UNIVERSITAT DE BARCELONA

Using patient-specific iPSC derived dopaminergic neurons to investigate Parkinson's disease: a new prospective in stem cell research and application

Roger Torrent Juan

UNIVERSITAT DE BARCELONA

Using patient-specific iPSC derived dopaminergic neurons to investigate Parkinson's disease: a new prospective in stem cell research and application.

Utilització de neurones dopaminèrgiques específiques de pacients derivades de cèl·lules pluripotents induïdes (iPSC) en la investigació de la malaltia de Parkinson: una nova perspectiva en la investigació amb cèl·lules mare i les seves aplicacions.

Memòria presentada per **Roger Torrent Juan** per optar al títol de
Doctor per la Universitat de Barcelona
Programa de Doctorat de **Biomedicina**
Línia de Recerca de **Neurociències**

Tesi doctoral realitzada sota la direcció de la **Dra. Antonella Consiglio** a
l'Institut de Biomedicina Universitat de Barcelona (IBUB)
Departament de Bioquímica de la Facultat de Biologia de la Universitat de Barcelona

Directora de la tesi:
Dra. Antonella Consiglio

Tutor de la tesi:
Dr. José Antonio del Río Fernández

Roger Torrent Juan

Barcelona, 2016

A la meva família i amics

AGRAÏMENTS

M'agradaria donar les gràcies a tots els qui han aportat un, o dos, o tres o fins a mil grans de sorra en el paviment d'aquest camí que m'ha dut fins aquí.

Primer de tot vull donar les gràcies a la meva directora de tesis, Antonella Consiglio, per haver-me brindat aquesta meravellosa oportunitat de treballar en el seu grup laboratori. Gràcies per la formació professional que m'has ensenyat, per inculcar-me el rigor constant que és necessari en un món com la investigació científica, i més encara en la recerca amb cèl·lules mare. Però tampoc vull oblidar-me de la teva empatia i paciència que has tingut en els moments més complicats, dels quals vull fer-te saber que sempre n'estaré plenament agraït. Gràcies també a l'Àngel Raya per haver compartit amb mi els seus coneixements, per haver-me deixat ser partícip dels seus "labmeetings", i per la seva també infinita paciència amb mi en tot moment i fins ara. Vull que sapigueu que sempre tindré un racó en la meva memòria de vosaltres, no només com a mestres, sinó també com a persones humanes.

Agraeixo també als membres del tribunal i al meu tutor, José Antonio del Río, per estar sempre disponible i disposat a ajudar-me sempre que ho he necessitat.

M'agradaria mencionar el plaer que ha estat col·laborar amb Juan José Toledo, Francisco Javier Villadiego, Mario Ezquerra, Rubén Santiago-Fernandez, Iria Carballo-Carbajal, Andrés Míguez, Isaac Canals, Noelia Brun, Daniel Grinberg i Lluïsa Vilageliu, sense els quals aquesta tesis no hagués estat possible.

Gràcies als meus pares, per haver-me alimentat, vestit, educat, i portat en aquest món tan complicat de la millor de les maneres com ningú podria haver imaginat. Gràcies per la vostra sempre desinteressada ajuda en els moments més difícils i per no haver deixat que em rendís en cap moment. Gràcies també a les meves germanes Mireia i Araceli, que han estat també el meu exemple a seguir, pels riures sempre sincers als meus acudits dolents, i a la felicitat contagiosa dels seus fills i filles Gemma, Gina, Glòria i Pau. També vull tenir un record especial pels meus cunyats Pedro i Gustavo en els sobretaules dels dinars familiars que hem compartit durant aquesta etapa.

Voldria subratllar també la dedicació i empenta que em van donar els meus professors de Batxillerat de l'escola IPSI, Jordi Dentard i Marta Domènech. Sempre els he tingut un grat record per la seva manera d'ensenyar ciència, i per haver-me encoratjat a cursar els estudis universitaris de biotecnologia.
Durant la universitat, sempre recordaré les classes o quasi diria monòlegs magistrals d'en Jordi Cairó, que sabia trobar l'equilibri perfecte entre la docència, el respecte, el rigor, el sentit de l'humor i donar-nos la motivació suficient per tirar endavant. Tampoc voldria oblidar-me de l'Elisabet Vila, que em va donar la meva primera oportunitat per treballar en un laboratori. Gràcies de tot cor també per l'experiència rebuda de part del l'Antonio Postigo i l'Ester Sánchez, els quals us considero els principals artífex del despertar de les meves inquietuds per arribar a ser doctor. Moltíssimes gràcies.
No em vull oblidar tampoc del tracte humà que vaig rebre de part d'en Fèlix Bosch durant la meva formació com a màster a la Universitat Pompeu Fabra.
Un record especial també per la meva temporada a Ferrer Internacional, per a la Gemmes, la Gloria, la Soraya i el Paco. Tan de bo segueixi trobant persones com vosaltres en els meus pròxims reptes professionals!

Sobretot vull donar les gràcies a l'Adriana Sànchez, que va creure que podia fer aquest camí, i que tantes i tantes coses em va ensenyar durant el seu últim any de doctorat. Valoro moltíssim l'esforç i paciència que vas tenir en totes les ensenyances que em vas donar. T'estaré tota la vida agraït.

Un record especial pel grup de laboratori de l'Iñaki.

Així, també vull agraïr a totes les persones que han format part del dia a dia al laboratori. Gràcies Yvonne per la teva dedicació, temps i paciència a la sala de cultius. Espero haver-t'ho posat fàcil. Aquesta tesis també va dedicada a tu i a tota la teva família. M'agradaria també

enrecordar-me del Sergio i l'Isaac, grandíssimes persones amb les que he après moltíssim i crec que també ens hem fet un tip de riure. Gràcies el sector "Peixos" Adriana, Cristina, Anna, i la ja Dra. Isil (Felicitats!). Moltíssimes gràcies a la també ja doctora Claudi (Enhorabona!), a la Senda, a la Raquel i l'Amèrica, a l'Alba Mateos, al Marcelet, l'Arnau, la Carola, la Dalel, la Maria Valls, al "José" Juan (que seràs el pròxim!), i al Juanlu (El pròxim del pròxim!), amb qui també he compartit moments fantàstics i anècdotes per recordar.

Un record superespecial per a tots els masters of the IBUBniverse. Angelique, gràcies sempre per el teu bon humor i les teves abraçades terapèutiques, gràcies Giulia també per la teva "contagiosa" alegria. De fet, gràcies a les dues per haver-me acompanyat a Cracòvia a fer la meva primera presentació oral davant de tant de públic. Armida, gràcies per haver estat com una tercera germana gran quan més ho he necessitat. Gràcies Irene per haver-me ajudat tant en aquesta última etapa del meu doctorat amb els experiments, al Carles pels teus coneixements i el teu rigor científic, i per els ànims que ocasionalment ens hem donat mútuament. Gràcies, Francesca, per la teva honestedat humana i professional. Moltíssimes gràcies, Neus, pels teus coneixements i ànims durant aquests últims anys. Menció especial a tots els estudiants de Màster i de Grau, i col·laboradors que han passat en algun moment o altre pel laboratori i l'han enriquit encara més: la Verònica, la Carla, la Helia, l'Ana Molgosa, la Judit, l'Ana Costa, la Caterina, la Laia, el Carles Terol, la Floriana, la Marta, l'Alba i el Chema.

Moltíssimes gràcies també a l'Elena Rebollo, per la dedicació i paciència que ha tingut durant les meves sessions al confocal SP5.

Moltes gràcies també al Dr. Rafael Padrós per tot el coaching rebut durant aquests anys.

Eternament agraït també a Rosa-Luxemburg i a Ós Bru, dos pilars fonamentals de l'amistat que han permès mantenir activa la meva vessant artística al llarg d'aquests anys. Gràcies Pol i Eli per compartir la vostra intel·ligència emocional amb mi, sempre que ho hem necessitat. Gràcies Tomàs i Nani per haver-me empès a fer el pas i independitzar-me de casa els pares (ells no sé si us ho agrairan tant, haha). Gràcies Iban, per les teves preguntes irreverents i per la teva paciència a la sala de controls.

Gràcies Cristian, Victor, Albert, Carles Ladrón de Guevara, Roger Torras, Aleix Sarri i Maria Martí, els millors amics que he tingut mai i que tan de suport m'heu demostrat al llarg de tants anys. Gràcies per formar part de tants projectes comuns.

Vull donar les gràcies a la Ksènia. Per tot el temps que hem compartit junts, pels viatges, les cases rurals, els estius a Cadaqués, Berlin i Istambul. Sobretot gràcies pel teu suport i pels sacrificis i riscos que vas assumir per poder venir fins a mi. Moltes gràcies als teus pares Victor i Tatiana per tota la seva generositat. Большое спасибо.

I què dir de la meva gata Marfa que ha omplert les meves mans de cicatrius, el meu mòvil de fotografies, i la vida de moments únics.

I finalment, vull dedicar aquesta tesi en memòria dels meus avis, en especial el meu avi patern Antoni Torrent Clavier, qui va ser víctima d'aquesta malaltia i que, tot i que no el vaig arribar a conèixer com hagués volgut, segur que allà on sigui aplaudeix la meva gesta, junt amb la meva àvia paterna Assumpció Torrent, així com també els meus avis materns Araceli Baruel i Josep Maria Juan.

“Acceptance doesn’t mean resignation;
it means understanding that something is what it is
and that there’s got to be a way through it”

Michael J. Fox

RESUM.

La malaltia de Parkinson (MP) és un desordre neurodegeneratiu incurable, principalment caracteritzat per la pèrdua progressiva de neurones dopaminèrgiques (DA) del mesencèfal, localitzades a la substancia nigra pars compacta (SNpc), i freqüentment acompanyat per la formació d'agregats proteics citosòlics insolubles en les neurones supervivents residuals, coneguts com a cossos de Lewy. La progressiva denervació dels terminals dopaminèrgics que projecten als ganglis basals i l'estriat causa una manca d'alliberament i ús de dopamina, provocant com a conseqüència una progressiva manifestació de dèficits motors, que acaben conduïnt a la invalidesa i mort prematura.

Actualment, la MP només es pot tractar amb teràpies simptomàtiques que compensen eficientment les deficiències locomotores durant un període al voltant dels 5 anys. No obstant, les teràpies existents no permeten curar ni aturar la progressió de la malaltia. La manca de models animals i cel·lulars adequats podrien explicar el coneixement fragmentari dels mecanismes patològics que condueixen a la MP, i posa en relleu la necessitat urgent de desenvolupar models experimentals fiables que puguin recapitular les principals característiques d'aquest trastorn. L'ús de cèl·lules mare amb pluripotència induïda (iPSC) ofereix una oportunitat sense precedents per a modelar malalties humanes, ja que poden ser generades a partir de pacients i diferenciades en tipus cel·lulars rellevants de la malaltia. Recentment, s'han descrit models basats en iPSC humanes per a l'estudi de la MP. Neurones derivades de iPSC provinents de pacients amb MP familiar i esporàdica recapitulen fenotips humans específics de la malaltia *in vitro*, com ara l'acumulació anormal d'α-sinucleïna, i alteracions en la maquinària de l'autofàgia.

En aquesta tesi doctoral s'ha investigat l'efecte neuroprotectiu de diferents compostos, incloent el factor neurotròfic GDNF, en el cultiu *in vitro* de neurones DA derivades de iPSC de pacients amb la mutació familiar G2019S al gen *lrrk2* (LRRK2-PD), i pacients esporàdics (ID-PD). Curiosament, s'ha trobat que sis setmanes després del tractament amb el GDNF, el nivell d'arborització dendrítica de les neurones DA derivades de LRRK2-PD i ID-PD-iPSC augmentà fins als nivells normals trobats en les neurones DA derivades d'individus control (Ctrl-iPSC). En comparació amb els cultius neuronals DA derivats de PD-iPSC sense el tractament, els efectes neuroprotectius estaven associats a una disminució en el número de neurones apoptòtiques, i a l'activació de vies de supervivència cel·lular, riu avall del complex receptor del GDNF GFR1α/RET, així com també la reducció de vesícules autofàgiques. A més, s'ha trobat que el GDNF és, en part, un requisit per a una correcta supervivència neuronal sistèmica en aquest model. Concretament, els nivells de GDNF a llarg temps de cultiu es troben dos vegades disminuïts tant en els cultius DA de ID-PD com els de LRRK2-PD, en comparació amb els nivells de les Ctrl. En conclusió, els nostres resultats demostren que les cèl·lules neuronals derivades de iPSC són models valuosos per a mesurar respostes a teràpies neuroprotectives, i per tant poden ajudar a identificar nous fàrmacs potencials, fomentant així el desenvolupament de tractaments per a la MP. La secreció diferencial de factors de supervivència dins del cultiu també destaca l'importància de l'ús d'aquesta tecnologia per a l'estudi de la contribució d'altres tipus neurals en la patogènesis de la MP.

ABSTRACT.
Parkinson's disease (PD) is an incurable neurodegenerative disorder, mainly characterized by a progressive loss of midbrain dopaminergic (DA) neurons, located in the substantia nigra pars compacta (SNpc), and frequently accompanied by the formation of insoluble cytosolic protein aggregates in the remaining surviving neurons, known as Lewy bodies. The progressive denervation of DA terminals that project to the basal ganglia striatum causes a lack of DA uptaking, and consequently a progressive manifestation of debilitating motor deficits, that leads to premature invalidity and death.
To date, only symptomatic therapies can compensate efficiently the locomotor deficiencies over a period of 5 years, however they do not cure or halt disease progression. A lack of suitable animal and cellular models might explain the fragmentary knowledge of the pathogenic mechanisms leading to PD, and highlights the urgent need for developing reliable experimental models that can recapitulate the key features of this disorder. The utilization of induced pluripotent stem cells (iPSC) offers an unprecedented opportunity to model human diseases, since they can be generated from patients and differentiated into disease-relevant cell types, such as neurons. Recently, human iPSC-based models of PD have been described. iPSC-derived neurons from patients with familial and sporadic PD recapitulate human disease phenotypes such as abnormal α-synuclein accumulation in vitro, and alterations in the autophagy machinery.
Here, we investigated the neuroprotective effect of several compounds, including the neurotrophic factor GDNF, in culture of iPSC-derived midbrain dopaminergic neurons from patients with a LRKK2 mutation or sporadic patients. Interestingly, we found that six weeks after GDNF treatment, the level of dendritic arborisation from DA neurons derived from ID-PD and LRRK2-PD-iPSC increased to normal levels found in Ctrl-iPSC derived DA neurons. The neuroprotective effects were associated to a decrease in the number of apoptotic cells, and to a GFR1α/RET downstream activation of cell survival pathways, as well as reduction of autophagosome vesicles, compared to the untreated PD-iPSC derived DA neurons. Additionally, we found that GDNF is, in part, a requirement for a properly systemic neuronal survival in this model, since levels of GDNF were found twice decreased within long-term DAn cultures derived from both ID-PD and LRRK2-PD, when compared to CTL. In conclusion, our data demonstrate that iPSC-derived neuronal cells are valuable models for measuring responses to neuroprotective therapies and they may help to identify potential new drugs, thus furthering the development of treatments for PD. The differential secretion of survival factors within the culture also highlights the importance of using this technology for studying the contribution of other neural cell types in the onset of PD.

CONTENTS

1. INTRODUCTION

1.1. Parkinson's Disease (PD).

When in 1817, the British physician James Parkinson wrote his monograph *Essay on the Shaking Palsy*, he hoped that he would persuade the scientific community that he had described an unrecognized disorder. Nevertheless, it was the father of neurology Jean Martin Charcot who named this disease in his honour as *maladie de Parkinson* (Parkinson's disease). To date, the main cause of Parkinson's disease (PD) remains as elusive as when it was first described, and a single cause has not been found and is unlikely to emerge.

Parkinson's disease is the second most common neurodegenerative disease after Alzheimer's, and it is characterized by a region-specific selective loss of dopaminergic (DA), neuromelanin-containing neurons from the substantia nigra pars compacta (SNpc), which connects with the caudate putamen through the nigrostriatal pathway. Therefore, there is a lack of DA uptaking primarily in the putamen that results in a progressive disruption of debilitating motor deficits (also known as "parkinsonism"), such as tremor, limb rigidity and slowness of movements (bradykinesia). Moreover, non-motor features, such as olfactory deficits, cognitive decline, depression, and disturbed sleep are also present in later stages of the disease [1–3]. Given that DA release in the caudate putamen is compromised, efforts of pharmacological substitution with dopamine agonists and anti-cholinergics, or Deep Brain Stimulation (DBS) were found to be successful treatments to reduce PD symptoms associated with motor impairment. These current symptomatic therapies can compensate efficiently the motor deficits over the first 5 years. However, they do not cure or halt disease progression. Furthermore, severe side effects over the years reduce overall medication efficacy [4]. The lack of a reliable treatment that can permit the cure of the disease remains still elusive.

The incidence of the disease rises prominently with age, with a prevalence of 1% at age of 65 and around 5% by the age of 85 [5]. Between 30-50% of DA neurons are lost during the first year of PD diagnosis, and this percentage increases dramatically after the following 4 years, reaching almost the 90% of them lost [6]. The fact that the disease is slowly progressive and changes in the behaviour are rarely noticed by the patient, a lag of 2-3 years from the first symptoms to diagnosis is frequent [1]. The mean duration of the disease is an average of 15 years, with a mortality ratio of 2 to 1 in the affected subjects. Due to an increased life expectancy of the Western world population, the prevalence of PD is anticipated to expand tragically and thus becoming an important part of the economic burden to the public health systems [7].

Approximately 90%–95% of all PD cases are sporadic with no family history. Although disease onset and age are highly correlated, PD occurs when complex mechanisms such as mitochondrial activity, autophagy, kinase signalling pathways or degradation via proteasome are deregulated by environmental influence or PD-specific mutation susceptibility. On the other hand, significant advances in understanding the mechanisms of disease pathogenesis have been made in the past two decades with the identification of distinct genetic loci at which pathogenic mutations are associated with parkinsonism, although these mutations only account for 5-10% of PD patients with family history [8].

1.1.1. Neuropathological features of Parkinson's Disease.

The main pathological hallmarks of PD include the progressive preferential loss of striatal-projecting DA neurons of the substantia nigra pars compacta (SNpc), and the presence of intraneuronal accumulation of insoluble proteins and protein fragments, known as Lewy Bodies (LB) in the remaining surviving neurons [9].

From SNpc, DA neurons project through the striatum, primarily to the putamen and secondly to the caudate. These DA neurons are of A9 subtype [10], characterized by strong neuromelanin pigmentation, and are responsible for the release of dopamine in the striatum to regulate the basal ganglia by means of mostly motor, but also associative and limbic domains. In PD, the

loss of A9-subtype DA neurons, displayed by a SNpc neuromelanin depigmentation [11], causes a progressive dysfunctionality in the motor circuitry of the basal ganglia (**Fig. 1**). In the onset of the disease, when the symptoms are already unequivocally, putamenal DA is depleted around 80%, and almost 50% of the DA neurons have already been lost. More important, the degree of terminal loss in the striatum appears to be more pronounced than the magnitude of the DA neuron loss in the SNpc. Striatal dopaminergic nerve terminals are the primary target of the degenerative process, therefore neuronal death in PD may result from a “dying back” process [9].

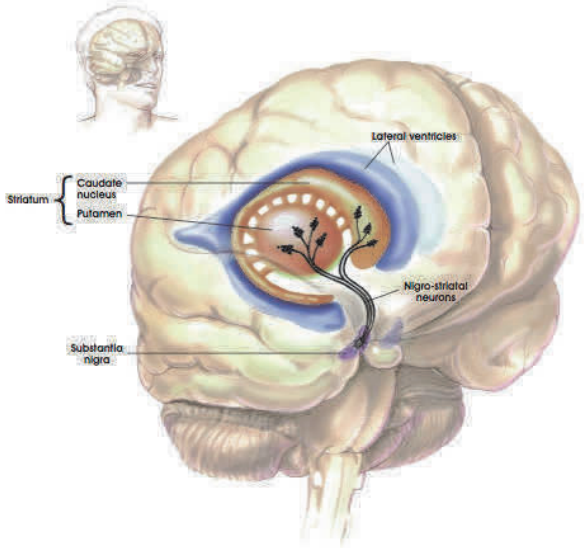

Figure 1. Schematic representation of the nigrostriatal pathway in the human brain.
In normal healthy brain, the nigrostriatal pathway is composed of A9 dopaminergic neurons whose cell bodies are located in the SNpc. Their processes project to the basal ganglia and synapse in the striatum, specifically in the putamen and caudate nucleus. In a PD brain, the nigrostriatal pathway degeneration is the consequence of a marked loss of A9 DA neurons that project to the putamen and a in a less extent in the caudate. (Extracted from http://stemcells.nih.gov/info/scireport/pages/chapter8.aspx)

Neuronal loss is typically accompanied by the presence of Lewy bodies (LB) and Lewy neurites (LN) in the substantia nigra, although they are also found in other brain regions of the central nervous system (CNS) [12]. LB are usually found as eosinophilic, intra-cytoplasmic inclusions, about 5-25 μm in diameter, with a dense central core, sorrounded by a clearer halo [9]. Ultrastructurally, its organization consists of a composition of a dense core of filamentous and granular material that is surrounded by radially oriented filaments (**Fig. 2**). Specifically, an abnormal, post-translationally modified, and aggregated form of the presynaptic protein α-synuclein is the major fibrillar component of LB and LN, among other numerous proteins, such as ubitiquin, Parkin and neurofilaments [13]. LB are not specific of PD, in fact, abundant LB and LN are found in the cerebral cortex in people with advanced age, and also in patients with "idiopathic dementia with Lewy Bodies" (DLB), a common late-life dementia that is clinically similar to Alzheimer's disease [14].

The loss of the nigrostriatal processes and subsequently loss of DA neurons in the SNpc results in a striatal dopamine deficiency which in turn leads to a cascade of dysfunctional events in the basal ganglia circuitry, and results in the development of the cardinal features of PD [15]. The basal ganglia (or basal nuclei) is a cluster of deep nuclei that includes the striatum, the SNpc and SN pars reticulate (SNpr), the globus pallidus pars interna (GPi) and pars externa (GPe), and the subthalamic nucleus (STN).

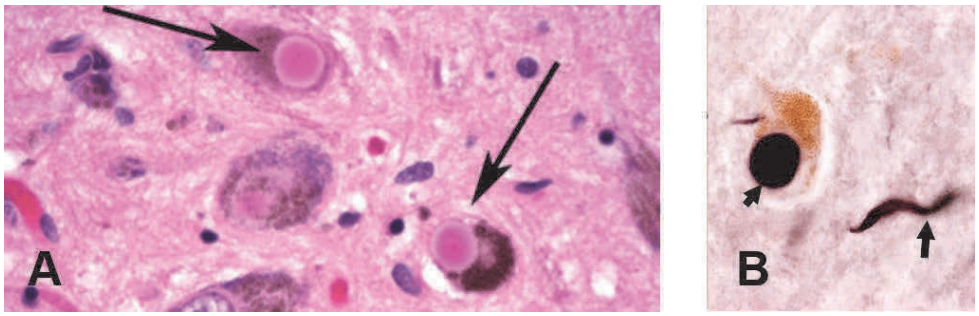

Figure 2. Histological cuts of postmortem PD brain's patients, showing Lewy bodies and Lewy neurites. A) Hematoxylin and eosin staining of Lewy Body (arrows) within a pigmented A9 DA neuron, showing the characteristic dense core surrounded by a more translucent halo. B) α-synuclein staining of a Lewy body (left arrow) and a Lewy neurite (right arrow) (2A Extracted from https://quizlet.com/80824024/nbme-neuro-flash-cards/ and 2B Extracted from Olanow and Brundin, 2013 [16])

Components of the basal ganglia are intimately connected with the thalamus and the cortical motor areas, through several segregated but parallel loops, that include not only motor, but also associative, and limbic domains. In the mid-1980s the description of a basal ganglia circuitry model reinforced the association between the basal ganglia and the abnormal movements events in PD [17].

In a normal state, the striatum receives cortical excitatory input and projects to output neurons in the monosynaptic GABAergic pathway (putamen-GPi), also known as the "direct" pathway, and in the polysynaptic "indirect" pathway (putamen-GPe-STN-GPi/SNpr). Dopamine is thought to excite D1 expressing neurons that comprise the "direct" pathway and project to GPi/SNpr, whereas it also inhibits neuronal activity of D2-bearing striatal neurons that comprise the "indirect" pathway, which project to the GPe. Besides, the STN is also activated by an excitatory projection from the cortex, called the hyperdirect pathway. In summary, activation of the "direct" pathway implies movement facilitation, whereas activation of the "indirect" pathway suppresses movements. However, in PD, when neuronal degeneration occurs in the SNpc and dopamine striatal depletion fall below 50-80%, respectively, the striatal physiology is disrupted, leading to an increased activity of the "indirect" pathway and an abnormal reduced activity of the "direct" pathway [18] (**Fig. 3**). These changes are thought to provoke the parkinsonian syndrome, characterized by the difficulty in making precise movement selection and execution (akinesia and bradikinesia), and are also tipically associated with increased muscle tone (rigidity), which can also be accompanied by tremor at rest.

Therefore, the classical model of the basal ganglia has provided a conceptual framework for better understanding the pathophysiology of PD, and other movement disorders. Indeed, it had a paramount role in revitalizing functional surgery such as Deep Brain Stimulation in PD patients and, for example, in defining the STN as a target [15].

1.1.2. The Clinical Prodrome.

As aforementioned, motor manifestations stem for the loss of DA neurons in the SNpc. However, certain non-motor features seem to precede the typical parkinsonism of PD, and are thought to be the result from the spreading of the pathology from the basal ganglia to other brain systems. These non-motor features include hyposmia, sleep disorders, dysautonomia, and neuropsychiatric disorders, such as depression, anxiety and apathy. In addition, patients in advanced stages of PD can suffer of dementia [19–21]. The clinically silent window between the non-motor molecular prodrome and the beginning of the first motor symptoms could last for decades, and probably varies from one patient to another, and this, together with a lag of 2-3 years in the clinical detection of the motor symptoms, makes the diagnostic a confounding challenge yet to be resolved.

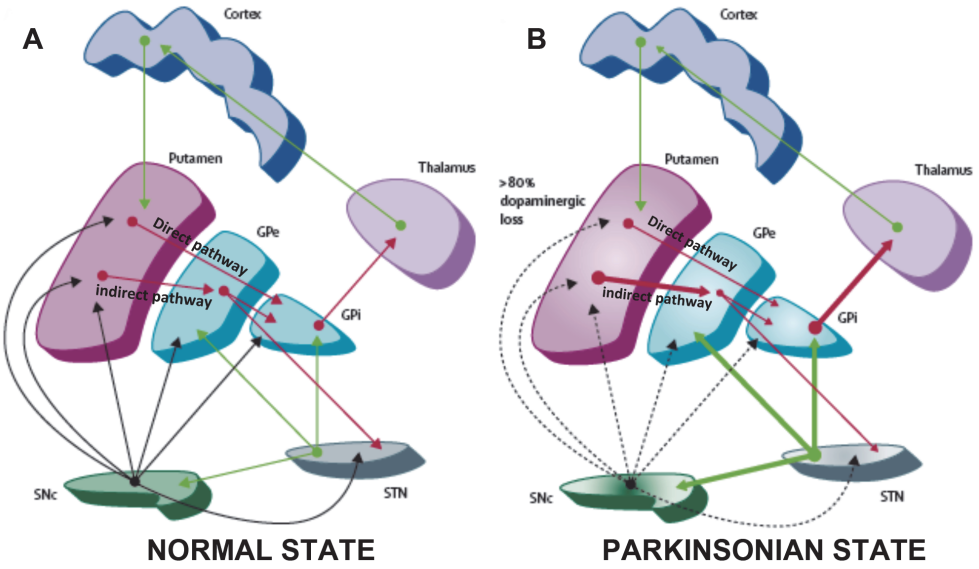

Figure 3. Scheme of the physiological model of the basal ganglia motor circuit.

Red arrows indicate inhibitory GABA-ergic projections, green arrows represent excitatory glutamatergic projections, and black arrows indicate dopaminergic innervation. The thickness of the arrows indicates the degree of activation of each projection. A) In the normal state, the striatum receives cortical excitatory input and projects to output neurons in the GPi through a direct pathway, and by a polysynaptic indirect pathway via the GPe and the STN. Dopamine is thought to inhibit neuronal activity in the indirect pathway and to excite neurons in the direct pathway. B) In the parkinsonian state, striatal physiology is disrupted. Dopamine D1 receptor-expressing striatal neurons in the direct pathway become hypoactive, whereas dopamine D2 receptor-bearing striatal neurons in the indirect pathway are hyperactive. The latter response leads to increased inhibition of the GPe, and disinhibition of the STN. Overactivity in STN neurons and reduced inhibition in the direct pathway provokes excessive excitation of neurons in the GPi and overinhibition of thalamocortical and brainstem motor centres, resulting in parkinsonism (From Obeso et al., 2014 [18]).

The clinical evolution of the prodromal non-motor features of PD might to some degree be explained by the proposal made by Braak and colleagues in 2003, about an ascending LB formation across the brain [22]. Based on studies of a large series of postmortem PD brains, they suggested a prion-like disease mechanism progression of α-synuclein accumulation from preclinical to symptomatic, and subsequently to an advanced disease stage, that spreads not randomly along axonal pathways interconnecting vulnerable brain regions in a constant pattern that they subdivided into six different stages. Summarizing, α-syn spreading it starts in the enteric and olfactory nervous system, followed by alterations in the brainstem, reaching the midbrain nigrostriatal DA neurons (third stage) that would start to degenerate, affecting finally the forebrain neurons that would suffer degeneration. This concept of premotor PD is gaining support, and even other several research groups have confirmed this staging pattern [23], although this is not applicable at least in 10% of PD cases, due to disease variants, which can be difficult to characterize [20]. However, about 10% of people older than 60 years of age who have died without evidence of neurological disease, LB are present in the brain, and despite being diagnosed with LB pathology, probably they were undergoing a presymptomatic early phase of PD that had not been detected yet [1]. This evidence suggests that the risk of developing PD could be ten times more, and the importance of an early diagnostic could determine a better treatment for these patients, who would be able to receive protective treatments instead of treating the motor symptoms.

1.2. Etiology of Parkinson's Disease

There are two main forms of PD: sporadic PD, which represents the majority of PD cases, and familial PD, accounting for 5-10% of PD cases [24]. Approximately 90- 95 % of all PD cases are sporadic with no known genetic mutation, most likely resulting from complex interactions among gene susceptibility and environmental factors. The most consistent risk factor associated to the development of the disease is aging, which has been interpreted as leading to the accumulation

of unrepaired cellular damage and to the failure compensatory mechanisms such as mitochondrial activity, autophagy or degradation via proteasome [8]. Other factors have been associated to the risk of developing PD such as exposure to toxins or chemicals. However no environmental cause of PD has yet been proven conclusively.
Studies of rare large families showing classical Mendelian inherited PD have allowed the identification of specific genes, the mutation of which is associated with increased risk of suffering PD, and recent genome-wide association studies (GWAS) have established additional susceptibility loci. The two genes associated to autosomal dominant PD are the Leucine-rich repeat kinase-2 (LRRK2) gene and the gene encoding α-syn (SNCA), while mutations in Parkin, DJ-1, PINK1, and ATP13A2 genes, cause early-onset parkinsonism [24], characterized by more atypical features of PD. In view of the known function of these proteins, especial attention has been drawn to the roles of mitochondrial dysfunction and oxidative stress in PD. However, the immediate cause(s) of neuronal cell death in any and all forms of PD are as yet undefined.
Although mutations in the PD-associated genes account for small number of PD cases, there is evidence that these genes may also contribute to the sporadic forms of the disease as well. For example, mutations in the LRRK2 gene are not only found in patients of autosomal dominant late-onset PD [26-27], but also in numerous cases of late-onset sporadic PD [25]. Therefore, it has been postulated that PD may result from a genetic mutation or a genetic predisposition to an environmental factor, or a combination of susceptibility genes that increases the risk of the disease [8,24]. This may represent the existence of different pathogenic mechanisms that converge on one or more common signaling pathways central to the loss of DAn, leading to the manifestation of clinical PD.

1.2.1. Risk Factors.

Aging is the strongest risk factor for development Parkinson's disease, although 10% of people with the disease are younger than 45 years of age. The mean age at onset is at 55, and the incidence increases markedly with age, from 20/100,000 overall to 120/100000 at age 70, with a lifetime risk of developing the disease of 1,5%. The incidence tends to decrease in the ninth decade of life, although the lecture of these observations could be artefactual or related to underdiagnosis of elderly people of that age [9].
Ageing has been described to actively lead to the accumulation of unrepaired cellular damage due to a progressive failure of compensatory mechanisms such as mitochondrial activity, autophagy or decreased proteasome activity [9]. Indeed, Collier and colleagues studied the effect on aging in non-human primates, by analyzing typical traits of PD patients, such as the presence of neurochemical and morphological changes in DA neurons in the brain of rhesus monkeys from different ages. The authors observed a decreased TH expression in the substantia nigra of aged monkeys, and this was associated with increased α-synuclein staining, and the presence of ubiquitin-positive inclusions, diminished lysosome activity, as well as excessive oxidative and nitrative damage, and a mild increased inflammation [26]. Moreover, DA neurons in the substantia nigra (A9) were more vulnerable to this age-associated degeneration than DA neurons in the ventral tegmental area (A10). From these observations they concluded that these age-related changes could be responsible for PD-associated changes in the nigrostriatal system and that, although being milder when compared to PD patients, ageing induces a pre-parkinsonian condition. How these cellular mechanisms of dopamine neuron demise during normal aging are accelerated or exaggerated in Parkinson's disease remains still not clear. Collier and colleagues hypothesized that the combination of a specific genetic contribution, environmental factors together with other unknown accelerants (prenatal infections, cellular predispositions, unknown factors), may alter the normal course of age-related dopamine neuron dysfunction that would eventually trigger the onset of PD phenotypes.
On the other hand, only some of the brain regions appear to be particularly vulnerable, while the majority of them do not degenerate and remain perfectly functional. In particular, hippocampus, putamen, hypothalamus or nucleus basalis of Meynert remain almost completely intact over

time. Others, like the neocortex, lose an average 10% of the total number of neurons throughout life. However, ventral tegmental area (VTA), retrorubral area and the SN are particularly sensitive to the aging process. Remarkably, all these regions mainly use DA for neurotransmission, which hints at a possible link between DA and a higher sensitivity to age-related degeneration [27].

Gender is another risk factor for suffering PD. Epidemiological studies have shown that both incidence and prevalence of PD have a female-to-male ratio of 1: 1.5-2, with a mean of 2.2 years older of age at onset in women compared with men, and also with a more benign form of the disease [1]. In fact, Haaxma and colleagues did a epidemiologic study in which differences in the onset of the disease between women were due two different issues: first, women have a higher initial striatal dopamine levels compared to men, that could delay the onset of the motor symptoms; secondly, later menopause and a longer fertile life span delayed the age at onset due to increased levels of oestrogen [28]. How oestrogen plays a role on neuroprotection is still unknown and in controversy, although oestrogen levels have been associated with increased presence of dopamine transporters and higher striatal dopamine concentrations. However, a longer fertile life span has also been linked with iron loss during menses and pregnancies, which in turn could suggest less presence of oxidative processes in the nigrostriatal systems due to the lack of iron, thus conferring indirect protection against oxidative stress by this hormone. Nevertheless, when disease progression is already ongoing no differences between gender are found, therefore oestrogens may have a mild role on neuroprotection in the preclinical stage, a no role when symptoms become clinically apparent [28].
On the other hand, other epidemiological studies have associated different habits and lifestyles with reduced risk of suffering PD, which includes diets high in uric acid, high levels of physical activity during midlife, cigarette smoking, and consumption of large amounts of caffeine. However, some of these findings could be more related to dopamine's role in reward pathways, rather than to any neuroprotective effect of nicotine or caffeine, and even there are studies that have shown inverse associations in some cases [29,30].

Given that around 90% of PD patients the disease is sporadic, many studies have been focused on the identification of environmental factors that could contribute to PD. For example, rural living together with exposure to herbicides and insecticides such as paraquat, MPTP or rotenone, and also heavy metals including manganese and iron, have been described to cause a parkinsonism picture. However, no other environmental substance has been associated with conclusive evidence to PD. In fact, PD is neither associated to race or creed, and there is literary and historical precedents of the disease, before the publication of James Parkinson's "Shaking Palsy" monograph, that make exclude PD as a post-industrial condition [1].

1.2.2. The Genetic contribution to Parkinson's disease

Studies of rare large families showing classical Mendelian inherited PD have allowed for the identification of 11 genes out of 16 identified disease *loci*, some of them are autosomal dominant forms (*SNCA, LRRK2*) and others are recessive (*PARK2, PINK1, DJ-1*) (**Table 1**). These genes have been identified, showing that mitochondrial or lysosomal dysfunctions, protein aggregation, the ubiquitin-proteasome system, and kinase signaling pathways all play a major role in the pathogenesis of PD. Moreover, recent genome-wide association studies (GWAS) have been helpful for identifying loci at which common genetic variants increase risk of developing apparently sporadic disease [24]. Altogether, this may represent the existence of different pathogenic mechanisms that can converge on one or more common pathways regarding the loss of DA neurons, and leading to the onset of the clinical manifestation of the disease. In addition, the lack of a family history that can appear in some dominant monogenic mutations can occur for multiple reasons, being early death as the most common event prior to the observation of the disease, a loss of follow up, and, more important, reduced penetrance

that can occur by positive influence of the environment or due to unidentified dominant de novo mutations that can compensate the effect of the others [8].
The elucidation of different genetic components has given rise to a multitude of cell and animal models enabling the dissection of molecular pathways involved in disease etiology.

PARK locus	Gene	Map position	Clinical phenotype	Pathology
PARK1/4	*SNCA*	4q21	Parkinsonism with common dementia	Lewy bodies
PARK2	*parkin*	6q25-q27	Early-onset, slowly progressing parkinsonism	Lewy bodies
PARK3	Unknown	2p13	Late-onset parkinsonism	Lewy bodies
PARK5	*UCHL1*	4p14	Late-onset parkinsonism	Unknown
PARK6	*PINK1*	1p35-p36	Early-onset, slowly progressing parkinsonism	One case exhibiting Lewy bodies
PARK7	*DJ-1*	1p36	Early-onset parkinsonism	Unknown
PARK8	*LRRK2*	12q12	Late-onset parkinsonism	Lewy bodies (usually)
PARK9	*ATP13A2*	1p36	Early-onset parkinsonism with Kufor–Rakeb syndrome	Unknown
PARK10	Unknown	1p32	Unclear	Unknown
PARK11	*GIGYF2*	2q36-q37	Late-onset parkinsonism	Unknown
PARK12	Unknown	Xq	Unclear	Unknown
PARK13	*Omi/HTRA2*	2p13	Unclear	Unknown
PARK14	*PLA2G6*	22q13.1	Parkinsonism with additional features	Lewy bodies
PARK15	*FBX07*	22q12-q13	Early-onset parkinsonism	Unknown
PARK16	Unknown	1q32	Late-onset parkinsonism	Unknown
FTDP-17	*MAPT*	17q21.1	Dementia, sometimes parkinsonism	Neurofibrillary tangles
SCA2	*Ataxin 2*	12q24.1	Usually ataxia, sometimes parkinsonism	Unknown
SCA3	*Ataxin 3*	14q21	Usually ataxia, sometimes parkinsonism	Unknown
Gaucher's locus	*GBA*	1q21	Late-onset parkinsonism	Lewy bodies

Table 1. Summary of PD-associated familial loci and genes
(from Martin et al., 2011).

a) Autosomal dominant forms of PD
So far at least two genes, *SNCA* and *LRRK2*, have been clearly shown to cause autosomal dominant PD, with an overall mutation frequency of ~5%. The pathogenic role of other dominant genes in PD, such as UCHL1, GIGYF2, HTRA2, is still controversial.

α-Synuclein (*SNCA*)
α-Synuclein is a small protein of 140 aminoacids (14 kDa), encoded by the *SNCA* gene, and it is expressed constitutively within the vertebrates brain. α-Synuclein is a member of a three synuclein family (α, β, γ). Although a considerable sequence homology exists between the three members of the synuclein family, what it makes α-synuclein unique is that it contains three differentiated domains: first, an acidic COOH-terminal region; second, seven imperfect repeats (KTKEGV) localized in the NH_2 terminus, which form an amphipathic α-helical domain, where the protein specifically associates with the lipid rafts on the membrane; and third, a highly amyloidogenic domain located in the midregion (NAC domain) which, by itself, has a high propensity to aggregate (**Fig. 4**).

Little is known about its biological function, although its localization in the presynaptic nerve terminals strongly suggests a role in the vesicle trafficking during neurotransmission release [31]. In fact, mouse models, either lacking or overexpressing α-synuclein, have shown abnormal changes in synaptic vesicle recycling and mobilization [32,33]. It is known that in healthy conditions α-synuclein adopts defined conformations to function in cells, and its alpha-helical rich conformations have been observed to associate with the lipid rafts on the membrane [34].
On the other hand, in the brain of PD patients, α-synuclein has an increased tendency to aggregate, and adopt different conformations initially from monomeric to β-sheet-rich structure forms, and ultimately oligomeric forms organized as protofibrils that can undergo to insoluble

polymers [24]. Moreover, aging may contribute to α-synuclein toxicity by age-related accumulation of oxidative and nitrative α-synuclein modifications [35]. The identification of the *SNCA* locus led to the important discovery that α-synuclein is the major fibrillar component of the Lewy bodies and Lewy neurites [13]. Nevertheless, a widely accepted hypothesis for α-synuclein toxicity proposes that protofibrils of α-syn are cytotoxic, whereas the LB fibrillar aggregates could represent a cytoprotective mechanism in PD [36].

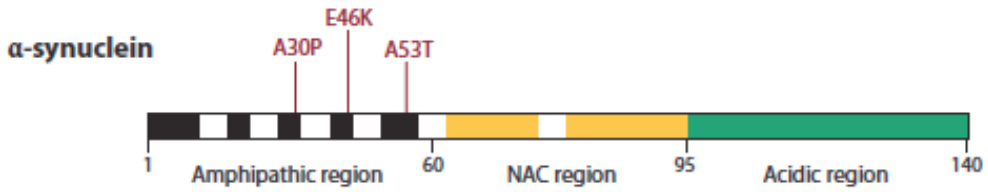

Figure 4. Schematic representation of the domains that constitute the protein α-synuclein.
Three missense mutations are represented above the protein organization. Moreover, duplications and triplications of different genomic sizes have been also reported (from Martin et al., 2011 [8]).

Two kind of genetic anomalies regarding *SNCA* have been described: point missense mutations that cause different variations of the protein, and multiplications of the entire locus, specifically duplications and triplications that provoke an overexpression of the wild-type protein. Only three point mutations have been identified: A53T, A30P and E46K, being the first the most common [8] (**Fig. 4**). Patients carrying the A53T mutation can present between a mild to a more sever phenotype, thus implying the existence of other factors that can modulate the phenotype. In patients carrying the A30P they present a similar idiopathic PD, and it has been shown that this mutation is associated with a reduced affinity to bind lipid rafts from the membrane, thus increasing the intracellular protein pool and thus potentiating its natural tendency to form aggregates. Patients carrying the E46K mutation manifests an early-age onset characterized by a sever parkinsonism and a diffuse Lewy body dementia.
On the other hand, numerous studies have linked familial PD with duplications and triplications in the *SNCA* (**Fig. 4**) [24]. In fact, the severity of the phenotype appears to be strongly correlated on the dosage of the *SNCA* gene. Whereas *SNCA* duplications are more associated with a typical late-onset PD phenotype, triplication of the same genomic region is more related to early-onset PD with dementia. The higher intracellular amount of this protein, caused by duplications and triplications, is thought to accelerate the formation of oligomers first and fibrillar aggregates later. So far, it has been proposed that PD, parkinsonism with dementia, and dementia with LB are causally related, and for this reason they have been grouped under the term of synucleinopathy disorders [37]. In addition, a link between sporadic PD and *SNCA* gene expression is supported by evidence of reduced epigenetic silencing of *SNCA* [38], and also *SNCA* promoter region polymorphisms that might increase its expression [39].

Leucine-rich repeat kinase 2 (*LRRK2*)
LRRK2 is a large protein that is ubiquitously and constitutively expressed in many organs and tissues. Although LRRK2 is present in brain regions relevant to the neuropathology of PD, its expression in A9 DA neurons is not particularly high [40]. LRRK2 is localized throughout the soma and dendritic processes of neurons. Little is known about the normal physiological functions of LRRK2, despite cell and animal models implicate it in a diverse array of functions, including mRNA translation, synaptogenesis, vesicular trafficking, autophagy, microtubule, and cytoskeletal network. This is not particularly surprising given its widespread distribution and broad interaction with different subcellular components, such as vesicular and membranous structures, the microtubule network, mitochondria, as well as other membranous-bound organelles [41].
The *LRRK2* gene consists of a genomic region of 144 kb, with 51 exons, encoding an unusually large 2,527 amino-acid multi-domain protein. LRRK2 contains three potential protein-protein

interaction domains that surrounds the central catalytic core, which include ankyrin repeats (ANK), armadillo repeat folds (ARM), leucine-rich repeats (LRR) and WD40 repeats, suggesting that LRRK2 is thought to serve as a scaffold for assembly of multiprotein signalling complexes. However, additional research is needed to identify the in vivo LRRK2 substrates relevant to PD. Moreover, what makes LRRK2 distinct from other proteins is that it singularly comprises two enzymes within a single polypeptide chain: a Roc GTPase domain followed by its associated C terminal of Roc (COR) domain, and a kinase domain of the tyrosine kinase-like (TKL) subfamily, homologous to other mitogen-activated protein kinase kinase kinase (MAPKKK) (**Fig. 5**) [8].

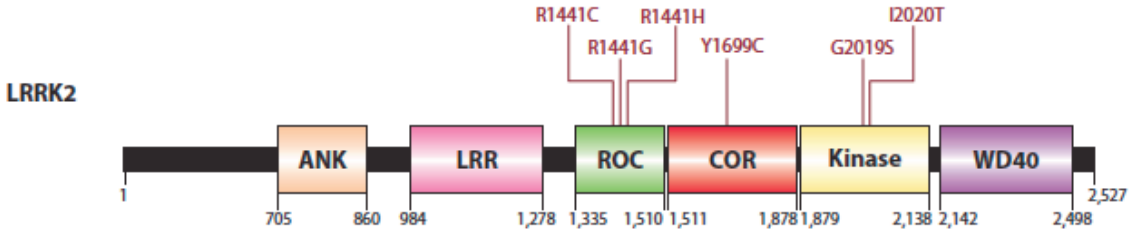

Figure 5. Schematic representation of the *LRRK2* gene and protein.
Several mutations in LRRK2 are known to be related with familial PD (from Martin et al., 2011 [8]).

The presence of both enzyme domains in the same protein has led to the hypothesis that LRRK2 may act as a cell signalling protein, although its intracellular functions are subject of intensive research indeed. In both primary cortical cells and rodent models, LRRK2 has been demonstrated to regulate neurite outgrowth in developing neurons, as knockout of endogenous LRRK2 in mouse neurons results in elongation of neuronal processes, and in neurons that express different pathogenic LRRK2 variants display reduced neurite process length and complexity [42]. Moreover, LRRK2 has been suggested to regulate protein translation through two different mechanisms: first, LRRK2 interacts genetically and physically with the eukaryotic translation initiation factor 4E-binding protein (4E-BP) by phosphorylating it, thus disrupting its binding to the eukaryotic translation initiation 4E (eIF4E), which could impact mitochondrial function and possibly neuronal viability [43]. Second, other studies reported that pathogenic LRRK2 impacts mRNA translation through negatively regulating miRNA activity [44].

LRRK2 mutations are the most common genetic cause of PD, and are found in patients with typical late-onset familial and sporadic PD [8]. PD directly attributable to LRRK2 mutations is typically indistinguishable from sporadic PD cases, potentially indicating common pathogenic pathways. Nearly 80 variants of LRRK2 gene are associated with PD so far, and most of them represent missense mutations. However, only seven are considered to be pathogenic and are segregated in a Mendelenian fashion. PD-causing mutations are mainly concentrated to the enzymatic GTPase (N1437H, R1441G/C/H), COR (Y1699C), and kinase domains (G2019S and I2020T) (**Fig. 5**).
In particular, G2019S mutation at the conserved Mg++-binding motif in the kinase domain is the most common genetic cause of PD. This mutation explains 1% of patients with sporadic PD, and 4% of patients with hereditary PD worldwide. In fact, the clinical phenotype of patients carrying this mutation is remarkably uniform, and undistinguishable from those patients with sporadic PD, characterized by a slow progression, Lewy pathology, and with a good response with DA treatments [45]. In contrast, in some cases, patients with LRRK2 mutations (R1441C, Y1699C, I2020T) other than G2019S frequently do not have Lewy body pathology, but can exhibit neurofibrillary tau tangles [46]. On the other hand, The G2019S can also be found in unaffected people. In fact, the penetrance of LRRK2 mutations in PD is generally incomplete, thus suggesting the importance of gene-environment interactions, or genetic background that can modulate the penetrance of a given LRRK2 mutation [24].

Recent studies support that most of the LRRK2 mutations are caused by an increase in LRRK2 kinase activity and a decrease in GTPase activity for kinase domain and Roc-COR mutations, respectively, thus inducing cell toxicity and death [47]. In fact, accumulating evidence has described an influence of the GTPase domain on LRRK2 kinase activity, although it is not clear if its effect is mediated either by LRRK2 self-regulation (autophosphorylation of the Roc domain), via phosphorylation of exogenous substrates that affect GTPase activity such as ArfGAP1, or a combination of both [25]. Therefore, a decrease in hydrolysis of GTP to GDP may cause a permanent activity of the kinase domain, thus suggesting a common biochemical effect of both kinase domain and Roc domain mutations in the kinase activity. In particularly, I2020T LRRK2 mutations has been described to increase its kinase activity through stabilization of the active-state conformation, and increased rate of phosphoryl transfer [48]. Moreover, G2019S mutation increases LRRK2 kinase activity, both autophosphorylation and phosphorylation of exogenous substrates, suggesting a gain-of-function of the kinase domain that will eventually exert neuronal toxicity. LRRK2 G2019S expression has been also associated with progressive neurite shortening that leads to gradual cell death in vivo and in vitro [42].
On the other hand, increased phosphorylation rates were observed in Roc domain mutants R1441C/G, supporting the existence of kinase-dependent mechanisms of LRRK2 toxicity. Furthermore, LRRK2 phosphorylates different ribosomal proteins, several of which have shown increased phosphorylation in the presence of G2019S and I2020T LRRK2 [25]. These mutations might increase bulk protein synthesis, thus leading to a depletion of valuable energy stores, inducing neuronal stress through an excess of the protein/degradation machineries, thus leading to the failure of overall protein quality control. In addition, there is a reported increase of cancer risk of patients carrying the G2019S mutations, given the fact that excess protein synthesis can result in the activation of certain oncogenic pathways [25].

b) Autosomal recessive forms of parkinsonism.
Nowadays, autosomal recessive PD (AR-PD) with homozygous or compound heterozygous mutations has been associated in four genes that include *PARK2* (parkin), PTEN induced putative kinase 1 (*PINK1*), *DJ-1* and *ATP13A2*. These genes are unequivocally associated with heritable, levodopa-responsive parkinsonism with early age at onset and, generally, no atypical signs. The penetrance of recessive genes is also age-dependent, and only the expression of the phenotype might simply be delayed [8]. Moreover, mutations in the encoding protein glucocerebrosidase (GCase) causes the lysosomal storage disorder Gaucher Disease, which has also been associated with a high risk in developing LB pathology and parkinsonism [49].

Parkin.
Parkin is an ubiquitin E3 ligase, primarily localized to the cytoplasm, which tags proteins through a process called ubiquitylation that leads to proteasomal degradation [50]. In addition to this, Parkin has been also reported to regulate mitochondrial quality control, by activating mitophagy and mitochondria biogenesis [51]. Parkin is suggested to exist in an autoinhibited state, and its activation is due to either its translocation to the mitochondria or association with its substrates [52].
Parkin is a 456-aminoacid protein that contains an N-terminal ubiquitin-like (UBL) domain, followed by three RING (Real Interesting New Gene) finger domains, separated by a 51-residue IBR (In-Between-Ring) domain in the C-terminal part (**Fig. 6**) [8].
Mutations in the PARKIN gene are the most frequent described cause of early-onset PD (<40-50 years), accounting for 10-20% of the cases worldwide and 50% of recessive familial forms [53,54]. To date, more than 170 different mutations have been described throughout the large sequence of this gene (1.35 Mb), including deletions, insertions and point mutations [55], that for the most part lead to a loss of parkin's catalytic activity [51]. Importantly, around 50% of parkin mutation carriers have exon rearrangements that, in the heterozygous state, are not detectable by sequencing alone [56].

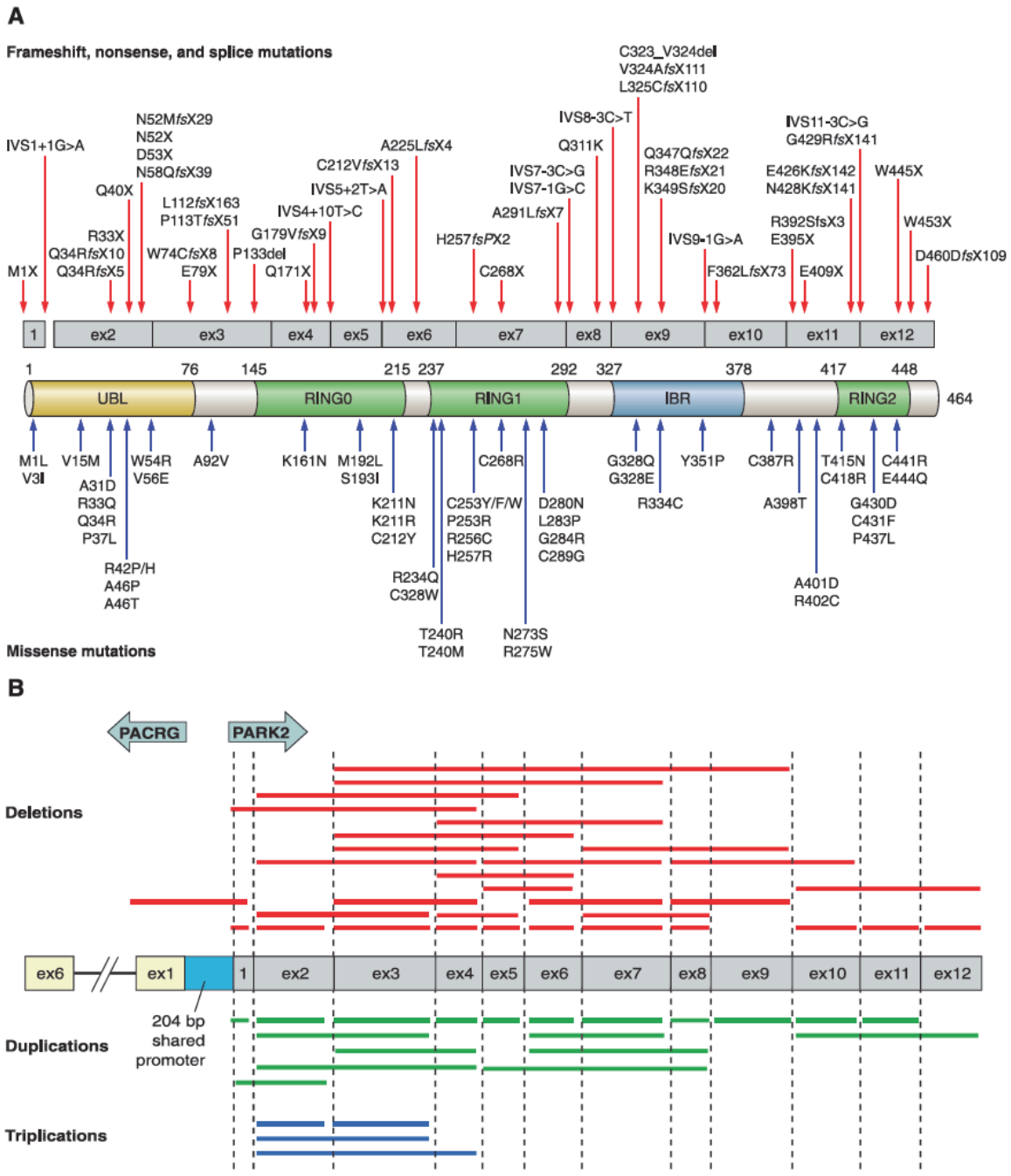

Figure 6. Schematic representation of *parkin* in the transcript level and the functional domains of the Parkin protein.

More than 170 different mutations have been described, comprising:
A) Pathogenic frameshift mutations, insertions and point mutations.
B) Missense mutations, exonic deletions, exonic duplications and triplication (from Corti et al., 2011 [8]).

Pathologically, PARKIN mutations carriers develop a clinical phenotype similar of that of sporadic patients, associated with loss of A9 DA neurons, but also a number of specific clinical features. In addition to an earlier age at onset, they have a relatively benign disease course, with slower disease progression, a better response to low doses of levodopa, but complicated signs with early motor fluctuations and the development of dyskinesias [8]. Interestingly, only half of the patients carrying Parkin mutations show LB formation [57].

As aforementioned, most of Parkin mutations are associated with a loss of function of the protein, implying the disruption of its E3 ligase activity or its interaction with E2 enzymes, provoking an accumulation of parkin substrates [24]. More interestingly, in addition to mutations impairing parkin's function, its enrichment with cysteines makes it prone to oxidative and nitrosative attack. In fact, parkin is inactivated by post-translational modifications, such as nitrosative, dopaminergic, and oxidative stress in sporadic PD, thus suggesting that Parkin dysfunction may be causative of both sporadic and genetic PD [58].
Given that loss of parkin function leads to accumulation of its substrates, identification of these substrates can help to understand the biomolecular mechanisms that lead to neurodegeneration in DA neurons. In fact, two potential pathophysiologic substrates of parkin have been identified recently: PARIS (ZNF746), and AIMP2 [58]. PARIS is a strong pathogenic substrate since it accumulates in familial PD with parkin mutations, sporadic PD, parkin knockout mice and MPTP intoxicated mice [59]. Work of Shin and colleagues showed that under pathological conditions, where parkin is inactivated in PD, PARIS levels accumulate leading to downregulation of transcription factor PGC-1α, thus decreasing mitochondrial biogenesis and accelerating the loss of DA neurons. On the other hand, AIMP2 is a parkin substrate that has been considered a strong candidate since it is present in LB inclusions of PD substantia nigra. Besides, its levels are elevated in the ventral midbrain in parkin KO mice and post-mortem brain from patients with parkin mutations or sporadic PD [60,61]. However, future studies are needed to explore the relationship of PARIS and AIMP2 in the pathogenesis of PD.

PTEN induced putative kinase 1 (PINK1)

Pink1 is a protein kinase, that can be found in the cytosol and also associated in the outer membrane of the mitochondria (OMM), where its kinase domain is thought to face the cytosol [62].
PINK1 is a 581-aminoacid protein with a N-terminal mitochondrial targeting signal (MTS) motif, a putative transmembrane (TM) region, and a serine/threonine kinase domain (**Fig. 7**) [8]. In cooperation with Parkin, Pink1 has been described to promote autophagy of damaged mitochondria, a pathway that is suggested to be aberrant in PD, thus leading to cellular dysfunction and cell death [51].

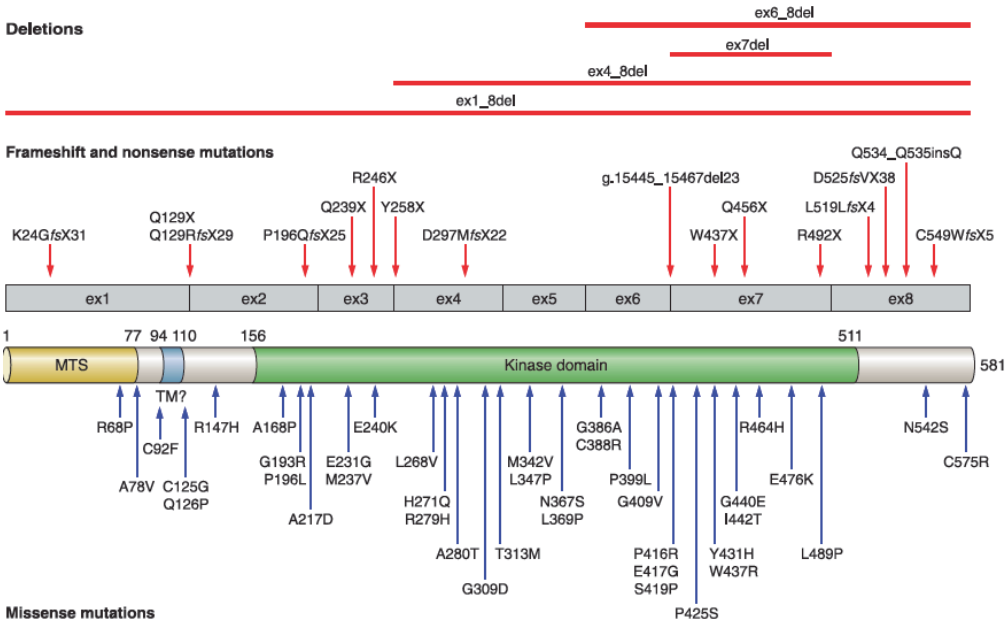

Figure 7. Schematic representation of *PINK1* on transcript level and the functional domains of the PINK1 protein.
Patogenic deletions, including a deletion of the whole gene are represented above the transcript level (red lines), followed by frameshift and nonsense mutations (red arrows). Missesense mutations are represented below the protein scheme (from Corti et al., 2011 [8]).

Homozygous and compound heterozygous mutations in PINK1 are the second most frequent cause of autosomal recessive early-onset of parkinsonism. Most of them are point mutations or small insertions, although large genomic deletions and rearrangements have also been described [63,64]. Mutations in the gene encoding the protein either destabilize the protein, or decrease its kinase activity [65], supporting the hypothesis that mitochondrial dysfunction and oxidative stress may play a role in the pathogenesis of genetic and sporadic PD (Moon et al., 2015).

The clinical phenotype of PINK1-related PD patients is broadly similar to that of parkin or DJ-1 related disease. Specifically, patients with PINK1 mutations tend to have better response to levodopa, a less severe disease and longer mean disease duration. In addition, patients with PINK1 mutations have an earlier onset and more frequent atypical symptoms, such as dystonia at onset, hyperreflexia, dyskinesias, and a higher prevalence of psychiatric disturbances [8].

DJ-1

DJ-1 is a 189-aminoacid single domain protein, member of the ThiJ/Pfp1 family of molecular chaperones (**Fig. 8**) [8]. In the presence of oxidative stress, it translocates from the cytoplasm to the outer mitochondrial membrane and is thought to play a role in neuroprotection under these conditions [66]. Specifically, oxidant-induced modification of DJ-1 at a conserved cysteine residue causes its relocalization to mitochondria, a step that appears to be necessary for its neuroprotection. DJ-1 knock-down experiments in neuroblastoma cells shown mitochondrial depolarization and fragmentations, thus suggesting that DJ-1 acts in parallel to the PINK1/Parkin pathway, maintaining the integrity and function of the mitochondrial pool [67]. DJ-1 is though to protect mitochondria and to mitigate cell death through different ways. First, by direct scavenging of H_2O_2 due to its peroxiredoxin-like peroxidase activity [68]. Second, DJ-1 can function as a redox-sensitive RNA-binding protein and regulates redox-dependent kinase signalling pathways, such as upregulation of the antioxidant glutathione, and the stabilization of Nrf2, a critical regulator of antioxidant gene transcription [69].

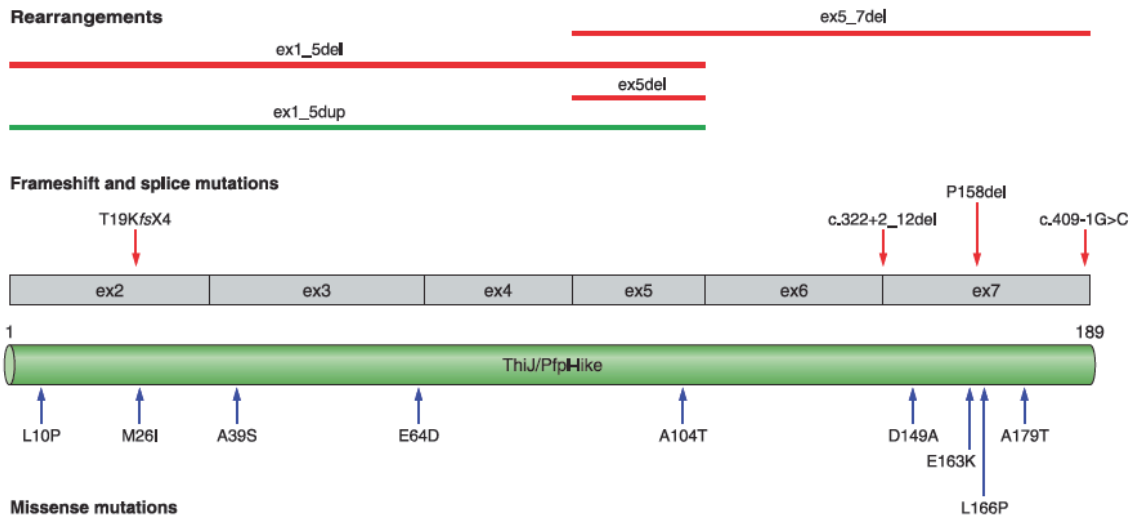

Figure 8. Schematic representation of *DJ-1* on transcript level and the functional domains of the DJ-1 protein.

Rare deletions (red lines) and duplications (green lines) are represented above the transcript scheme, followed by frameshift and splice mutations. Missense mutatinos are represented below the protein scheme (from Corti et al., 2011 [8]).

Only 1% of early-onset PD accounts for mutations in DJ-1. Mutations in this gene include large homozygous deletions, homozygous missense mutation L166P, missense mutations in coding and promoter regions, frame-shift and splice-site mutations, and also exonic deletions have been found in some populations [8]. Mutations in DJ-1 destabilizes the protein, provoking a rapid proteasomal degradation, that is thought to interfere with its neuroprotective mechanism.

The DJ-1 phenotype is also characterized with early-onset and slow disease progression, and closely resembles that of patients with parkin and PINK1 mutations. However, little is known about genotype/phenotype correlations due to the small number of DJ-1 patients.

Lysosome type 5 P-type ATPase (ATP13A2)

ATP13A2 is a large transmembrane protein with putative ATPase acitivity, located in the lysosomes. ATP13A2 has been been associated with Kufor-Rakeb Syndrome, a recessive inherited atypical motor disorder [70], characterized by a levodopa-responsive juvenile parkinsonism, with akinesia, supranucelar gaze palsy, pyramidal signs, dementia, and progressive brain atrophy. Although little is known about its function, ATP13A2 is localized across endosomal and lysosomal membranes and functions as a cation pump. ATP13A2 loss of function was shown to increase neuronal sensitivity to zinc and impaired lysosomal function leading to α-synuclein accumulation [71]. Seven missense mutations in this gene have been identified [72]. Interestingly, ATP13A2 mRNA levels in the substantia nigra of patients with classical late-onset PD were found ~10fold higher than in control brains [73].

Glucocerebrocidase (GBA1)

Only <10% of all PD cases account for rare forms of PD that follows Mendelian inheritance, representing 2% of late-onset and 50% of early-onset familial PD. However, Genome-wide association studies (GWAS) in PD have demonstrated a number of additional significant genetic associations with the disease. Probably the most exciting of all these genetic associations with PD, is the identification that mutations of the glucocerebrocidase gene (GBA1) are associated as a significant risk factor for developing PD [74].

The lysosomal enzyme glucocerebrocidase (GCase) is encoded by the GBA1 gene, which is located in the chromosome 1q21. It has 11 exons, 10 introns and is 7.6 kb in total, with a 16kb downstream nearby 5.6 kb pseudogene [75]. GCase functions by metabolising glucocerebrocidase to glucose and ceramide. Mutations in GBA1 provoke reduced GCase activity, causing the autosomal recessive lysosomal storage rare disorder Gaucher disease (GD) [76]. Almost 300 GBA mutations have been identified in patients with GD: point mutations, insertions and deletions, as well as complex alleles derived from the recombination or gene conversion between the GBA gene and its highly homologous pseudogene that represent ~20% of the pathogenic mutations in GBA (**Table 2**) [77]. The proportion of PD patients that carry GBA1 mutations is estimated to be between 5-10%, however this range may be underestimated in some populations. Interestingly, Gaucher patients and asymptomatic heterozygous gene carriers are recognised to be almost equal at risk of developing PD [74]. Thus, GBA1 mutations represent the most important risk factor for PD identified to date, being even more common than other PD associated genes such as LRRK2 or SNCA.

Carriers of GBA1 mutations with PD are clinically and pathologically undistinguishable from idiopatic PD without GBA1. PD-GBA1 exhibit clinical features related to early-onset, levodopa-responsive PD, experiencing hallucinations and symptoms of cognitive decline or dementia. The pathology of GBA1-PD patients appears to be identical to that of idiopathic disease, characterized widespread and abundant α-synuclein pathology and prominent diffuse Lewy body-type pathology in the neocortex [78].

Specifically, the presence of a mutation in GBA1 is directly associated with reduction of the GCase activity, although the degree of this varies between mutation. Whereas homozygous Caucher patients may have <1% residual activity, heterozygous carriers may have 50-60% residual activity, depending on the mutation [74].

The loss of activity is not induced by decreased transcription, but associated with decreased protein levels of GCase. Specifically mutant GCase protein it has been reported to be trapped in the endoplasmic reticulum (ER), thus triggering the unfolded protein response and ER-associated degradation (ERAD), which are found to be increased in the GBA1 brains [79].

Study:	Population	Mutations screened	Neurological disease	N affected	N control	% Affected	% Control	Common mutations/ phenotype:
Asselta et al. (2014)	Italian	Exon 9-10	PD, DLB, CBD, PSP	2766 total 2350 PD 29 DLB 118 MSA 100 PSP 34 CBD 135 undefined Parkinsonism	1111	4.5% PD 13.8% DLB 0.85% MSA 2.0% PSP 0.0% CBD 3.7% undefined Parkinsonism	0.63%	p.N370S, p.L444P
Mitsui et al. (2015)	Multiple	GD linked *GBA* variants	MSA	574 Japanese, 223 European, 172 North-American	900 Japanese, 315 European, 294 North-American	Japanese: 1.65% European: 1.35% North-American: 2.91%	Japanese: 0.89% European: 0.63% North-American: 0.34%	Linked to MSA-C p.R120W, p.G202R, p.F213I, p.N370S, p.G377S, p.D409H, p.L444P, p.L444R, RecNciI
Clark et al. (2015)	North-American, Ashkenazi Jewish	GBA exons	LBD ADLBV AD	59 LBD 68 ADLBV 71 AD	33	47.5% LBD 23.5% ADLBV 8.5% AD	3%	p.R496H p.R463C p.L444P p.D409H p.N370S p.T369M P.E326K p.H255Q p.W184R c.84GGIns
Nalls et al. (2013)	Multiple	Whole GBA gene	DLB, PDD	721 DLB 151 PDD	1962	7.50% DLB 5.96% PDD	0.87%	p.N370S, p.L444P
Srulijes et al. (2013)	European	p.N370S p.L444P (94%) GBA exons (6%)	MSA	183 MSA-P 97 MSA-C 64 MSA-non specified	325	0.58% MSA	0%	p.N370S p.T369M
Sun et al. (2013)	Chinese	p.L444P	MSA, ET	54 MSA 109 ET	657	0%	0.15%	–
Tsuang et al. (2012)*	North-American	GBA exons	DLB, DLB-AD, AD	80 DLB 231 DLB-AD 251 AD	381	8.8% DLB 4.8% DLB-AD 1.2% AD	1%	p.N370S p.E326K p.T369M
Jamrozik et al. (2010)	Polish	p.N370S, p.L444P	MSA, CBD PSP	34 MSA-P 31 MSA-C 34 PSP 5 CBD	0	0% MSA-P 0% MSA-C 0% PSP 0% CBD	–	–
Clark et al. (2010)	Ashkenazi Jewish	GBA exons	ET	117	62	7.7%	4.8%	p.N370S p.R469H p.E326K p.R44C
Clark et al. (2009)	North-American	GBA exons	DLB AD	95 DLB 60 AD	32	28% DLB 10% AD	3%	p.N370S p.E326K p.T369M
Farrer et al. (2009)*	North-American	GBA exons	DLB	101	99	7.9%	1%	IVS 2 + 1 p.H255Q c.1263-1317del p.E326K
Nishioka et al. (2009)	Caucasian	GBA exons	DLB	59 DLB	99	6.8% DLB	1.0%	p.N370S p.L444P p.A292T p.E388K
Segarane et al. (2009)	British	GBA exons	MSA	108 MSA	259	0.92% MSA	1.17%	p.R262H

TABLE 2. Summary table of the frecuency of GBA mutations in parkinsonian syndromes and other neurodegenerative diseases.

Abbreviations: AD = Alzheimer's disease; ADLBV = Alzheimer's disease variant with Lewybodies; CBD = corticobasal degeneration; DLB = Lewy body dementia; ET = Essential tremor; LBD = Lewy Body diseases; MSA = Multiple system atrophy; MSA-C = Multiple system atrophy cerebellar type; MSA-P = Multiple system parkinsonian type; PD = Parkinson's disease; PDD = Parkinson's disease dementia (from Barkhuisen et al., 2015 [77]).

In addition, there is now evidence to support an age-related decline of GCase activity in the ageing brain that may act as predisposing factor for α-syn accumulation and PD [49].

The link between the inverse correlation with GCase and SNCA levels has been demonstrated both in vivo and in vitro in different studies. Some have found that overexpression of mutant GBA1 increased SNCA levels [80]. Moreover, accumulation of SNCA has been seen in cortical neuronal cultures from GBA1 knockout mice and in the brains of these mice [81]. In fact, an analysis of Lewy Body density load in PD brain found an inverse relationship with GCase activity [82]. However, the molecular and biochemical basis for the interaction between both proteins has yet to be elucidated.

1.3. Mechanisms involved in PD pathogenesis.

As aforementioned, little is known about the exact mechanisms leading to A9 DA neuron death in PD. it is suggested that PD occurs when several mechanisms such as protein aggregation and spreading, mitochondrial activity, autophagy or degradation via proteasome become dysregulated in a complex chain of events, triggered by the combination of an environmental influence and/or a PD-specific mutation susceptibility.

1.3.1 Pathogenic protein aggregation and spreading.

It is in 1912 when Friedrich Heinrich Lewy first described the inclusion bodies, which would become the main histopathological hallmark of PD, later reffered to as "Lewy bodies" and "Lewy neurites" by Konstantin Nikolaevich Tretiakoff in 1919. The composition of those inclusion would remain unknown until 1997, when two key discoveries were made, with a substantial effect on PD research: first, the identification of point mutations in the gene encoding α-synuclein (SNCA) in familial forms of PD [83], and second, the finding that aggregated forms of misfolded α-synuclein are the major fibrillar component of Lewy body pathology, among other numerous proteins, such as ubitiquin, parkin and other neurofilaments [13].

To date, the mechanisms regarding the initiation of α-synuclein misfolding and aggregation, the cellular specificity, and the progression of α-syn pathology in synucleopathies remains poorly understood. However, accumulative evidences have strenghten the concept that α-synuclein may be transmissible from cell to cell, acting as a self-propagating pathogenic protein (prion-like protein), thereby contributing to the progression and extension of PD. This hypothesis stems from two sets of discoveries. First, as aforementioned, Braak staging hypothesis suggested an ascending LB formation across the brain, following a caudo-rostral pattern, thereby explaining the clinical prodrome and progression of most of sporadic forms of PD [22]. Following this hypothesis, further evidence from three independent groups reported that embryonic mesencephalic neurons grafted into the striatum of some PD patients develop LB-like structures, more than 9 years after brain surgery, thus speculating that misfolded α-synuclein can be transmitted between cells, thus initiating aggregation in neighbouring neurons [84–86].

The exact molecular mechanism involved in α-synuclein aggregation and how aggregates can cause selective DA neuron loss is poorly understood (**Fig. 9**). On one hand, wild-type α-synuclein has shown a spontaneous tendency to form amyloid fibrils in vitro, a feature that has been accentuated in the A53T, A30P and E46K mutant variants of α-synuclein [87]. On the other hand, as mentioned in previous chapters, there is a dosage effect directly related between α-syn cytotoxicity and its overexpression, due to the effect of supernumerary copies of the SNCA gene [88]. Cellular dysfunction might be related to conformational changes of α-synuclein, although controversy have risen regarding which of the forms are more toxic than others. Although some studies claimed a direct correlation between fibrillar inclusion bodies and neurodegeneration[89] several others have aimed that oligomeric intermediates causes cellular dysfunction and cell death [90]. Remarkably, Winner and colleagues established a direct in vivo demonstration of the toxicity of α-synuclein oligomeric forms in murine models. They developed recombinant α-synuclein variants able to accelerate fibril-promoting variants, as well as others able to form stable oligomer forms. Lentivirus encoding of these α-syn variants were injected in the substantia nigra of adult rats. Specifically, high loss of DA neurons was only found in the mutants that favoured α-syn oligomerization, compared with the mutants that formed fibrils more quickly. In addition, compared to fibril forms, α-syn oligomer forms were found to bound strongly to cell membranes, thus confirming the role of this oligomeric forms in membrane disruption, cellular dysfunction, and cell death. Therefore, this study demonstrated a direct link of membrane-associated α-syn oligomers and DA neurodegeneration in a murine model, thus reinforcing the concept that oligomeric prefibrillar α-syn, rather than its fibrils, may represent the pathogenic species of α-syn in PD [91].

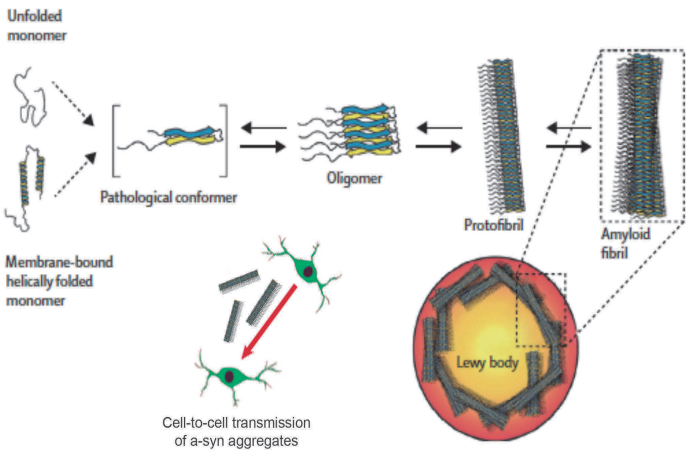

Figure 9. α-Syn aggregation in PD.

α-Synuclein exists in various conformations but it has predominantly two strucural isoforms that can undergo substantial structural changes, resulting in the formation of β-sheet-rich assemblies, that can aggregate into several types of small oligomeric species that remain stabilised by β-sheet interactions, and then into higher-molecular-weight insoluble protofibrils, which can polymerise into amyloidogenic fibrils resembling those identified Lewy bodies. α-Syn aggregates are thought to be transmitted from one DA neuron to another in a prion-like manner (modified from Dehay et al., 2015 [92])

On the other hand, as it had been shown with in vitro recombinant α-syn preformed fibrils [93], 2012), Recasens and colleagues demonstrated that injection of nigral LB containing pathological α-syn, that was previously purified from postmortem PD brains and subsequently inoculated into either the SN or striatum of C57BL/6J mice and rhesus monkeys, was enough to initiate a PD-like pathological process characterized by diffuse cytosolic and presynaptic accumulations of pathological α-synuclein. Importantly, LB-induced pathogenic effects required both human α-syn present in PD-derived LB extracts and host expression of α-syn. Specifically, exogenous α-syn was quickly internalized within host neurons and triggered the pathological conversion of endogenous α-syn, thus resulting in a progressive nigrostriatal neurodegeneration in both mice and macaque monkeys [94]. However, the mechanism of this pathological conversion is not clear whether if it starts directly through a seeding prion process [95], or rather indirectly as a general response to cellular stress, such as deleterious microglial response, thus contributing to the overall progression of the disease [92].

Moreover, the native state of α-synuclein is extensively under discussion, as it has been found either as a folded monomer [96], or as a predominantly helically folded tetramer [97,98]. Taken together, this data suggests that α-syn may exist in various conformations and oligomeric states in a dynamic equilibrium, which can be modulated by external factors, post-translational modifications and disease-related mutations, thus accelerating the formation of toxic forms of the protein. At this point, toxic forms of oligomeric α-synuclein can lead to the disruption of different cellular components, affecting vesicle trafficking, neurotransmission release, and the integrity and functionality of several organelles (**Fig. 10**) [92].

Interestingly, several studies have shown that the presence of nitration [35], and oxidation of α-synuclein derived from oxidised derivatives of dopamine increase, decrease the propensity of α-syn to form fibrils and stabilise oligomers, and might thus enhance toxicity [99]. Moreover, it has been shown that phosphorylation of α-synuclein at Ser129 promotes fibril formation [100]. In conclusion, the existence of toxic versus non-toxic α-synuclein strains could underlie the differences in disease propagation between individuals, cell types, and synucleopathies, and the formation of LB may represent a protective form of the protein thereby decreasing the content of relevant toxic species of α-synuclein [92].

Moreover, although in not all the cases, an interaction of LRRK2 with α-syn has been accepted. Evidences for a role of α-syn in LRRK2 toxicity come from studies on human dopamine neuron cultures demonstrating increase α-syn levels in several mutated forms of LRRK2 PD patient iPSC-derived DA neurons [101,102].

There are two hypotheses that can explain this connection. First, that pathogenic LRRK2 stimulates general mRNA translation, thus leading to increased translation of α-syn mRNA, which would account for synucleopathies seen in PD patients carrying LRRK2 mutations.

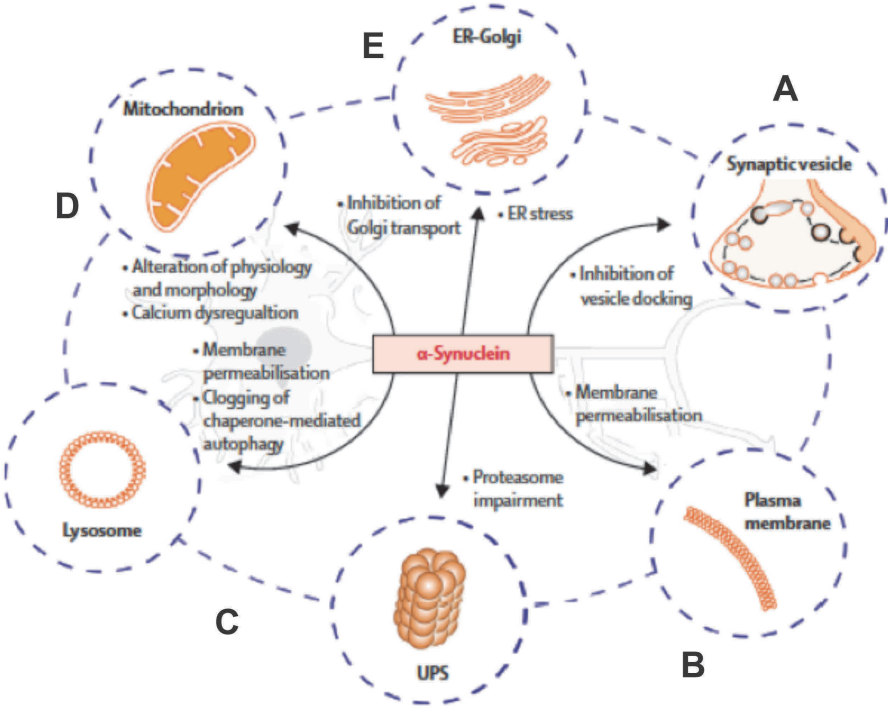

Figure 10. Schematic representation of interaction between the toxic oligomeric forms of α-syn and the affected cellular compartments.

A) Disruption of the normal function of α-syn in neurotransmission release, where it may act as a negative regulator of DA release; B) Strong interaction with organelles and plasma membranes through pore formations or perforations, that can dysregulate calcium and cation homeostasis; C) Impairing the efficiency of some protein-degradation mechanisms; D) Impairing mitochondrial structure and complex I activity, as well as mitochondrial dynamics and mitophagy; E) disrupting ER-Golgi vesicular transport, which results in ER-stress (Modified from Dehay et al., 2015 [92]).

Second, pathogenic LRRK2 may promote oligomerization of α-syn, which can impair its degradation through the chaperon-mediated autophagy [103,104]. However, LRRK2 and α-syn are not connected in invertebrate models, mainly because α-syn is not expressed, although they do manifest LRRK2 toxicity. Therefore, given that there is an absence of Lewy bodies in some PD patients with mutations in LRRK2 or other familial PD genes, altogether bolsters the hypothesis that LRRK2 toxicity can be independent of α-syn [25].

1.3.2. Mitochondrial dysfunction

Almost since the dawning of PD research, association with mitochondria and PD was the first link to be described, when people intoxicated with inhibitors of the mitochondrial complex I (MPTP) developed acute parkinsonism, thus revealing severe lesions in the brain, particularly in the nigrostriatal system [105]. Indeed, some animal models are based in the induction of brain lesions by the administration of mitochondrial inhibitors, such as MPTP, paraquat, rotenone, in order to generate PD-related phenotypes [106].

Mitochondrial dysfunction has emerged as one of the key mechanisms underlying the pathogenesis of both sporadic and familial PD. Two decades ago, it was already known that the activity of the mitochondrial respiratory complex I (NADH-quinone oxidoreductase) is reduced in the substantia nigra of PD patients [107]. Specifically, correlation between reduced electron transfer rates, with increased levels of protein carbonyls (oxidative modification of proteins) in several catalytic subunits of complex I were found in parkinsonian brains, suggesting that excessive oxidative damage of complex I subunits can lead to its dysfunction [108]. Interestingly, compared with other brain areas, A9 DA neurons in the substantia nigra appear to be more vulnerable to impairments of complex I activity, probably due to lower mitochondria

content, and increased levels of reactive oxigen species (ROS) generated as a result of dopamine metabolism and iron content [109].
To date, strong evidence from the characterization of the contribution of PD related genes suggests a causal involvement of mitochondrial dysfunction and oxidative stress in PD pathogenesis. Among these genes, the gene encoding E3 ubiquitin ligase Parkin, the mitochondrial serine-threonine kinase Pink1 and the chaperon DJ-1 have been considered to have prominent functions in mitochondrial homeostasis. Hence, both genetic mutations and disease-specific post-translational modifications in these PD-related proteins are linked to PD pathogenesis, thus underlying that some pathogenic mechanisms from sporadic and familial PD can converge [110].

Mitochondria are dynamic organelles, with their morphology constantly being modified by fission and fusion events, all while they are being shuttled throughout the cell. The balance between biogenesis and mitophagy is crucial to adjust the bioenergetic demands of the cell, while minimizing the accumulation of damaged mitochondria.
In particular, Parkin has key functions in mitochondrial homeostasis. First, in normal conditions Parkin ubiquitinates PARIS, a transcription repressor of PGC1α, thus enabling the activation of mitochondrial biogenesis pathways [59]. Specifically, Parkin is present in mitochondria of proliferating cells, enhancing transcription and replication of mitochondrial DNA (mtDNA) [111], thus suggesting a recruitment of Parkin to mitochondria in order to promote mitochondrial biogenesis during cell mitosis (**Fig. 11A**). Indeed, a clear correlation has been found between the occurrence of PD and a decrease in the activity of PGC1α [112]. On the other hand, recent evidences suggests that Parkin operates together with PINK1 in a common genetic pathway in maintaining mitophagy and mitochondrial integrity, with PINK1 acting upstream of Parkin [113–116]. In fact, loss of function of either PINK1 and Parkin in Drosophila results in altered mitochondrial dynamics and impaired mitochondrial function in DA neurons, suggesting that the balance of fission to fusion is pushed towards fusion in these mutants [110].
In normal conditions, PINK1 is localized in the outer membrane of the mitochondria (OMM), where it is cleaved in a voltage-dependent manner to a smaller fragment, and rapidly degraded. However, in depolarized mitochondria no cleavage occurs and PINK1 is sequestered in the OMM, triggering a kinase-dependent process that will translocate parkin to the mitochondria. Once recruited to mitochondria, Parkin ubiquitinates several OMM proteins, including Mitofusin 1 and 2 (Mfn1, Mfn2), voltage-dependent anion channels (VDACs) or Miro. Subsequently, the parkin ubiquitination process recruits the autophagic adapter protein P61/SQSTM1, thus allowing the recruitment of other components of the autophagy machinery, and preventing the fusion of damaged mitochondria with other healthy mitochondria (**Fig. 11B**). Therefore, PINK1/Parkin pathway is thought to promote mitochondrial fission rather than mitochondrial fusion [110].

Nevertheless, although the evidence points to the PINK1/Parkin pathway affecting fission and fusion, it is not well understood how this could cause specific DA neuron degeneration. On one hand, the fusion of two damaged mitochondria that harbor mutations in different genes can allow functional complementation to occur by the diffusion of RNA and protein components across the newly formed mitochondria, thus rescuing the mitochondrial function. However, point mutations and deletions caused by the vulnerability of mtDNA to ROS as a result of ATP production, leads tu accumulative lesions that with aging can expand in the cellular pool of mitochondria, resulting in impaired mitochondrial function in PD, such as decreased activity of complex I, IV, mtDNA deletions, as well as the presence of swollen and dysfunctional mitochondria inside neurons [51].
On the other hand, mitochondrial fission allows the autophagic degradation of damaged mitochondria, which often leads to the segregation of damaged components to one of the resulting mitochondria. Indeed, as aforementioned, fission is a prerequisite for mitophagy [117].

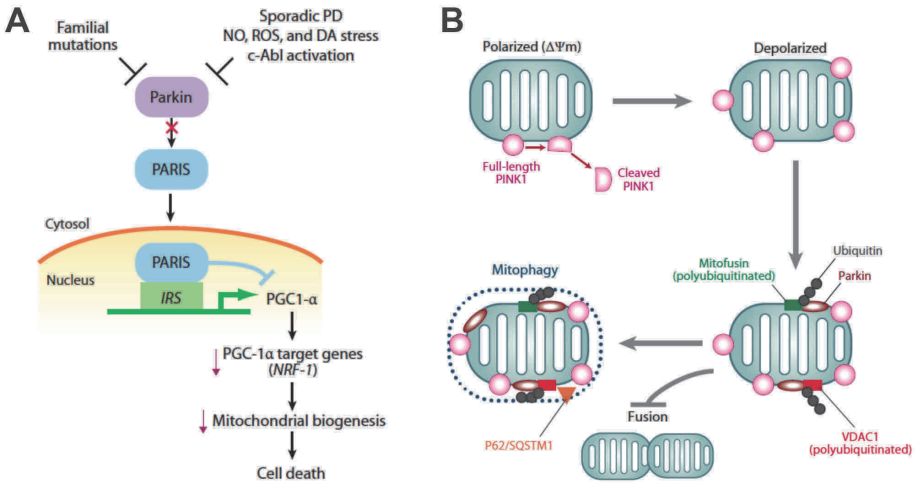

Figure 11. Parkin and PINK1 and their interaction related with mitochondrial homeostasis.

A) Parkin controls the expression of PGC1**α** through PARIS. PARIS is a transcriptional repressor that selectively downregulates PGC1**α** by binding to insulin response sequences (IRSs) in the *PGC1**α*** gene promoter. This leads to downregulation of NRF-1, which transcriptionally controls mitochondrial biogenesis, resulting in DA neuron degeneration. Parkin loss of function is either caused by mutations in familial PD or triggered by nitrosative, oxidative or DA stress in sporadic PD.

B) A model of interaction of PINK1 and parkin in regulating mitochondrial turnover. In depolarized mitochondria, Pink1 is not cleaved and remains in the mitochondria where it recruits parkin to mitochondria. Once localized to mitochondria, parkin polyubiquitinates mitofusin and voltage-dependent anion channel 1 (VDAC1). This ubiquitination recruits the autophagic adapter protein P62/SQSTM1, which in turns triggers mitophagy of dysfunctional mitochondria, thus preventing fusion of the damaged mitochondria with other healthy mitochondria. (modified from Büeler et al., 2009 [110])

In addition, fission is also required for normal respiration and ATP synthesis [118] and favours the transport of mitochondria to synapses to promote synaptogenesis [119]. In fact, dysregulation of mitochondrial transport may be implicated in PD. Given the increased requirements of neurons for mitochondrial transport and how far neurites extend from the cell soma, loss of either PINK1 or parkin could provoke a suboptimal mitochondria to be shuttled to axon terminals, undermining local energy production.

Moreover, different properties have been abscribed to DJ-1. As aforementioned, the redox-regulated chaperone DJ-1 is present mostly in the cytosol, but it is rapidly translocated to the mitochondria during conditions of oxidative stress, thus confering neuroprotection in different ways [66,120,121]. On one hand, DJ-1 can prevent misfolding of different subunits of mitochondrial respiratory complexes, in particular complex I, since loss of DJ-1 is associated with increased sensitivity to complex I inhibitors. Alternatively, under oxidative stress conditions, DJ-1 dissociates from mRNA related to glutathione metabolism, mitochondrial proteins and members of the PTEN/PI3 kinase cascade, restoring translation to full activity [122]. On the other hand, its chaperon role is thought to prevent also protein misfolding. For this reason, DJ-1 may prevent oligomerization and aggregation of α-synuclein in an oxidation-dependent manner [123], thus probably preventing α-syn toxicity.

All in all, is substantially evident that DJ-1, Pink1 and parkin share similar function in preserving mitochondrial integrity, although DJ-1 does not act in the same pathway as PINK1 and parkin, despite acting in a parallel pathway with common effects (**Fig. 12**). Therefore, the role of these three proteins against oxidative stress is important in those neurons, such as DA neurons, which need a strict mitochondria quality control, necessary for their high energetic demands.

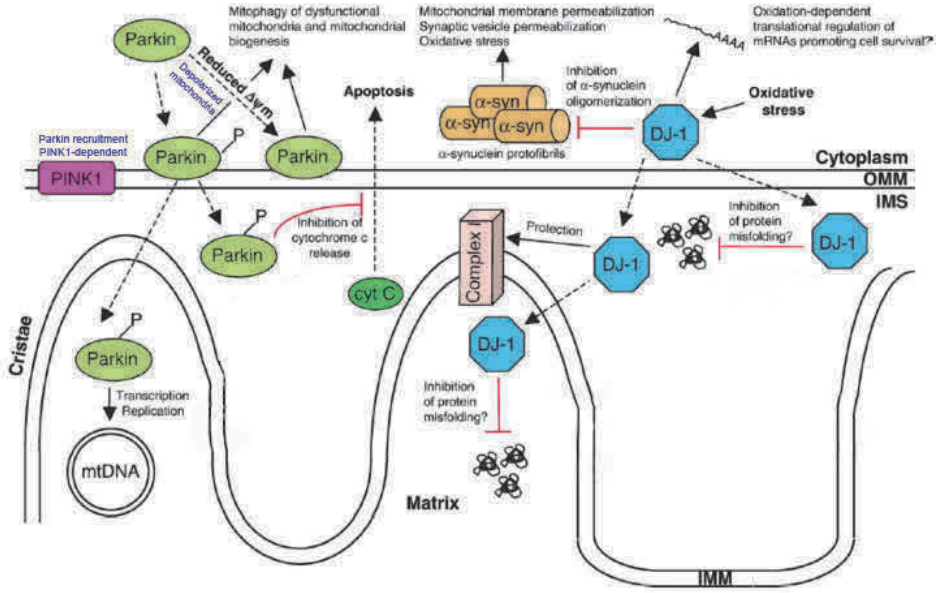

Figure 12. A simplified model for the dynamic regulation and maintenance of mitochondrial integrity by PINK1, Parkin, and DJ-1.

Pink1 controls the localization and activities of its target (effector) proteins, such as Parkin, by direct or indirect phosphorylation. Phosphorylation of Parkin triggers its translocation from the cytosol into mitochondria, where it exerts its mito-protective effects. As well, oxidative stress-induced mitochondrial dysfunction triggers the rapid and specific translocation of cytosolic Parkin to depolarized mitochondria, consequently promoting mitophagy. Other important functions of Parkin are; to reduce cytochrome C release, thus suppressing apoptotic stress-activated protein kinase pathway; to stimulate mitochondrial biogenesis; and possibly to promote mitochondrial fission via the ubiquitination of mitochondrial fission and/or fusion proteins. On the other hand, DJ-1 protects mitochondrial complex I against oxidative stress-mediated activation. Moreover, as a chaperone, DJ-1 may prevent the misfolding and aggregation of oxidized mitochondrial proteins, as well as the aggregation and toxicity of α-synuclein. As well, DJ-1 may regulate the translation of mRNA coding for proteins required for glutathione metabolism, mitochondrial function and cell survival in an oxidation-dependent manner (modified from Büeler et al., 2009 [110]).

The role of the interaction between α-synuclein and mitochondria still remains poorly understood. However, association between α-synuclein and mitochondria are known to be highly dependent on membrane lipid composition. On one hand, alterations in membrane lipids and reduced activities of the electronic transport chain (ETC) complexes I and III were observed in mitochondria from mice lacking binding of α-synuclein [124]. Indeed, it is not surprising that α-syn could have a physiological role in mitochondria since other evidences have demonstrated that α-syn binding to mitochondria brings stability to the ETC complexes, and that its antioxidant capacity is completely dependent on its associations with cellular membranes [125].

On the other hand, hippocampus, striatum and substantia nigra has shown to contain several-fold higher mitochondrial α-synuclein content in PD patients when compared to healthy individuals, thus suggesting that mitochondrial accumulation of α-synuclein in PD contributes to the known mitochondrial complex I defects of the disease [126]. It is suggested that the natural capacity of α-synuclein to interact with cellular membranes might be modified via post-translational modifications like phosphorylation, nitration or oxidation, thus causing increased aggregation and toxicity and losing its physiological function in this organelle (**Fig. 13**) [96]. Indeed, α-synuclein protofibrils are known to form annular pores in membranes, suggesting that permeabilization of intracellular membranes, including synaptic vesicles and mitochondria, may be involved in α-synuclein toxicity [127,128].

Moreover, α-synuclein has been shown to bind to the PGC1a promoter under conditions of oxidative stress, thus contributing to a vicious cycle, where interaction of α-syn with PCG1a,

impairs mitocondrial biogenesis pathways, and increases accumulation of defective mitochondria and susceptibility to α-syn toxicity [129]. It has been further shown that α-syn inhibits the fusion of mitochondria and to alter the structure of their crests [130,131], therefore the resulting mitochondrial membrane depolarization, together with a smaller size make them prone to become targets for mitophagy [132], thus negatively contributing to the overall energy demanding of the neuron. In addition, α-syn impairs axonal transport and delivery of mitochondria, as it has been shown to interact with motor proteins like kinesin [133]. Given that mitochondrial transport within DA axons is slower than in other neuronal cell types [134], impairing transport in DA neurons can have a significant impact, since their long-projections have a high energetic demand, making them vulnerable to the α-syn pathology.

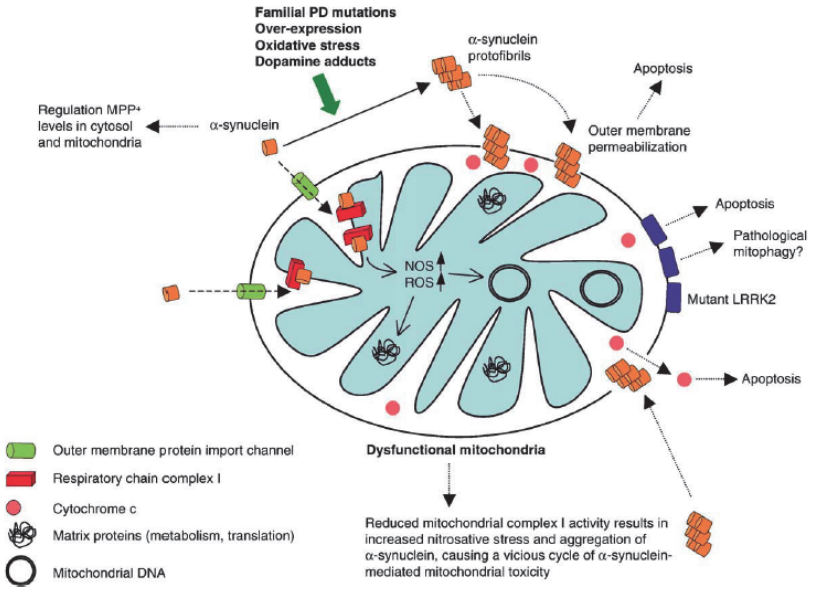

Figure 13. Contribution of α-syn an LRRK2 in mitochondria dysfunctionality.

α-Synuclein controls synaptic vesicle dynamics and may regulate mitochondrial membrane lipid composition and complex I activity. Familial PD mutations, oxidative stress (nitration) and dopamine adducts accelerate the formation of toxic α-synuclein protofibrils, which may permeabilize the outer mitochondrial membrane, resulting in the loss of the mitochondrial membrane potential, cytochrome c release and apoptosis. Increased mitochondrial levels of α-synuclein in PD have been associated with reduced complex I activity and oxidative stress. Therfore, mitochondrial dysfunction may result in further oxidative stress that promotes aggregation of α-synuclein, generating a vicious cycle of α-synuclein-induced mitochondrial damage. On the other hand, LRRK2 distributes diffusely in the cytoplasm, but about 10% of the protein is associated with the outer mitochondrial membrane. Over-expression of familial mutant LRRK2 proteins causes caspase- and Apaf-1-dependent apoptosis. In addition, increased autophagy associated with expression of G2019S LRRK2 may result in excessive (pathological) degradation of mitochondria (modified from Büeler et al., 2009 [110]).

Furthermore, a although the physiological role of LRRK2 is not yet fully understood, it has been shown that LRRK2's kinase activity mediates mitochondrial fission and fusion dynamics [135,136]. LRRK2 is associated with intracellular membranes, including lysosomes, transport vesicles and mitochondria [41]. In particular, LRRK2 can be associated with the mitochondrial outer membrane, although the function of LRRK2 in relation to mitochondria is presently unclear (**Fig.13**). Transient over-expression of familial PD mutant LRRK2 (G2019S, Y1699C and R1441C) has been shown to induce Apaf-1 required neuronal death, which can be blocked by caspase-inhibitors, showing that mutant LRRK2 causes mitochondria-dependent apoptosis. Moreover, patients with a G2019S mutation have a decrease in mitochondrial membrane potential and ATP deficits. Overexpression of either wild-type or mutant (R1441C or G2019S) LRRK2 causes mitochondrial fragmentation, reduced mitochondrial fusion, and increased Dynamin related protein (Drp1) recruitment to mitochondria by direct interaction with LRRK2 in vitro [25]. Overexpression of G2019S mutant LRRK2 caused neurite retraction and shortening in differentiated neuroblastoma cells, which correlated with increased autophagy [137]. In fact,

increased autophagy may also affect mitochondria, possibly resulting in a deregulated mytophagy in neurites. Besides, LRRK2 G2019S mutation also provokes more sensitiveness to toxins in mitochondria [101,135]. Overall, these evidences may suggest that overactivity of the kinase of LRRK2 due to either gain-of-function mutations or its overexpression might play a role in the phenotypes observed.

1.3.3. Oxidative and Nitrosative stress

Oxidative and nitrosative stress have been shown to be increased in idiopathic and genetic cases of PD. PD patients exhibit high levels of oxidized lipids, proteins and DNA and are also associated with reduced GSH levels [138–140]. Due to the presence of ROS-generating enzymes like Tyrosine Hydroxylase and monoamine oxidase B (MAO-B), DA neurons are particularly prone to oxidative stress. Therefore, it is suggested that the accumulation of reactive oxygen and nitrogen species (ROS and RNS) can affect different pathways that contribute to the pathogenesis of PD (**Fig. 14**).

Oxidative stress can be generated mainly by three mechanisms. First, generation of ROS is an inevitable outcome of oxygen dependent respiration that takes place in mitochondria. Mitochondria generate energy in the form of ATP from macromolecules via Krebs cycle and electronc transport chain (ETC). High energy end products of Krebs cycle, NADH and FADH2, generate a proton gradient through the ETC, across the inner mitochondrial membrane, which drives the oxidative phosphorylation of ADP to ATP by the ATP synthase. However, ROS result when electrons donated by NADH and FADH2 leak from the ETC, mainly from complex I (Lin et al., 2006), thus leading to the partial reduction of molecular oxygen to superoxide (O^{-}_{2}). Mitochondria are protected from this by superoxide dismutase (SOD), which metabolizes superoxide to hydrogen peroxide (H_2O_2), which in turn it can be converted to H_2O and O_2 by catalase. The conversion of O^{-}_{2} and H_2O_2 into non-toxic species is crucial for cell survival, since this toxic forms can react with other molecules to generate additional ROS, such as hydroxyl radicals, that can be extremely toxic to the cell [141].

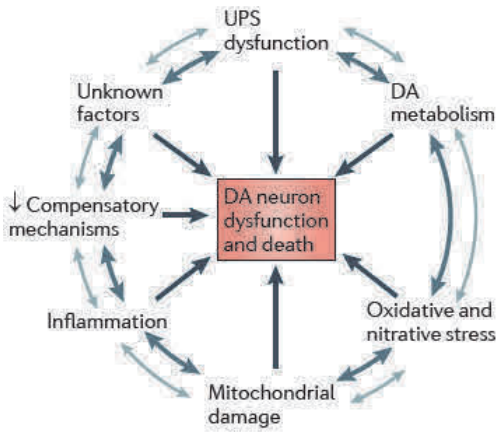

Figure 14. Oxidative and nitrosative stress activates mechanisms that contribute to A9 dopaminergic death.

Dopamine metabolism, inflammation and exicitoxicity contribute to the generation of excessive ammount of ROS and RNS. Excessive amount of oxidatively damaged proteins can overwhelm the proteolytic system and therefore results in the further accumulation of misfolded or aggregated proteins that can compromise the survival of SNc DA neurons. In addition, ROS and RNS can directly affect the performance of proteolytic system by the modification of specific components in the system, specifically affecting the mitochondrial integrity and function, creating a pathogenic feedforward loop that leads to increased protein aggregation and compromised ATP production, which in turn blocks energy dependent stress coping mechanisms, thus leading to dopaminergic neuron cell death (modified from Collier et al., 2011 [26]).

Second, generation of ROS in the process of inflammation acts as a defense mechanism against small pathogens. However, excessive production of ROS can cause a chronic inflammation that can have deleterious effects. Specifically, neuronal loss in PD is associated with chronic neuroinflammation, which is controlled primarily by the activation of the microglia, the major resident immune cells in the brain [142]. Activation of microglia is not only neurotoxic through the production of cell damaging extracellular ROS, but also through the initiation of redox signalling in microglia that amplifies the pro-inflammatory response [143] to astrocytes and oligodendrocytes [144], which eventually would produce modulators of inflammatory that augment microglial activation, chemotaxis and proliferation. Microglial activation has been found with a greater density in the SNpc [145] and in the olfactory bulb of both sporadic and familial

PD patients [146,147], as well as in PD animal models [148,149] and it has been associated with different PD-associated genes like SNCA or LRRK2 [150,151]. Indeed, extracellular α-syn released from neuronal cells is an endogenous agonist for Toll-like receptor 2 (TLR-2), which triggers the activation of the microglial inflammatory responses [150]. Moreover, LRRK2 increases proinflammatory cytokine release from activated primary microglial cells which results in neurotoxicity [152]. In contrast, LRRK2 inhibition it has been shown to attenuate microglial inflammatory responses [151,153].
Third, DA neurons are more exposed to ROS and RNS than other neurons due to the metabolism of DA itself. DA is a relatively unstable molecule in nature that undergoes autooxidation mechanism in the nigrostriatal tract system thereby producing ROS [154]. In addition, the unstored cytosolic fraction undergoes spontaneous or MAO-B-mediated degradation to form toxic DA derivates, such as DA quinones, toxic reactive species that can modify proteins such as α-synuclein and parkin [155–157].

Another major contributor of oxidative stress is the metabolism of nitric oxide (NO). NO is generated in biological tissues by specific nitric oxide synthases (NOS) [158]. NO acts as an important biological signalling oxidative molecule in a large variety of diverse physiological processes like neurotransmission, among others [159]. When the generation of RNS in a system exceeds the system's ability to eliminate and neutralize them it provokes nitrosative stress. Nitrosative stress leads to nitrosylation reactions, which again can modify the structure of the proteins, such as α-synuclein or parkin [35,160–162], thus inhibiting the normal functioning of proteins. In addition, S-nitrosylations have been found to regulate gene transcription, vesicular trafficking, receptor mediated signal transduction, and apoptosis [163].
NO is generated by three isoforms of nitric oxide synthase (NOS): inducible NOS (iNOS), endothelial NOS (eNOS), and neuronal NOS (nNOS). For instance, overstimulation of NMDAR by its ligand glutamate results in excitotoxicity [164]. Specifically, overstimulation of NMDAR results in the influx of Ca^{2+}, which leads to the activation of nNOS [165], that eventually will produce NO, thus reacting with other ROS and forming highly toxic peroxynitrite ($ONOO^-$). Consequently, peroxynitrite will induce cellular damage through protein nitration (i.e. peroxynitrite-induced aggregation of α-syn), lipid peroxidation and DNA fragmentation [166,167].

Oxidative stress is also playing important roles in affecting the normal function of familial PD-related gene products in the process of neurodegeneration. For example, ROS and RNS are known to cause protein misfolding and aggregation. Indeed, nitrated or oxidative damaged protein aggregates are prominent in brain tissues from PD patients [168]. For instance, oxidative damaged α-syn, as well as nitrated α-syn, are more prone to aggregation and therefore it is selectively deposited into the LB. Nitrated α-syn is more resistant to proteolysis and prone to aggregation, and reduced lipid binding and solubility in cells. In addition, nitrated α-syn is more immunogenic, which might explain why increased inflammatory response such as gliosis and T cell activation is common in PD patients [169,170].

α-Syn can undergo other oxidative modifications. One that gained most attention is the addition of DA adduct on α-syn [171]. This modification stabilizes the toxic α-syn protofibrils, and that inhibits from further aggregation into less toxic insoluble fibrils [172]. α-Syn protofibrils would lead to the permeabilization of synaptic vesicles, thus increasing intracellular DA, which could further enhance DA modification of α-syn and consequently, the formation of more α-syn protofibrils. Moreover, toxic forms of α-syn have shown to interact with complex I [126]. Besides, DA conjugated α-syn is resistant to CMA degradation as well as capable of blocking other proteins from degradation via this pathway [173]. Taken together, these studies provide potential pathogenic mechanisms of how wild-type α-syn and oxidative stress can contribute to the neurodegenerative process in PD.

Neurons are metabolically very active as such they depend a lot on the mitochondria energy production in the form of ATP. Any untoved or pathological situation which leads to mitochondrial dysfunction can cause a lot of increase in ROS.
Pathological studies supports that complex I dysfunction is commonly observed in PD patients, suggesting that mitochondrial function can also be affected by ROS [174]. For example, studies have found that oxidative damage such as S-nitrosylation of complex I can inhibit its normal activity [175]. In fact, mitochondrial respiratory chain subunits are also sensitive to NO- and ONOO- mediated damage, thus resulting in disorganization and inhibition of the respiratory complexes. For instance, ROS production can cause peroxidation of the mitochondrial lipids cardiolipin, and as such leads to the release of cytochrome C oxidase in the cytosol, which is known to cause apoptosis [176].
Moreover, hydroxyl radicals derived from generated ROS in the mitochondria are highly reactive and can damage different macromolecules inside mitochondria, like proteins, DNA and lipids. Specifically, accumulative unrepaired damage of mtDNA leads to defective complex I. Indeed, inhibition of complex I can result in increased formation of superoxides, thus amplifying the generation of more ROS. Therefore, the redox sensitive of the complex I activity [174], can generate a pathogenic vicious cycle, that can result in the shutdown of ATP biosynthesis, that consequently will provoke the inhibition of ATP dependent cytoprotective pathways, seriously compromising the survival of neurons [177].

1.3.4. Dysfunction UPS and autophagy.
Most of accumulated proteins in LBs are involved in protein clearance and quality control. In fact, major causative mutations in familial PD are linked to genes in the Ubiquitine Proteasomal System (UPS) or the Autophagic pathways, including α-synuclein, PINK1, Parkin, and LRRK2.
UPS is responsible for a highly selective degradation of short-lived intracellular and membrane proteins, as well as misfolded or damaged proteins in the cytosol, nucleus or endoplasmic reticulum. Specifically, ubiquitin targets suceptible proteins and only the unfolded ubiquitinated proteins pass through the narrow pore of the proteasome barrel [178]. The causative link of UPS dysfunction in the patogenesis of PD come from the observation that ubiquitin-positive LBs were observed in post-mortem analysis of PD patients [89]. In addition, proteasomal activity has been found decreased in different brain areas in patients with idiopathic PD [179]. Increased OS can lead to impaired function of the UPS, but also familial recessive Parkin mutations have shown a decrease in ubiquitin-ligase enzymatic activity in the SNpc [8]. This supports the hypothesis that failure of the UPS can lead to the neurodegeneration underlying PD.

On the other hand, protein clearance by means of autophagy is an important process in the protein quality control cell system. In contrast to the UPS, the role of autophagy relies on maintaining cellular homeostasis by degrading bulky citoplasmic material including damaged organelles and misfolded accumulated proteins. Indeed, autophagy is crucial for the clearance of aggregated proteins that represent a pathological hallmark of several neurodegenerative disorders such as PD [104]. Three different forms of autophagy have been identified: macroautophagy, microautophagy and chaperone-mediated autophagy (CMA). Whether autophagy has a protective role or contributes to cell death in PD still remains controversial.

Increased concentrations of aggregated α-synuclein in PD suggest a defective handling of protein clearance pathways. In vivo evidence suggests that normal soluble α-syn is degraded mainly by UPS and CMA [180], whereas more complex conformations, including aggregates, are disposed by the autophagy lysosomal pathway [181]. Specifically, α-synuclein and also LRRK2 contain a chaperone-mediated autophagy recognition motif, which enables its recognition by chaperone HSC70, facilitating a specific translocation into the lysosome through the lysosome-associated membrane receptor protein, LAMP2A, thus triggering their degradation via the CMA pathway. Dysfunction in CMA has been described in both familial [103,182–184], and sporadic PD [173]. Specifically it has been demonstrated that mutant forms

of α-synuclein (A30P and A53T) and of LRRK2 (G2019S and R1441C) are successfully recognized and delivered to the lysosomal membrane, but fail to reach the lysosomal lumen thus blocking their degradation via CMA [103,182]. Whereas α-syn mutants binds with abnormal high affinity to LAMP2A, preventing their own degradation [182], in the case of LRRK2, its mutant forms bind with enhanced affinity in the presence of other substrates, interfering with the proper organization of the active CMA translocon [103]. Therefore, mutant LRRK2 and α-syn not only block their own degradation, but also inhibit the degradation and promote accumulation of other CMA substrates [103,182]. In the particular case of mutant LRRK2, it exacerbates the intracellular accumulation of α-syn, in part by preventing its clearance through CMA, thus promoting its aggregation into toxic oligomers that can further compromise CMA activity in a vicious cycle, and contributing to the seeding of the protein aggregates characteristic of PD (**Fig. 15**).

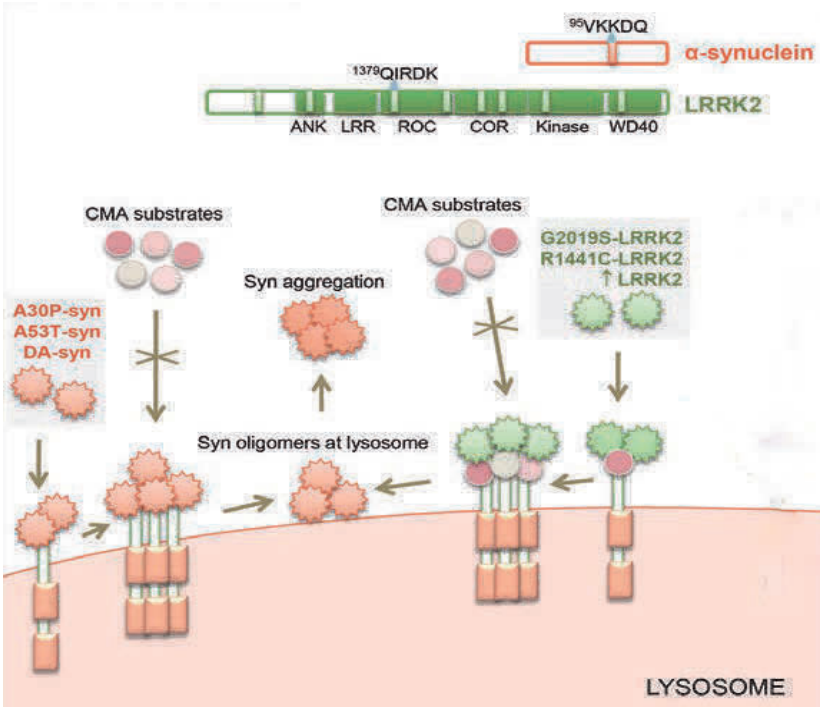

Figure 15. Impairment of CMA by pathogenic α-syn and LRRK2 proteins, contributing to neurodegeneration.

Both α-synuclein and LRRK2 bear CMA-targeting motifs (top), and are degraded by CMA. Mutant forms of these proteins bind anomally to LAMP2A, albeit different mechanisms, leading to blocakage of their own degradation as well as degradation of other CMA substrates. DA-modified α-synuclein and abnormally high levels of wild-type LRRK2 also impair CMA. Moreover, alterations of CMA by mutant LRRK2 show toxic effects on α-synuclein aggregation (modified from Cuervo et al., 2014 [104]).

Furthermore, alterations of CMA have also been implicated in sporadic PD. As aforementioned, oxidative derivates of DA can modify α-synuclein conformation, and this has been shown to reduce the ability to be degradated by CMA, in a similar manner to that of familial α-syn mutants. In detail, DA-modified α-syn inhibits its own degradation as well as other CMA substrates, promoting its multimerization in toxic oligomeric and protofibrils forms at the lysosomal membrane [173]. In addition, in the absence of post-translational modifications, increase of cellular levels of either α-syn or LRRK2 far from a tolerable threshold, can have a similary inhibitory effect to the CMA activity, even potentiating each other's toxic effect [103]. It is suggested that the accumulation of abnormal α-synuclein acts in a vicious cycle, progressively inhibiting the CMA pathway. Therefore, subsequently activation of macroautophagy could act as a compensatory mechanism [182], since abnormal presence of autophagic vacuoles is observed in brains of PD patients, in comparison with healthy brains [185].

As aforementioned, autophagy is also involved in the turnover of dysfunctional mitochondria, mainly controlled by Parkin and PINK1, which are responsible of activating mitophagy of damaged mitochondria. Loss of function of either Parkin or Pink1 has been found to fail in activating mitophagy thus suggesting a common PD pathogenic mechanism. On the other hand some in vitro data obtained in neuronal cultures and yeast model of aging also point that wild-type as well as mutated α-syn aggregates can up-regulate macroautophagy as compensatory mechanism aimed to reduce the misfolded portein burden [178]. As a consequence, abormal activated autophagy could induce to an undiscriminated clearance of both functional and dysfunctional mitochondria, which can lead to pathogenic degradation in the neurites, and subsequently neuronal death.

1.4. Treatment of PD

To date, Parkinson's disease is still an incurable progressive disease. Current treatments are still symptomatic, focused on mitigating the motor affectations caused by the lack of DA in the caudate putamen due to the nigrostriatal dopaminergic denervation. Symptomatic treatments notably improve quality of life and functional capacity, but they do not cure or halt disease progression, and are not effective with non-motor manifestations of the disease. The pharmacological substitution of DA with levodopa (L-dopa) is the most widely used treatment for PD, although other pharmacological and surgical treatments are recommended in specific conditions.

1.4.1. Current treatments: Symptomatic treatments

Current treatments for PD are divided into pharmacological and surgical treatments. DA replacement therapy is the major medical approach for treating PD. Among the variety of dopaminergic agents, levodopa remains the "gold standard" treatment for PD motor symptoms since its efficacy and tolerability is firmly established for more than 30 years of use in clinical practice [186,187]. Specifically, levodopa is a precursor of dopamine, able to cross the blood-brain barrier, whereas dopamine itself cannot. Once in the brain, levodopa exerts its symptomatic benefits through the conversion to dopamine, by the enzyme L-amino acid decarboxylase. This strategy allows the restoration of dopamine levels in the striatum and leads in many cases to the improvement of motor symptoms. To date, levodopa is routinely administered in combination with a decarboxylase inhibitor (Benzerazide, carbidopa), in order to prevent formation of dopamine in the peripheral tissues, which can result in adverse effects such as nausea and vomiting. Levodopa treatment it is well known to improve motor symptoms and patients' quality of life. Most people can be maintained over the first 5 years of the disease on 300-600 mg/d of L-dopa, and motor symptoms initially improve by 20-70%, depending on the patient's condition [1]. However, levodopa has a short half-life in plasma, which eventually results in short-duration responses with a "wearing-off" effect (a gradual waning of the effect of dopaminergic treatment on motor symptoms before the next dose). Moreover, after 4-6 years of chronic treatment, severe motor complications arise. These motor complications specifically comprise "on-off" fluctuations (when symptoms can reappear and disappear randomly) and dyskinesias (involuntary movements and tics). Non-motor side effects such as confusion, hallucinations, and sleep disorders are also present in some patients. Risk factors are levodopa treatment itself, younger age at onset (less than 60 years of age), and longer disease duration [4,188]. In individual studies, the percentage of fluctuations and dyskinesia may range from 10 to 60% of patients at 5 years of treatment, and up to 80-90% in later years [187].

Therefore, motor complications remains a major unmet need for the management of PD symptoms. Several treatments have been developed during the last decades, in order to find ways to prolong the duration of striatal dopamine receptors stimulation for longer than what is achieved by the short half-life of oral levodopa in plasma. On one hand, dopamine agonists (Pramipexole, ropinirole, rotigotine, pergolide, and apomorphine) were found to be efficacious to delay the occurrence of motor complications when used before levodopa [189,190]. In fact, these are popular first-line treatment for young-onset PD patients (under 55 years), although

levodopa is later usually necessary within 3 years of diagnosis, when there is not a good control of the motor symptoms with the agonist alone. Moreover, supplementation of levodopa with dopamine agonists are helpful for smoothing motor fluctuations, and, in many cases, they permit lowering levodopa doses. However, the long-term results of the open extensions of those trials questioned the clinical relevance of delaying the onset of dyskinesia, since this "protective" effect is lost once L-dopa has been initated [191–194]. In addition, DA agonists expose the risk of troublesome adverse reactions, including daytime somnolence or impulse disorders. Nevertheless, to date new formulations DA agonists such as apomorphine are currently under different clinical trials (**Table 3**).

Drug and formulation	New studies in the period 2013-2015	Main results	Safety	Development/marketing status
New formulations of levodopa				
Duodopa	1 R, DB, DD trial vs levodopa IR	Reduced daily OFF-time, increased "good" ON-time	Related to the device or infusion	Commercialized in USA and Europe
IPX066	1 R, DB, DD vs levodopa IR 1 R, DB, DD trial vs entacapone	Reduced daily OFF-time, increased "good" ON-time	Same as levodopa IR	Commercialized in USA
New COMT or MAO-B inhibitors				
Opicapone	2 R, DB, vs placebo or entacapone	Increased L-dopa exposure, reduced off-time	Dyskinesia, insomnia, dizziness, nausea	In Phase III
Safinamide	1 R, DB vs placebo	Increased "good" ON-time	Dyskinesia, worsening of PD, cataract, back pain, depression, headache, and hypertension	Comercialized in Europe. NDA submitted to FDA
New formulation of apomorphine (DA agonist)				
Inhaled apomorphine	3 R, DB vs placebo	Greater motor improvements after a single dose	Somnolence, yawning, flushing, dysgeusia, dissiness, orthosatic hypotension	In Phase III

TABLE 3. A selection of new drugs or formulations for the treatment of motor complications in the 2013-2015 period. DB = double-blind; DD = Double-dummy; IR = Immediate-release; R = Randomized; "Good" ON-time = ON-time without troublesome dyskinesias (modified from Rascol et al., 2015 [195]).

On the other hand, other compounds have been used as a complement of levodopa in order to prevent the breakdown of dopamine, both the endogenous and the product formed from levodopa. Particularly, dopamine is also metabolised either by catechol-O-methyl transferase (COMT) to form 3-O-methyldopa, or by the enzyme monoamine oxidase B (MAO-B), which metabolizes dopamine to 3,4-dihydroxyphenylacetic acid (DOPAC). For this reason, the co-administration of levodopa together with either COMT inhibitors (Entacapone, Opicapone) or MAO-B inhibitors (rasagiline, safinamide) has been found to extend plasma half-life of DA and levodopa, thereby prolonging the duration of action of DA therapies (**Table 3**) [195]. Specifically, Safinamide is a novel third-generation MAO-B inhibitor, that also modulates dopamine reuptake and glutamate release [196]. Safinamide, as a complement of DA therapies, has been shown to significantly improve motor symptoms, activities of daily living, quality of life, and cognition ratings compared with placebo [197], proved to be safe [198], and demonstrated to improve dyskinesias [199,200].

Furthermore, improving oral levodopa pharmacokinetics or developing new modes of delivery to achieve more constant plasma levels may reduce or prevent motor oscillations and drug-induced dyskinesias (Poewe et al., 2015). For instance, the novel extended release L-Dopa (ER-LD) formulations Duodopa and IPX006 (Rytary®) are promising candidates that recently have been marketed and approved in Europe and USA in the beginning of year 2015 (**Table 3**). These formulations are thought to be used for the treatment of motor fluctuations in people with advanced PD. Specifically, continuous intrajejunal infusion of Levodopa-Carbidopa (LD-CD) intestinal gel (Duodopa) circumvents gastric emptying problems and provides more stable plasma concentrations than oral formulations. Duodopa has been shown to have a robust improvement in motor symptoms, as well as an increase of daily on-time without troublesome of dyskinesias, and these effects were maintained up to 2 years. On the other hand, IPX066 (Rytary®) is a novel extended release LD-CD capsule containing combined immediate and sustained-release pellets, that dissolves at different rates along their gastrointestinal passage. In different studies, IPX066 has been found to reduce daily OFF-time, compared with immediate-release formulations, as well as no increase in dyskinesias, although adverse events such as insomnia, nausea and falls were reported in particular cases. However, how far these new ER-LD formulations instead of standard LD formulations can impact the delay onset of motor complications in advanced PD remains still unknown.

A better understanding of the basal ganglia physiology has led to the development of surgical treatments in PD, known as Deep Brain Stimulation (DBS). DBS can provide additional help for specific patients whose symptoms are not controlled sufficiently by dopaminergic medications in advanced stages of PD. DBS is a surgical treatment involving the implantation of a medical device, which can send electrical impulses in a region of the basal ganglia, mainly GPi, the STN or the ventral medial nucleus of the thalamus (VIM). The optimal target point for DBS is based on the type of motor symptoms of each patient manifests (**Table 4**).

	STN	GPi	Vim
PD features	Medically intractable motor fluctuations, dyskinesia, or tremor. Major disability from off-symptoms.	Medically intractable motor fluctuations. Major disability from dyskinesias.	Medically intractable tremor. No major disability from other parkinsonian symptoms. High risk for STN.
Concerns	Dysarthria and dysphagia. Balance and gait problems non–dopa-responsive. Psychiatric problems.	STN a concern because of age, psychiatric history, or cognition problems.	Speech and balance problems.

GPi = globus pallidus internus; STN = subthalamic nucleus; Vim = ventral intermediate nucleus of the thalamus.

Table 4. Target selection criteria for Deep Brain Stimulation Criteria in PD.
(from Limousine et al., 2009).

In 1987, VIM became the first target in the modern era of DBS, which allowed a clear and immediate effect on tremor, although no effects in dyskinesia, motor fluctuation, rigidity and bradikinesia. Later in the 90's, other regions for DBS became available. Specifically, both STN-DBS and GPi-DBS are an effective option to improve motor symptoms and manage long-term motor complications resulting from levodopa treatment (Weaver et al., 2012), although only STN-DBS allows a reduction of the levodopa dosage (Follet et al., 2010; Okun et al., 2012). However, this strategy presents mainly two limitations. First, it is only suitable for a small group of patients. For instance, preoperative indicators for a good outcome are younger age and shorter disease duration (Schüpbach et al., 2013), as well as high levodopa-response (Bronstein et al., 2011). More important, dementia and other psychiatric problems are the most common exclusion criteria (Bronstein et al., 2011). In fact, decisions for or against DBS should be individualized, taking into account the degree of disability, risk factors for complications, general life expectancy and patient's motivation. For example, GPi-DBS is especially

considered for those patients with risk of psychiatric problems after STN-DBS, and a preferred choice in the older population (Limousine et al., 2008). Moreover, VIM-DBS can be a useful treatment for patients with a more severe tremor, who are also not suitable for other DBS strategies (Limousine et al., 2008). Second, as with dopaminergic treatments, DBS has only a symptomatic effect and does not alter the progression of the disease. Moreover, after five years after DBS, many features decline with disease progression, as gait, balance, cognitive functions and speech often deteriorate, and a number of patients also develop dementia (Limousine et al 2008).

1.4.2. Disease-modifying drugs for PD. What is in the pipeline?

The drug development pipeline for PD has been, and remains, largely focused on symptomatic treatment. Progress in this area has been steady over the past 10 years [201]. Phase I clinical trials show a trend toward increasing year over year, and the number of phase II and phase III, despite some fluctuations year-to-year, remains essentially stable. Moreover, over the last decade there has been an average of 4.7 new molecular entities entering phase I and phase III clinical trials each year, and 9.6 new molecular entities entering the phase II annually. However, these data do not discriminate between drugs designed for symptomatic treatments and those for disease-modifying therapies [202].

Furthermore, recent advances in the genetic contribution of Parkinson's have helped in the identification of new potential therapeutic targets and strategies that have fed into the drug development pipeline, which eventually could converge with the common pathogenesis of the disease [202]. These new therapies, that might be called "experimental", including also cell replacement therapies and gene therapy for PD, are currently being tested in animal models and small groups of PD patients in order to assess their efficacy and reliability.

Coenzyme Q10 and Creatine

Targeting mitochondria functionality or enhancing neuron bioenergetics might be considered strategies to protect neuronal death in PD. For instance, drugs pointing to this strategy comprise the electron carrier for complexes II/I Coenzyme Q10, and Creatine, which once converted to phosphocreatine, can act as a short-term energy source. Unfortunately, clinical trials comprising these two compounds were futile in their primary outcomes [203]. However, the major role that mitochondrial dysfunction plays in PD should not exclude other attempts that are currently ongoing (**Table 5**).

PPAR-γ and GLP-1r agonists

A recent meta-analysis of changes observed in post-mortem human PD samples pointed that PGC1α is a potential target for disease intervention [112]. Therefore fine-tune regulation of endogenous PGC1α in neurons by different compounds may be a good strategy to pursue, since PGC1α is considered an important regulator of mitochondrial biogenesis and energy metabolism. In particular, PPAR-γ agonists, such as rosiglitazone and pioglitazone, are commonly used in the treatment of Type II diabetes (T2D), and they were thought to have potential also for the treatment of PD [204]. Preclinical studies showed that rosiglitazone protects DA neurons toxic animal models of PD, and pioglitazone can improve parkinsonian syndrome in rhesus monkeys [205,206]. Both drugs have shown to reduce the production of proinflammatory cytokines by reactive microglia [148,207]. Moreover, a recent epidemiological study on people with T2D revealed a lower incidence of PD in patients on glitazone drugs [208]. However, pioglitazone underwent a multi-center, double-blind phase II clinical trial in early PD patients, and failed to shown any improvement of the disease outcome [209], thus suggesting that the preclinical neurotoxin-inducing neuroinflammatory models may not reflect the human condition of PD (**Table 5**) [210].

Study	Drug	Mechanism of Action	Trial Design	Subjects	Follow-up Period	Primary Outcome Measures	Results/ Status
PSG et al., 2014	Coenzyme Q10 (1200 mg/d or 2400 mg/d) + vitamin E (1200 IU/d)	Bioenergetic	Multi-center, randomized, double-blind, placebo-controlled, phase III trial	Early PD subjects not requiring DA therapy (n=600)	16 months	Change in total UPDRS score	Prematurely terminated due to futility
NET-PD et al., 2015a	Creatine (10g/d)	Bioenergetic	Multi-center, randomized, double-blind, placebo-controlled, phase III trial	Early PD subjects not receiving DA therapy (n=1741)	4 years (median)	Difference in decline of clinical status defined by 5 outcome measures	Prematurely terminated due to futility
NET-PD et al., 2015b	Pioglitazone (15 mg/d or 45 mg/d)	PPAR-γ agonist	Multi-center, randomized, double-blind, placebo-controlled	Early PD subjects on rasagiline or selegiline (n=210)	44 weeks	Change in total UPDRS score	Futility
NCT02168842	Isradipine (immediate release; 10 mg/d)	Dihydropyridine calcium channel blocker	Multi-center trial (USA, Canada), randomized, double-blind, placebo-controlled, phase III trial	Early PD subjects not requiring DA therapy (n=336)	36 months	Change in total UPDRS score	Recruiting
NCT02424708	GSH (intranasal; 300 mg/d or 600 mg/d)	Antioxidant	Dual-center (USA), randomized, double-blind, placebo-controlled, phase II trial	PD subjects (n=45)	12 weeks	Change in total UPDRS score	Recruiting
NCT01470027	N-acetyl-cysteine (1800 mg/d or 3600 mg/d)	GDH precursor: Antioxidant	Single-center (USA), randomized, double-blind, placebo-controlled, phase I/II trial	PD subjects on no medications for PD (n=60)	4 weeks	Change in cerebral GSH levels measured by proton magnetic resonance spectroscopy	Recruiting
NCT01174810	Exenatide (5-10µg/ twice a day)	GLP-1R agonist	Open-label, single-center, randomized controlled phase II trial	Moderate PD patients (n=45)	12 month	Effect on motor and cognitive functions	Improvements at 12 months with persistent effects after 12 months of drug withdrawal

Table 5. Clinical trials of disease-modifying therapies for PD from 2013 to 2015.
(modified from Kalia et al., 2015 [203])

Other T2D compounds, such as agonists of the glucagon-like peptide R1 receptor (GLP-1R) system have been shown to be neuroprotective in PD models as well as in other brain diseases [78,211]. Specifically, A proof-of-concept clinical trial that enrolled 45 patients with moderate disease, were subcutanously injected with Exenatide for 12 months. Treated subjects had a mean improvement in motor and cognitive functions, and the drug demonstrated reasonable safety [211]. However, limited conclusions can be drawn from this study, since there is a lack of placebo controls, therefore additional clinical trials have been considered and are on the way (**Table 5**).

Antioxidant and antiiflammatory compounds

Furthermore, antioxidant and antiinflammatory properties of different drugs have also been studied for their potential as a disease-modfying therapy for PD. First, it has been shown that early PD patients with higher plasma urate levels, confers antioxidant properties [212,213], confering to these patients a slower disease progression. A precursor or urate called Inosine, has been found to elevate urate levels and to be safe in a select population of early PD patients, supporting further investigation of this compound as a potential disease modifying therapy [214]. Second, the use of calcium channel blockers has been associated with reduced risk of

developing PD [215]. In particular, Isradipine is a dihydropyridine calcium channel blocker with relatively high affinity for Cav1.3 channels, approved for treatment of hypertension. In a phase II random clinical trial (RCT) 12 month study, Isradipine has been well tolerated with few adverse effects, and to date, a phase III RCT is currently ongoing to assess its efficacy as a disease modifying therapy in PD (**Table 5**). Third, gluthathione (GSH) is an endogenous antioxidant within the brain, and loss of GSH has been implicated in PD. To date, a phase I/II study is underway evaluating whether GSH levels are decreased in PD subjects by using proton magnetic resonance spectroscopy, as well as to assess if levels of GSH can increase after supplementation with N-acetylcysteine, a GSH precursor (**Table 5**) [203].

On the other hand, targeting microglia activation, the increased production of ROS and pro-inflammatory cytokines, using drugs or neuroprotective substances is therefore a valid path to consider for therapy. Interestingly, the study of and evaluation of large ochorts of individuals, those who use non-steroidal anti-inflammatory drugs (NSAIDs), specifically ibuprofen, have been found to exhibit a lower risk of developing PD. Indeed, treatment with NSAID's is protective in toxic animal models, thus suggesting an association between anti-inflammatory treatments and a decrease in the potential of developing PD. In addition to NSAID's, Minocycline possesses potent neuroprotective and anti-inflammatory activity in various inflammatory rodent models in PD, and it has been carried into clinical trials as well. Specifically, analysis of patients following minocycline treatment suggests that microglial activation was perturbed, however motor assessments failed to show any clinical benefit, thus suggesting that anti-inflammatory agents by themselves fail to improve the motor clinical outcomes in the human condition of PD [210].

Targeting implicated genes on PD

Several of the genetic loci directly implicated in PD are currently the subject of drug development efforts. On one hand, accumulating genetic evidence implicates dysfunction of kinase activities and phosphorylation pathways in the pathogenesis of PD. For instance, targeting LRRK2's kinase function has generated a lot of interest from both pharmaceutical and research institutions. Several studies have shown that is feasible to design highly selective LRRK2 inhibitors capable of crossing the blood brain barrier, thus being LRRK2 an attractive target for PD therapeutics [216]. Although the study of LRRK2 inhibitors is still in a preclinical stage, recent studies have move forward in the characterization of the potential safety and efficacy liabilities of different promising small molecules that selectively target LRRK2 kinase activity. However, lung toxicity may be the primary clinical safety liability of LRRK2 kinase inhibitors in patients, since this effect was seen in LRRK2 KO mice [217], and when treating with specific LRRK2 inhibitors in non-human primates [218]. Interestingly, Fell and colleagues described a highly selective LRRK2 inhibitor called Mli-2. When administered in-diet during 15 weeks, Mli-2 was found to achieve chronic LRRK2 inhibition in rodents. MLi-2-induced LRRK2 inhibition was well tolerated since no adverse effects on body weight, food intake, or behavioural activity were observed, although a mild phenotype in lung cells similar to the one found in LRRK2 KO mice was found [219]. Concurrently, Daher and colleagues developed a rat model of lentiviral overexpression of α-synuclein, in which they demonstrated that G2019S LRRK2 expression exacerbates α-syn-induced neuroinflammation and dopaminergic neurodegeneration, and that these effects can be reverted by chronic in-diet administration of a potent LRRK2 inhibitor, developed by Pfizer (PF-06447475) [151]. In particular, this LRRK2 inhibitor demonstrated a clear superiority in potency, specificity, and bioavailability compared with other published LRRK2 kinase inhibitors [218,220]. Moreover, no abnormalities such as the ones observed in LRRK2 KO rats or in non-human primates treated with LRRK2 kinase inhibitors were found after a 4-week period of time. However, tolerability and safety of LRRK2 kinase inhibitors needs further evaluation, particularly in non-human primates [218]. Likewise, setting the time-onset and dosage, as well as the primary outcomes to assess on-target LRRK2 inhibition in human clinical trials still need to be identified.

On the other hand, extracellular α-syn might play a crucial role in PD when its missfolded forms are transferred from one neuron to another [221]. Therefore, immunotherapy focused on clearing extracellular forms of α-synuclein has been proposed [222]. Specifically, immunotherapeutic approaches are aimed to target and enhance the clearing of misfolded or post-translationally modifed α-syn. Preclinical studies along these research lines have shown promising results [223,224]. In particular, α-syn overexpressing transgenic rodent models have demonstrated the capability of antihuman α-syn to ameliorate doaminergic neuronal cell loss, decrease microglial activation, as well as reduce levels of protein propagation, and attenuating also motor deficits [225,226].

Study	Drug	Mechanism of Action	Trial Design	Estimated Enrollment	Follow-up Period	Primary Outcome Measures	Status
NCT02216188	PD01A + Adjuvant (sucutaneous injection; 15μg or 75μg booster x1)	Active immunization against α-syn	Single-center (Austria), randomized, single-blind, follow-up, phase I trial	PD subjects who previously received PD01A and untreated controls (n=32)	6 months	Safety and tolerability	Enrolling by invitation
NCT01885494	PD01A + Adjuvant (subcutaneous injection; 15μg or 75 μg x4)	Active immunization against α-syn	Single-center (Austria), observational, follow-up, phase I, extension trial	PD subjects who previously received PD01A and untreated controls (n=32)	52 weeks	Safety and tolerability	Active but not recruiting
NCT02267434	PD03A + Adjuvant (subcutaneous injection; 15μg or 75 μg x4)	Active immunization against α-syn	Dual-center (Austria), randomized, single-blind, placebo-controlled phase I trial	Early PD subjects (n=36)	52 weeks	Safety and tolerability	Recruiting
NCT02095171 NCT02157714	PRX002 (intravenous infusion)	Passive immunization against α-syn	Multi-center (USA), randomized, double-blind, placebo-controlled, phase 1 trial	PD subjects (n=60)	6 months	Safety and tolerability; several pharmacokinetic parameters	Recruiting

Table 6. Ongoing clinical trials based on immunotherapies against α-synuclein.
(Modified from Kalia et al., 2015).

Currently, various immunotherapies based upon active (injection of recombinant α-syn) and passive immunization (injection of domain-specific anti-α-syn antibodies) procedures are in clinical testing or are being planned for PD patients (**Table 6**). For instance, Roche and Protena further developed and commercialized PRX002 to specifically target α-syn. A phase I clinical trial was recently completed, finding that the vaccine was safe and well tolerated. Administration of the antibody was associated with a rapid and dose-dependent reduction of free serum α-syn levels, with no more than 10% subjects under adverse effects. A promising second phase trial is underway in order to assess dose response, tolerability, pharmacokinetics, exploratory biomarkers and immunogenicity [210].

On the other hand, AFFITOPE PD01A, is va accine developed to produce antibodies that are specific for phosphorylated form of α-syn, responsible for the induction of a neurotoxic proinflammatory cascade through microglial activation. Phase I clinical trial was completed, safe and tolerable, and half of the patients developed α-syn antibodies suggesting that the vaccine is effective as well. Further investigations are underway to test its clinical benefits in PD, among other parkinsonian-associated diseases. Altogether, these studies show that α-syn-targeted immunotherapies may have the potential to attenuate neuroinflammatory-associated neurotoxicities and as such, delay dopaminergic neurodegeneration associated with PD [210]. However, some pitfalls targeting α-syn must be on consideration. T cell infiltration, as well as altered IgG production and ehanced MHCII expression has been found [225], thus suggesting that antibody-mediated therapies might contribute to an inflammatory state operative during PD.

Moreover, given that α-syn is a remarkably abundant protein in the brain and blood, and its normal physiology is not well elucidated, non-specifically lowering α-syn levels could have biological serious consequences. Therefore a robust immune response without cross-reactivity with common nonpathogenic forms of α-syn is preferable. In addition, targeting a host self-protein is much more challenging than protecting the host from foreign antigens. If safety of α-syn-targeted immunotherapies can be well established, further development to more specifically target of the toxic forms of α-syn is expected [210].

1.4.3. Cell replacement therapies

Alternatively, cell replacement therapies (CRT) are aimed to restore and replace the DA-secreting cells in the damaged striatum and SNpc, thus recovering DA supply in the striatum and replacing the function of DA neurons lost during the course of the disease. Conceived as a long-lasting therapy to substitute pharmacological treatment, in the last 20 years, approximately 300-400 PD patients have been transplanted with human fetal mesencephalic tissue and results have varied from success to failure. Human fetal mesencephalic tissue contains DA progenitors that are committed to DA neuron fate, and the risk of tumorigenicity seems to be low or absent [227]. In 1990s, in the best cases, patients were able to withdraw their anti-parkinsonian medications, since dopamine signalling was restored in the grafted striatum, with the reactivation of relevant cortical motor areas [228,229]. These encouraging results provided proof-of-principle that CRT could become a feasible therapy for PD. However, when including more complex clinical trials, such as double-blind, controlled trials [230], or patients with moderately advanced PD [231], the results were from modest to no recovery. In fact, in some cases human fVM transplants did not demonstrate significant improvements in patients with PD, especially when compared with newer surgical approaches such as DBS in that moment [232]. In addition, adverse effects raise in the form of graft-induced dyskinesias (GID) in some cases [231], due to either non-homogenous distribution of DA cells across the striatal complex, giving rise to hot spots of innervation [233], or presence of grafted innervated serotonergic neurons that release dopamine in an unregulated fashion [234]. However, several factors emerged that were associated with positive outcomes in this surgery, which includes younger age and less-advanced disease clinically, preserved striatal DA innervation, receipt of grafts with more than 100000 or more DA nigral neurons, adequate immunotherapy to avoid rejection of the graft, and a grafting technique that allowed an homogenously innervation of the damaged striatum [227]. In fact, it has been demonstrated that in some cases grafted DA neurons could survive for as long as 16 years after transplantation [84–86]. Interestingly, in one of these studies in post-mortem brains of PD patients that had been transplanted 9-14 years before, disease-free DA neurons (no Lewy Body) were found [86]. On the other hand, LB and α-synuclein aggregates were found in grafted cells of patients that were transplanted 11-16 years before [84,85], as well reduced dopamine staining, thus suggesting the aforementioned hypothesis of host-to-graft disease propagation [22]. However, since no host-to-graft propagation can happen in patients surviving 10 years after transplantation [86], this indicates that CRT could have a longer therapeutic window than current symptomatic treatments, and even longer in some cases (**Figure 16**).

The main limitation of this CRT is the source of the donor tissue. Human fetal mesencephalic tissue is obtained from 6-9 week-old aborted human fetuses; therefore ethical implications to this approach are evident. In addition, the amount of aborted fetuses needed per patient can vary from 6 to 10 fetuses, and the survival of DA cells after transplantation, in the best cases reached a 10% of the transplanted cells [235]. Therefore, there is a need of alternatives of cell sources of A9 DA neurons in large supply, with less ethical contentious, that eventually could garantee a feasible transplantation in terms of safety and efficacy, for treating PD. Human pluripotent stem cells (both human embryonic stem cells (hESC) and induced pluripotent stem cells (iPSC)) meet these criteria.

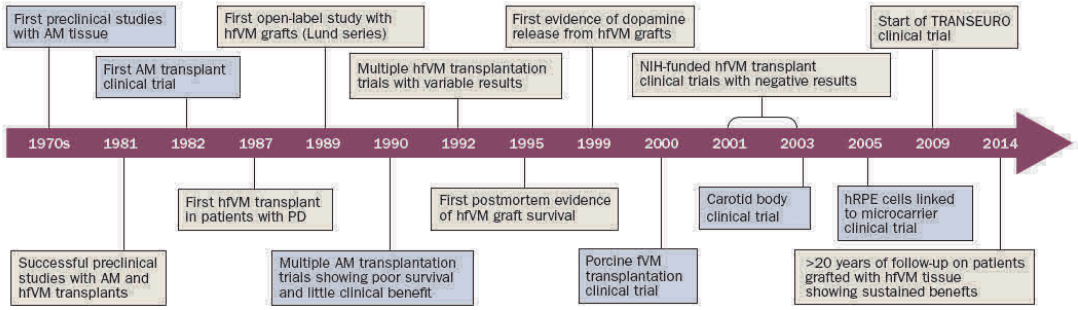

Figure 16. Timeline of cell-based therapies for use in patients with PD, highlighting the key preclinical and clinical studies.

Yellow boxes: Trials of human fetal tissue transplants
Blue boxes: Trials involving cells from other sources
Abbreviations: AM = Adrenal medullary; fVM = fetal ventral mesencephalic; GIDs = graft-induced dyskinesias; hfVM = human fVM; hRPE = human retinal pigmentary epithelial (modified from Barker et al., 2015 [227]).

A number of protocols have been developed in which hESC-derived neural progenitor cells were patterned in co-culture with murine stromal cell lines such as PA6 and MS5 [236–239], with astrocytes [240], or cultured with fibroblast growth factor 8 (FGF8) and sonic hedgehog (SHH) [241]. Some of these early protocols produced relatively high numbers of TH-positive neurons that were capable of releasing dopamine, but none of them generated cells co-expressing two transcription factors required for proper midbrain dopaminergic neuron specification, namely, FOXA2 and LMX1A. Moreover, the incomplete and non-synchronized differentiation of the cells led to tumour formation in vivo in some cases [239,240].

In 2006, the demonstration that pluripotency can be induced in human fibroblasts sparked a major revolution in the field [242]. Induced pluripotent stem cells (iPSCs) have become a source of patient-specific and disease-specific neurons, specially as, in theory, this approach would avoid many of the ethical issues associated with making hESC lines. However, like hESC-derived dopaminergic neurons, the midbrain properties of the cells were unclear, and their in vivo performance in standard animal models of PD was modest [243,244]. It is only recently that it has been possible to obtain efficient generation of authentic midbrain dopamine neurons from human ES cells. The protocols recently developed by Kriks and Kirkeby are particularly promising [245,246]. The procedure is based on a floor plate intermediate [247], and involved stepwise exposure of the cells to extrinsic factors activating sonic hedgehog (SHH) and Wnt signaling, in combination with neuronal differentiation survival factors, such as Brain-derived neurotrophic factor (BDNF), Glial cell-derived neurotrophic factor (GDNF), ascorbic acid, and cyclic adenosine monophosphate (cAMP). The cells generated in these protocols express all markers of authentic midbrain dopamine neurons and they have been shown to survive and function after transplantation to the striatum, in both rodent and primate PD models [245,246]. Rigorous preclinical testing in animal models of PD has shown that these floor plate-derived dopaminergic neurons can function with equal potency and efficacy as fetal dopaminergic neurons [248]. Importantly, they have a remarkable capacity for long-distance, target-specific outgrowth. In addition the protocol is quite fast, efficient and synchronized, thus circumventing the problems of tumour formation and neural overgrowth seen with the older protocols. Based on these promising findings, improving and standarizing these protocols, and adapting them to good laboratory practice (GLP)/GMP conditions, will be able to move this technology closer to clincial translation [227].

Furthermore, the use of integration-free iPSC in this regard, encourages the performing of CRT with autografts in PD patients, with no need to use immunosuppressive drugs when cell replacement surgery is performed. Recently, the autologous transplantation of iPSC-derived neurons into the striatum of healthy non-human primates has been demonstrated to be advantageous when compared to allogenic grafts, at least in terms of immune response and cell

survival [249]. However, some concern regarding mutations or epigenetic markers in cells that can persist should be taken, since patient-derived iPSC are still more vulnerable to PD [102,250]. Therefore the future cell therapeutic strategies should pay attention to the correct epigenetic status of the reprogrammed dopaminergic cells, especially when using patient's own cells. However, the very recent development of gene editing tools could help in solving this problem [251].

1.4.4. Neuroprotective treatments using neurotrophic factors: GDNF and NRTN.

Neuroprotection is a therapeutic strategy intended to slow or cease neuronal loss and, therefore, to alter the natural progression of the disease. Contrary to symptomatic treatments, neuroprotective therapies are aimed to act on the pathogenic mechanisms underlying the clinical manifestations of the disease. Neurotrophic factors (NTFs) have been considered for many years promising targets for neuroprotection in neurodegenerative disorders, although they still need to be translated into viable clinical trials. Several neurotrophic factors have been described such as nerve growth factor, brain-derived neurotrophic factor (BDNF), astrocyte-derived neurotrophic factor, among others. However, the most promising ones are the glial cell-derived neurotrophic factor (GDNF) family members: both GDNF itself and its structurally related trophic protein neurturin (NTRN), have become the most extensively studied dopaminergic NTFs to date [252].

GDNF and NRTN, as well as the other GDNF-family ligands artemin and persephin, are distant members of the transforming growth factor-β (TGF-β) superfamily [253]. GDNF-family ligands share the receptor tyrosine kinase Ret. However, activation of Ret requires the association with GDNF Family Receptor alpha (GFRα), of which four subtypes have been described with different affinities for each ligand. In particular, GDNF homodimer specifically binds to two GFRα-1, forming a high affinity complex with the recruitment of Ret. With the formation of the Ret-GFRα-1 complex, transphosphorylation of Ret tyrosine kinases residues is induced, which in turn activates downstream signaling molecules, such as the mitogen-activated protein kinase RAS/ERK1-2/MAPK pathway, and the phosphatidylinositol 3-kinase PI3K/Akt/mTORC1, thus triggering several cellular pathways involved in apoptosis, metabolism, and redox homeostasis [253–255] (**Fig. 17**). Moreover, it is also known that ablation of Ret does not produce a phenotype similar to GDNF-deficiency [256], since GDNF can also bind to an alternative signaling system when GFRα-1 form a complex with the receptor NCAM-140 [257]. However, the role of this alternative complex on dopamine neurons remains unclear [255].

GDNF properties were first described in 1993, when Lin et al. observed a specific triggered action by GDNF on the survival of *in vitro* rat E16 midbrain DA neurons, selectively stimulating dopamine uptake and neurite outgrowth in tyrosine hydroxylase positive (TH+) neurons [258]. Interestingly, the study of gene-deleted animals have revealed that GDNF, GFRα-1, as well as RET KO mice die after birth due to a lack of kidney development [259–261]. However, those animals have an intact nigrastriatal dopaminergic system, thus suggesting that GDNF is not crucial for the embryonic development of DA neurons [261]. On the other hand, conditional deletions of GDNF in the adult mice revealed that GDNF is absolutely required for the survival of DA neurons throughout the adult life of mammals [262].

Subsequently, initial *in vitro* observations were followed by preclinical studies of GDNF effects on PD animal models based on toxin-induced damage of midbrain DA neurons. Given that GDNF does not cross the blood brain barrier, initial *in vivo* studies were based in the injection or infusion of recombinant GDNF directly into the brain. Several independent studies reported neurochemical and behavioral motor improvements in unilaterally 6-OHDA-lesioned rats following administration of GDNF [263–266]. More increasing evidence of the potent neurotrophic properties of GDNF come from the first non-human primate data in a MPTP-induced parkinsonian monkey model, showing functional improvement of parkinsonian features along with increased levels of striatal DA in GDNF-treated monkeys [267].

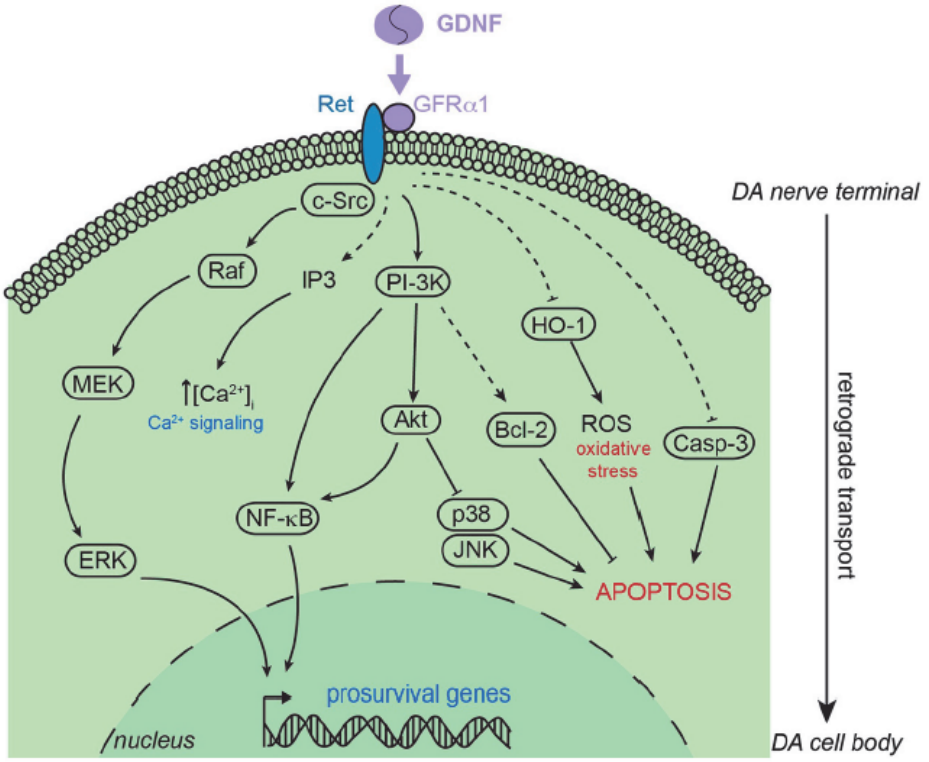

FIGURE 17. Schematic representation of the main signaling pathways involved in the neuroprotective action of GDNF on DA neurons.

Gdnf mainly stimulates the GFRα1-RET coupling, which triggers intracellular kinase signaling cascades leading to pro-survival genes expression, calcium signaling and pro-apoptosis factors inhibition. Dashed arrows indicate indirect stiumulation or inhibition.

Abbreviations: Akt = Protein Kinase B; Bcl-2 = B cell lymphoma 2; Casp-3 = Caspase-3; c-Src = proto-oncogene tyrosine-protein kinase Src; ERK = extracellular signal-regulated kinase; HO1, heme oxygenase 1; IP3 = inositol tri-phosphate; JNK = c-Jun N-terminal kinase; MEK = mitogen extracellular signal-regulated kinase; NF-κB = nuclear factor κB; PI-3K = phosphatidylinositol 3 kinase; Raf = Raf kinase; ROS = reactive oxygen species (from d'Anglemont de Tassigny et al., 2015 [255])

Altogether, the encouraging performance of GDNF in both in vitro and animal studies opened a new perspective for PD pathogenesis and therapy, and early intracerebral application of this protein was examined in human clinical trials. However, since NTFs do not cross the blood-brain-barrier, and are rapidly biometabolized in vivo, clinical application requires them to be delivered intracerebrally.

In 2003, recombinant human GDNF (Liatermin®, Amgen Inc.) was infused intraventricularly in 38-50 patients enrolled in a randomised, placebo controlled double-blind trial [268]. Unexpectedly, intraventricular GDNF delivery did not elicit significant motor improvements but resulted in strong adverse effects, such as depression, anorexia, nausea and vomiting. Postmortem analysis in one patient revealed a very poor biodistribution and bioavailability of the injected GDNF, making unlikely to elicit any effect in the striatum or SN. On the other hand, positive results were found in two open-label trials, when these studies infused GDNF directly into the putamen instead of intraventricularly [269,270]. A significant motor improvement in both on- and off-medication phases was found in patients with advanced PD, and, importantly, there was no suffering from the aforementioned severe events. Unfortunately, the success of these open-label trials were mitigated when an Amgen Inc. sponsored randomised, placebo-controlled phase II trial using intraputaminal delivery of GDNF did not reproduce the promising therapeutic effects from previous open-label trials, due to a lack of significant motor improvements between the GDNF-treated and the placebo group [271]. Indeed, this trial was prematurely halted, when it was reported that some patients enrolled in this study developed neutralizing antibodies, which could potentially cross-react with endogenous GDNF, whereas in a parallel toxicology study some monkeys developed cerebellar damage [272]. The problems derived from delivering

NTFs to brain cells across the blood-brain-barrier have hampered the progress in using these molecules as a neurorestorative trophic treatment. In fact, it seems challenging and unsustainable to treat a chronic disorder, such as PD, by a regular and rudimentary injection of high doses of GDNF directly into the brain. During these last ten years, alternative and innovative delivery methods have been developed and tested in order to exploit the benefit of the potent trophic action of GDNF on DA neurons in a more reliable manner (**Fig. 18**) (reviewed elsewhere [255]).

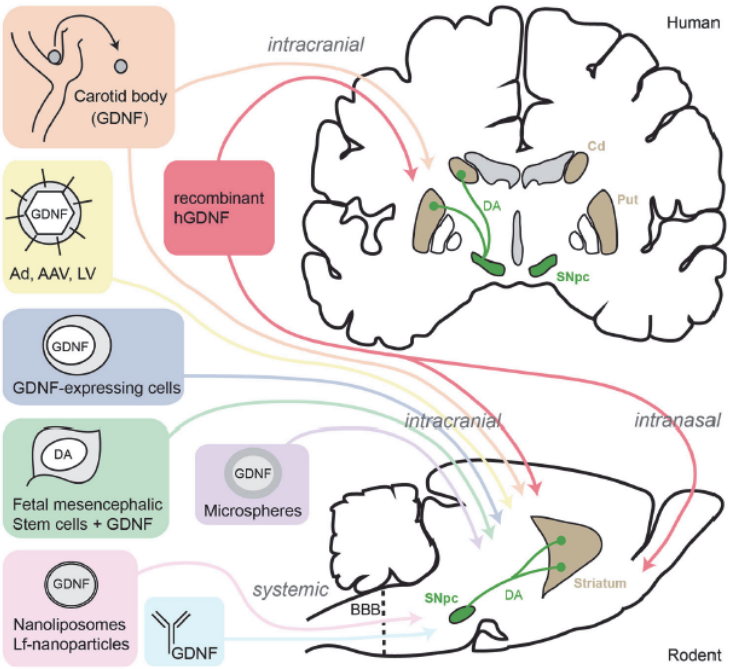

Figure 18. Schematic summary of GDNF-delivery strategies tested in human PD patients and rodent models.

Abbreviations: AAV = adeno-associated virus; Ad = adenovirus; LV = lentivirus; Lf = Lactoferrin; SNpc = Substantia nigra pars compacta; DA = Dopamine; Cd, Caudate nucleus; Put = Putamen; BBB = Blood-brain-barrier (from d'Anglemont de Tassigny et al., 2015)

It has not been until 2013, that after following a safety trial enrolling 6 PD patients, a new phase II clinical trial involving 36 patients was initiated at the Frenchay Hospital in Bristol (UK), implementing a novel infusion strategy for GDNF protein (EUCTR2013-0038). The trial is still ongoing (**Table 7**), and it uses an optimised delivery port, aiming to overcome the problems encountered in the previous trial [273].

In parallel with the studies based on delivery of GDNF peptide, considerable efforts in the preclinical stage have been made towards the development of in vivo gene transfer by recombinant viral vectors expressing the *Gdnf* gene. The vector construct harbors a cassette that contains the gene of interest, but lacks the viral genome machinery, thus impeding the virus replication and the likelihood of immune response. Therefore, the modified virus can be injected directly into the desired brain region. As aforementioned, the human chronic condition of PD requires a continuous therapy over the course of months, years or probably during the whole life of the patient, in order to sustain DA neuron survival and function [252]. Adenoassociated virus serotype 2 (AAV-2) and lentivirus (LV) are the most promising candidates to provide a sustained long-term expression of a gene such as GDNF, in the absence of troublesome inflammatory or immune reactions. In particular, AAV vectors have been successfully used for gene transfer into the brain of rodents and nonhuman primates (NHP), and are very effective in transducing neurons in the SN, GP and Striatum [274]. In addition, AAV is known to be safe in humans, many of whom already harbor the virus [252]. Interestingly, the use of AAV-GDNF have shown to protect DA neurons after toxic lesions in rodent (6-OHDA) and also successfully confirmed in non-human primates (MPTP) . Specifically, although both SN and striatal delivery of AAV-GDNF injections promote neuroprotective effects of nigral neurons, only when AAV-GDNF is transduced in the striatum, is capable to promote the preservation of the striatal dopaminergic fibers, and importantly the recovery of motor functions [275]. More important, AAV-GDNF

treatment is also effective when administered after the neurodegenerative process is initiated in both rodents and, more importantly, in non-human-primate monkeys, thus partially restoring both motor and striatal dopaminergic function. Specifically in non-human-primate monkeys, the work of Bankiewicz group has focused in the optimization of a novel AAV2-GDNF delivery [276] using a system mediated by convection-enhanced delivery (CED) [277], and have shown promising results. To date, a phase II clinical trial using this novel delivery method is currently ongoing (NCT01621581) (**Table 7**) [273].

Study/Clinical -trials.gov ID	Condition	Trial Design	Subjects enrolled	Results/Status
Nutt et al., 2003 [268]	Intraventricularly infusion delivery of GDNF (range of doses from 25 to 4000 µg/d)	Randomised, placebo controlled double-blind multi-center trial	PD patients (n=50)	No motor improvements; strong adverse effects (depression, anorexia, nausea and vomiting) after 8 months of treatment.
Patel et al., 2005 [269]	Intraputaminal bilateral direct infusion of GDNF (doses from 14,4 to 28,8 µg/d)	Open-label phase I trial	PD patients (n=5)	Sustained and progressive improvement in motor symptoms and no serious adverse side effects afer 1 year of treatment
Slevin et al., 2005 [270]	Intraputaminal unilateral direct infusion of GDNF (30µg/d)	Open-label phase I trial	Advanced PD patients (n=10)	Significant motor improvement in both on- and off-medication phases, without severe side effects after 6 months of treatment.
Lang et al., 2006 [271]	Intraputaminal bilateral direct infusion of GDNF (15µg/d)	Randomised, placebo-controlled phase II trial	Advanced PD patients (n=38)	No clinical benefit when compared with placebo-treated patients, and the presence of an immunological response against recombinant GDNF prematurely halted the clinical trial.
EUCTR2013-0038	Recombinant GDNF (9-11 mg/ml) intermittent bilateral intraputamen infusions via convection enhanced delivery (CED)	Open-label, controlled, Phase II trial	PD patients (n=42)	Ongoing Phase II, with the aim on studying the Effect on OFF-state motor function between 18 months and 9 months of treatment
NCT01621581	AAV2-GDNF (convection enhanced delivery (CED) to bilateral putamen) using 4 different doses	Single-center (USA), open-label, dose escalation safety study, phase I trial	Advanced PD subjects (n=24)	Recruiting for Safety and tolerability and several clinical measures
Marks et al., 2010 [278]	AAV2-Neurturin (injection into bilateral putamen)	Multicenter, double-blind, phase II randomized control trial	Moderately advanced PD subjects (n=12)	No significant difference between treated vs sham-surgery group.
Olanow et al., 2015 [279]	AAV2-Neurturin (injection into bilateral SNpc and putamen)	Multi-center, randomized, double-blind, sham surgery-controlled, phase II trial	Advanced PD subjects (n=51)	No statistically significant difference between treated and control grups, although significant motor-off benefits were observed in early-diagnosed PD patients, compared with late-diagnosed subjects.

TABLE 7. Summary of human clinical trials using trophic factors as a disease-modifying approach for PD.

On the other hand, preclinical studies have shown that NRTN can also promote the survival of DA neurons in culture as well as protect dopamine neurons in rodent and non-human primate neurotoxin models of PD [273]. Sharing 40% of homology with GDNF, NTRN binds to GFRα-2,

albeit at lower affinity also can bind to GFRα1. Given the variability in its distribution between animals, infusion method is not optimal for PD treatment [280–282] and therefore gene delivery of NTRN offers an interesting alternative. In particular, CERE-120, a recombinant AAV2-based vector encoding for human NTRN has been developed by Ceregene Inc. Delivery of CERE-120 to the striatum has shown long-lasting efficacy, as judged by SN cell protection, preserved innervation of the striatum, as well as behavioral recovery in the rat 6-OHDA lesion model [283]. Moreover, CERE-120 administered to parkinsonian monkeys 4 days after MPTP lesion has shown similar positive results, thus providing a long-lasting improvement in motor behavior, that persisted almost for one year [284,285].

With this promising data, Ceregene Inc. initiated a Phase I clinical trial using 12 patients with advanced PD, in order to assess safety and tolerability of CERE-120 bilateral delivery to the putamen, and no serious adverse effects were reported and a significant reduction in PD was observed (**Table 7**). Subsequently, a Phase II double-blinded trial failed to meet its primary endpoint (UPDRS motor off), although modest clinical benefit was observed [278]. Interestingly, histopathological examinations were conducted in the brains of 2 PD patients who died from non-CERE-120 related events. These patients showed clear expression of relevant NTRN levels in the putamen, but no evidence for TH induction in the SNpc, probably caused by an increased striatal DA fibers denervation, probably more exacerbated in the human advanced PD versus the preclinical toxin-induced animal models, thus causing a loss of retrograde transport in nigrostriatal neurons [252]. Consequently, Ceregene's most recent open-label trial assessed the safety and efficacy of simultaneously CERE-120 delivery to both SNpc and striatum, with no severe relevant complications found up to 24 months [286]. The success of this open-label trial led to a placebo-controlled double-blind phase 2 clinical trial with 51 patients involved (**Table 7**). Again, this trial did not show statistically significant benefit overall, but it did demonstrated significant efficacy in a small group of patients with early stage PD [279], thus suggesting the necessity for earlier intervention approaches of NTF therapy in progressive neurological diseases such as PD, if significant clinical neuroprotection or neurorestorative benefits want to be achieved.

1.5. Modeling Parkinson's Disease.

To date, despite much progress has been done in the last four decades, the understanding of the relationship of genetic targets with the cellular mechanisms that drive neuronal death in PD is still very fragmentary, thus challenging the development of new disease-modifying therapies. In previous chapters, it has been described how several molecules and trophic factors showing promising neuroprotective actions in preclinical experiments have failed to do so in rigorous clinical trials, therefore suggesting that the current models have poor predictive power to determine the human clinical success of a given drug. In fact, there are many different causes of PD that it is plausible to think that an agent that provides neuroprotection in one form of the disease will not be protective for all the patients.

On the other hand, examinations of postmortem PD brains are constrained by the fact that these samples typically represent persons who died in late stages of their disease. The molecular abnormalities found may not be representative of problems earlier in the pathogenesis, and the characteristics of neurons in these specimens may reflect the "survivors" and not those of neurons that have died. For these reasons representative cell and animal models are potentially of great value if they reproduce essential early disease characteristics.

Therefore, we have yet to develop cellular or animal models that appropriately mimic the human disease process in order to elucidate unknown mechanisms underlying PD, but also to be used as powerful drug screening and testing platforms, hoping that an eventual better prediction in the clinical trials might come from them.

1.5.1 Animal models of PD

It is remarkable to mention that an ideal animal model should recapitulate most of the features of PD, such as loss of A9 DA neurons and LB formation in a progressive and age-dependent fashion, thus presenting symptoms and alterations reminiscent of those observed in PD patients that suffer from similar genetic backgrounds. In addition, the non-motor features of the disease would be ideally also relevant. Unfortunately, such a perfect model does not exist to date [106].

Animal models of PD have been the most widely used platforms to investigate the pathogenesis and pathophisiology of this neurodegenerative condition. The first attempts at translating preclinical findings to positive clinical trial outcomes stems from toxin-based animal models, which can replicate the neurodegeneration of nigral DA neurons, typical of PD [287]. In the last decade, with the identification of PD-associated genes, genetic models for preclinical investigation have arisen, specifically the development of various mammalian (rodent and primates), as well as non-mammalian transgenic models (Drosophila and C. elegans), that replicate most of the disease-causing mutations identified for monogenic forms of familial PD. Considering the advantages and limitations of each animal model, the selection of a model allows for a potential therapy to be tested against a specific pathogenic mechanism. However, multiple models can also be used, impacting in several different mechanisms involved in PD pathogenesis (for instance, the influence of a given mutation to α-synuclein toxicity). Hence, using both toxin-based and genetic-based models to study PD can also be relevant for aspects that can be found in both sporadic and genetic forms of PD.

Neurotoxic animal models of PD

Among the different neurotoxin-based mammalian models of PD that are presently available, the 6-hydroxidopamine (6-OHDA) and the 1-methyl-4-phenyl-1,2,3,6-tetrahydropyridine (MPTP) are the best characterized and most widely used models, since they have been useful platforms for the development of therapeutic strategies aimed to treat motor symptoms and to study alterations of the basal ganglia that occur in PD.

In particular, the neurotoxin 6-OHDA is a hydroxylated analogue of DA that has been used to model PD in rats [288]. The toxin, which needs to be delivered by local injection, has a high affinity for the dopamine transporter (DAT), responsible for the transport of the toxin inside DA neurons. Injecting 6-OHDA into either the SNpc or the medial forebrain bundle (MFB) triggers a massive degeneration of the nigrostriatal pathway, reaching the highest level of nigral cell loss and striatal DA depletion achievable in PD animal models (90-100%) [289]. Alternatively, injecting 6-OHDA in the striatum [290,291] produces a more gradually human-like progressive model of nigrastriatal degeneration, which produces degeneration of 30-75% of DA neurons.

On the other hand, one classical systemic model is based on the administration of MPTP, a compound that is selectively toxic for DA neurons. Unlike 6-OHDA, MPTP crosses the blood-brain barrier and, once in the brain it is metabolized to its active form MPP+. MPP+ is internalized by A9 DA neurons through the dopamine transporter DAT and blocks the mitochondrial complex I activity, provoking mitochondrial dysfunctionalities, that eventually trigger a rapid neurodegeneration. Administration of MPTP to primates causes a levodopa-responsive parkinsonian syndrome, representing the best PD-like clinical pictures achieved in experimental animals [292]. To date, the MPTP-monkey model remains the gold standard for preclinical testing of therapeutic strategies for PD. Although MPTP can be adminstered to rodents as well, in particular rats are highly resistant to MPTP [293], and must be delivered directly as MPP+ into the SNpc. Moreover, MPTP-induced mouse brains mice display phenotypes similar to the defects observed in humans, including motor symptoms and a loss of DA neurons [294]. However, the major limitations of both 6-OHDA and MPTP is that DA neurodegeneration is not accompanied by the formation of the main neuropathological hallmark of PD, which is the presence of LB-like cytoplasmic inclusions. Nevertheless, the 6-OHDA rat model and the MPTP primate model have contributed enormously to translate animal experimentation into clinical practice, including pharmacological symptomatic treatments and

deep brain stimulation [287]. These models, along with the MPTP mouse model, are helping to elucidate the pathogenic mechanism of neurodegeneration in PD. Thanks to these models, the role of oxidative stress [295], apoptosis [296], mitochondrial dysfunction [107], and inflammation [297] have been identified as important key players in the phyisiopathology of PD. However, for instance, none of the neuroprotective strategies such as GDNF or NTRN, that have worked in the preclinical stage using these models, have thus far been sucessfully translated to a clinical setting to treat PD patients. Therefore, there is a need of a more complex physiological model that could display the main neuropathological hallmarks along with an age-dependent gradual neurodegeneration, similar to the human clinical condition.

Genetic animal models of PD

As aforementioned, the identification of monogenic forms of PD has provided noteworthy insights into the molecular pathways involved in PD etiology. Moreover, GWAS studies have also provided evidence that familial and sporadic forms of PD may converge in some aspects of the disease. These discoveries have led to the generation of different genetic models, which may prove to be a more realistic approach to study PD.

Many different species are useful for genetic manipulation, including rat, mice, *Drosophila melanogaster*, *Caenorhabditis elegans*. Different strategies have been pursued depending on the nature of the gene contribution in the PD pathogenesis. In the case of autosomal genes such as LRRK2 and SNCA, overexpression of either wild-type or mutated forms of a protein is usually performed. On the other hand, in the case of autosomal recessive genes such as PARKIN, PINK1 and DJ-1, a loss of function is found in PD patients carrying mutations in one of those genes, therefore knockout or knockdown approaches are used in this case.

Drosophila and C. elegans genetic models

Several invertebrate models, such as *D. melanogaster and C. elegans* have become popular experimental models, and they provide potent genetic tools. Their use has been extended not only to drug-screening and genetic factors or mutations that may modify neurodegeneration, but also it offers the possibility to identify evolutionary conserved pathways. α-Synuclein overexpression models of either mutated or wild-type forms in both animals provokes a selective loss of DA neurons in both animals, and particularly in Drosophila the appearance of LB-like inclusions [298]. However, these results should be interpreted cautiosly, since α-synuclein is not naturally expressed in both Drosophila and C. elegans. Therefore, the main limitations in using these invertebrates is that they lack some pathways and genes present in humans [106].

More interesting is to see that in the absence of α-syn, overexpression of LRRK2 resulted in the induction of neurodegeneration of DA neurons in invertebrates [299–301], thus suggesting that LRRK2 toxicity is independent of α-syn, thus explaining the absence of LB in some patients carrying mutations in LRRK2.

Furthermore, studies in both Parkin and Pink1 transgenic flies exhibit similar phenotypes suggesting interplay between these two genes. In addition to this, it has been described that transgenic expression of Parkin ameliorated PINK1 loss-of-function phenotypes, while transgenic expression of PINK1 did not have any effect on Parkin los-of-function animals [114,115], indicating that Parkin and PINK1 may function in a common pathway, in which PINK1 plays upstream to Parkin.

Rodent genetic models

Since the identification of *SNCA* was the first gene to be linked to familial PD, the relevance of this protein in neuronal survival and synaptic function has been highlighted with several transgenic animal models of α-synuclein. Several transgenic mouse lines, expressing wild-type or mutated *SNCA* under the control of panneuronal promoters, have been created, leading to a wide range of phenotypes, such as defective mitochondria, defective motor activity, and progressive nigrostriatal degeneration [302]. It is worth mentioning that, compared with

panneuronal *Thy1*, *Prh1* or *Pdgfa* promoters [303], non of these features were seen when SNCA was overexpressed under the control of TH promoter [304]. This suggests that PD might not originate specifically in dopaminergic neurons, and that these neurons are affected only during the progression of the disease, which would be in line with the aforementioned hypothesis of Braak and colleagues [22].

Moreover, the study of extracellular function of aggregated α-synuclein has recently increase the attention of researchers. As aforementioned, aggregated α-syn released into the extracellular space [305] can affect synaptic transmission and plasticity [306], or taken up by other neurons through endocytosis [307], thus somehow promoting the aggregation of α-syn in a prion-like fashion. Prion-like mechanisms have been observed in several animal studies designed for this aim. First evidence comes from brain homogenates of old mice expressing A53T mutant α-syn (manifestating motor disabilities and α-syn accumulation), were intracerebrally inoculated in young mice from the same line without a phenotype, and that triggered motor defects in these young animals [308]; second, as aforementioned, Recasens and colleagues demonstrated that injection of nigral LB containing pathological α-syn, that was previously purified from postmortem PD brains and subsequently inoculated into either the SN or striatum of C57BL/6J mice and rhesus monkeys, was enough to elicit a PD-like pathological process characterized by diffuse cytosolic and presynaptic accumulations of pathological α-synuclein, accompanied by a progressive nigrostriatal neurodegeneration in both mice and macaque monkeys [94].
Moreover, other novel strategies are based in allowing a fine temporal and spatial modulation of α-syn, using viral vectors. Unlike transgenic insertion, viral vector approaches allow for the targeted and differential expression of the desired transgene in a restricted brain area at a certain time. Infecting either substantia nigra or striatum of adult animals has been achieved using a single injection [309]. Lo Bianco and colleagues showed that rats lentiviral overexpression of either wild-type or the A30P or A53T mutant forms of α-synuclein in the SNpc resulted in a specific loss of dopaminergic neurons, as well as the appearance of α-synuclein inclusions [310]. In fact, the same group found that GDNF did not provide trophism in rats in which the LV-α-synuclein vector was injected into the SN. More important, Decressac et al., not only confirmed these observations [311], but also suggested that the unresponsiveness to GDNF by the nigral cells were due to an induced downregulation of Nurr1, caused by the α-synuclein overexpression, which in turn results in a reduced expression of the RET receptor [312].
Therefore, the use of α-synuclein overexpressing viral vectors constitutes a flexible mean to rapidly produce an accute α-synuclein toxicity, in order to study its effect in a restricted neuronal population, and to study their interactions with different compounds or treatments [310–312], and also the interaction with other PD-related genes, such as LRRK2 [151].

On the other hand LRRK2 models have also been a matter of study. As PD-related autosomal mutations are mostly considered as gain-of-function mutations, mice and rat overexpressing either wild-type or G2019S LRRK2 were created, and results are very variable. While mice overexpressing wild-type LRRK2 did not induce PD-relevant phenotypes, when mice were overexpressing G2019S LRRK2, they display an age-dependent reduction of dopamine release and appearance of motor symptoms, despite no dopaminergic neuron loss was observed [313]. In contrast, a different study showed dopaminergic neuron loss in mice overexpressing LRRK2 but here motor deffects were lacking [314]. Rat conditionally expressing G2019S LRRK2 have also been generated [315] and, although no signs of neuronal loss were detected, an impaired DA uptake by DAT was observed. On the other hand, adenoviral overexpression of G2019S LRRK2 driven in adult rats resulted in a progressive degeneration of nigrostriatal neurons [316].
In addition, it is worth to aformention the work of Daher et al., which recently developed transgenic rats expressing G2019S-LRRK2 from a human-derived Bacterial Artifficial Chromosome (BAC). When intranigral adenoviral overexpression of α-synuclein was induced in

adult rats, unlike the wild-type, G2019S-LRRK2 transgenic rats exacerbated neuroinflammation and dopaminergic neurodegeneration caused by α-synuclein overexpression. It is suggested that the increased toxic effect was attributed to the enhanced kinase activity associated with the G2019S mutation, since chronic administration of a potent LRRK2 kinase inhibitor abated this toxic effect [151].

Regarding the genes that cause autosomal recessive mutations, Parkin, Pink1 and DJ-1 mutant mice failed to show nigrostriatal degeneration and LB pathology [106]. However, KO mice for these genes exhibited mild alterations in the nigrostriatal circuit, as well as DA neuronal sensitiviness to oxidative stressors or insults [68]. Moreover, like in the Drosophila model, both Parkin and Pink1 transgenic animal models exhibit similar phenotypes, including mitochondrial defects [317,318], suggesting interplay between these two genes.

In conclusion, it is not currently clear the reasons why none of the genetic transgenic animal models exhibit clear PD features, such as robust neurodegeneration. In the case of LRRK2, it could be due to the fact that LRRK2 mutations are partially penetrant and the presence of other genetic factors, such as α-synuclein toxicity, or other environmental factors may be required for PD-related neurodegeneration [151]. Another possible explanation could be the activation of compensatory mechanisms during development that may prevent loss of DA neurons. However, most models are only suitable to adress one particular issue. However, the combination of different genetic and environmental factors could ultimately provide new and useful animal models of PD.

1.5.2. Cellular models of PD

The development of cellular models from human origin has become an urgent need and of particular interest for a considerable number of research groups. These models have been used for the investigation of PD-related pathogenic mechanisms, as well as useful platforms to develop and discover new drug compounds for the treatment of PD. For instance, since these models are easy-handling for genetic modifications, they can be used with the aim of deciphering concrete molecular functions of different genes and proteins responsible of the pathogenic mechanisms that take part in the PD progression. In addition, cell-based PD models have emerged as powerful tools for drug discovery. With the implementation of these models in the high-throughput screening for candidate drugs, they have permited a considerable reduction of the number of experimental animals in similar studies in the preclinical stage.

Among different cell lines established, the human neuroblastoma cell line SH-SY5Y is the most used cell line for studying neurodegeneration and neurotoxicity in the context of PD research. Derived from a metastatic neuroblastoma more than 40 years ago, this cell line can easily be expanded and further it differentiates to cells that express DA markers, such as TH, DAT, and VMAT2 [319,320]. Both neurotoxin-induced neurodegeneration and genetic modification of SH-SY5Y cells have been used in attempts to model PD. For instance, overexpression of wild-type human α-syn was shown to promote inclusion formation in SH-SY5Y cells [321]. Moreover, extracellular addition of α-syn oligomers caused transmembrane seeding of α-syn aggregation in a dose- and time-dependent manner [322]. In addition, overexpression of G2019S mutant LRRK2 caused neurite retraction and shortening in differentiated SH-SY5Y, which correlated with increased autophagy [137]. On the other hand, when using them as toxin-induced models, rotenone, MPP+ or 6-OHDA have caused the degeneration of SH-SY5Y cells, thus suggesting their use for the identification of drugs that may prevent neurodegeneration [323]. However, SH-SY5Y cells stems from cancerous origin, and they are not authentic DA neurons, being difficult to differentiate them into a post-mitotic mature dopaminergic state [324].

All in all, although these cellular models of PD, mostly based on human neuronal tumor cell lines, have provided helpful insights into alterations in specific subcellular components (such as

proteasome, lysosome and mitochondrion), the relevance of these findings for PD pathogenesis is not always immediate. These models do not, however, investigate the defective mechanisms within the predominantly affected cell in PD, the DA neuron.

1.6. Induced Pluripotent Stem Cells.

The development of human induced pluripotent stem cells (iPSC) from patient somatic cells offered a remarkable opportunity to generate disease-specific iPSC [325], with the aim to reproduce at a cellular and molecular level the mechanisms involved in disease progression in the type of cell of particular interest. The use of iPSC not only offers the possibility of addressing important questions such as the functional relevance of the molecular findings, the contribution of individual genetic variations, patient-specific response to specific interventions, but also helps to recapitulate the prolonged time-course of the disease (**Fig. 19**).

In 2007, the group of Yamanaka described a procedure of induced cell reprogramming, based in the reprogramming of human fibroblasts to a pluripotent state, after transiently ectopic overexpression of just four transcription factors: OCT4, SOX2, KLF4 and c-MYC (Takahashi et al., 2007). Subsequent studies have also demonstrated that iPSC can be generated using only three factors (OCT4, SOX2, and KLF4) [326], thus avoiding the use of c-Myc, which is considered an oncogene. This safety measure allows preventing induced-transformation processes upon eventual reactivation of this transgene. Therefore, although is less efficient than doing it with 4 factors, in the resulting reprogrammed iPSC with this procedure, less clonal variation should be caused by the absence of insertional mutagenesis caused by c-Myc.

Moreover, the efficiency of reprogramming can depend on the cell type employed. For instance, it has been reported that reprogramming efficiency starting from keratinocytes (1%) is significantly higher than starting from fibroblasts (0,01%) [327]. Human iPSC share many characteristics with human embryonic stem cells (hESC), including similarities in their morphologies, gene expression profiles, self-renewal ability, and capacity to differentiate into cell types of the three embryonic germ layers in vitro and in vivo by the generation of teratomas [328].

The “first generation” iPSC have been generated using retroviral or lentiviral transduction with vectors encoding the reprogramming factors, which can result in multiple genomic integrations of the viral transgenes. For this reason, although they are efficiently silenced at the end of reprogramming, the risk of mutagenesis and tumorigenecity that can result from these insertions make them not useful for cell therapy clinical applications [329]. However, initial proof-of-principle studies showed that they are useful for disease modelling purposes [330–332]. The residual expression of reprogramming genes can, not only create problems during cell differentiation, but overall iPSC do not need a constant overexpression of reprogramming genes. Indeed, the reprogramming process by which a somatic cell acquires pluripotent potential is not a genetic transformation, but an epigenomic one [333], therefore only a transient expression of reprogramming genes needs to be activated. Alternative methods to the retro- or lenti-viral infection, have been recently adopted. These include the use of non-integrating viral vectors such as Sendai virus [334], episomal vectors [335], protein transduction [336], or transfection of modified mRNA transcripts [337]. These methods of reprogramming are relevant in the context of any future clinical applications of iPSCs in the field of transplantable replacement cell therapies.

1.6.1. Generation of PD-Specific iPSCs.

In few years, neurodegenerative research has quickly advanced with the help of stem cell technology reprogramming somatic cells, into induced pluripotent stem cells (iPSC). An important advantage of induced cell reprogramming is represented by the possibility of generating iPSC from patients showing sporadic or familial forms of the disease. These *in vitro* models are composed of cells that carry the patients’ genetic variants, some known and others not, that are key to the contribution of disease onset and progression. Moreover, given that

iPSC can be further differentiated into neurons, this technology potentially provides, for the first time, an unlimited source of native phenotypes of cells specifically involved in the process related to neuronal death in neurodegeneration *in vitro.* Therefore, a critical issue for disease modeling with iPSC is the availability of reliable and reproducible protocols that could efficiently direct pluripotent stem cells towards the specific cell types affected in Parkinson's disease.

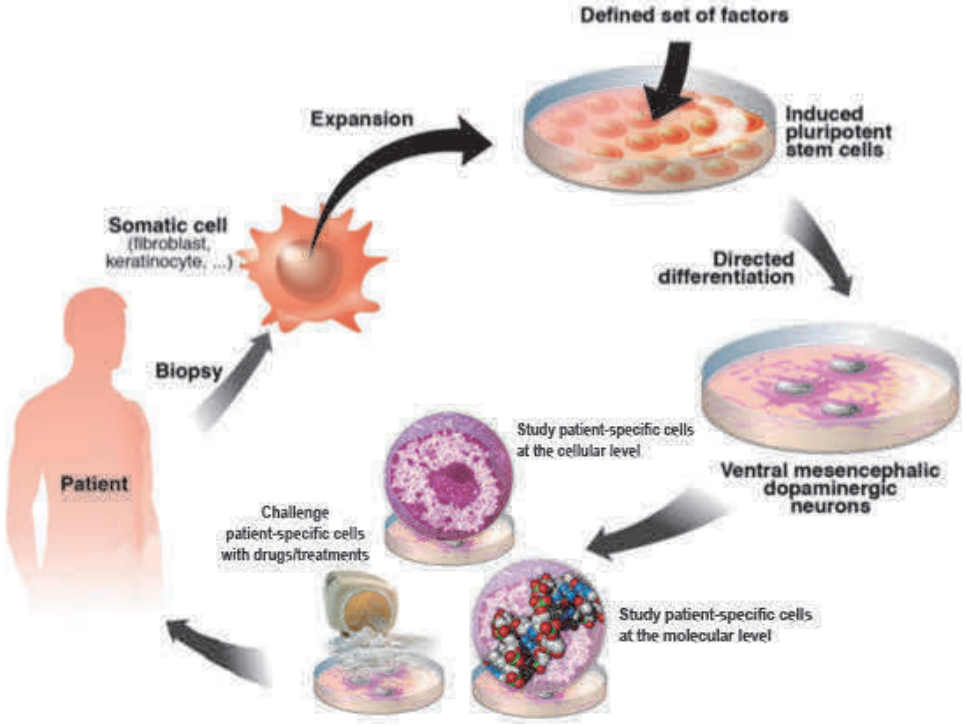

Figure 19. Generation and use of iPSC modelling in PD.

Somatic cells from a diseased patient are isolated and then reprogrammed to a pluripotent state (iPSCs). iPSCs can be maintained in culture or induced to differentiate along tissue- and cell-type specific pathways. Differentiated cells can be used to elucidate disease mechanism pathways at the cellular and molecular level, as well as for the development of novel therapies.

Indeed, at first it was unclear whether disease-specific features of neurodegenerative disorders that usually progressively appear over several years were reproducible *in vitro* over a period of only a few days to a few months. As a consequence, iPSC were initially used to model successfully neurodevelopmental phenotypes and a variety of monogenic early-onset diseases [301,330,331,338–340]. However, studies using iPSC derived from patients with monogenic and sporadic forms of PD have demonstrated the appearance of key features of PD pathophysiology when these iPSC differentiate and maturate into dopaminergic neurons. These key features comprise α-syn accumulation, autophagic clearance and mitochondrial dysfunctions, among other PD-specific pathological mechanisms [341] (see **Table 8**). Therefore, despite the typical late-onset of this disorder, these studies suggest that the key cellular and molecular pathological mechanisms may have started before the clinical onset of the disease. Moreover, several inducible factors that cause cell stress, such as mitochondrial toxins [342], long-term culture maturation [102], growth factor deficiency, or even modulated aging with induced expression of progerin (a protein causing premature aging) [343], have also been used to accelerate and reproduce the phenotypes found during disease progression. The cumulative effect of these abnormalities during disease progression, along with the effect of environmental influence, has been shown to progressively encourage neurodegeneration [102,342].

1.6.2. Modeling Sporadic and Familial PD Using iPSC.

Over the last few years, many laboratories have now successfully recapitulated in vitro some of the characteristics of PD, using iPSC as a model. However, given that PD is a progressive aging disease that affects several cellular mechanisms involving different cell types, each iPSC model highlights only some PD-associated characteristics. Nevertheless, each one of these models has helped to understand some of the fundamental underlying mechanisms as a proof-of-concept. In the last few years, iPSC-model reliability has rapidly improved and has paved the way for the discovery of new complex biomolecular interactions in the pathogenesis of PD. Thus, iPSC modeling has shown to be promising as a tool for studying new therapies in the future (**Table 8**).

Recently, iPSC-derived DA neurons carrying a triplication of SNCA have been generated [344,345]. These cells showed enhanced α-syn mRNA and protein levels [344] and increased cell death vulnerability when exposed to oxidative-stress inducers [345]. Using an iPSC model based on the rare missense A53T SNCA mutation, Chung et al. observed early pathogenic phenotype in patient-derived neurons, compared to isogenic gene-corrected controls. In particular, they observed a connection between nitrosative and ER stress in the context of α-syn toxicity. Interestingly, the levels of CHOP (CCAAT enhancer binding protein homologous protein), a component of ER stress-induced apoptosis, did not change, indicating that in this model cellular pathology was still at an early stage [346]. iPSC-derived DAn, carrying the A53T SNCA mutation, also showed α-syn aggregation, altered mitochondrial machinery, thus enhancing basal ROS/RNS production [342]. The increase of RNS production leads to S-nitrosylation of the pro-survival transcription factor MEF2 and its consequent inhibition, reducing the expression of the mitochondrial master regulator PGC1α and genes that are important for the development and survival of A9 DA neurons [347]. Interestingly, Ryan et al., postulated that the MEF2-PGC1α pathway contributes to the appearance of late-onset phenotypes in PD due to the complex interaction between environmental factors and gene expression. Indeed, when PD-associated pesticides were added below EPA-accepted levels, this was enough to exacerbate oxidative/nitrosative stress, inhibiting MEF2-PGC1α and inducing apoptosis, a late-onset phenotype [342].

Interestingly, α-syn is one of the main pathological readouts for many of the sporadic and familial PD cases that are not related with mutations in SNCA [348]. As aforementioned, the clinical link between the lysosomal storage disorder Gaucher disease (GD) and PD appears to be based on the fact that mutations in acid GBA1 gene, which causes GD, contribute to the pathogenesis of synucleinopathies [81,349]. GBA1 encodes the lysosomal enzyme β-Glucocerebrocidase (GCase), which cleaves the β-glucosyl linkage of GlcCer. Functional loss of GCase activity in iPSC-derived neurons has been associated with compromised lysosomal protein degradation, which in turn induces α-syn accumulation, resulting in neurotoxicity through aggregation-dependent mechanisms [81]. In addition, iPSC-derived neurons carrying the heterozygous mutation in GBA1 also have shown increased levels of GlcCer, changes in the autophagic/lysosomal system and calcium homeostasis, which may cause a selective threat to DA neurons in PD [349]. On the other hand, it is worth mentioning the work of Woodard and colleagues, who investigated key PD pathogical features in iPSC-derived DA neurons from two 68-year-old, monozygotic male twins carrying heterozygous *GBA* N370S mutation, with the particularity that one was diagnosed at the age of 63, and the other is asymptomathic. Interestingly, regardless of disease status, differentiated DA neurons carrying GBA N370S had significantly higher α-syn levels. Intriguingly, MAO-B levels were found increased in the affected twin, resulting in an overall decrease in DA levels and a lower DA:DOPAC ratio, although it remains unclear how MAO-B level is upregulated in the affected twin [350].

Similarly to mutations in GBA1, mutations in PINK1 and Parkin genes are also associated with early onset recessive forms of familial PD, and their mutations cause a PD characterized by mitochondrial stress as a main feature. As aforementioned, under physiological conditions, Parkin, which is localized in the cytoplasm, is translocated to damaged mitochondria in a

PINK1-dependent manner triggering mitophagy [351]. This has been confirmed in iPSC-derived DA neurons carrying a mutation in PINK1. In these cells, Parkin recruitment to mitochondria was impaired and only over-expression of WT PINK1 was able to rescue the function [352]. On the other hand, iPSC models for mutation in Parkin revealed an increase of oxidative stress. Jiang and colleagues showed that iPSC from patients carrying mutations in Parkin enhanced the transcription of monoamine oxidase, the spontaneous release of dopamine and significantly decreased dopamine uptake, increasing susceptibility to reactive oxygen species [353]. Although the incremented oxidative stress has been confirmed in a study from Imaizumi et al., they did not observe differences in monoamine oxidase expression levels. On the contrary, the oxidative stress was accompanied by a compensation mechanism that involved the activation of the reducing Nrf2A pathway [354]. Moreover, in another study, Ren et al., associated Parkin mutations with a reduction of length and complexity of neuronal processes, with a stronger impact on DA TH+ neurons. This phenotype was correlated with a dicrease in the microtubule network stability, since overexpression of parkin reverted this phenotype, thus suggesting a prominent role of parkin in stabilizing microtubules to maintain the length and complexity of neuronal processes [355]. In addition, the work of Shaltouki et al. found reduced mitochondrial fraction in iPSC-derived Parkin-mutant DA neurons, provoking a decrease in mitochondrial membrane potential, and accompanied by a reduction in the neuronal survival. Moreover, the phenotype was recapitulated also in isogenic Parkin$^{-/-}$ lines [356].

Mutations in LRRK2 have been one of the most studied mutations in PD, not only because they are the most common cause of familial PD, but also because clinical symptoms of LRRK2-PD are similar to those of idiopathic PD. The most common mutation is the G2019S, which results in hyper-activity of the LRRK2 kinase domain. Although penetrance of this gene has shown to be variable between individuals' age, iPSC model of a G2019S LRRK2-PD has recapitulated characteristic features of PD, such as accumulation of α-syn, increase in genes responsible for oxidative stress and enhanced susceptibility to hydrogen peroxide, which is displayed through caspase-3 activation [101]. Furthermore, the expression of key oxidative stress-response genes and α-syn were found to be increased in neurons from LRRK2-iPSC, when compared to those differentiated from control iPSC or hESC.
Of interest, our group has generated iPSC lines from seven patients with idiopathic PD and four patients carrying G2019S mutation in the LRRK2 gene [102]. We observed morphological alterations in PD-derived iPSC vmDAn (fewer and shorter neurites) as well as an increase in the number of apoptotic neurons over a long-time culture (75 days). Moreover, we found an accumulation of α-syn in LRRK2-iPSC derived DAn after a 30 days culture. In addition, sporadic forms of PD are not as well defined, given that they may be caused by several genetic variants, as well as a strong environmental effect. However, our study revealed that DA neurons derived from idiopathic PD patients, also showed an increased susceptibility to degeneration in vitro after long-term culture [102]. Importantly, the appearance of the neurodegenerative phenotypes in differentiated DAn from either idiopathic or LRRK2-associated PD was shown to be the consequence, at least in part, of impaired autophagy. Blockade of autophagy by lysosomal inhibition showed a specific reduction in autophagic flux by LC3-II immunoblotting, suggesting that the clearance of autophagosomes was compromised [102] (**See section 1.7. for detailed information**).
Proteins may also enter the autophagic process directly at the lysosome level, via chaperone-mediated autophagy (CMA). Increased co-localization of α-syn with LAMP2A puncta in iPSC-derived LRRK2-G2019S DAn revealed a compromised degradation of α-syn by CMA [103]. Indeed, although both wild-type and mutant LRRK2 were found to block CMA, G2019S LRRK2 protein was more resistant to the CMA-mediated degradation, resulting in accumulation of other CMA substrates, including α-syn accumulation [103]. Furthermore, a similar phenotype was induced by over-expression of wild-type or G2019S LRRK2 in control iPSC-derived cultures [102] and rescued by LRRK2 inhibition [357]. Indeed, the work of Reinhardt et al., shown that iPSC-derived DAn cultures from isogenic G2019S LRRK2 lines (mutation being the sole

experimental variable) exhibited an increased mutant-specific apoptosis and decreased neurite outgrowth, as well as alterations in the expression of several pERK (phosphorylated ERK) controlled genes, all of which could be rescued by the inhibition of LRRK2. Moreover, the genetic correction of LRRK2 mutation resulted in the phenotypic rescue of differentiated neurons with improved neurite length to levels comparable to those of controls.
Moreover, Ohta and colleagues first described the phenotypes of iPSC lines derived from patients carrying the I2020T mutation of LRRK2, which has been described to be more susceptible to post-translational degradation than WT and G2019S LRRK2 [358]. Specifically, when iPSC-I2020T were differentiated to DA neurons, those neurons exhibited reduced levels of LRRK2 protein and AKT phosphorylation, accompanied with an increased vulnerability to oxidative stress, when compared to controls. In addition, patient iPSC-derived neurons had reduced dopamine release probably caused by reduced levels of protein and mRNA levels of the SNARE proteins. More important, increased levels of tau phosphorylation were found in I2020T-neurons, consistently affected by reduced AKT levels unable to regulate kinase activity of GSK-3β, and that results were consistent with post-mortem analysis from one of the patients [359].
On the other hand, in a very recently published study, G2019S iPSC-derived DA neurons displayed the same morphological phenotypes as previously published elsewhere [102,357,360]. However, the same mutation showed a different and specific phenotype only when iPSC were differentiated to peripheral sensory neurons. Specifically, G2019S iPSC-derived sensory neurons displayed a significantly more and larger neurite cytoskeletal aggregates compared to healthy control, accompanied by impaired calcium signaling and increased levels of p62 and LC3-II [361]. Moreover, a proportion of these aggregates were positive for tau, as well as other axonal and microtubule proteins, that were likely distinct from the composition of classical α-synuclein positive Lewy bodies and Lewy neurites. These data emphasizes the specific role of LRRK2 contributing to neurite integrity by affecting microtubule stability, independently of α-syn aggregation pathology, and suggests that the observation of neurite aggregates within sensory neurons is consistent with PD patients exhibiting peripheral nervous system impairment and may be a pathological feature of PD.

1.6.3. Patient-Derived Stem Cells Could Improve Drug Research for PD.

An important goal of humanized stem cell-based PD model systems is the screening of potential new drugs that could affect the neurodegenerative process at several levels during its development in specifically affected human cells (**Table 8**). Moreover, the availability of such patient-specific stem cell-based model systems could help identifying new pharmacological strategies for the design of personalized therapies. Recently, iPSC-derived forebrain neurons have been used as a platform to screen disease-modifying drugs, highlighting the possibilities of iPSC technology as an *in vitro* cell-based assay system for AD research [362]. A recent study has also taken a significant leap towards personalized medicine for PD patients, by investigating signs of the disease in patient-specific iPSC-derived neurons and testing how the cells respond to drug treatments [360]. The study showed that neurons derived from PD patients carrying mutations in the *PINK1* or *LRRK2* genes display common signs of distress and vulnerability such as abnormalities in mitochondria and increased vulnerability to oxidative stress. However, they found that oxygen consumption rates were lower in cells with mutations in *LRRK2* and higher in cells with the mutations in *PINK1*. Notably, they were able to rescue the phenotype caused by toxins to which the cells were exposed to with various drug treatments, including the antioxidant coenzyme Q10 and rapamycin. Most importantly, the response of iPSC-derived neurons was different depending on the type of PD, where drugs that prevented damage to neurons with mutations in *LRRK2,* did not protect neurons with mutations in *PINK1* [360]. Furthermore, in the work of Ren et al. chronic treatment with taxol mimicked the effect of parkin overexpression by enhancing neurite length and complexity in patient neurons with parkin loss of function mutations [355].

Moreover, Ryan and colleagues performed a high-throughput screening (HTS) to identify molecules that are capable of protecting DAn from the toxic effect of PD-associated pesticides. They observed that the MEF2-PGC1α pathway contributes to the late-onset PD phenotypes due to the interaction between environmental factors and gene expression [342]. They performed HTS for small molecules capable of targeting the MEF2-PGC1α pathway and they identify isoxazole as new potential theraupetic drug. Isoxazole, not only drove the expression of both MEF2 and PGC1α, but also protected A53T-SNCA DA neurons from pesticide-induced apoptosis. On the other hand, Chung and colleagues investigated yeast and iPSC PD models in parallel to discover and reverse phenotypic responses to α-syn. In conjunction to what was previously reported, they showed a connection between α-syn toxicity, accumulation of NO and ER stress [346]. Moreover, they showed that the ubiquitin ligase Nedd4 and its chemical activator NAB2 can rescue the α-syn toxicity in patient-derived neurons, opening a door to a new potential drug treatment.

Furthermore, in the work of Woodard et al., WT GBA overexpression lowered α-synuclein levels in the GBA N370S twins-derived neurons, and treatment with rasagiline (MAO-B inhibitor) improved the ratio DA:DOPAC of the mDA neurons only from the affected twin, which were found to have increased levels of this enzyme [350].

Gene	Publication	Mutation	N. Patients	Isogenic controls	Cell type differentiation	Findings
SNCA	Devine et al., 2011 [344]	Triplication	1	NO	Floor-plate DAn diff. (21-30 d): 28-37% $TH^+/TUJ1^+$	mRNA doubled expression of SNCA
	Byers et al., 2011 [345]	Triplication	1	NO	DAn diff. (50 d): 6-11% TH^+	Double expression of SNCA, increased susceptibility to OS
	Chung et al., 2013 [346]	A53T	2	YES	Neuronal diff. (56-84 d): DAn yield not specified.	Increased nitrosative stress, and ER stress, reversed by adding NAB2.
	Ryan et al., 2013 [342]	A53T	1	YES	Kriks's Floor-plate DAn diff.: ~80% A9 DAn of total neurons.	Diminished spare respiration mitochondrial capacity; increased ROS/RNS and attenuation of MEF2/PGC1a neuroprotective pathway
GBA1	Mazzulli et al., 2011 [81]	N370S/84GG insertion	1	NO	DAn diff. (30d): 80% $TUJ1^+$, 10% $TH^+/TUJ1^+$	Formation of soluble α-syn oligomers, correlated by a decline of lysosomal proteolysis.
	Schöndorf et al., 2014 [349]	GBA1 (RecNcil/wt) GD (N370S; L444P)	4 GBA1 4 GD	YES	Kriks's Floor-plate DAn diff: 15-20% $TH^+/GIRK2^+/FOXA2^+/VMAT2^+$ There is also further purification of DAn by FACS	Causal relation of GBA1 mutations with increased α-syn and LB inclusions, correlated with autophagic/lysosomal system impairment
	Woodard et al., 2014 [350]	GBA N370S	Monozygotic twins: 1 symptomathic 1 asymptomathic	NO	Krik's floorplate DAn diff, and purification of the culture as described (Yuan et al., 2011): 80% of DA neurons.	Impaired α-synuclein clearance in mDA neurons carrying GBA N370S regardless of disease status. Elevated MAO-B level in the symptomathic line, impairing DA production. Overexpression of GBA and inhibition of MAO-B activity rescued α-synuclein accumulation and DA release phenotypes.
Parkin	Jiang et al., 2012 [353]	Exon 3/5 deletion	2	NO	DAn diff. (70 d): yield not specified	Loss of Parkin function; decreased DA uptake and incorrectly folded DAT protein, with increased OS susceptibility. Transduction of WT PARK2 reversed OS sensitiveness.
	Imaizumi et al., 2012 [354]	Exons 2-4 and 6,7 homozygous deletion	2	NO	DAn diff (10 d): yield not specified	Abnormal mitochondrial morphology and impaired mitochondrial homeostasis.
	Shaltouki et al., 2015 [356]	Deletions or point mutations. PARK2 KO isogenic lines	4	NO	Generation of NSC and dopaminergic differentiation as described in Swistowski et al., 2009	Alteration in mitochondrial volume, due a decrease in mitochondrial membrane potential, and accompanied by a gradual decline in the number of surviving dopaminergic neurons.
	Ren et al., 2015 [355]	Heterozygous deletions (exon 3; exon5). Homozygous deletion (exon 3)	2	NO	DAn differentiation (90 d): Protocol as described in Jiang et al., 2012	Less extensive and elaborated neuronal processes with a specifically stronger impact in TH^+ DA neurons, due to a reduced microtubule stability The phenotype was reverted by either ectopic overexpression of Parkin, or taxol chronic treatment.

TABLE 8. Summary of the described PD iPSC modeling publications.
(modified from Torrent et al., 2015 [341])

Gene	Publication	Mutation	N. Patients	Isogenic controls	Cell type differentiation	Findings
Parkin PINK1	Miller et al., 2013 [343]	PINK1 (Q456X) Parkin (V324a)	1 1	NO	Kriks's Floor-plate DAn diff. yield not specified	Loss of dendrite lenght and decreased neuronal survival, as seen by decreased p-Akt values, when exposing mDA neurons to progerin.
PINK1	Seibler et al., 2013 [352]	C1366T, C509G	3	NO	Floor-plate DAn diff.: 11-16% $TH^+/TUJ1^+$	Endogenous mutant PINK1 diminished Parkin recruitment to the mitochondrial membrane under the presence of valynomycin. WT PINK1 rescued Parkin recruitment.
(PINK1)	Cooper et al., 2012 [360]	Q456X	2	NO	DAn diff. (22 d): 35% $TUJ1^+$; 10% TH+	Increased vulnerability of neural cells to chemical stressors, with common defects in protecting against OS.
LRRK2	Nguyen et al., 2011 [101]	G2019S, R1441C	2	NO	Floor-plate DAn diff. (30-35d): 3,6-5% TH^+	α-syn accumulation, increased OS genes, and increased susceptibility to hydrogen peroxide.
	Sánchez-Danès et al., 2012 [102]	G2019S	7 Sporadic 4 LRRK2 (G2019S)	NO	DAn diff (Lentiviral-mediated forced expression LMX1A of neural precursors) (75 d): 55% $TH^+/TUJ1^+$ (Majority TH^+GIRK2^+)	Reduced neurite lenght and number. Accumulation of α-syn in LRRK2 DAn. Reduction of autophagic flux and accumulation of early autophagosomes.
	Orenstein et al., 2013 [103]	G2019S	4 LRRK2 (G2019S)	NO	As described in Sánchez-Danès et al., 2012	Blockage of the CMA degradation pathway due to accumulated α-syn with correlated increased expression of LAMP-2A.
	Reinhardt et al., 2013 [357]	G2019S	2	YES	Floor-plate DAn diff. (30-35d): 20% TH/TUJ1/DAPI	Decreased neurite lenght levels. Increased ERK activation levels, and discover of novel genes dysregulated in LRRK2 DAn.
	Schwab et al,. 2015 [361]	G2019S	2 homozygous 1 heterozygous (no onset of disease)	NO	Differentiation of peripherin-positive peripheral sensory neurons, as previously described in Fasano et al., 2010 [247]	Aberrant presence of larger neurite aggregates, specifically from LRRK2 G2019S iPSC-derived peripheral sensory neurons, accompanied by an overall increase in tau and phosphorylated tau levels. Impaired calcium signaling, accompanied by increased levels of p62 and LC3-II. Phenotype partially reverted after pharmacological inhibition of LRRK2 kinase activity.
	Ohta et al., 2015 [359]	I2020T	2 LRRK2 (I2020T)	NO	DAn as described in Imaizumi et al., 2012 [354]	Reduced levels of LRRK2 protein and AKT phosphorylation, correlated with a dysregulated kinase activity of GSK-3β, that increased levels of tau phosphorylation. Vulnerability to oxidative stress. Reduction of DA release, consistent of reduced levels of proteins related with vesicle trafficking (SNARE).

TABLE 8. Cont.

All in all, all these data encourage the use of iPSC technology as a tool to discover potential therapeutic drugs. However, concluding for what recent studies have unveiled up until now focusing only on genetic forms of PD, it remains to be determined whether this advanced technology can be used also in sporadic patients with uncertain genetic cause of the disease.

1.7. Studying Parkinson's disease with an *in vitro* human iPSC model.

The current thesis is a follow-up study based on the previously work published by Sánchez-Danès et al. [102,363].

Briefly, a total of 15 individuals have been recruited: 7 patients diagnosed with idiopathic PD (ID-PD), with no family history of disease and no known PD-related mutations; 4 unrelated patients diagnosed with familial PD carrying the G2019S mutation in the LRRK2 gene (LRRK2-PD); and 4 healthy individuals with no history of neurological disease (Ctrl). Individuals in each group were also selected so that no significant bias in gender or age occurred. Primary cultures of epidermal keratinocytes and dermal fibroblasts were established from all individuals, and were used for reprogramming at passage 2-4. By using retroviral delivery of OCT4, KLF4, and SOX2 2-6 independent iPSC lines per individual, were generated (**Table 9**). Of these, 2 lines per patient were thoroughly characterized and shown to be fully reprogrammed to pluripotency.
For the directed differentiation of iPSC toward vmDA neurons (the cell type most affected in PD), a 30-day protocol implemented in the laboratory that relies on lentiviral-mediated forced expression of the ventral midbrain determinant LMX1A, together with DAn patterning factors (Sanchez-Danes et al., 2011) was applied. Co-culture of iPSC-derived DAn on top of neonatal mouse cortical astrocytes allowed longer time cultures, after which DAn differentiated from either ID-PD- or LRRK2-PD-iPSC showed morphological alterations, including reduced numbers of neurites and neurite arborization, and accumulation of autophagic vacuoles, which were not evident in DAn differentiated from Ctrl-iPSC. Further induction of autophagy and/or inhibition of lysosomal proteolysis greatly exacerbated the DAn morphological alterations, indicating autophagic compromise in DAn from ID-PD- and LRRK2-PD-iPSC.

Overall, this study demonstrated the potential of iPSC-based technology, not only in deciphering familial-PD-related phenotypes, but also phenotypes derived from patients with an unknown genetic cause (ID-PD), thus suggesting that the cause of increased susceptibility of ID-PD-derived DAn to undergo degeneration is encoded also in the genome of ID-PD patients.
The efficient differentiation of the PD relevant cell type (A9 DA neuron), the ability to maintain DAn cultures over a long-term culture span, and the use of multiple patients per condition, which allowed controlling the inherent variability between lines, have been of relevant importance in order to achieve this work, and opened the door to use this model as a platform for the study of compounds that could prevent the appearance of the aberrant phenotypes present at long-term points.

	Patient			Disease					iPSC						
	Code	Sex	Age[a]	Age onset	Family history	Mutation	Initial symptoms[b]	LDopa response	# of Lines	Clones selected	Karyotype	Transgene silencing[c]	Pluripotency markers[c]	*In vitro* differentiation[c]	Teratoma assay[c]
CONTROL	SP09	M	66						4	SP09.2	46,XY	Passed	Passed	Passed	N/P
										SP09.4	46,XY	Passed	Passed	Passed	Passed
	SP11	F	48						3	SP11.1	46,XX	Passed	Passed	Passed	Passed
										SP11.4	46,XX	Passed	Passed	Passed	N/P
	SP15	F	47						4	SP15.2	46,XX	Passed	Passed	Passed	Passed
										SP15.3	46,XX	Passed	Passed	Passed	N/P
										SP15.4	47,XX + 20	Passed	Passed	N/P	N/P
	SP17	M	52						3	SP17.1	47,XY + 20	Passed	Passed	Passed	N/P
										SP17.2	46,XY	Passed	Passed	Passed	Passed
										SP17.3	46,XY	Passed	Passed	Failed	N/P
ID-PD	SP01	F	63	58	No	No	T and B	N/A	4	SP01.1	46,XX	Passed	Passed	Passed	Passed
										SP01.4	46,XX	Passed	Passed	Passed	N/P
	SP02	M	55	48	No	No	T	N/A	2	SP02.1	46,XY	Passed	Passed	Passed	Passed
										SP02.2	46,XY	Passed	Passed	Passed	N/P
	SP04	M	46	40	No	No	B	Good	2	SP04.1	46,XY	Passed	Passed	Passed	N/P
										SP04.2	46,XY	Passed	Passed	Passed	Passed
	SP08	F	66	60	No	No	T	Good	4	SP08.1	46,XX	Passed	Passed	Passed	Passed
										SP08.2	46,XX	Passed	Passed	Passed	N/P
										SP08.3	46,XX	Failed	N/P	N/P	N/P
	SP10	M	58	50	No	No	D	Good	2	SP10.1	46,XY	Passed	Passed	Passed	N/P
										SP10.2	46,XY	Passed	Passed	Passed	Passed
	SP14	M	55	51	No	No	B	Good	2	SP14.1	46,XY	Passed	Passed	Passed	Passed
										SP14.2	46,XY	Passed	Passed	Passed	N/P
	SP16	F	51	48	No	No	B	N/A	4	SP16.2	46,XX	Passed	Passed	Passed	Passed
										SP16.3	46,XX	Passed	Passed	Passed	N/P
LRRK2-PD	SP05	M	66	52	Yes	LRRK2	B	Good	2	SP05.1	46,XY	Passed	Passed	Passed	Passed
										SP05.2	46,XY	Passed	Passed	Passed	N/P
	SP06	M	44	33	Yes	LRRK2	T	Good	6	SP06.1	46,XY	Passed	Passed	N/P	N/P
										SP06.2	46,XY	Passed	Passed	Passed	Passed
	SP12	F	63	49	Yes	LRRK2	T	Good	4	SP12.3	46,XX	Passed	Passed	Passed	Passed
										SP12.4	46,XX	Passed	Passed	Passed	N/P
	SP13	F	68	57	Yes	LRRK2	T	Good	4	SP13.2	46,XX	Passed	Passed	Passed	N/P
										SP13.4	46,XX	Passed	Passed	Passed	Passed

N/A, information not available; N/P, test not performed.
[a]Age at biopsy.
[b]T, tremor; B, bradykinesia; D, foot dystonia.
[c]Tests performed as exemplified in Fig 1.

TABLE 9. Summary of iPSC lines generated.
(From Sánchez-Danès et al., 2012 [102]).

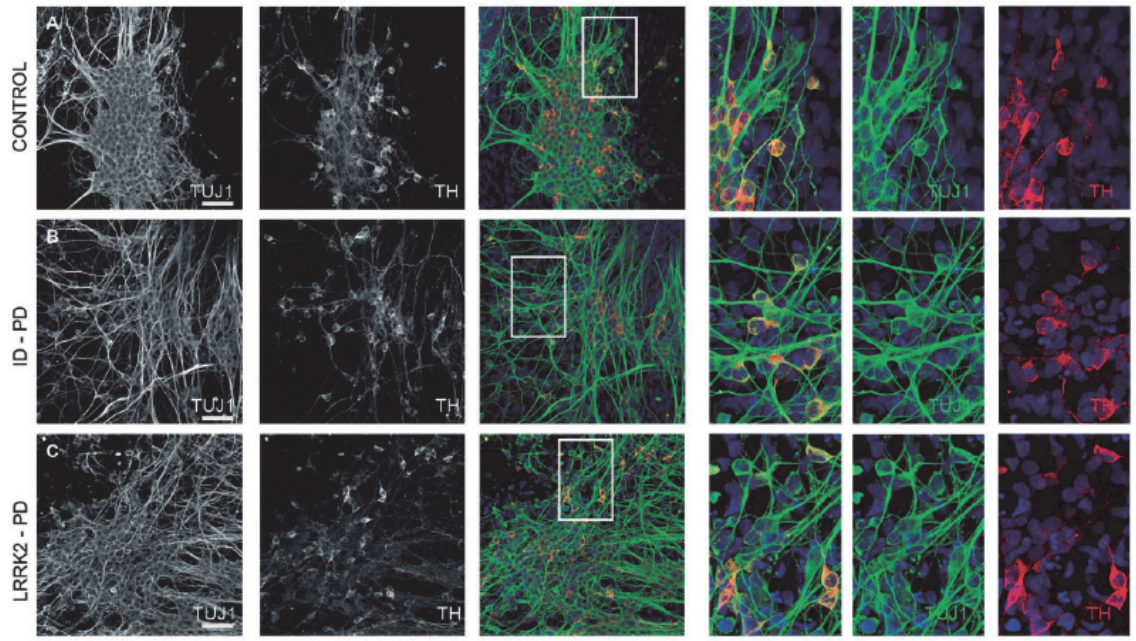

Figure 20. Differentiation of DA neurons from PD patient-specific iPSC.
iPSC derived from ID-PD, LRRK2-PD and CTL were differentiated into DA neurons for 30 days and then analysed by immunofluorescence for the expression of TUJ1 (green) and TH (red). Quantitative analyses of cells stained positive for TUJ1 (left bars) or TUJ1 and TH (right bars) show the same capacity to differentiate into neurons between different type of lines (from Sánchez-Danès et al., 2012 [102]).

Spontaneous phenotypes of PD-familial- and PD-sporadic-specific vmDA neurons.

α-synuclein immunodetection specific from LRRK2-PD vmDA neurons.

DAn differentiated from either CTL or the PD-group were morphologically and phenotypically indistinguishable after the 30-day protocol of DA neuronal differentiation in culture, in agreement with previous reported literature (**Fig. 20**) [364]. However, most DAn derived from LRRK2-PD iPSC showed diffuse cytoplasmic accumulations of SNCA (**Fig. 21**), although did not form obvious aggregates or inclusions. In contrast, the majority of DAn differentiation from CTL of ID-PD exhibited barely detectable levels of endogenous α-synuclein in their cytoplasm. These results are consistent with the previously published works in which LRRK2 and SNCA have been found to participate in intersecting pathways [47], as well as evidences highlighting the role of LRRK2 and its mutation G2019S as an accelerator of α-synuclein toxicity [151,365]. These results demonstrate the ability of iPSC-based cellular systems to recapitulate PD-related pathology and to model a monogenic form of PD.

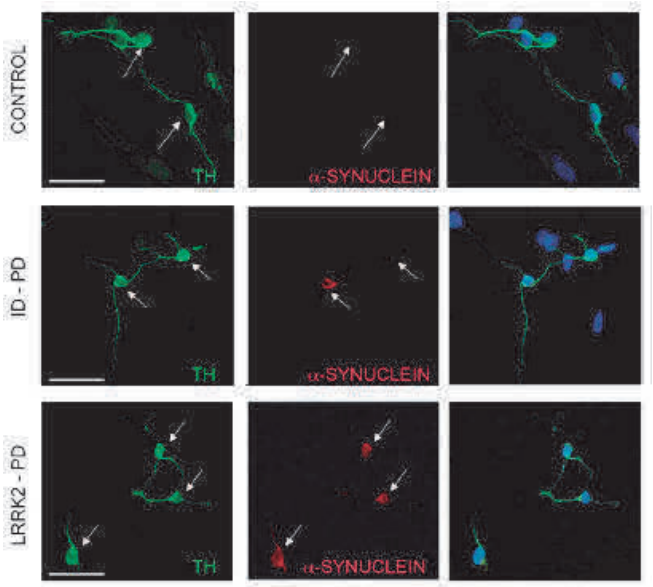

Figure 21. Abnormal accumulation of α-synuclein in LRRK2-PD vmDA neurons.
(from Sánchez-Danès et al., 2012).

Morphological alterations over long-term culture.

NPCs were co-cultured over a monolayer of primary murine cortical astrocytes (Johnson et al., 2007), thus supporting viable cultures of vmDA neurons for up to 75 days. Therefore, culture-related stress conditions generated after a long time span of the DA neuron culture was expected to exacerbate the susceptibility to degenerate of the DA neurons derived PD patients in a different manner as CTLs. In fact, DA neurons from CTL lines were morphologically homogeneous and mature, exhibiting complex dendritic arborisations. In contrast, DAn differentiated from both ID-PD or LRRK2-PD developed a range of altered morphologies over long-term culture, mostly presenting fewer and simpler processes, reminiscent of immature neurons, others with clear signs of degenerations, including very short or absent neurites, vacuolated soma, fragmented nucleus, as well as positive staining for cleaved-caspase 3 (**Fig 22A**). In fact, confocal analysis of TH neurons, demonstrated both number and length of neurites of CTL DAn were significantly higher than those from both ID-PD and LRRK2-PD.

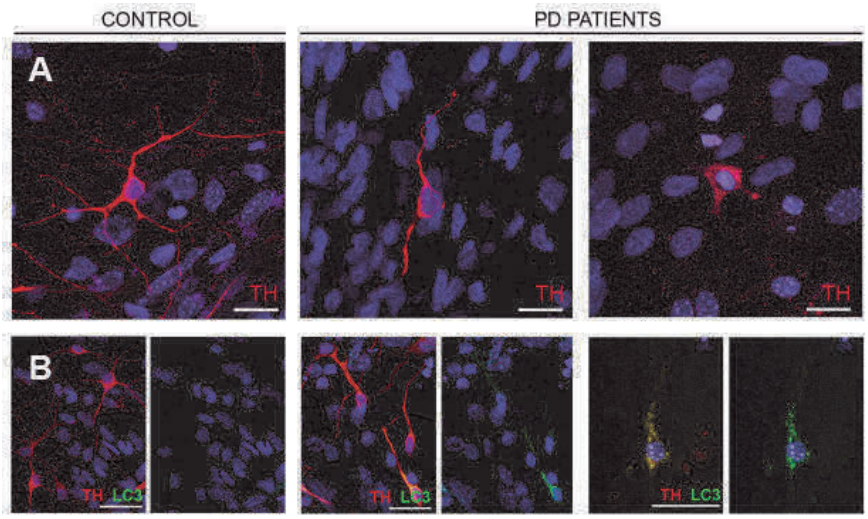

Figure 22. Disease-specific phenotypes from DA neurons iPSC-derived LRRK2-PD and ID-PD patients.

A) Morphologic alterations of either ID-PD or LRRK2-PD, showing decreased and shorter neurite arborisation.
B) Increased presence of LC3 positive autophagosomes in either LRRK2-PD and ID-PD vmDA neuons (modified from Sánchez-Danès et al., 2012 [102]).

Impaired autophagy of PD-specific vmDA neurons.

Neurite shortening has been correlated with increased autophagy [137]. Therefore, since both LRRK2-PD and ID-PD DA neurons displayed aberrant arborisation, autophagy status become a good candidate to look in detail.

At 75 days of culture, DAn differentiated from CTL showed a diffuse cytoplasmic LC3 staining with very few autophagosomes. On the other hand, a marked increase in LC3-positive puncta was evident in untreated DAn differentiated from both ID-PD or LRRK2-PD, thus suggesting either a massive upregulation of autophagosome formation, or a compromise in the clearance of autophagic compartments in these cells (**Fig. 22B**). In fact, autophagic clearance was analysed by comparing the degradation of LC3-II in the whole culture by immunoblot (LC3-flux assay). Given that part of LC3 located in the inner membrane of the autophagosome is degraded along with the cargo when these compartments fuse to lysosomes (autophagolysosomes), consequently the increase in levels of LC3-II upon blockage of lysosomal proteolysis provides information on autophagic clearance. As expected, basal-steady state levels of LC3-II were increased in the PD-derived cells, when compared to CTLs. Moreover, blockage of lysosomal degradation resulted in an increase in LC3-II in all cell lines, thus reducing siginificantly the autophagic flux in PD-derived cells. These data suggests that the increased in the abundance of LC3 in PD-iPSC-derived neurons when compared to controls was due, mainly to a blockage in their clearance. In fact, Ultrastructural analysis by electronic microscopy showed a more abundant of autophagic vacuoles prior to their fusion with lysosomes in the PD groups as well as more abundant lipid droplets, whereas in the CTL the predominant form in the CTLs was the autophagolysosome. Moreover, the defective autophagic clearance was also confirmed by a reduced co-localization between the autophagosome marker LC3 and LAMP1 lysosome markers in the PD group, in comparison with the CTL group.

Interplay of LRRK2 with chaperon-mediated autophagy (Orenstein et al., 2013).

As aforementioned in the chapter 1.3.4., α-synuclein and also LRRK2 contain a chaperone-mediated autophagy recognition motif, which enables their specific degradation via CMA pathway. A recently published paper from Orenstein et al., revealed that, as well as some A30P and A53T mutation forms of α-syn, degradation of G2019S-LRRK2, as well as other pathogenic mutations (R1441C) of this protein, is compromised. Specifically in this work, different studies

with neuronal cell lines, primary neuronal mouse cultures, and lysosomes from different LRRK2 transgenic mouse models, support the conclusion that the mutant form of LRRK2 (G2019S) binds with enhanced affinity in the presence of other substrates, interfering with the proper organization of the active CMA translocon. This leads to the accumulation of LRRK2 itself and other substrates, including α-syn, which its impaired degradation can undergo to the aggregation of toxic forms of the protein. Interestingly, part of the work by Orenstein has been done in collaboration, confirming that the LRRK2-mediated blockage of LAMP2-A was also shown in iPSC-derived DA neurons. Specifically, to adress the contribution of changes in CMA activity to the abnormally high levels of α-syn in the LRRK2-PD derived cells (Sánchez-Danès et al., 2012b), LAMP2-A was knocked down in differentiated neurons by lentiviral transduction of the GFP-tagged short hairpin RNA against LAMP2-A. Knockdown of LAMP2A in cells cultured for 75 days, increased α-syn content in both CTL and LRRK2-PD, however the proportional increase compared to untransduced cells was lower in the LRRK2-PD DA neurons, thus indicating an already compromised CMA of α-syn in these neurons [103].

2. OBJECTIVES

1. To assess the ability of some compounds, including GDNF, to prevent disease phenotypes of PD patient-specific iPSC-derived DAn

2. To evaluate GDNF expression within human DAn cultures derived from PD patient-specific iPSC as well as Ctrl-iPSC

3. MATERIAL AND METHODS.

PD patients and generation of iPSC-derived DAn.
We have used nine iPSC lines previously generated and characterized in our laboratory, as previously described [102]. Three iPSC lines have been used from healthy donors (SP09#4, SP11#1 and SP17#2) and six from PD patients: three of them had the G2019S mutation on LRRK2 gene (SP05#1, SP06#2 and SP12#3) and the other three were sporadic cases, with no familiar history of PD (SP04#2, SP08#1 and SP02#1). Expanded subject information, cell characterization, and technical details are extensively described in this precedent work [102], and it is also summarized in **chapter 1.7.1.**

For directed differentiation of iPSC to ventral dopaminergic neurons (vmDAn), we used a protocol based on the lentiviral-mediated forced expression of the vmDAn determinant LMX1A together with DAn patterning factors and co-culture with either murine cortical astrocytes or mouse PA6 feeding cells. Briefly, iPSC were transduced with LV.NES-LMX1A.GFP and processed as previously described [102,363]. iPS cells were mechanically aggregated to form EBs. EBs were cultured 10 days in suspension in N2B27 medium, consisting of DMEM/F12 medium (Life Technologies), Neurobasal medium (Life Technologies), 0.5x B27 supplement (Life Technologies), 0.5x N2 supplement (Life Technologies), 2mM GlutaMAX (Life Technologies), and penicillin-streptomycin (Life Technologies). In this stage, N2B27 was supplemented with SHH (100 ng/ml, R&D, 1314-SH), FGF-8 (100 ng/ml, Peprotech cat. no. 100-18B), and bFGF (10 ng/ml). Generated neural progenitor cells (NPCs) clumps were seeded as described in the next paragraph.

For long-term culture subjected to neuroprotective treatments, NPCs were seeded on top of post-natal mouse primary cortical astrocytes, prepared as described elsewhere [366] and maintained in N2B27 medium. When cultures reached 21 days of DAn differentiation, 3 different long-term treatments were initiated with MEK kinase inhibitors PD098059 (PD09; 10 μM; cat n. 513000, Calbiochem), and UO126 (UO; 10 μM; cat n.662005; Calbiochem), and GDNF (20ng/ml; CYT-305; Prospec). The correspondent dose of each compound was administered as described elsewhere [367–370]. Each compound was added when medium was changed, thus corresponding twice a week. DAn differentiations under long-term treatment were kept culturing until they reached 75 days of culture, and a total of 6 weeks of treatment.

For GDNF signalling studies, NPCs were seeded on top of PA6 for 21 days in N2B27 medium, as described [363]. 24 hours before the culture reached 21 days cells were treated with the same medium without B27 (Nutrient Limited Medium: NLM), to avoid interferences in the GDNF pathway by factors present in B27, such as insulin (reference). 20 ng/ml GDNF was added to the DAn culture and samples were subjected to protein extraction at different time of exposure (0 min, 5 min, 10 min, 15 min), in order to evaluate peak activation of the pathway under study.

Immunofluorescence staining.
Cells were fixed with 4% paraformaldehyde in PBS for 15 minutes. Samples were washed with TBS 3 times for 15 minutes, and blocking and permeabilization was done with TBS with 0,3% triton X-100 and 3% Normal Donkey Serum. In the case of ICC done for autophagic markers, mild permeabilization was done with TBS 0,01% Triton X-100 and 3% Normal Donkey Serum. The following antibodies were used: rabbit anti-TH (Sigma, 1:1000), mouse anti-TH (Chemicon, MAB5280, 1:1000), rabbit anti-cleaved Caspase3 (Cell Signalling 1:400), rabbit anti-GFRα1 (Santa-Cruz 1:50), rabbit anti-LC3 (Cell Signalling, 1:100), rabbit anti-PV. Secondary antibodies used were all the Alexa Fluor Series from Invitrogen (1:500). To visualize nuclei, slides were stained with 0.5 μg/ml DAPI (4', 6-diamidino-2-phenylindole) and then mounted with PVA-DABCO. Images were taken using Leica SP5 confocal microscope.

Neurite analysis.
Neurite analysis was done at the end-point of the long-term culture (75 days) on isolated iPSC-derived DA neurons differentiated on top of cortical mouse astrocytes, either treated with PD098059, UO126, or GDNF for 6 weeks, fixed and stained for TH. We randomly selected between 15-20 isolated DAn per iPSC line, so that we could unambiguously abscribe neurites to a single DAn. We took images using Leica SP5 confocal microscope, and analysed with the ImageJ plugin NeuronJ, in order to determine the number and lenght of neurites per cell.

Soma Size analysis.
Quantification of DAn neuronal bodies was done by analysing occupied cell body area by TH staining, and subsequently quantified by ImageJ software of 15 random DA neurons per line, from the fixed cell cultures at 75 days of DAn differentiation, with or without long-term GDNF treatment.

Neuronal population counting.
To assess changes in the TH+ neuron density population from the DA cultures at 75 days of culture (treated and not treated with GDNF), we selected 15-20 representative pictures taken with SP5 confocal microscope, at 40x of magnification, and we counted the number of TH+ neurons that were present per field, by using the Cell Counter Plugin from ImageJ or FIJI.
On the other hand, we also quantify the percentual proportion of TH/TUJ1 remaining at 75 days, as well as PV/TUJ1 in CTL, PD and PD+GDNF cultures, using the same plugin.

Measurement of Intracellular Reactive Oxygen Species (ROS) formation.
The dye $DCFH_2$-DA, which is oxidized for fluorescent DCF by hydroperoxides, was used to measure relative levels of cellular peroxides, as described elsewhere [369]. After long-term culture with or without GDNF treatment, 100 µl of dye in ethanol was added to the culture media at a final concentration of 500 µM, and incubated for 30 min at 37ºC. In order to obtain a dissociated culture for the ROS assay, cells were washed twice with cold PBS, and then scraped from the dish with a pipet tip into 200 µl of 1% triton X-100 in PBS. 50 µl of cell suspension was measured in triplicate by a fluorescence microplate reader at an excitation wavelenght of 485 nm and an emission wavelenght of 530 nm. The remaining 50µl from the cell suspension was used for measuring protein Bradford quantification, in order to relativize the obtained values with protein quantity of the culture. 100µl of ethanol (without $DCFH_2$-DA) was added to another cell sample to correct for autofluorescence generated by the cells. The same volume of 1% Triton X-100 buffer with $DCFH_2$-DA without cells was set up as a blank control. A positive control of the dye was assessed in a cell sample overdosed of H_2O_2. The experiment was repeated three times.

Protein Extraction and Western blotting.
Proteins were extracted from fresh pellets using RIPA protein buffer, supplemented with protease inhibitors (Roche ref: 11873580001), sodium Orthovanadate (1mM, Sigma), sodium fluoride (50mM, Sigma) and phenylmethylsulfonyl fluoride (PMSF; 100 μM). Considering all the steps at 4ºC, the lysis buffer was added to fresh pellets, and the pellet was disaggregated by making up and down, and then vortexing every 5 minutes, in a total of 20 minutes. After this, the lysate was centrifugated 5 minutes at 13200 rpm. Subsequently, Bradford quantification was done, and proteins were denaturalized in loading buffer for 5 minutes at 98ºC. Proteins were separated using SDS-polyacrilamide gel electrophoresis (SDS-PAGE) and transferred to PVDF membrane. The membrane was probed with anti-ERK and -pERK (1:1000, Cell Signaling), anti-S6 kinase and -pS6 kinase (1:1000, Cell Signalling) and α-tubulin (1:10000, Sigma T6074).

LC3 analysis.
As aforementioned, LC3 staining was performed in all samples analysed at the same time, in order to avoid variability in the LC3 signal. Furthermore, Between 15 and 20 random images of DA neurons were taken with SP5 confocal using always the same image acquisition settings. Imaging analysis were done with imageJ, using an algorythm that allowed us to count objectively the relative occupied area of LC3 in the TH+ neuron area. Furthermore, LC3 mean fluorescence intensity within the neuron was also evaluated using the same algorythm.

Detection GDNF by ELISA.
In collaboration with the Cell Therapy and Molecular Physiology laboratory group (Instituto de Biomedicina de Sevilla, IbiS) directed by professor Juan José Toledo y Aral, GDNF protein content was estimated from the culture medium of differentiated iPSC-derived DA neurons, at different time points 3 wks (21 days), 5 wks (35 days) and 9 wks (75 days). Briefly, 1 ml of medium of each culture was concentrated by centrifugation at 3800 g for 60 min at 4ºC using 3000 Da centrifugal filter devices (Millipore, Billerica, MA, USA). ELISA (enzyme-linked immunosorbent assay) was performed following the manufacturers instructions, except, as previously described, with the anti-GDNF monoclonal and anti-hGDNF polyclonal antibodies used at 1:500 and 1:250 respectively [371,372]. Absorbance at 450 nm was measured in a plate reader (Thermo Electron Corporation, Vantaa, Finland).

RT-qPCR analyses.
Total mRNA was extracted using guanidinium thiocynate-phenol-chloroform (TRIzol, Invitrogen). One microgram of mRNA was used to synthesize cDNA with the SuperScript III Reverse Transcriptase Synthesis Kit (Invitrogen). Quantitative PCR analyses were done in triplicate on 50 ng with Platinum Syber Green qPCR Super Mix (Invitrogen) in an ABI Prism 7000 thermocycler (Applied Biosystems). All results were normalized to GAPDH. The primers used were: hGFRα1-R: TGACCTTCAGACCAAACTGCTCCA; hGFRα1-F: AAACACATCCATG-CTGGGATGCAC; hRET-R: TGTACTGGACGTTGATGCCACTGA; hRET-F: TCCTCTTGCTCC-ACTTCAACGTGT; hNCAM-140-R: TCAGGATGACATCTCGGCCTTTGT; hNCAM-140-F: AAG-TGTGTGGTTACAGGCGAGGAT; hGAPDH-R: AGGGATCTCGCTCCTGGAA; hGAPDH-F: GC-ACCGTCAAGGCTGAGAAC.

4. RESULTS.

The nine lines used, derived from patients carrying the G2019S LRRK2 mutation, idiopathic PD patients and healthy controls were described previously [102] (see **chapter 1.7.**) As discussed above, in that study, was showed that over long-time culture (2.5 months), vmDAn differentiated from PD-iPSC exhibited morphological alterations, including fewer and shorter neurites, and an increase in the number of apoptotic neurons, signs that were not evident in DAn differentiated from control iPSC (**Fig. 23a**). Here we evaluated the effect of MEK kinase inhibitors PD098059 and UO126 as well as of GDNF using PD-specific iPSC derived DA neurons. With this purpose, we differentiatiated iPSC from patients carrying the G2019S LRRK2 mutation, idiopathic PD patients and healthy controls towards vmDA neurons on top of murine cortical astrocytes as previously described [102]. At 21 days of DA neuronal differentiation, healthy controls and PD DA neurons did not show any signs of disease.. At this time point, we treated the dopaminergic cultures with each compound for 75 days, the time in which PD phenotypes normally occur in patient-specific DA neurons [102] (**Fig. 23a**).
After six weeks of treatment, in each of the PD mDA neurons, treatment with MEK kinase inhibitors did not improved neuronal survival (**Fig 23b**). In particular, both UO126 and PD098059 are non-competitive MEK inhibitors, that were expected to protect DA neurons by reducing the overall kinase activity induced by the kinase gain-of-function G2019S mutation of LRRK2 in the LRRK2-PD [137,373], and by the increased susceptibility of both ID-PD and LRRK2-PD to culture-related stress conditions, such as oxidative stress, known to constitutively induce kinase cascade signaling pathways mediating cell death [374]. However, inhibition of MEK did not protect against PD phenotypes, and this could be probably due to an excessive inhibition caused by a prolonged treatment, or to a low specificity of these inhibitors against the pathways affected by LRRK2 gain-of-function mutation.

GDNF exerts a potent trophic effect in cell survival and cell differentiation in iPSC-derived patient-specific DA neurons.
On the contrary, long-term treatment with GDNF dramatically increased dopaminergic neuronal survival and differentiation in both LRRK2-PD and ID-PD, and also in CTL although in a lesser extent. First, we found that the average of TH+ neurons per field was significantly higher in the GDNF-treated PD cultures when compared with untreated PD cultures, which were below the average of the untreated healthy CTLs (**Fig 23c**). Second, we proved that DA neuronal death caused by apoptosis was also prevented in both GDNF-treated LRRK2-PD and ID-PD. Specifically, immunofluorescence co-localization of the apoptosis marker Cleaved Caspase-3 with TH among overall TH+ positive neurons was markedly absent in both GDNF-treated LRRK2-PD and ID-PD, in comparison with their untreated homologues, thus demonstrating that GDNF long-term treatment protected from DA neuronal death (**Fig 24**).

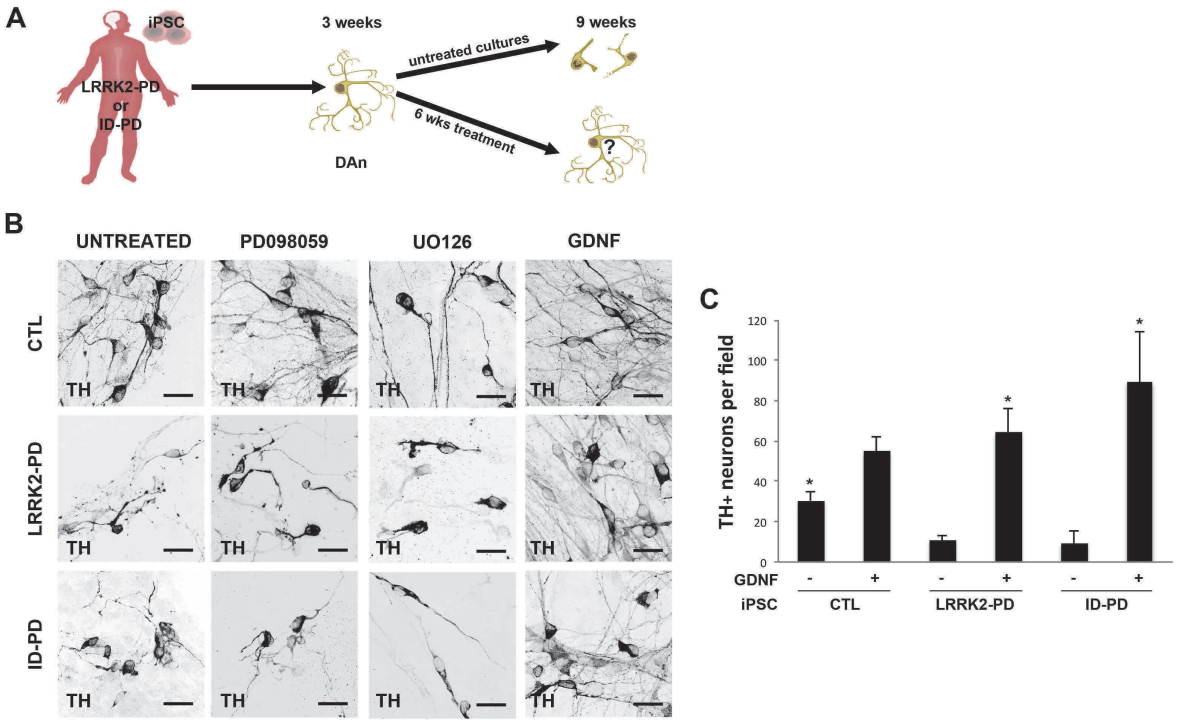

Figure 23. Long-term culture with GDNF increased neuronal survival of iPSC-derived DA neurons.

A) CTL, ID-PD and LRRK2-PD iPSC lines were differentiated into DA neurons for 21 days on top of a monolayer of post-natal murine cortical astrocytes. Then they were subsequently cultured in the presence of kinase inhibitors PD098059 (10µg/ml), U0126 (10µg/ml), and GDNF (20ng/ml), reaching 75 days in total, by the time neurodegeneration occurs.

B) Representative images of DA neurons immunostained with the specific DA marker Tyrosine Hydroxylase marker, at 75 days of culture under different treatments, or without treatment. Scale bar represent 25 µm.

C) Quantitative analyses of DA neuron population are represented by the average of TH+ neurons that are present in 15 random images from CTL (n=3), LRRK2-PD (n=3) and ID-PD (n=2), with and without GDNF long-term treatment. Asterisks denote statistically significant differences between; untreated CTL vs either untreated ID-PD or LRRK2-PD; untreated CTL vs GDNF-treated CTL; untreated LRRK2-PD vs GDNF-treated LRRK2-PD; untreated ID-PD vs GDNF-treated ID-PD. Data are presented as mean ± s.e.m (*p<0,05).

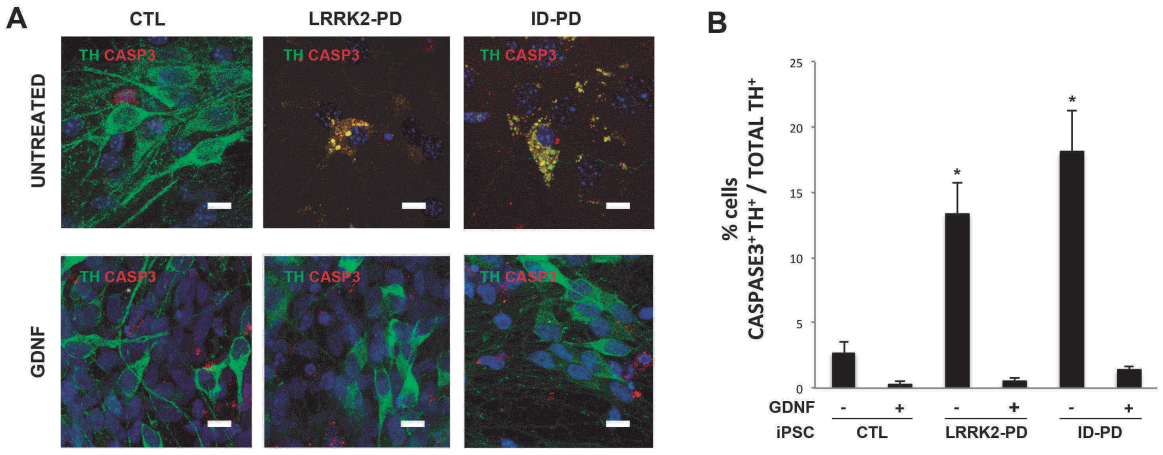

Figure 24. GDNF promotes cell survival of human DA neurons.

A) Immunofluorescence analysis of DA neurons differentiated from PD iPSC cell lines for 75 days, with or without long-term GDNF treatment, co-stained for TH (green), apoptotic marker Cleaved Caspase-3 (red), and DAPI (blue). Scale bars represent 10 µm.

B) Quantitative analysis of the percentage of DA neurons at day 75, double positive for CASP3 and TH, among total DA neurons (TH^+) with and without long-term GDNF treatment. Analysis was performed by taking 15-20 images in SP5 confocal microscopy per each line (Control n=2; ID-PD n=2, and LRRK2 n=2), and by making the average in each line per condition. Asterisks denote statistically significant differences between: untreated CTL vs either untreated ID-PD or LRRK2-PD; untreated LRRK2-PD vs GDNF-treated LRRK2-PD; untreated ID-PD vs GDNF-treated ID-PD. Data are presented as mean ± s.e.m. (*p<0,05).

GDNF neuroprotective signal transduction on iPSC-derived patient-specific DA neurons. Since GDNF was exerting a potent trophic effect on cell differentiation and cell survival, it was important to assess that DA neurons express the receptor machinery in order to trigger specifically these trophic actions. Interestingly we found that the GDNF receptor (GFRα1) is present in the differentiated DA neurons by the time we started the protective treatment (21 days) (**Fig. 25a**). Moreover, RT-qPCR experiments revealed that both GFRα1 and RET progressively increase their expression during the long-term treatment with GDNF when compared with untreated samples at their respective time-points (**Fig. 25b**). On the other hand, the alternative pathway that involves the coupling of GFRα1 and NCAM-140 [257] could be involved in a lesser extent, since NCAM-140 expression values remain stable if compared with RET expression.

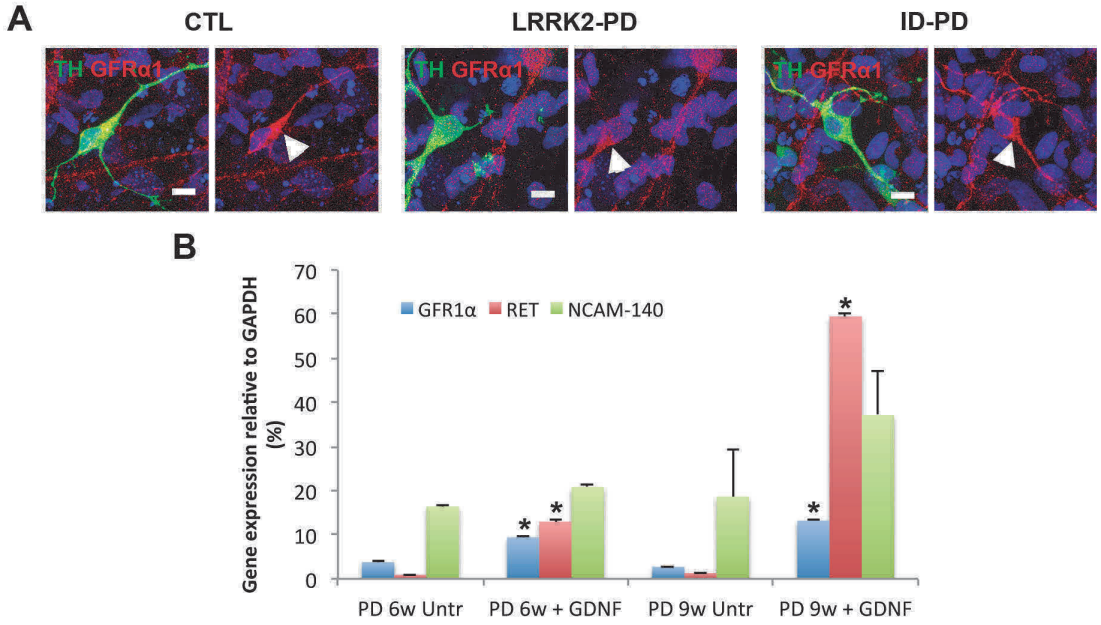

Figure 25. Expression of the GFRα1-RET complex in DA neuronal cultures.
A) Immunofluorescence staining of DA neurons at 21 days of culture on top of a monolayer of PA6. DA neurons were co-stained for TH (green), GDNF receptor GFRα1 (red), and DAPI (blue). Scale bar represents 10μm.
B) RT-qPCR analysis of the expression levels with or without GDNF long-term treatment, of the GDNF receptors GFRα1, RET and NCAM (cell line SP04# 2). Data is represented in triplicates. Asterisks denote statistically significant differences between untreated vs long-term GDNF-treated at 6 and at 9 weeks of DAn differentiation. Data are presented as mean ± s.e.m. (*p<0,001).

In addition, we confirmed the GFRα1-RET downstream activation of both PI3K/Akt/mTORC1 and RAS/ERK1-2/MAPK after GDNF exposition [253–255]. In particular, by adding GDNF at 21 days of DAn differentiation culture, and extracting protein at different time points, immunoblot analysis showed that ERK1-2 pathway is quickly transiently activated, and its activation peak is approximately of 6 fold-increase in both CTL, and PD DAn cultures, compared with non-exposed samples (**Fig. 26a-b**). It is important to note that transiently activation of ERK1-2 has been shown to be neuroprotective [375,376], as it has been demonstrated that triggers cell survival by stimulating the activity or expression of anti-apoptotic proteins [377]. On the other hand, sustained activation of ERK can trigger an accumulation of death-promoting factors, thus leading to apoptotic cell death, which is not observed in this case [376,378]. Moreover, AKT pathway was also found activated in both CTL and PD cultures, as demonstrated by approximately a 2 fold-increase activation of a downstream effector of this pathway, p70 S6 kinase (p70 S6K) (**Fig. 26c-d**). Specifically, AKT also induces cell survival by inhibiting the activity of apoptotic proteins [377]. In addition, the phosphorylation of p70 S6K has been used as a marker of activation of mTOR, whose activation is known to suppress autophagy by

inhibiting the ULK complex, responsible of the preautophagosomal structures, that lead to the complete formation of macroautophagosomes [379]. Given the reported dysfunctional autophagy clearance in this model [102], and that mTORC1 is active after GDNF exposure, influence of GDNF in regulating autophagy clearance was suggested to be another of the protective benefits of this molecule (See below).

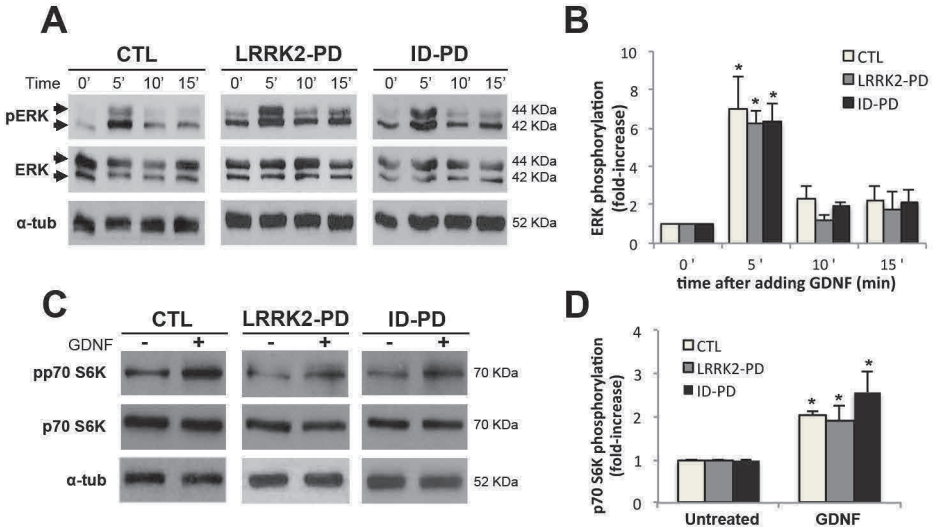

Figure 26. GDNF activation of both GFRα1-RET downstream pathways MAPK/ERK1-2 and PI3K/Akt/mTOR in DAn cultures.

A-B) Western Blot of ERK activation signalling pathway. DAn differentiations at 21 days, were exposed to 20ng/ml of GDNF, and pellets were collected at different times after GDNF exposition, in order to check transient activation of ERK pathway. Blots have been analysed with ImageJ software (NIH), by densitometry quantification. Experiments were done in triplicate, and data is presented as mean ± s.e.m, *p<0,05.

C-D) Activation of AKT downstream pathway p70 S6 Kinase in controls and both ID-PD and LRRK2 DAn differentiation at 21 days of culture after 5 minutes of GDNF exposition. Experiments were done in triplicate, and data is presented as mean ± s.e.m. *p<0,05.

GDNF prevents from neurite denervation of iPSC-derived patient-specific DA neurons.

As well as neuronal survival and cell differentiation, GDNF trophic actions are also well known to promote neurite outgrowth [10,253–255]. In fact, at day 75, long-term GDNF patient-specific DA neurons are characterized by longer and arborised neuronal processes that innervate different neuronal areas of the culture, a feature that was unfrequently found in their untreated homologues. Specifically, neurite number and length quantification resulted in a notable maintainance in the complexity and elongation of the processes of patient-specific DA neurons that were long-term cultured with GDNF, achieving similar values as the untreated DA neurons from healthy CTL (**Fig. 27a-c**). In addition, an increase in the soma area was also observed **(Fig.28 a-b)**, a trophic effect that has also been described elsewhere [380].

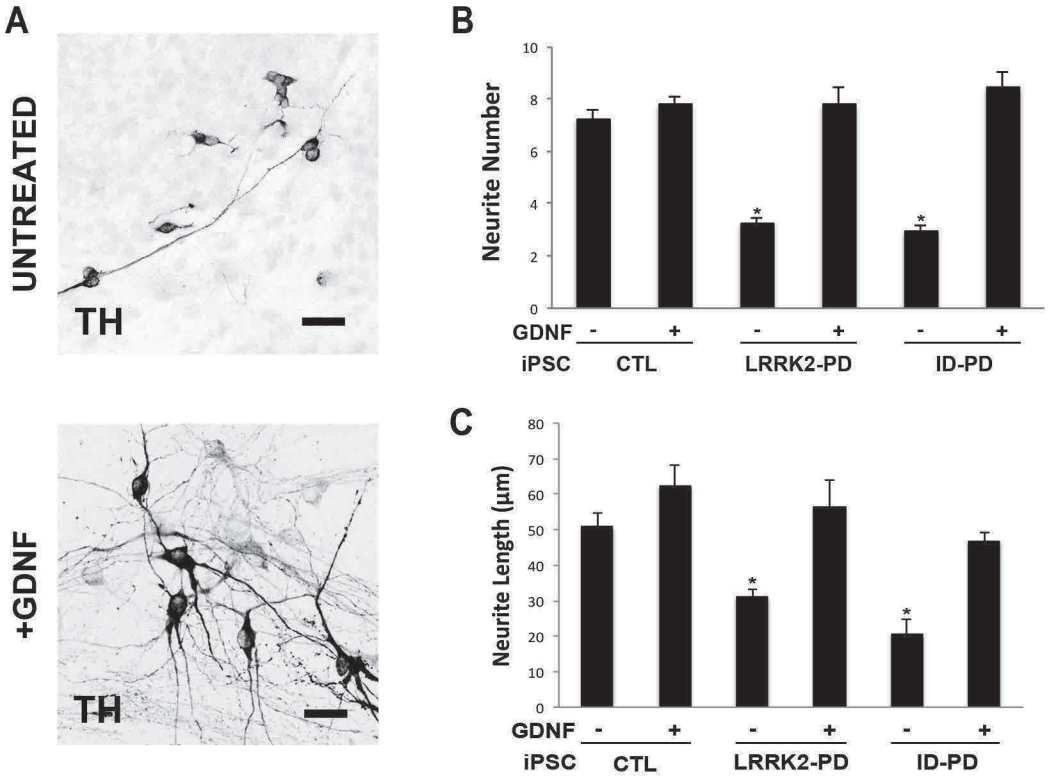

Figure 27. Immunofluorescence analysis of neurite length and number after GDNF treatment.

A) Representative images after 75 days of DAn differentiation, untreated (ID-PD: SP04 #2) and long-term GDNF-treated (LRRK2-PD: SP05 #1). Scale bar represents 25 µm.

B) Quantitative analysis of neurite number in DA neurons differentiated for 75 days of culture with and without long-term GDNF treatment. Data for each condition is the average of neurite number in a DA neuron, and it has been analysed respectively in 3 CTL lines (not treated: 99 DAn; GDNF: 48 DAn), 3 LRRK2-PD lines (not treated: 76 DAn; GDNF: 54 DAn) and 3 ID-PD lines (not treated: 88 DAn; GDNF: 51 DAn). Asterisks denote statistically significant differences between: untreated CTL vs either ID-PD or LRRK2-PD; untreated LRRK2-PD vs GDNF-treated LRRK2-PD; untreated ID-PD vs GDNF-treated ID-PD. The data show mean ± s.e.m. neurite number, measured with NeuronJ plugin of ImageJ software (NIH) (*p<0.001).

C) Quantitative analysis of neurite lenght in DA neurons differentiated for 75 days with or without long-term GDNF treatment. Data for untreated and GDNF-treated CTL is the average of 570 and 378 neurites, respectively from 3 different lines; for untreated and GDNF-treated of 3 LRRK2-PD lines is 251 and 411, respectively; and for untreated and GDNF-treated of 3 ID-PD lines is 288 and 464, respectively. Asterisks denote statistically significant differences between: untreated CTL vs either ID-PD or LRRK2-PD; untreated LRRK2-PD vs GDNF-treated LRRK2-PD; untreated ID-PD vs GDNF-treated ID-PD. Data show mean ± s.e.m in µm, measured with NeuronJ plugin of ImageJ software (NIH) (*p<0.001).

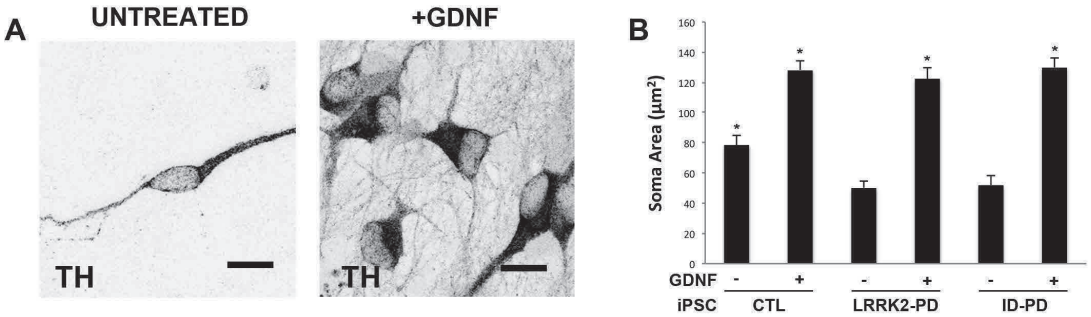

Figure 28. Immunofluorescence analysis of soma size after GDNF treatment.

A-B) Cell bodies from 15 random TH+ DAn neurons (3 CTLs, 3 LRRK2-PD and 3 ID-PD), at 75 days of culture were quantified with ImageJ software (NIH). Values represent the mean soma area ± s.e.m in μm^2. Scale bar 10 µm. Asterisks denote statstically significant differences between; untreated CTL vs either untreated LRRK2-PD or ID-PD; untreated group vs GDNF-treated group of each iPSC line. (*p<0.001).

GDNF-induced neurite outgrowth is related with the prevention of macroautophagic vesicles accumulation in iPSC-derived patient-specific DA neurons.

Autophagy has been shown to play key roles in maintaining neurite length [137,381], and there is evidence that deregulated autophagy may be a pathogenic mechanism of PD [382]. mTOR signalling cascade is also related to neurite elongation and branching in the central nervous system [383]. Given that we have demonstrated that GDNF protects from DAn neurite degeneration, and that mTOR is active, as judged by the phosphorylation of p70 S6K, we wanted to assess if GDNF has also an influence in terms of autophagosome clearance. Interestingly, at day 75, LC3, a marker of autophagic vesicles, has an increased relative presence inside the soma and neurites of patient-specific DA neurons [102], as well as increased mean fluorescence intensity of its signal. In contrast, long-term GDNF-treated patient-specific DA neurons were found with fewer LC3 expressing vesicles, similar to the levels found in the untreated healthy CTLs, as well as lower mean fluorescence intensity (**Fig. 29a-d**). These results suggest that GDNF protects from dysfunctional autophagosome accumulation in patient-specific DA neurons, therefore preventing their susceptibility to degenerate.

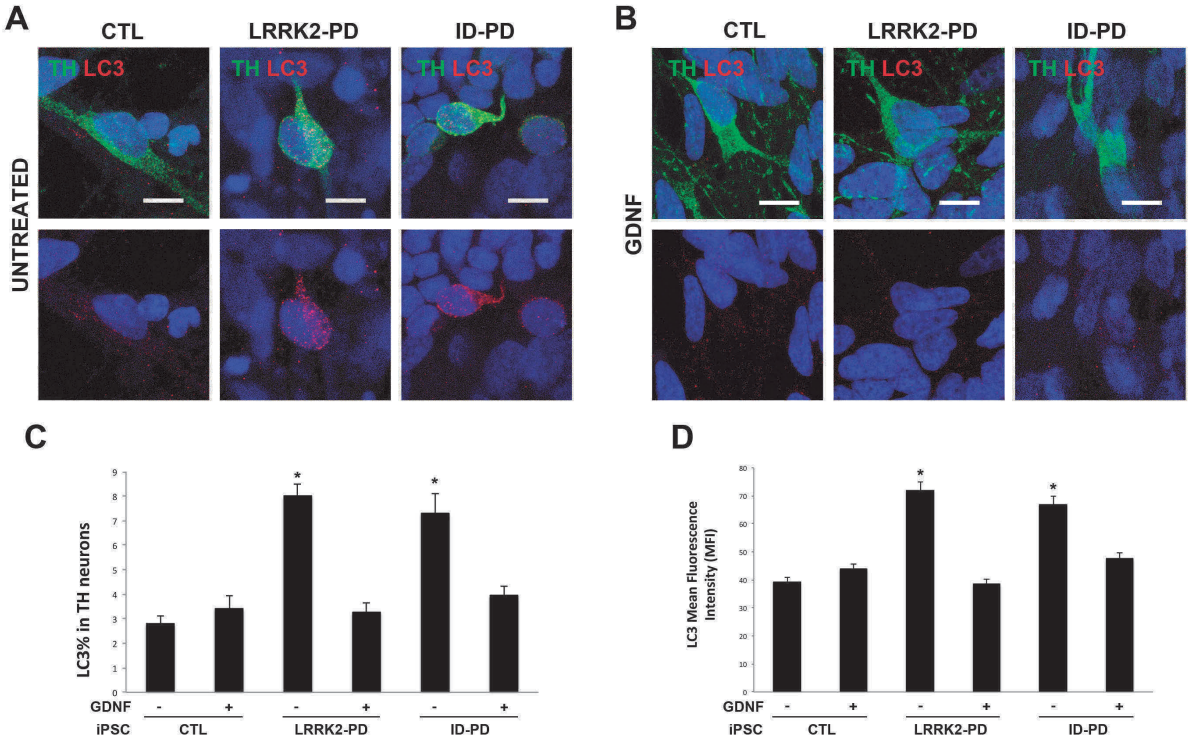

Figure 29. Long-term PD GDNF-treated DAn differentiation cultures reduce accumulation of LC3^{+} autophagosomes.

A-B) Representative images of the presence of aggregated forms of LC3 in PD DA neurons cultured for 75 days. Preventive treatment with GDNF reduces this aggregated forms that we show in untreated PD samples. Immunofluorescence of TH (green), LC3 (red) and DAPI (blue) were performed all in the same day to avoid differences in the emission of the fluorescence of the samples. Scale bars, 10 µm.

C-D) Quantification of LC3 presence in TH+ neurons. between 15 and 20 images of random DA neurons were taken with SP5 confocal using always the same image acquisition settings. We count first the relative occupied area of LC3 in the neuron area. Given that image acquisition settings used were the same for all the samples, we also quantified the LC3 mean fluorescence intensity within the neuron. 2 CTL, 2 LRRK2-PD, and 2 ID-PD DAn differentiations were used for this analysis. Asterisks denote statistically significant differences between: untreated CTL vs either untreated LRRK2-PD or ID-PD; untreated LRRK2-PD vs GDNF-treated LRRK2-PD; untreated ID-PD vs GDNF-treated ID-PD. Data are presented as mean ± s.e.m. (*p<0,01).

GDNF prevented from ROS generation in iPSC-derived patient-specific DA neuronal cultures.

Moreover, we have also demonstrated the antioxidative properties of GDNF [263,265,369]. We used the dye $DCFH_2$-DA, a molecule that reacts with intracellular peroxides releasing a fluorescent signal that can be subsequently detected. At day 75, we exposed untreated and GDNF-treated DAn cultures to $DCFH_2$-DA, and we found that patient-specific DA neuronal cultures have almost twice of ROS levels relative to the levels found in healthy untreated CTLs. However, preventive treatment with GDNF showed a significant prevention of this ROS generation, thus suggesting that GDNF also protects DA cultures from culture-stress conditions such as oxidative stress (**Fig. 30**).

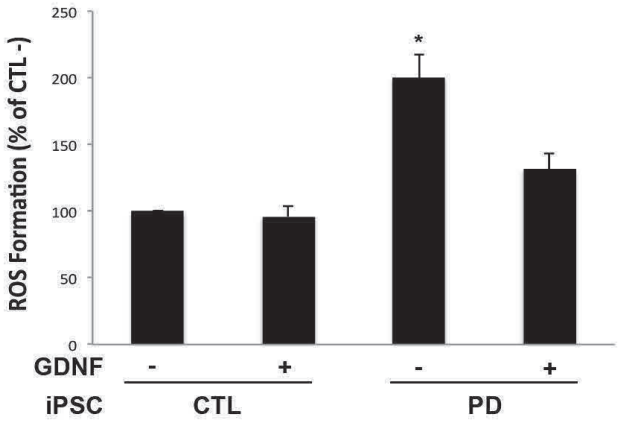

Figure 30. GDNF long-term treatment prevented ROS formation in patient-specific DAn cultures.

Asterisk denotes statistically significant differences between: Untreated CTL vs Untreated PD; Untreated PD vs GDNF-treated PD (*p<0,01). Experiments have been perfomed three times, in triplicate, with two CTLs, one LRRK2-PD and one ID-PD.

Study of the endogenous contribution of secreted GDNF within iPSC-derived patient-specific DA neuronal cultures.

Protective treatment with GDNF has shown to prevent PD DA neurons from cell death, neurite denervation, dysregulated autophagy and ROS formation. Given that some of these features were described in this model [102], we hypothesized that different endogenous GDNF expression and secretion within the DA cultures could influence iPSC-derived patient-specific DA neurons to degenerate. In order to answer this question, we collected medium supernatants at different time points of the DA neuronal differentiation on top of murine cortical astrocytes (3, 5, and 9 weeks). In collaboration with the Cell Therapy and Molecular Physiology laboratory group (Instituto de Biomedicina de Sevilla, IBiS) directed by professor Juan José Toledo y Aral, ELISA quantification of these supernatants was performed. Results from these experiments revealed that, at 75 days of culture (9 weeks), both LRRK2-PD and ID-PD DAn cultures showed a 2-fold lower content of secreted GDNF when compared with healthy CTLs (**Fig. 31**). These data confirmed our hypothesis, and suggest that a decreased GDNF content in patient-specific DA cultures could be in part responsible for the higher susceptibility of patient-specific DA neurons to degenerate *in vitro*.

Moreover, we investigated the type of cell possibly responsible in producing and secreting GDNF within the DA cultures. Interestingly, Hidalgo-Figueroa et al. demonstrated that the 95% of GDNF produced in the rodent striatum is produced by PV^+ interneurons, a type of GABAergic neurons that represent only ~0,7% of neostriatal neurons [384]. Based on these recent findings, we investigated whether PV^+ neurons were differently present between PD and CTLs. Here, we show that at day 75, PV^+ neurons were completely absent in patient-specific PD DA cultures.

However, PV^+ neurons in Ctrl DA cultures at day 75 (**Fig. 32a-b**) were found, although they were scarce, when compared with the absolute values of the overall population of TH^+ or $TUJ1^+$ neurons (**Fig. 32d-f**). Interestingly, absolute values of TH^+ and $TUJ1^+$ neurons in patient-specific DA cultures are significantly lower when compared with CTLs. Therefore, we suggest here that not only TH+ neurons die at day 75, but also the overall neuronal population of cells might be compromised as well. In fact, when we analysed the neuronal population of patient-specific DA cultures that underwent a long-term GDNF treatment after 75 days, we found that this treatment helped to preserve the neuronal networks and, surprisingly it promoted the generation of PV neurons within the culture (**Fig 32c, d-f**). This finding is notably promising, because it highlights the importance of studying other neuronal types that might have relevant and still unknown roles in the onset and progression of PD.

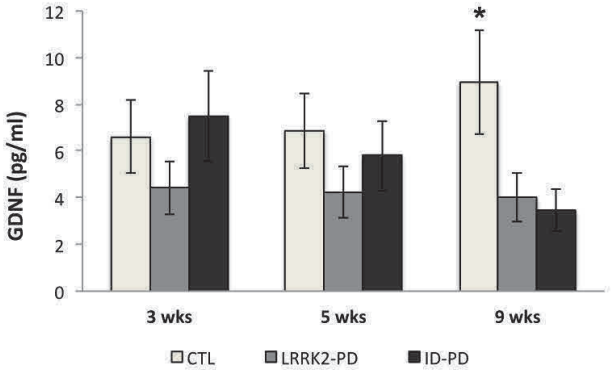

Figure 31. Long-term DAn differentiation cultures doubled the concentration of GDNF compared with ID-PD and LRRK2-PD samples.

A) ELISA analysis of supernatants at different time points. Asterisk denotes a statistically significant difference of GDNF concentration at 9 weeks between CTL vs either LRRK2-PD or ID-PD (n=15; *p<0,05).

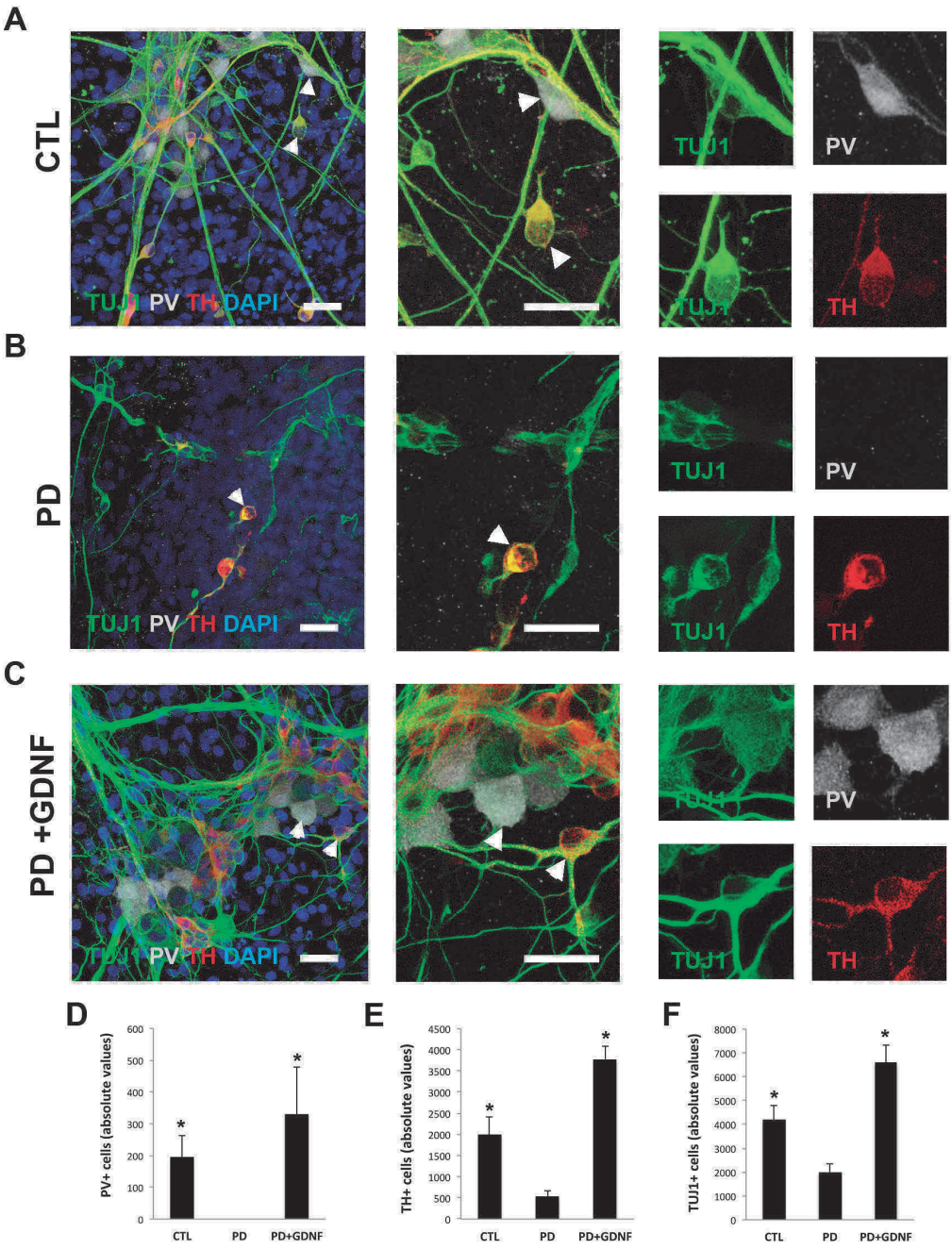

Figure 32. Parvalbumin neurons may have a protective role in DA neurons.

A-C) Representative images of iPSC-derived neuronal cultures at 75 days of DAn differentiation: untreated CTL, untreated PD and long-term GDNF treated PD (TUJ1 green, TH red, PV grey, and DAPI blue)**.** Scale bar represents 25 µm.

A) Representative image of a DA culture of a healthy CTL (SP09 #4) at day 75, showing a neuronal network composed by $TH^+/TUJ1^+$ positive neurons, $PV^+/TUJ1^+$ neurons, as well as other unidentified neuronal lineages ($TUJ1^+$).

B) Representative image of a patient-specific PD line (SP12 #3) at day 75, showing a modest neuronal network, characterised by the absence of $PV^+/TUJ1^+$, and the presence of fewer $TH^+/TUJ1^+$ neurons, as well as other unidentified neuronal lineages ($TUJ1^+$).

C) Representative image of a DA culture of a long-term GDNF-treated patient-specific PD line (SP05 #1) at day 75. The culture shows a major systemic improvement, characterised by a complex neuronal network, composed by the presence of $PV^+/TUJ1^+$, and increased presence of $TH^+/TUJ1^+$ neurons, as well as other unidentified neuronal lineages ($TUJ1^+$).

D-F) Quantitative analyses of neuronal population (PV+, TH+ and TUJ+ cells) in absolute numbers at day 75, (untreated CTL n=3; untreated PD n=4; and long-term GDNF-treated PD n=2). Asterisks denote statistically significant differences between: CTL vs PD; and PD vs PD+GDNF (*p<0,05).

5. DISCUSSION.

iPSC-modeling in PD: Application for the study of neuroprotective strategies.

In this thesis, we have implemented a recently published human iPSC model of LRRK2-G2019S familial and sporadic PD [102], for the study of different compounds in the prevention of the appearance of *in vitro* PD-related cellular and molecular phenotypes.

The obvious advantage of studying PD using patient-specifc iPSC, is that cells are from human origin, and therefore, they carry the precise human genetic background that may lead to the onset of the disease. Moreover, our method of neuronal differentiation, based on the forced lentiviral overexpression of LMX1A in neural progenitors, results in the efficient generation of DA neurons. In addition, the generated DA neuron population is enriched in the A9-subtype [363], which is the predominant subtype of DA neurons in the SNpc and it has also been demonstrated that this subtype is more prone to degenerate than other DA neurons such as the A10-subtype from the ventral tegmental area (VTA) [10,385]. Therefore, any disease-related cell phenotype that has been identified with this approach can be extrapolated to the clinical manifestations and progression of the disease.

In summary, this model recapitulates the pathological features of PD, since DAn differentiation of either LRRK2-PD and ID-PD over a long-term culture is characterized by morphological alterations comprising DA neuronal loss, reduced neurite arborisation, as well as dysfunctional autophagy, that are not evident in the healthy controls [102]. It is worth to mention that, in this model, the 75-day time-span in the cultured neurons is critical for the appearance of these PD-related phenotypes. Hence, culture-related stress conditions are thought to influence in the susceptibility of PD-iPSC-derived DA neurons to degenerate *in vitro*, thus somehow mimicking *in vivo* DA neuronal aging of PD patients, which has been demonstrated to be the most important PD-related risk factor.

On the other hand, at the early time point of DA neuronal differentiation (21 days), both ID-PD and LRRK2-PD DA neurons are morphologically similar to healthy CTLs. However, at this time point only LRRK2-PD DA neurons are found to accumulate a diffuse cytoplasmic α-synuclein accumulation [102], which could indicate of a LRRK2-G2019S-specific pathological mechanism that may start before the onset of the disease.

Given the likelihood that any disease-modifying drug for PD will need to be taken on a continual, life-long basis, assessment of efficacy and safety of a drug that will be administered chronically is crucial. Hence, since either PD or CTL DA neurons are morphologically undistinguishable at this time point, we hypothesized that starting a long-term chronic treatment at an early time, a compound that might be beneficial for PD DA neurons should confer neuroprotection against the susceptibility to degenerate, induced by culture-related stress conditions. Therefore, with this strategy, we pursued the prevention of the appearance of the aberrant phenotypes found after 75 days of DA neuronal differentiation.

The observation that the common G2019S mutation of LRRK2 causes a gain of function of the kinase activity suggests that altered phosphorylation of downstream LRRK2 targets may have a pathological outcome. This made us hypothesize that DAn derived from LRRK2-PD patients could be treatable with chronic exposure to kinase inhibitors, thus attenuating the overall upregulated phosphorylation of LRRK2 downstream pathways, such as the MEK1-2 kinases. In particular, G2019S-LRRK2 has been found to trigger neuritic autophagy and reduced neurite shortening in SH-SY5SY cells, and this was attenuated with the addition of the MEK1-2 UO126 inhibitor [137]. Moreover, excessive oxidative stress caused by the 6-OHDA in B65 cells also triggered a sustained kinase activation that was related to the activation of cellular pathways committed to cell death [374]. Therefore, previously published data suggested that abnormal patterns of kinase activation, either induced by G2019S mutation or the influence of the environment may contribute to DA neuronal cell death [137,373,374].

However, although the doses used of both PD098059 and UO126 were used between the range of other previous studies that used these molecules [137,367,368,373,374,386], in this model the chronic inhibition of MEK1-2 signaling does not protect against the appearance of PD phenotypes. Hence, future studies should target specifically LRRK2 protein, as it has been successfully performed in, for instance, the work of Reinhardt et al., *in vitro* [357], or the recently published study of Daher et al., *in vivo* [151]. More important, studying the correct range of doses of a given compound in order not to abate completely the physiological activity of, for instance LRRK2, is a question that should be considered in future studies [216].

On the other hand, one of the most important advantages of working with this model is that, to date, this cell-based model is still one of the fewest that has successfully attempted at modelling idiopathic PD through iPSC technology [102]. Although sporadic PD represents a heterogeneous category of disease-causing mechanisms, the result of a complex interaction between unknown gene susceptibility and environmental factors (in this case culture-related stress conditions), at least in the cases studied, has led to the same result of DA neuronal degeneration and loss. Moreover, PD directly attributable to LRRK2 mutations, specifically the G2019S, is typically indistinguishable from sporadic PD cases, potentially indicating common pathogenic pathways. Therefore, using a trophic factor such as GDNF, which is known to have such multifunctional benefitial properties [253–255], seemed a good candidate in order to protect both LRRK2-PD and ID-PD DA neurons from long-term aberrant PD phenotypes.
Indeed, GDNF long-term treatment has protected both LRRK2-PD- and ID-PD-derived DA neurons to degenerate. Specifically, long-term GDNF-treated patient-specific DA neurons increased neuronal survival, as well as neurite outgrowth and arborisation. In terms of morphology our data is consistent with previous studies in vivo [265,267,380] and in vitro [258,369]. Indeed, we found that GDNF activates both GFRα1-RET downstream pathways PI3K/Akt/mTORC1 and RAS/ERK1-2/MAPK, thus leading to neuritogenesis, neuronal survival, and cell differentiation.

On one hand, activation of the RAS/ERK1-2/MAPK pathway has been found to increase neuritogenesis [253,254], and to induce neuronal survival and differentiation by directly stimulating the expression of different prosurvival genes, including anti-apoptotic proteins, such as B cell lymphoma-2 (Bcl-2) [377], thus protecting neurons from apoptotic cell death. Moreover, after the addition of GDNF, we show that the RAS/ERK1-2/MAPK pathway is rapidly and transiently activated after acting on midbrain DA neurons, a mechanism that has been previously described elsewhere [376]. Moreover, RAS/ERK1-2/MAPK pathway was found more activated than PI3K/Akt/mTORC1 (6-fold vs 2-fold). We suggest that, given that we show that NCAM-140 is expressed within the culture, the activation of an alternative pathway involving the coupling of GFRα1-NCAM140, could be the cause of a more pronounced activation of this pathway, since this alternative pathway has also been described to activate ERK1-2 through the phosphorylation cascade of Fyn and FAK proteins [254].
On the other hand, PI3K/Akt/mTORC1 pathway was found active through the analysis of a downstream effector that is a substrate of the activated form of mTORC1: p70 S6 Kinase (S6K). In particular, whereas ERK1-2 promotes cell survival by directly stimulating the expression of prosurvival genes, Akt is thought to suppress apoptosis by inhibiting the activities of pro-apoptotic proteins of, for instance Forkhead or Bad, indirectly by suppressing GSK-3 apoptotic activities, thus increasing IAP-1 and IAP-2, Bcl-2 or Bcl-XL levels [377]. Moreover, intrastriatal infusion of GDNF has been found to prevent lactacystin-induced DA neuron loss by inhibiting the pro-apoptotic molecules Jun N-terminal kinase (JNK) and p38 and activating the pro-survival Akt and MAPK pathways [387].

Importantly, this model previously demonstrated that DA neurons from patients presented defects in autophagy clearance and found a correlation between neurite retraction and

autophagy impairment in disease-specific DA neurons. Indeed, many neurodegenerative diseases have been assocaited with defects in the autophagy compartment [388], and the correlation between neurite retraction and activation of autophagy has been previously described [137]. The phosphorylation of S6K has been used as a readout for the acivation of mTOR, whose activation is known to suppress autophagy by inhibiting the ULK complex, which is responsible of the preautophagosomal structures, that lead to the complete formation of macroautophagosomes [379]. In addition, mTOR signaling cascade is also related to neurite elongation and branching in the central nervous system [383]. Therefore, a contribution of the long-term treatment of GDNF in preventing the accumulation of LC3 positive autophagic vesicles within the disease-specfic DA neurons was also expected, as the results show.

Furthermore, since culture-related stress conditions are suggested to influence in the susceptibility of PD-iPSC-derived DA neurons to degenerate *in vitro*, we hypothesized that by the end of the day 75 of culture, patient-specific DA neurons should have increased ROS levels compared with CTL lines. Indeed, we have demonstrated that patient-specific DA neurons have almost twice of ROS levels relative to the levels found in healthy untreated CTLs. On the other hand, GDNF long-term treatment can promote antioxidant defense mechanisms against ROS, since there is a significant prevention of ROS generation in patient-specfici DA neurons that almost reached the levels found in untreated CTLs. In fact, in previous studies striatal GDNF administration moderately enhanced the activity of certain enzymes involved in the enzymatic detoxification of ROS, comprising superoxide dismutase, catalase and glutathion peroxidase [389]. Moreover, in several animal models of PD using mitochondrial toxins, which are based in the increase of oxidative stress and mitochondrial dysfunctionality, preventive treatment with GDNF has been shown to protect the nigrostriatal pathway [275]. Specifically, GDNF administration in the rat striatum prevents 6-OHDA-induced ROS formation [390], and it has also found to protect in vitro hESC-derived DA neurons from MPP+ toxicity, in part by attenuating the formation of ROS and caspase-3 activation [369].

It is worth to mention that GDNF delivery by either AAV or LV vectors was not effective in preventing or minimising neurodegeneration caused by the overexpression of α-syn with AAV-α-synuclein vector in rodent models [311]. Specifically, overexpession of α-syn showed to downregulate the expression of Nurr1, and subsequently the GDNF receptor RET, thus reducing the availability of the receptor and consequently blocking the intracellular signalling response to GDNF in the striatum [312]. This study highlighted the fact that GDNF treatments would not be the first choice to treat advanced PD patients with a high degree of synucleopathy and, also important, with reduced concentrations of Nurr1, or mutations in the Nurr1 gene, as it has been described elsewhere [391–393].
However, in this model we did not address differences of Nurr1 expression between CTL and both LRRK2-PD and ID-PD. Moreover, we suggested that the increased cytoplasmic α-synuclein staining found in the early time point in LRRK2-PD DA cultures [102] is probably not sufficient, or not containing a toxic α-syn predominant form able to block the activation of GDNF signaling pathways. In fact, the degree of activation of both AKT and ERK pathways in the LRRK2-PD is the same as the ID-PD and the healthy CTLs. Therefore, we suggest that further studies should address the response of GDNF to patient-specific DA neurons at later time points in which already compromised phenotypes, such as increased accumulation forms of α-synuclein, could differently modulate the degree of its trophic response. Hence, in addition to its known neuroprotective role, these studies could help to understand whether GDNF also has a rescue role in a more reliable physiological background than the AAV-α-syn overexpression rodent models.

Endogenous expression of GDNF.

It was proposed that changes in the levels of neurotrophic factors, such as GDNF, due to alterations in the activity, release or synthesis, associated with ageing or genetic factors, might be involved in the neurodegenerative process of PD [394,395].

However, postmortem studies analysing the distribution in the human parkinsonian brain have yielded conflicting results. On one hand, in situ hybridization studies failed to detect GDNF mRNA in the human midbrain [396], and no significant differences were found in GDNF content in the caudate-putamen and SN between PD and control samples [397]. On the other hand, using immunohistochemistry, large reductions in GDNF content are reported in surviving PD SN neurons [398], and more recently, using rt-PCR, modest but significantly increased levels of a GDNF isoform were found in the putamen of PD patients with marked nigral neuronal loss [399].

Interestingly, our data shows that by the end of the 75 day of DA differentiation, endogenous levels of GDNF within the DA culture of patient-specific lines are significantly 2-fold decreased when compared with healthy CTLs. Although our model doesn't represent the vast complexity of the brain or for instance the nigrostriatal pathway, the results obtained suggest that a lack of GDNF trophic support might be, in part, responsible for the aberrant phenotypes found at 75 days after long-term DA differentiation. Moreover, the concentration levels of GDNF were accurately measured by ELISA [371,372] in the magnitude of pg/ml. However, it should be noted that GDNF expression in neuronal tissues is commonly lower than that of peripheral organs, like for instance the kidney [254]. Consistently, Mogi et al measured GDNF protein levels by ELISA in lysates of different regions of the brain and found that GDNF concentration was also found in a low range of values, that varied between 10–70 pg/mg total protein, depending on the analysed brain region [397]. However, whether alterations in GDNF synthesis and release have any causative pathogenic role in PD is still poorly understood.

Parvalbumin neurons and GDNF production.

On the other hand, given that we found differential endogeneous levels of GDNF between CTLs and PD DAn cultures, we wanted to understand the nature of the cells that could be producing GDNF in the culture. However, immunostaining analysis of GDNF expression performed with antibodies are challenged by specificity considerations [255].

Interestingly, the use of the mouse *GDNF-LacZ* model has been of great value in order to adress the GDNF expression in the adult mice brain [261]. In particular, the *LacZ* expression driven by the *Gdnf* promoter, and subsequently revealed by X-gal staining (β-galactosidase activity), has revealed that GDNF expression in the adult mouse brain is restricted to the dorsal and ventral striatum, and there is no expression in the SN [262]. Interestingly, GFRα1-Ret share distinct patterns, and are broadly expressed in the adult CNS, a fact that can explain the appearance of adverse effects in previous clinical trials when GDNF was delivered intraventricularly [268]. Moreover, although GDNF receptor mRNAs are not detected in the striatum, they are highly expressed in the SNpc [400], thus indicating that in the striatum GDNF may specifically act on SNpc DA neurons that conform the nigrostriatal pathway, and is retrogradely transported to their cellular bodies in the SNpc [401], and therefore no other striatal cells seem to benefit from its trophic action.

So far, the identity of the striatal neurons expressing GDNF is not completely defined, and the site and mechanisms of GDNF as well as the signals regulating GDNF production are also basicaly unknown. However, the aforementioned use of the GDNF-LacZ mouse model has demonstrated that almost 95% of the GDNF positive striatal neurons are Parvalbumin (PV) GABAergic interneurons, and in a much lesser extent choinergic (ACh) or somatostatinergic (SS) interneurons [384]. Moreover, in contrast with previous works suggesting a role in the glia (astrocytes and microglia) in producing GDNF after local brain injury [402], in the Gdnf-LacZ mouse model none of the GDNF expressing cells are of astrocyte or microglia origin, even after 7-21 days after MPTP lesion [384].

More surprisingly, PV GABAergic neurons represents only approximately ~0.7% of all striatal neurons [403], in contrast with medium spiny projecting neurons (MSNs), which represents almost the 95% of the rodent striatal neurons. However, the particular condition of the PV interneurons makes them prone to be responsible in GDNF expression. In fact, PV interneurons are sparsely distributed over the striatum, and their striatal topology coincided with the area innervated by dopaminergic terminals from the SNpc [404]. PV neurons are “fast-spiking” cells, thought to constitute a unique network that is highly interconnected by electrical synapses due to dendrodendritic gap junctions, which enable them to fire almost synchronously [405], thus providing trophic support to neighboring neurons such DA terminals with their soma in the SNpc (**Fig. 33**). In fact, PV neurons are thought to be a target of choice for pharmacological modulation of GDNF expression [255].

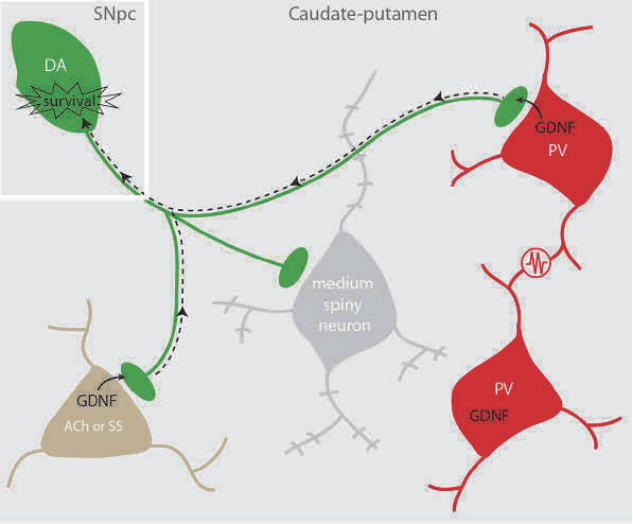

Figure 33. Protection of the dopaminergic nigrostriatal pathway by striatal GDNF.
Dopaminergic (DA) neurons (green) located in the SNpc innervate the caudate putamen to modulate the activity of GABAergic medium spiny neurons (gray), parvalbumin (PV)-positive interneurons (red) and other cholinergic (ACh) or somatostatin (SS) interneurons (brown). PV neurons form an ensemble of synchronized cells through multiple dendrodendritic electrical synapses (resistance in the scheme), and release GDNF at the nerve terminals to provide trophic support to DA neurons via retrograde signaling (dotted arrow) (Modified from d’Anglemont de Tassigny et al., 2015 [255]).

However, despite these recent advances in the identification of GDNF-producing interneurons in the rodent striatum, the nature of the cells that produce GDNF in the human striatum remains as yet unidentified. Moreover, given the low percentage of PV that may participate in the secretion of GDNF we were skeptical in finding PV neurons in our DA cultures. Nevertheless, we have shown that PV neurons can be found in our culture when analysed at day 75, although they were scarce and, most important, they were only found in CTLs, in which endogenous GDNF levels were found 2-fold increase when compared with PD DA cultures. Specifically, at day 75 absolute values of the neuronal population of CTL DA cultures revealed an increased number of neurons when compared with PD DA cultures, comprising predominantly TH neurons and in much lesser extent PV neurons. Moreover, since the overall neuronal population in PD DA cultures is compromised if compared with CTLs, we suggest that this is probably affecting the proper maturation of the neuronal culture, thus impeding the generation of PV neurons. In fact, when we treat PD DA cultures with GDNF, it helped to protect and improve the overall neuronal population and, surprisingly, it promoted also the generation of PV neurons within the culture.

Nevertheless, since we could not address by immunofluorescence if the generated PV neurons were secreting GDNF in our culture, the connection between the presence of PV neurons in CTL cultures and higher levels of GDNF is modest, and further studies need to address this question. Nevertheless, these data is importantly promising and it strongly encourages the study of other neuronal and neural cell types that could influence in the onset and progression of PD.
In fact, to date, no studies have been performed analysis in the status of striatal PV interneurons in postmortem PD brains. In contrast, PV neurons have already been the aim of the study in other neurological diseases such as Hungtington Disease (HD) and Tourette Syndrome (TS) [406–408]. First, Reiner et al. have shown in postmortem studies that PV striatal

interneurons are rapidly lost in HD, and that the progression of loss from motor striatum coincides with the dystonia emergence of this disease [406]. Second, Kataoka et al. also showed a depletion of PV cells in the striatum of postmortem TS brains [407]. Interestingly, both studies show that PV neurons are not abundant in the striatum of human normal brains as it was shown in the mice striatum [384]. Third, a TS family study revealed a common genetic variant in the *GDNF* gene, associated with the disease, and they suggested a possible connection between impaired production of GDNF and depletion of PV neurons in TS [408]. Hence, further studies should address the status of PV neurons in postmortem PD brains, which will give some clues in how this type of neuron can affect the progression of PD. In addition, using iPSC technology in order to study different neural types [409,410], might help in understanding the different roles that specifically each brain cell type has in the maintenance and survival of the DA nigrostriatal pathway and in the pathogenesis of PD.

Future directions.

Despite all recent advances in the research of trophic therapies, disease-modifying therapies using either GDNF or NTRN, still have not demonstrated their efficiency in more complex clinical studies. The reasons are likely multifactorial, including technical delivery issues [271,278], and also due to unanticipated biological complexities probably caused by the advanced stage [279], and due to synucelopathy toxicity that mitigates the activity of neurotrophic factors [312]. Moreover, in advanced PD patients, the degeneration of the striatal terminals to nigral cell bodies, are thought to impair an effective retrograde transfer of GDNF to the SNpc [411]. However, after almost one decade since the last clinical trial with GDNF, currently new clinical approaches based on new technologies for GDNF protein delivery are arising and incoming results from them will be heard in the coming year (**Table 7**).

Importantly, a major possible inconvenient of viral vector delivery gene therapies is that transferred genes could be uncontrollably overexpressed. Indeed, GDNF can lead to GDNF-induced cerebellar toxicity [412], thus masking the potential benefits of GDNF [413]. Therefore, pharmacological modulation of GDNF-expressing viral vectors that could express it in a more physiological manner, although still in its initial stages of development, is particularly attractive when considering new therapeutic approaches to protect nigrostriatal degneration and concomitantly prevent adverse effects from sustained high GDNF delivery [255].

As aforementioned, between 30-50% of DA neurons are lost during the first year of PD diagnosis, and this percentage increases dramatically after 4 years of the first diagnosis, reaching almost the 90% of them [6]. This dramatic feature has obvious implications for the timing of clinical trials that test neuroprotective treatments such as trophic therapies.

In fact, our model has demonstrated that, in an early time-point, iPSC-PD-derived DA neurons do respond cellular and molecularly to the neuroprotective long-term chronic treatment of GDNF in multifactorial ways, comprising neurite outgrowth, increased cell survival, reduced ROS levels and prevented the accumulation of macroautophagic vesicles.

On the other hand, the clinical study from Olanow et al., using AAV-NTRN delivery in both SNpc and caudate did demonstrate significant efficacy in a small group of patients with early stage PD [279] (**Table 7**). This suggests the necessity for earlier intervention approaches of neurotrophic therapy in progressive neurological diseases such as PD, if significant clinical neuroprotection or neurorestorative benefits want to be achieved.

Therefore, early intervention will be crucial for success. In fact, improving early diagnostics, as well as moving to a diagnosis prior to the emergence of movement impairment, will be key to developing effective new treatments. For effective therapies, stratification of PD patients according to their aetiology is also crucial as these may vary between patient groups. It seems plausible that not one single but a combined therapy is required to effectively combat cell degeneration and restore neuronal functions in PD.

Finally, advanced PD patients should not lose hope in finding a cure for PD. To date, different targets have emerged in the research of disease-modifying therapies that eventually will be able to fit the needs of each condition [203,273]. For instance, it is worth noting that PD patients that suffer from acute synucleopathies in a long future they might be able to benefit from α-syn-targeted immunotherapies that may have the potential to attenuate neuroinflammatory-associated neurotoxicities, as well as α-syn accumulation in the brain.
Moreover, independently of the levels of α-synuclein, advanced PD patients suffer from a massive loss of DA neurons. Therefore, restorative therapies to improve their condition probably have to go through cell replacement therapies combined with the addition of an adequate trophic support to help in reinnervating the affected parts of the brain, such as the striatum. CRT, although still in its initial phases, in which safety and efficiency issues are still a matter of debate, should be available not in a very long future. In addition, with better and safer GDNF delivery approaches on the way, restorative therapies in advanced PD patients should not be considered utopic.

6. CONCLUSIONS.

1. We have implemented the use of iPSC-derived patient-specific DA neurons for the study of neuroprotective strategies.

2. GDNF long-term chronic treatment is neuroprotective in iPSC-derived patient-specific DA neurons. Specifically, GDNF has shown to:

2.1. Increase neuronal survival by preventing neuronal death and promoting DA neuronal differentiation.

2.2. Increase neurite elongation and arborisation of DA neurons.

2.3. Activate cell survival pathways PI3K/Akt/mTORC1 and RAS/ERK1-2.

2.4. Protect from the accumulation of macroautophagic vesicles in DA neurons.

2.3. Prevent ROS generation in DA cultures, thus protecting from culture-stress conditions, such as oxidative stress.

3. We found a 2-fold-decreased in the endogenous GDNF levels within the long-term DAn differentiation cultures from both LRRK2-PD and ID-PD cultures. We suggest that a lack of GDNF in our culture could be responsible in part of the increased susceptibility of PD-related DA neurons to undergo neurodegeneration.

4. We suggest that the increased presence of GDNF in CTL is due to the specific presence of Parvalbumin neurons in the DA neuronal cultures. PV neurons are thought to be the main type of neuron that secrete GDNF in the striatum. However, further studies based in the analysis of postmortem PD brains, as well as the use of iPSC technology towards the differentiation of other neronal types such as GABAergic PV interneurons, are needed to study the specific contribution of this neuronal type in the maintenance and survival of the DA nigrostriatal pathway and in the pathogenesis of PD.

7. REFERENCES

1. Lees, A. J.; Hardy, J.; Revesz, T. Parkinson's disease. *Lancet* **2009**, *373*, 2055–2066.

2. Obeso, J. A.; Rodriguez-Oroz, M. C.; Goetz, C. G.; Marin, C.; Kordower, J. H.; Rodriguez, M.; Hirsch, E. C.; Farrer, M.; Schapira, A. H. V; Halliday, G. Missing pieces in the Parkinson's disease puzzle. *Nat. Med.* **2010**, *16*, 653–661.

3. Schapira, A. H. V; Tolosa, E. Molecular and clinical prodrome of Parkinson disease: implications for treatment. *Nat. Rev. Neurol.* **2010**, *6*, 309–17.

4. Fahn, S. Description of Parkinson ' s Disease as a Clinical Syndrome. *Ann N Y Acad Sci* **2003**, *991*, 1–14.

5. de Rijk, MC, Launer, LJ, Berger, K, Breteler, MM, Dartigues, JF, Baldereschi, M, Fratiglioni, L, Lobo, A, Martinez-Lage, J, Trenkwalder, C, Hofman, A. Prevalence of Parkinson's disease in Europe: A collaborative study of population-based cohorts. Neurologic Diseases in the Elderly Research Group. *Neurology* **2000**, *54*, S21–3.

6. Kordower, J. H.; Olanow, C. W.; Dodiya, H. B.; Chu, Y.; Beach, T. G.; Adler, C. H.; Halliday, G. M.; Bartus, R. T. Disease duration and the integrity of the nigrostriatal system in Parkinson's disease. *Brain* **2013**, *136*, 2419–2431.

7. Wittchen, H. U.; Jacobi, F.; Rehm, J.; Gustavsson, A.; Svensson, M.; Jönsson, B.; Olesen, J.; Allgulander, C.; Alonso, J.; Faravelli, C.; Fratiglioni, L.; Jennum, P.; Lieb, R.; Maercker, A.; van Os, J.; Preisig, M.; Salvador-Carulla, L.; Simon, R.; Steinhausen, H.-C. The size and burden of mental disorders and other disorders of the brain in Europe 2010. *Eur. Neuropsychopharmacol.* **2011**, *21*, 655–679.

8. Corti, O.; Lesage, S.; Brice, A. What Genetics Tells us About the Causes and Mechanisms of Parkinson's Disease. *Physiol. Rev.* **2011**, *91*, 1161–1218.

9. Dauer, W.; Przedborski, S. Parkinson's Disease. *Neuron* **2003**, *39*, 889–909.

10. Hegarty, S. V.; Sullivan, A. M.; O'Keeffe, G. W. Midbrain dopaminergic neurons: A review of the molecular circuitry that regulates their development. *Dev. Biol.* **2013**, *379*, 123–138.

11. Marsden, C. Neuromelanin and Parkinson's disease. *J Neural Transm Suppl* **1983**, *19*, 121–41.

12. Forno, LS, DeLanney, LE, Irwin, I, Langston, J. Electron microscopy of Lewy bodies in the amygdala-parahippocampal region. Comparison with inclusion bodies in the MPTP-treated squirrel monkey. *Adv Neurol* **1996**, *69*, 217–28.

13. Spillantini, M. G.; Crowther, R. A.; Jakes, R.; Hasegawa, M.; Goedert, M. alpha-Synuclein in filamentous inclusions of Lewy bodies from Parkinson's disease and dementia with lewy bodies. *Proc. Natl. Acad. Sci. U. S. A.* **1998**, *95*, 6469–73.

14. Gibb, WR, L. A. A comparison of clinical and pathological features of young- and old-onset Parkinson's disease. *Neurology* **1988**, *38*, 1402–6.

15. Obeso, J. a.; Marin, C.; Rodriguez-Oroz, C.; Blesa, J.; Benitez-Temiño, B.; Mena-Segovia, J.; Rodríguez, M.; Olanow, C. W. The basal ganglia in Parkinson's disease: Current concepts and unexplained observations. *Ann. Neurol.* **2008**, *64*, 30–46.

16. Olanow, C. W.; Brundin, P. Parkinson's disease and alpha synuclein: is Parkinson's disease a prion-like disorder? *Mov. Disord.* **2013**, *28*, 31–40.

17. Rodriguez-Oroz, M. C.; Jahanshahi, M.; Krack, P.; Litvan, I.; Macias, R.; Bezard, E.; Obeso, J. a. Initial clinical manifestations of Parkinson's disease: features and pathophysiological mechanisms. *Lancet Neurol.* **2009**, *8*, 1128–1139.

18. Obeso, J. A.; Rodriguez-Oroz, M. C.; Stamelou, M.; Bhatia, K. P.; Burn, D. J. The expanding universe of disorders of the basal ganglia. *Lancet* **2014**, *384*, 523–531.

19. Langston, J. W. The parkinson's complex: Parkinsonism is just the tip of the iceberg. *Ann. Neurol.* **2006**, *59*, 591–596.

20. Hawkes, C. H. The prodromal phase of sporadic Parkinson's disease: Does it exist and if so how long is it? *Mov. Disord.* **2008**, *23*, 1799–1807.

21. Chaudhuri, K. R.; Schapira, A. H. V Non-motor symptoms of Parkinson's disease: dopaminergic pathophysiology and treatment. *Lancet Neurol.* **2009**, *8*, 464–74.

22. Braak, H.; Tredici, K. Del; Rüb, U.; de Vos, R. A. .; Jansen Steur, E. N. .; Braak, E. Staging of brain pathology related to sporadic Parkinson's disease. *Neurobiol. Aging* **2003**, *24*, 197–211.

23. Muller, Christian; de Vos, Rob; Braak, H. Staging of Sporadic Parkinson Disease-Related alpha -Synuclein Pathology: Inter- and Intra Rater Reliability. *J. Neuropathol. Exp. Neurol.* **2005**, *64*, 623–627.

24. Martin, I, Dawson, VL, Dawson, T. Recent Advances in the Genetics of Parkinson's Disease. *Annu Rev Genomics Hum Genet* **2011**, *12*, 301–25.

25. Martin, I.; Kim, J. W.; Dawson, V. L.; Dawson, T. M. LRRK2 Pathobiology in Parkinson's Disease. *J. Neurochem.* **2014**, *131*, 554–565.

26. Collier, T. J.; Kanaan, N. M.; Kordower, J. H. Ageing as a primary risk factor for Parkinson's disease: evidence from studies of non-human primates. *Nat. Rev. Neurosci.* **2011**, *12*, 359–66.

27. Reeve, A.; Simcox, E.; Turnbull, D. Ageing and Parkinson's disease: Why is advancing age the biggest risk factor? *Ageing Res. Rev.* **2014**, *14*, 19–30.

28. Haaxma, C. A.; Bloem, B. R.; Borm, G. F.; Oyen, W. J. G.; Leenders, K. L.; Eshuis, S.; Booij, J.; Dluzen, D. E.; Horstink, M. W. I. M. Gender differences in Parkinson's disease. *J. Neurol. Neurosurg. Psychiatry* **2007**, *78*, 819–24.

29. Thacker, E. L.; Chen, H.; Patel, A. V.; McCullough, M. L.; Calle, E. E.; Thun, M. J.; Schwarzschild, M. A.; Ascherio, A. Recreational physical activity and risk of Parkinson's disease. *Mov. Disord.* **2008**, *23*, 69–74.

30. Gao, X.; Chen, H.; Choi, H. K.; Curhan, G.; Schwarzschild, M. A.; Ascherio, A. Diet, Urate, and Parkinson's Disease Risk in Men. *Am. J. Epidemiol.* **2008**, *167*, 831–838.

31. Yavich, L, Tanila, H, Vepsäläinen, S, Jäkälä, P. Role of alpha-synuclein in presynaptic dopamine recruitment. *J Neurosci* **2004**, *24*, 11165–70.

32. Abeliovich, A.; Schmitz, Y.; Fariñas, I.; Choi-Lundberg, D.; Ho, W. H.; Castillo, P. E.; Shinsky, N.; Verdugo, J. M.; Armanini, M.; Ryan, A.; Hynes, M.; Phillips, H.; Sulzer, D.; Rosenthal, A. Mice lacking alpha-synuclein display functional deficits in the nigrostriatal dopamine system. *Neuron* **2000**, *25*, 239–252.

33. Cabin, DE, Shimazu, K, Murphy, D, Cole, NB, Gottschalk, W, McIlwain, KL, Orrison, B, Chen, A, Ellis, CE, Paylor, R, Lu, B, Nussbaum, R. Synaptic vesicle depletion correlates with attenuated synaptic responses to prolonged repetitive stimulation in mice lacking alpha-synuclein. *J Neurosci* **2002**, *22*, 8797–807.

34. Fortin, DL, Troyer, MD, Nakamura, K, Kubo, S, Anthony, MD, Edwards, R. Lipid rafts mediate the synaptic localization of alpha-synuclein. *J Neurosci* **2004**, *24*, 6715–23.

35. Giasson, B. I.; Duda, J. E.; Murray, I. V; Chen, Q.; Souza, J. M.; Hurtig, H. I.; Ischiropoulos, H.; Trojanowski, J. Q.; Lee, V. M. Oxidative damage linked to neurodegeneration by selective alpha-synuclein nitration in synucleinopathy lesions. *Science* **2000**, *290*, 985–989.

36. Wakabayashi, K.; Tanji, K.; Mori, F.; Takahashi, H. The Lewy body in Parkinson's disease: Molecules implicated in the formation and degradation of α-synuclein aggregates. *Neuropathology* **2007**, *27*, 494–506.

37. Trojanowski, J. Q.; Lee, V. M.-Y. Parkinson's Disease and Related Synucleinopathies are a New Class of Nervous System Amyloidoses. *Neurotoxicology* **2002**, *23*, 457–460.

38. Jowaed, A.; Schmitt, I.; Kaut, O.; Wullner, U. Methylation Regulates Alpha-Synuclein Expression and Is Decreased in Parkinson's Disease Patients' Brains. *J. Neurosci.* **2010**, *30*, 6355–6359.

39. Puschmann, A, Wszolek, ZK, Farrer, M, Gustafson, L, Widner, H, Nilsson, C. Alpha-synuclein multiplications with parkinsonism, dementia or progressive myoclonus? *Park. Relat Disord* **2009**, *15*, 390–2.

40. Higashi, S.; Biskup, S.; West, A. B.; Trinkaus, D.; Dawson, V. L.; Faull, R. L. M.; Waldvogel, H. J.; Arai, H.; Dawson, T. M.; Moore, D. J.; Emson, P. C. Localization of Parkinson's disease-associated LRRK2 in normal and pathological human brain. *Brain Res.* **2007**, *1155*, 208–219.

41. Biskup, S.; Moore, D. J.; Celsi, F.; Higashi, S.; West, A. B.; Andrabi, S. a.; Kurkinen, K.; Yu, S. W.; Savitt, J. M.; Waldvogel, H. J.; Faull, R. L. M.; Emson, P. C.; Torp, R.; Ottersen, O. P.; Dawson, T. M.; Dawson, V. L. Localization of LRRK2 to membranous and vesicular structures in mammalian brain. *Ann. Neurol.* **2006**, *60*, 557–569.

42. MacLeod, D.; Dowman, J.; Hammond, R.; Leete, T.; Inoue, K.; Abeliovich, A. The Familial Parkinsonism Gene LRRK2 Regulates Neurite Process Morphology. *Neuron* **2006**, *52*, 587–593.

43. Imai, Y.; Gehrke, S.; Wang, H.-Q.; Takahashi, R.; Hasegawa, K.; Oota, E.; Lu, B. Phosphorylation of 4E-BP by LRRK2 affects the maintenance of dopaminergic neurons in Drosophila. *EMBO J.* **2008**, *27*, 2432–2443.

44. Gehrke, S.; Imai, Y.; Sokol, N.; Lu, B. Pathogenic LRRK2 negatively regulates microRNA-mediated translational repression. *Nature* **2010**, *466*, 637–641.

45. Healy, D. G.; Falchi, M.; O'Sullivan, S. S.; Bonifati, V.; Durr, A.; Bressman, S.; Brice, A.; Aasly, J.; Zabetian, C. P.; Goldwurm, S.; Ferreira, J. J.; Tolosa, E.; Kay, D. M.; Klein, C.; Williams, D. R.; Marras, C.; Lang, A. E.; Wszolek, Z. K.; Berciano, J.; Schapira, A. H.; Lynch, T.; Bhatia, K. P.; Gasser, T.; Lees, A. J.; Wood, N. W. Phenotype, genotype, and worldwide genetic penetrance of LRRK2-associated Parkinson's disease: a case-control study. *Lancet Neurol.* **2008**, *7*, 583–590.

46. Ujiie, S, Hatan, T, Kubo, S, Imai, S, Sato, S, Uchihara, T, Yagishita, S, Hasegawa, K, Kowa, H, Sakai, F, Hattori, N. LRRK2 I2020T mutation is associated with tau pathology. *Park. Relat Disord* **2012**, *18*, 819–23.

47. Cookson, M. R. The role of leucine-rich repeat kinase 2 (LRRK2) in Parkinson's disease. **2010**, *2*.

48. Ray, S.; Bender, S.; Kang, S.; Lin, R.; Glicksman, M. a; Liu, M. The Parkinson disease-linked LRRK2 protein mutation I2020T stabilizes an active state conformation leading to increased kinase activity. *J. Biol. Chem.* **2014**, *289*, 13042–53.

49. Rocha, E. M.; Smith, G. A.; Park, E.; Cao, H.; Brown, E.; Hallett, P.; Isacson, O. Progressive decline of glucocerebrosidase in aging and Parkinson's disease. *Ann. Clin. Transl. Neurol.* **2015**, *2*, 433–438.

50. Dawson, T. M.; Dawson, V. L. The role of parkin in familial and sporadic Parkinson's disease. *Mov. Disord.* **2010**, *25*, 32–39.

51. Scarffe, L. A.; Stevens, D. A.; Dawson, V. L.; Dawson, T. M. Parkin and PINK1: much more than mitophagy. *Trends Neurosci.* **2014**, *37*, 315–324.

52. Byrd, R. A.; Weissman, A. M. Compact Parkin only: insights into the structure of an autoinhibited ubiquitin ligase. *EMBO J.* **2013**, *32*, 2087–9.

53. Lücking, CB, Dürr, A, Bonfitati V, Vaughan, J, De Michele, G, Gasser, T, Harghangi, BS, Meco, G, Denèfle, P, Wood, NW, Agid, Y, Brice, A. F. P. D. G. S. G. E. C. on G. S. in P. D. Association between early-onset Parkinson's disease and mutations in the parkin gene. *May* **2000**, *343*, 1560–7.

54. Periquet, M.; Latouche, M.; Lohmann, E.; Rawal, N.; De Michele, G.; Ricard, S.; Teive, H.; Fraix, V.; Vidailhet, M.; Nicholl, D.; Barone, P.; Wood, N. W.; Raskin, S.; Deleuze, J. F.; Agid, Y.; Dürr, A.; Brice, A.; Bonnet, a. M.; Borg, M.; Broussolle, E.; Damier, P.; Destée, a.; Durif, F.; Feingold, J.; Fénelon, G.; Martinez, M.; Penet, C.; Pollak, P.; Rascol, O.; Tison, F.; Tranchant, C.; Vérin, M.; Viallet, F.; Warter, J. M.; Gasser, T.; Müller-Myhsok, B.; Breteler, M.; Harhangi, S.; Oostra, B.; Bonifati, V.; Vanacore, N.; Fabrizio, E.; Filla, a.; Meco, G. Parkin mutations are frequent in patients with isolated early-onset parkinsonism. *Brain* **2003**, *126*, 1271–1278.

55. Nuytemans, K.; Theuns, J.; Cruts, M.; Van Broeckhoven, C. Genetic etiology of Parkinson disease associated with mutations in the SNCA, PARK2, PINK1, PARK7, and LRRK2 genes: a mutation update. *Hum. Mutat.* **2010**, *31*, 763–780.

56. Hedrich, K.; Eskelson, C.; Wilmot, B.; Marder, K.; Harris, J.; Garrels, J.; Meija-Santana, H.; Vieregge, P.; Jacobs, H.; Bressman, S. B.; Lang, A. E.; Kann, M.; Abbruzzese, G.; Martinelli, P.; Schwinger, E.; Ozelius, L. J.; Pramstaller, P. P.; Klein, C.; Kramer, P. Distribution, type, and origin of Parkin mutations: review and case studies. *Mov. Disord.* **2004**, *19*, 1146–57.

57. Mori, H, Kondo, T, Yocochi, M, Matsumine, H, Nakagawa-Hattori, Y, Miyake, T. Pathologic and biochemical studies of juvenile parkinsonism linked to chromosome 6q. *Neurology* **1998**, *51*, 890–2.

58. Dawson, T. M.; Dawson, V. L. Parkin plays a role in sporadic parkinson's disease. *Neurodegener. Dis.* **2014**, *13*, 69–71.

59. Shin, J.-H.; Ko, H. S.; Kang, H.; Lee, Y.; Lee, Y.-I.; Pletinkova, O.; Troconso, J. C.; Dawson, V. L.; Dawson, T. M. PARIS (ZNF746) repression of PGC-1α contributes to neurodegeneration in Parkinson's disease. *Cell* **2011**, *144*, 689–702.

60. Ko, H. S.; Lee, Y.; Shin, J.-H.; Karuppagounder, S. S.; Gadad, B. S.; Koleske, A. J.; Pletnikova, O.; Troncoso, J. C.; Dawson, V. L.; Dawson, T. M. Phosphorylation by the c-Abl protein tyrosine kinase inhibits parkin's ubiquitination and protective function. *Proc. Natl. Acad. Sci. U. S. A.* **2010**, *107*, 16691–16696.

61. Imam, S. Z.; Zhou, Q.; Yamamoto, A.; Valente, A. J.; Ali, S. F.; Bains, M.; Roberts, J. L.; Kahle, P. J.; Clark, R. a; Li, S. Novel regulation of parkin function through c-Abl-mediated tyrosine phosphorylation: implications for Parkinson's disease. *J. Neurosci.* **2011**, *31*, 157–163.

62. Zhou, C.; Huang, Y.; Shao, Y.; May, J.; Prou, D.; Perier, C.; Dauer, W.; Schon, E. a; Przedborski, S. The kinase domain of mitochondrial PINK1 faces the cytoplasm. *Proc. Natl. Acad. Sci. U. S. A.* **2008**, *105*, 12022–7.

63. Cazeneuve, C.; Sân, C.; Ibrahim, S. a.; Mukhtar, M. M.; Kheir, M. M.; LeGuern, E.; Brice, A.; Salih, M. a. A new complex homozygous large rearrangement of the PINK1 gene in a Sudanese family with early onset Parkinson's disease. *Neurogenetics* **2009**, *10*, 265–270.

64. Marongiu, R.; Brancati, F.; Antonini, A.; Ialongo, T.; Ceccarini, C.; Scarciolla, O.; Capalbo, A.; Benti, R.; Pezzoli, G.; Dallapiccola, B.; Goldwurm, S.; Valente, E. M. Whole gene deletion and splicing mutations expand the PINK1 genotypic spectrum. *Hum. Mutat.* **2007**, *28*, 98.

65. Beilina, A.; Van Der Brug, M.; Ahmad, R.; Kesavapany, S.; Miller, D. W.; Petsko, G. a; Cookson, M. R. Mutations in PTEN-induced putative kinase 1 associated with recessive parkinsonism have differential effects on protein stability. *Proc. Natl. Acad. Sci. U. S. A.* **2005**, *102*, 5703–5708.

66. Canet-Avilés, R. M.; Wilson, M. a; Miller, D. W.; Ahmad, R.; McLendon, C.; Bandyopadhyay, S.; Baptista, M. J.; Ringe, D.; Petsko, G. a; Cookson, M. R. The Parkinson's disease protein DJ-1 is neuroprotective due to cysteine-sulfinic acid-driven mitochondrial localization. *Proc. Natl. Acad. Sci. U. S. A.* **2004**, *101*, 9103–9108.

67. Thomas, K. J.; McCoy, M. K.; Blackinton, J.; Beilina, A.; van der Brug, M.; Sandebring, A.; Miller, D.; Maric, D.; Cedazo-Minguez, A.; Cookson, M. R. DJ-1 acts in parallel to the PINK1/parkin pathway to control mitochondrial function and autophagy. *Hum. Mol. Genet.* **2011**, *20*, 40–50.

68. Andres-Mateos, E.; Perier, C.; Zhang, L.; Blanchard-Fillion, B.; Greco, T. M.; Thomas, B.; Ko, H. S.; Sasaki, M.; Ischiropoulos, H.; Przedborski, S.; Dawson, T. M.; Dawson, V. L. DJ-1 gene deletion reveals that DJ-1 is an atypical peroxiredoxin-like peroxidase. *Proc. Natl. Acad. Sci. U. S. A.* **2007**, *104*, 14807–14812.

69. Clements, C. M.; McNally, R. S.; Conti, B. J.; Mak, T. W.; Ting, J. P.-Y. DJ-1, a cancer- and Parkinson's disease-associated protein, stabilizes the antioxidant transcriptional master regulator Nrf2. *Proc. Natl. Acad. Sci. U. S. A.* **2006**, *103*, 15091–15096.

70. Williams, D. R.; Hadeed, A.; Najim al-Din, A. S.; Wreikat, A. L.; Lees, A. J. Kufor Rakeb disease: Autosomal recessive, levodopa-responsive Parkinsonism with pyramidal degeneration, supranuclear gaze palsy, and dementia. *Mov. Disord.* **2005**, *20*, 1264–1271.

71. Perrett, R. M.; Alexopoulou, Z.; Tofaris, G. K. The endosomal pathway in Parkinson's disease. *Mol. Cell. Neurosci.* **2015**, *66*, 21–28.

72. Di Fonzo, A, Chien HF, Soca, M, Giraudo, S, Tassorelli, C, Iliceto, G, Fabbrini, G, Marconi, R, Fincati, E, Abbruzzese, G, Marini, P, Squitieri, F, Horstink, MW, Montagna, P, Livera, AD, Stocchi, F, Goldwurm, S, Ferreire, JJ, Meco, G, Martignoni, E, Lopia, V. ATP13A2 missesense mutations in juvenile parkisnonism and young onset Parkinson's disease. *Neurology* **2007**, *68*, 1557–62.

73. Ramirez, A.; Heimbach, A.; Gründemann, J.; Stiller, B.; Hampshire, D.; Cid, L. P.; Goebel, I.; Mubaidin, A. F.; Wriekat, A.-L.; Roeper, J.; Al-Din, A.; Hillmer, A. M.; Karsak, M.; Liss, B.; Woods, C. G.; Behrens, M. I.; Kubisch, C. Hereditary parkinsonism with dementia is caused by mutations in ATP13A2, encoding a lysosomal type 5 P-type ATPase. *Nat. Genet.* **2006**, *38*, 1184–1191.

74. Schapira, A. H. V. Glucocerebrosidase and Parkinson disease: Recent advances. *Mol. Cell. Neurosci.* **2015**, *66*, 37–42.

75. Horowitz, M, Wilder, S, Horowitz, Z, Reiner, O, Gelbart, T, Beutler, E. The human glucoerebrosidase gene and pseudogene: structure and evolution. *Genomics* **1989**, *4*, 87–96.

76. Grabowski, G. A. Series Lysosomal Storage Disease 1 Phenotype, diagnosis, and treatment of Gaucher's disease. *Lancet* **2008**, *372*, 1263–1271.

77. Barkhuizen, M.; Anderson, D. G.; Grobler, A. F. Advances in GBA-associated Parkinson's disease – Pathology, presentation and therapies. *Neurochem. Int.* **2015**.

78. Neumann, J.; Bras, J.; Deas, E.; O'Sullivan, S. S.; Parkkinen, L.; Lachmann, R. H.; Li, A.; Holton, J.; Guerreiro, R.; Paudel, R.; Segarane, B.; Singleton, A.; Lees, A.; Hardy, J.; Houlden, H.; Revesz, T.; Wood, N. W. Glucocerebrosidase mutations in clinical and pathologically proven Parkinson's disease. *Brain* **2009**, *132*, 1783–1794.

79. Ron, I.; Horowitz, M. ER retention and degradation as the molecular basis underlying Gaucher disease heterogeneity. *Hum. Mol. Genet.* **2005**, *14*, 2387–2398.

80. Cullen, V.; Sardi, S. P.; Ng, J.; Xu, Y.-H.; Sun, Y.; Tomlinson, J. J.; Kolodziej, P.; Kahn, I.; Saftig, P.; Woulfe, J.; Rochet, J.-C.; Glicksman, M. A.; Cheng, S. H.; Grabowski, G. A.; Shihabuddin, L. S.; Schlossmacher, M. G. Acid β-glucosidase mutants linked to gaucher disease, parkinson disease, and lewy body dementia alter α-synuclein processing. *Ann. Neurol.* **2011**, *69*, 940–953.

81. Mazzulli, J. R.; Xu, Y.-H.; Sun, Y.; Knight, A. L.; McLean, P. J.; Caldwell, G. A.; Sidransky, E.; Grabowski, G. A.; Krainc, D. Gaucher Disease Glucocerebrosidase and α-Synuclein Form a Bidirectional Pathogenic Loop in Synucleinopathies. *Cell* **2011**, *146*, 37–52.

82. Murphy, KE, Gysbers, AM, Abbott, SK, Tayebi, N, Kim, WS, Sidransky, E, Cooper, A, Garner, B, Halliday, G. Reduced glucerebrosidase is associated with increased alpha-synuclein in sporadic Parkinson's disease. *Brain* **2014**, *137*, 834–848.

83. Polymeropoulos, M. H.; Lavedan, C.; Leroy, E.; Ide, S. E.; Dehejia, A.; Dutra, A.; Pike, B.; Root, H.; Rubenstein, J.; Boyer, R.; Stenroos, E. S.; Chandrasekharappa, S.; Athanassiadou, A.; Papapetropoulos, T.; Johnson, W. G.; Lazzarini, A. M.; Duvoisin, R. C.; Iorio, G. Di; Golbe, L. I.; Nussbaum, R. L. Mutation in the α -Synuclein Gene Identified in Families with Parkinson ' s Disease Mutation in the _ -Synuclein Gene Identified in Families with Parkinson ' s Disease. *Science (80-.).* **1997**, *276*, 2045–2047.

84. Kordower, J. H.; Chu, Y.; Hauser, R. A.; Freeman, T. B.; Olanow, C. W. Lewy body–like pathology in long-term embryonic nigral transplants in Parkinson's disease. *Nat. Med.* **2008**, *14*, 504–506.

85. Li, J.-Y.; Englund, E.; Holton, J. L.; Soulet, D.; Hagell, P.; Lees, A. J.; Lashley, T.; Quinn, N. P.; Rehncrona, S.; Björklund, A.; Widner, H.; Revesz, T.; Lindvall, O.; Brundin, P. Lewy bodies in grafted neurons in subjects with Parkinson's disease suggest host-to-graft disease propagation. *Nat. Med.* **2008**, *14*, 501–503.

86. Mendez, I.; Viñuela, A.; Astradsson, A.; Mukhida, K.; Hallett, P.; Robertson, H.; Tierney, T.; Holness, R.; Dagher, A.; Trojanowski, J. Q.; Isacson, O. Dopamine neurons implanted into people with Parkinson's disease survive without pathology for 14 years. *Nat. Med.* **2008**, *14*, 507–9.

87. Choi, W.; Zibaee, S.; Jakes, R.; Serpell, L. C.; Davletov, B.; Anthony Crowther, R.; Goedert, M. Mutation E46K increases phospholipid binding and assembly into filaments of human α-synuclein. *FEBS Lett.* **2004**, *576*, 363–368.

88. Ibáñez, P.; Bonnet, a-M.; Débarges, B.; Lohmann, E.; Tison, F.; Pollak, P.; Agid, Y.; Dürr, a; Brice, a Causal relation between alpha-synuclein gene duplication and familial Parkinson's disease. *Lancet* **2004**, *364*, 1169–1171.

89. Dawson, T. M.; Dawson, V. L. Molecular Pathways of Neurodegeneration in Parkinson ' s Disease. *October* **2003**, *302*, 819–822.

90. Caughey, B.; Lansbury, P. T. PROTOFIBRILS, PORES, FIBRILS, AND NEURODEGENERATION: Separating the Responsible Protein Aggregates from The Innocent Bystanders. *Annu. Rev. Neurosci.* **2003**, *26*, 267–298.

91. Winner, B.; Jappelli, R. In vivo demonstration that α-synuclein oligomers are toxic. *Proc. Natl. Acad. Sci.* **2011**, *108*, 4194–4199.

92. Dehay, B.; Bourdenx, M.; Gorry, P.; Przedborski, S.; Vila, M.; Hunot, S.; Singleton, A.;

Olanow, C. W.; Merchant, K. M.; Bezard, E.; Petsko, G. A.; Meissner, W. G. Targeting α-synuclein for treatment of Parkinson's disease: mechanistic and therapeutic considerations. *Lancet Neurol.* **2015**, *14*, 855–866.

93. Luk, KC, Kehm, V, Carroll, J, Zhang, B, O'Brien, P, Trojanowski, JQ, Lee, V. Pathological alpha-synuclein transmission initiates Parkinson-like neurodegeneration in nontransgenic mice. *Science (80-.).* **2012**, *338*, 949–953.

94. Recasens, A.; Dehay, B.; Bové, J.; Carballo-Carbajal, I.; Dovero, S.; Pérez-Villalba, A.; Fernagut, P.-O.; Blesa, J.; Parent, A.; Perier, C.; Fariñas, I.; Obeso, J. A.; Bezard, E.; Vila, M. Lewy body extracts from Parkinson disease brains trigger α-synuclein pathology and neurodegeneration in mice and monkeys. *Ann. Neurol.* **2014**, *75*, 351–362.

95. Osterberg, V. R.; Spinelli, K. J.; Weston, L. J.; Luk, K. C.; Woltjer, R. L.; Unni, V. K. Progressive aggregation of alpha-synuclein and selective degeneration of lewy inclusion-bearing neurons in a mouse model of parkinsonism. *Cell Rep.* **2015**, *10*, 1252–60.

96. Lashuel, H. A.; Overk, C. R.; Oueslati, A.; Masliah, E. The many faces of α-synuclein: from structure and toxicity to therapeutic target. *Nat. Rev. Neurosci.* **2012**, *14*, 38–48.

97. Bartels, T.; Choi, J. G.; Selkoe, D. J. α-Synuclein occurs physiologically as a helically folded tetramer that resists aggregation. *Nature* **2011**, *477*, 107–110.

98. Dettmer, U.; Selkoe, D.; Bartels, T. New insights into cellular α-synuclein homeostasis in health and disease. *Curr. Opin. Neurobiol.* **2016**, *36*, 15–22.

99. Norris, E. H.; Giasson, B. I.; Ischiropoulos, H.; Lee, V. M.-Y. Effects of oxidative and nitrative challenges on alpha-synuclein fibrillogenesis involve distinct mechanisms of protein modifications. *J. Biol. Chem.* **2003**, *278*, 27230–40.

100. Fujiwara, H.; Hasegawa, M.; Dohmae, N.; Kawashima, A.; Masliah, E.; Goldberg, M. S.; Shen, J.; Takio, K.; Iwatsubo, T. alpha-Synuclein is phosphorylated in synucleinopathy lesions. *Nat. Cell Biol.* **2002**, *4*, 160–164.

101. Nguyen, H. N.; Byers, B.; Cord, B.; Shcheglovitov, A.; Byrne, J.; Gujar, P.; Kee, K.; Schüle, B.; Dolmetsch, R. E.; Langston, W.; Palmer, T. D.; Pera, R. R. LRRK2 Mutant iPSC-Derived DA Neurons Demonstrate Increased Susceptibility to Oxidative Stress. *Cell Stem Cell* **2011**, *8*, 267–280.

102. Sánchez-Danés, A.; Richaud-Patin, Y.; Carballo-Carbajal, I.; Jiménez-Delgado, S.; Caig, C.; Mora, S.; Di Guglielmo, C.; Ezquerra, M.; Patel, B.; Giralt, A.; Canals, J. M.; Memo, M.; Alberch, J.; López-Barneo, J.; Vila, M.; Cuervo, A. M.; Tolosa, E.; Consiglio, A.; Raya, A. Disease-specific phenotypes in dopamine neurons from human iPS-based models of genetic and sporadic Parkinson's disease. *EMBO Mol. Med.* **2012**, *4*, 380–395.

103. Orenstein, S. J.; Kuo, S.-H.; Tasset, I.; Arias, E.; Koga, H.; Fernandez-Carasa, I.; Cortes, E.; Honig, L. S.; Dauer, W.; Consiglio, A.; Raya, A.; Sulzer, D.; Cuervo, A. M. Interplay of LRRK2 with chaperone-mediated autophagy. *Nat. Neurosci.* **2013**, *16*, 394–406.

104. Cuervo, A. M.; Wong, E. Chaperone-mediated autophagy: roles in disease and aging. *Cell Res.* **2014**, *24*, 92–104.

105. Langston, JW, Ballard, P, Tetrud, JW, Irwin, I. Chronic Parkinsonism in humans due to a product of meperidine-analog synthesis. *Science (80-.).* **1983**, *219*, 979–80.

106. Valadas, J. S.; Vos, M.; Verstreken, P. Therapeutic strategies in Parkinson's disease: what we have learned from animal models. *Ann. N. Y. Acad. Sci.* **2015**, *1338*, 16–37.

107. Schapira, AH, Mann, VM, Cooper, JM, Dexter, D, Daniel, SE, Jenner, P, Clark, JB, Marsden, C. Anatomic and disease specificity of NADH CoQ1 reductase (complex I) deficiency in Parkinson's disease. *J Neurochem* **1990**, *55*, 2142–5.

108. Keeney, PM, Xie, J, Capaldi, RA, Bennet Jr, J. Parkinson's Disease Brain Mitochondrial Complex I Has Oxidatively Damaged Subunits and Is Functionally Impaired and Misassembled. *J. Neurosci.* **2006**, *26*, 5256–5264.

109. Chinta, S. J.; Andersen, J. K. Redox imbalance in Parkinson's disease. *Biochim. Biophys. Acta - Gen. Subj.* **2008**, *1780*, 1362–1367.

110. Büeler, H. Impaired mitochondrial dynamics and function in the pathogenesis of Parkinson's disease. *Exp. Neurol.* **2009**, *218*, 235–246.

111. Kuroda, Y, Mitsui, T, Kunisige, M, Shono, M, Akaike, M, Azuma, H, Matsumoto, T. Parkin

enhances mitochondrial biogenesis in proliferating cells. *Hum. Mol. Genet.* **2006**, *15*, 883–895.

112. Zheng, B.; Liao, Z.; Locascio, J. L.; Lesniak, K. A.; Roderick, S. S.; Watt, M. L.; Eklund, A. C.; Zhang-James, Y.; Kim, P. D.; Hauser, M. A.; Grunblatt, E.; Moran, L. B.; Mandel, S. A.; Riederer, P.; Miller, R. M.; Federoff, H. J.; Wullner, U.; Papapetropoulos, S.; Youdim, M. B.; Cantuti-Castelvetri, I.; Young, A. B.; Vance, J. M.; Davis, R. L.; Hedreen, J. C.; Adler, C. H.; Beach, T. G.; Graeber, M. B.; Middleton, F. A. PGC-1a, A potential therapeutic target for early intervention in Parkinson's disease. *Sci. Transl. Med.* **2010**, *2*, 52ra73.

113. Narendra, D.; Tanaka, A.; Suen, D.-F.; Youle, R. J. Parkin is recruited selectively to impaired mitochondria and promotes their autophagy. *J. Cell Biol.* **2008**, *183*, 795–803.

114. Clark, I. E.; Dodson, M. W.; Jiang, C.; Cao, J. H.; Huh, J. R.; Seol, J. H.; Yoo, S. J.; Hay, B. A.; Guo, M. Drosophila pink1 is required for mitochondrial function and interacts genetically with parkin. *Nature* **2006**, *441*, 1162–6.

115. Park, J.; Lee, S. B.; Lee, S.; Kim, Y.; Song, S.; Kim, S.; Bae, E.; Kim, J.; Shong, M.; Kim, J.-M.; Chung, J. Mitochondrial dysfunction in Drosophila PINK1 mutants is complemented by parkin. *Nature* **2006**, *441*, 1157–61.

116. Yang, Y.; Gehrke, S.; Imai, Y.; Huang, Z.; Ouyang, Y.; Wang, J.-W.; Yang, L.; Beal, M. F.; Vogel, H.; Lu, B. Mitochondrial pathology and muscle and dopaminergic neuron degeneration caused by inactivation of Drosophila Pink1 is rescued by Parkin. *Proc. Natl. Acad. Sci. U. S. A.* **2006**, *103*, 10793–8.

117. Youle, R. J.; van der Bliek, A. M. Mitochondrial fission, fusion, and stress. *Science* **2012**, *337*, 1062–5.

118. Benard, G.; Bellance, N.; James, D.; Parrone, P.; Fernandez, H.; Letellier, T.; Rossignol, R. Mitochondrial bioenergetics and structural network organization. *J. Cell Sci.* **2007**, *120*, 838–48.

119. Detmer, S. A.; Chan, D. C. Functions and dysfunctions of mitochondrial dynamics. *Nat. Rev. Mol. Cell Biol.* **2007**, *8*, 870–9.

120. Ashley, A. K.; Hanneman, W. H.; Katoh, T.; Moreno, J. A.; Pollack, A.; Tjalkens, R. B.; Legare, M. E. Analysis of targeted mutation in DJ-1 on cellular function in primary astrocytes. *Toxicol. Lett.* **2009**, *184*, 186–91.

121. Junn, E.; Jang, W. H.; Zhao, X.; Jeong, B. S.; Mouradian, M. M. Mitochondrial localization of DJ-1 leads to enhanced neuroprotection. *J. Neurosci. Res.* **2009**, *87*, 123–9.

122. van der Brug, M. P.; Blackinton, J.; Chandran, J.; Hao, L.-Y.; Lal, A.; Mazan-Mamczarz, K.; Martindale, J.; Xie, C.; Ahmad, R.; Thomas, K. J.; Beilina, A.; Gibbs, J. R.; Ding, J.; Myers, A. J.; Zhan, M.; Cai, H.; Bonini, N. M.; Gorospe, M.; Cookson, M. R. RNA binding activity of the recessive parkinsonism protein DJ-1 supports involvement in multiple cellular pathways. *Proc. Natl. Acad. Sci. U. S. A.* **2008**, *105*, 10244–9.

123. Shendelman, S.; Jonason, A.; Martinat, C.; Leete, T.; Abeliovich, A. DJ-1 is a redox-dependent molecular chaperone that inhibits alpha-synuclein aggregate formation. *PLoS Biol.* **2004**, *2*, e362.

124. Ellis, C. E.; Murphy, E. J.; Mitchell, D. C.; Golovko, M. Y.; Scaglia, F.; Barceló-Coblijn, G. C.; Nussbaum, R. L. Mitochondrial lipid abnormality and electron transport chain impairment in mice lacking alpha-synuclein. *Mol. Cell. Biol.* **2005**, *25*, 10190–201.

125. Zhu, M.; Qin, Z.-J.; Hu, D.; Munishkina, L. A.; Fink, A. L. Alpha-synuclein can function as an antioxidant preventing oxidation of unsaturated lipid in vesicles. *Biochemistry* **2006**, *45*, 8135–42.

126. Devi, L.; Raghavendran, V.; Prabhu, B. M.; Avadhani, N. G.; Anandatheerthavarada, H. K. Mitochondrial Import and Accumulation of alpha-Synuclein Impair Complex I in Human Dopaminergic Neuronal Cultures and Parkinson Disease Brain. *J. Biol. Chem.* **2008**, *283*, 9089–9100.

127. Lashuel, H. A.; Hartley, D.; Petre, B. M.; Walz, T.; Lansbury, P. T. Neurodegenerative disease: amyloid pores from pathogenic mutations. *Nature* **2002**, *418*, 291.

128. Ding, T. T.; Lee, S.-J.; Rochet, J.-C.; Lansbury, P. T. Annular alpha-synuclein protofibrils are produced when spherical protofibrils are incubated in solution or bound to brain-derived membranes. *Biochemistry* **2002**, *41*, 10209–17.

129. Siddiqui, A.; Chinta, S. J.; Mallajosyula, J. K.; Rajagopolan, S.; Hanson, I.; Rane, A.; Melov, S.; Andersen, J. K. Selective binding of nuclear alpha-synuclein to the PGC1alpha promoter under conditions of oxidative stress may contribute to losses in mitochondrial function: implications for Parkinson's disease. *Free Radic. Biol. Med.* **2012**, *53*, 993–1003.

130. Nakamura, K.; Nemani, V. M.; Azarbal, F.; Skibinski, G.; Levy, J. M.; Egami, K.; Munishkina, L.; Zhang, J.; Gardner, B.; Wakabayashi, J.; Sesaki, H.; Cheng, Y.; Finkbeiner, S.; Nussbaum, R. L.; Masliah, E.; Edwards, R. H. Direct membrane association drives mitochondrial fission by the Parkinson disease-associated protein alpha-synuclein. *J. Biol. Chem.* **2011**, *286*, 20710–26.

131. Kamp, F.; Exner, N.; Lutz, A. K.; Wender, N.; Hegermann, J.; Brunner, B.; Nuscher, B.; Bartels, T.; Giese, A.; Beyer, K.; Eimer, S.; Winklhofer, K. F.; Haass, C. Inhibition of mitochondrial fusion by α-synuclein is rescued by PINK1, Parkin and DJ-1. *EMBO J.* **2010**, *29*, 3571–89.

132. Brunk, U. T.; Terman, A. Lipofuscin: mechanisms of age-related accumulation and influence on cell function. *Free Radic. Biol. Med.* **2002**, *33*, 611–9.

133. Prots, I.; Veber, V.; Brey, S.; Campioni, S.; Buder, K.; Riek, R.; Böhm, K. J.; Winner, B. α-Synuclein oligomers impair neuronal microtubule-kinesin interplay. *J. Biol. Chem.* **2013**, *288*, 21742–54.

134. Kim-Han, J. S.; Antenor-Dorsey, J. A.; O'Malley, K. L. The parkinsonian mimetic, MPP+, specifically impairs mitochondrial transport in dopamine axons. *J. Neurosci.* **2011**, *31*, 7212–21.

135. Ryan, B. J.; Hoek, S.; Fon, E. A.; Wade-Martins, R. Mitochondrial dysfunction and mitophagy in Parkinson's: from familial to sporadic disease. *Trends Biochem. Sci.* **2015**, *40*, 200–10.

136. Yan, M. H.; Wang, X.; Zhu, X. Mitochondrial defects and oxidative stress in Alzheimer disease and Parkinson disease. *Free Radic. Biol. Med.* **2013**, *62*, 90–101.

137. Plowey, E. D.; Cherra, S. J.; Liu, Y. J.; Chu, C. T. Role of autophagy in G2019S-LRRK2-associated neurite shortening in differentiated SH-SY5Y cells. *J. Neurochem.* **2008**, *105*, 1048–1056.

138. Bosco, D. A.; Fowler, D. M.; Zhang, Q.; Nieva, J.; Powers, E. T.; Wentworth, P.; Lerner, R. A.; Kelly, J. W. Elevated levels of oxidized cholesterol metabolites in Lewy body disease brains accelerate alpha-synuclein fibrilization. *Nat. Chem. Biol.* **2006**, *2*, 249–53.

139. Nakabeppu, Y.; Tsuchimoto, D.; Yamaguchi, H.; Sakumi, K. Oxidative damage in nucleic acids and Parkinson's disease. *J. Neurosci. Res.* **2007**, *85*, 919–34.

140. Zeevalk, G. D.; Razmpour, R.; Bernard, L. P. Glutathione and Parkinson's disease: is this the elephant in the room? *Biomed. Pharmacother. = Biomédecine pharmacothérapie 62*, 236–49.

141. Tsang, A. H. K.; Chung, K. K. K. Oxidative and nitrosative stress in Parkinson's disease. *Biochim. Biophys. Acta - Mol. Basis Dis.* **2009**, *1792*, 643–50.

142. Barcia, C.; Fernández Barreiro, A.; Poza, M.; Herrero, M.-T. Parkinson's disease and inflammatory changes. *Neurotox. Res.* **2003**, *5*, 411–8.

143. Surace, M. J.; Block, M. L. Targeting microglia-mediated neurotoxicity: the potential of NOX2 inhibitors. *Cell. Mol. Life Sci.* **2012**, *69*, 2409–27.

144. Perry, V. H. Innate inflammation in Parkinson's disease. *Cold Spring Harb. Perspect. Med.* **2012**, *2*, a009373.

145. Lawson, L. J.; Perry, V. H.; Dri, P.; Gordon, S. Heterogeneity in the distribution and morphology of microglia in the normal adult mouse brain. *Neuroscience* **1990**, *39*, 151–70.

146. McGeer, P. L.; Yasojima, K.; McGeer, E. G. Association of interleukin-1 beta polymorphisms with idiopathic Parkinson's disease. *Neurosci. Lett.* **2002**, *326*, 67–9.

147. Doorn, K. J.; Drukarch, B.; van Dam, A.-M.; Lucassen, P. J. Hippocampal proliferation is increased in presymptomatic Parkinson's disease and due to microglia. *Neural Plast.* **2014**, *2014*, 959154.

148. Pisanu, A.; Lecca, D.; Mulas, G.; Wardas, J.; Simbula, G.; Spiga, S.; Carta, A. R. Dynamic changes in pro- and anti-inflammatory cytokines in microglia after PPAR-γ agonist neuroprotective treatment in the MPTPp mouse model of progressive Parkinson's disease.

Neurobiol. Dis. **2014**, *71*, 280–91.

149. Stott, S. R. W.; Barker, R. A. Time course of dopamine neuron loss and glial response in the 6-OHDA striatal mouse model of Parkinson's disease. *Eur. J. Neurosci.* **2014**, *39*, 1042–56.

150. Sacino, A. N.; Brooks, M.; McKinney, A. B.; Thomas, M. A.; Shaw, G.; Golde, T. E.; Giasson, B. I. Brain injection of α-synuclein induces multiple proteinopathies, gliosis, and a neuronal injury marker. *J. Neurosci.* **2014**, *34*, 12368–78.

151. Daher, J. P. L.; Abdelmotilib, H. A.; Hu, X.; Volpicelli-Daley, L. A.; Moehle, M. S.; Fraser, K. B.; Needle, E.; Chen, Y.; Steyn, S. J.; Galatsis, P.; Hirst, W. D.; West, A. B. Leucine-rich Repeat Kinase 2 (LRRK2) Pharmacological Inhibition Abates α-Synuclein Gene-induced Neurodegeneration. *J. Biol. Chem.* **2015**, *290*, 19433–19444.

152. Gillardon, F.; Schmid, R.; Draheim, H. Parkinson's disease-linked leucine-rich repeat kinase 2(R1441G) mutation increases proinflammatory cytokine release from activated primary microglial cells and resultant neurotoxicity. *Neuroscience* **2012**, *208*, 41–8.

153. Moehle, M. S.; Webber, P. J.; Tse, T.; Sukar, N.; Standaert, D. G.; DeSilva, T. M.; Cowell, R. M.; West, A. B. LRRK2 inhibition attenuates microglial inflammatory responses. *J. Neurosci.* **2012**, *32*, 1602–11.

154. Slivka, A.; Cohen, G. Hydroxyl radical attack on dopamine. *J. Biol. Chem.* **1985**, *260*, 15466–72.

155. Mallajosyula, J. K.; Chinta, S. J.; Rajagopalan, S.; Nicholls, D. G.; Andersen, J. K. Metabolic control analysis in a cellular model of elevated MAO-B: relevance to Parkinson's disease. *Neurotox. Res.* **2009**, *16*, 186–93.

156. Stokes, A. H.; Hastings, T. G.; Vrana, K. E. Mini-Review Cytotoxic and Genotoxic Potential of Dopamine. *J. Neurosci Res* **1999**, *665*, 659–665.

157. LaVoie, M. J.; Ostaszewski, B. L.; Weihofen, A.; Schlossmacher, M. G.; Selkoe, D. J. Dopamine covalently modifies and functionally inactivates parkin. *Nat. Med.* **2005**, *11*, 1214–21.

158. Ghafourifar, P.; Asbury, M. L.; Joshi, S. S.; Kincaid, E. D. Determination of mitochondrial nitric oxide synthase activity. *Methods Enzymol.* **2005**, *396*, 424–44.

159. Bergendi, L.; Benes, L.; Duracková, Z.; Ferencik, M. Chemistry, physiology and pathology of free radicals. *Life Sci.* **1999**, *65*, 1865–74.

160. Lipton, S. A.; Choi, Y.-B.; Takahashi, H.; Zhang, D.; Li, W.; Godzik, A.; Bankston, L. A. Cysteine regulation of protein function--as exemplified by NMDA-receptor modulation. *Trends Neurosci.* **2002**, *25*, 474–80.

161. Chung, K. K. K.; Thomas, B.; Li, X.; Pletnikova, O.; Troncoso, J. C.; Marsh, L.; Dawson, V. L.; Dawson, T. M. S-nitrosylation of parkin regulates ubiquitination and compromises parkin's protective function. *Science* **2004**, *304*, 1328–31.

162. Yao, D.; Gu, Z.; Nakamura, T.; Shi, Z.-Q.; Ma, Y.; Gaston, B.; Palmer, L. A.; Rockenstein, E. M.; Zhang, Z.; Masliah, E.; Uehara, T.; Lipton, S. A. Nitrosative stress linked to sporadic Parkinson's disease: S-nitrosylation of parkin regulates its E3 ubiquitin ligase activity. *Proc. Natl. Acad. Sci. U. S. A.* **2004**, *101*, 10810–4.

163. Chung, K. K. K. Say NO to neurodegeneration: role of S-nitrosylation in neurodegenerative disorders. *Neurosignals.* **2007**, *15*, 307–13.

164. Calabrese, V.; Butterfield, D. A.; Scapagnini, G.; Stella, A. M. G.; Maines, M. D. Redox regulation of heat shock protein expression by signaling involving nitric oxide and carbon monoxide: relevance to brain aging, neurodegenerative disorders, and longevity. *Antioxid. Redox Signal. 8*, 444–77.

165. Dawson, V. L.; Dawson, T. M.; London, E. D.; Bredt, D. S.; Snyder, S. H. Nitric oxide mediates glutamate neurotoxicity in primary cortical cultures. *Proc. Natl. Acad. Sci. U. S. A.* **1991**, *88*, 6368–71.

166. Szabó, C.; Ischiropoulos, H.; Radi, R. Peroxynitrite: biochemistry, pathophysiology and development of therapeutics. *Nat. Rev. Drug Discov.* **2007**, *6*, 662–80.

167. Reynolds, A.; Laurie, C.; Mosley, R. L.; Gendelman, H. E. Oxidative stress and the pathogenesis of neurodegenerative disorders. *Int. Rev. Neurobiol.* **2007**, *82*, 297–325.

168. Danielson, S. R.; Andersen, J. K. Oxidative and nitrative protein modifications in

Parkinson's disease. *Free Radic. Biol. Med.* **2008**, *44*, 1787–94.

169. Goedert, M. Alpha-synuclein and neurodegenerative diseases. *Nat. Rev. Neurosci.* **2001**, *2*, 492–501.

170. Benner, E. J.; Banerjee, R.; Reynolds, A. D.; Sherman, S.; Pisarev, V. M.; Tsiperson, V.; Nemachek, C.; Ciborowski, P.; Przedborski, S.; Mosley, R. L.; Gendelman, H. E. Nitrated alpha-synuclein immunity accelerates degeneration of nigral dopaminergic neurons. *PLoS One* **2008**, *3*, e1376.

171. Conway, K. A.; Rochet, J. C.; Bieganski, R. M.; Lansbury, P. T. Kinetic stabilization of the alpha-synuclein protofibril by a dopamine-alpha-synuclein adduct. *Science* **2001**, *294*, 1346–9.

172. Mazzulli, J. R.; Mishizen, A. J.; Giasson, B. I.; Lynch, D. R.; Thomas, S. A.; Nakashima, A.; Nagatsu, T.; Ota, A.; Ischiropoulos, H. Cytosolic catechols inhibit alpha-synuclein aggregation and facilitate the formation of intracellular soluble oligomeric intermediates. *J. Neurosci.* **2006**, *26*, 10068–78.

173. Martinez-Vicente, M.; Talloczy, Z.; Kaushik, S.; Massey, A. C.; Mazzulli, J.; Mosharov, E. V; Hodara, R.; Fredenburg, R.; Wu, D.-C.; Follenzi, A.; Dauer, W.; Przedborski, S.; Ischiropoulos, H.; Lansbury, P. T.; Sulzer, D.; Cuervo, A. M. Dopamine-modified alpha-synuclein blocks chaperone-mediated autophagy. *J. Clin. Invest.* **2008**, *118*, 777–88.

174. Swerdlow, R. H.; Parks, J. K.; Miller, S. W.; Tuttle, J. B.; Trimmer, P. A.; Sheehan, J. P.; Bennett, J. P.; Davis, R. E.; Parker, W. D. Origin and functional consequences of the complex I defect in Parkinson's disease. *Ann. Neurol.* **1996**, *40*, 663–71.

175. Clementi, E.; Brown, G. C.; Feelisch, M.; Moncada, S. Persistent inhibition of cell respiration by nitric oxide: crucial role of S-nitrosylation of mitochondrial complex I and protective action of glutathione. *Proc. Natl. Acad. Sci. U. S. A.* **1998**, *95*, 7631–6.

176. Bhat, A. H.; Dar, K. B.; Anees, S.; Zargar, M. A.; Masood, A.; Sofi, M. A.; Ganie, S. A. Oxidative stress, mitochondrial dysfunction and neurodegenerative diseases; a mechanistic insight. *Biomed. Pharmacother.* **2015**, *74*, 101–110.

177. Schapira, A. H. V Mitochondrial dysfunction in neurodegenerative diseases. *Neurochem. Res.* **2008**, *33*, 2502–9.

178. Moon, H. E.; Paek, S. H. Mitochondrial Dysfunction in Parkinson's Disease. *Exp. Neurobiol.* **2015**, *24*, 103–16.

179. McNaught, K. S. P.; Belizaire, R.; Isacson, O.; Jenner, P.; Olanow, C. W. Altered proteasomal function in sporadic Parkinson's disease. *Exp. Neurol.* **2003**, *179*, 38–46.

180. Webb, J. L.; Ravikumar, B.; Atkins, J.; Skepper, J. N.; Rubinsztein, D. C. alpha-Synuclein Is Degraded by Both Autophagy and the Proteasome. *J. Biol. Chem.* **2003**, *278*, 25009–25013.

181. Ebrahimi-Fakhari, D.; Cantuti-Castelvetri, I.; Fan, Z.; Rockenstein, E.; Masliah, E.; Hyman, B. T.; McLean, P. J.; Unni, V. K. Distinct roles in vivo for the ubiquitin-proteasome system and the autophagy-lysosomal pathway in the degradation of α-synuclein. *J. Neurosci.* **2011**, *31*, 14508–20.

182. Cuervo, a. M. Impaired Degradation of Mutant -Synuclein by Chaperone-Mediated Autophagy. *Science (80-.).* **2004**, *305*, 1292–1295.

183. Mak, S. K.; McCormack, A. L.; Manning-Bog, A. B.; Cuervo, A. M.; Di Monte, D. A. Lysosomal degradation of alpha-synuclein in vivo. *J. Biol. Chem.* **2010**, *285*, 13621–9.

184. Vogiatzi, T.; Xilouri, M.; Vekrellis, K.; Stefanis, L. Wild type alpha-synuclein is degraded by chaperone-mediated autophagy and macroautophagy in neuronal cells. *J. Biol. Chem.* **2008**, *283*, 23542–56.

185. Anglade, P.; Vyas, S.; Javoy-Agid, F.; Herrero, M. T.; Michel, P. P.; Marquez, J.; Mouatt-Prigent, A.; Ruberg, M.; Hirsch, E. C.; Agid, Y. Apoptosis and autophagy in nigral neurons of patients with Parkinson's disease. *Histol. Histopathol.* **1997**, *12*, 25–31.

186. Cotzias, G. C.; Papavasiliou, P. S.; Gellene, R. Modification of Parkinsonism--chronic treatment with L-dopa. *N. Engl. J. Med.* **1969**, *280*, 337–45.

187. Levine, C. B.; Fahrbach, K. R.; Siderowf, A. D.; Estok, R. P.; Ludensky, V. M.; Ross, S. D. Diagnosis and treatment of Parkinson's disease: a systematic review of the literature. *Evid. Rep. Technol. Assess. (Summ).* **2003**, 1–4.

188. Golbe, L. I. Young-onset Parkinson's disease: a clinical review. *Neurology* **1991**, *41*, 168–73.

189. Rascol, O.; Brooks, D. J.; Korczyn, A. D.; De Deyn, P. P.; Clarke, C. E.; Lang, A. E. A five-year study of the incidence of dyskinesia in patients with early Parkinson's disease who were treated with ropinirole or levodopa. *N. Engl. J. Med.* **2000**, *342*, 1484–91.

190. Pramipexole vs levodopa as initial treatment for Parkinson disease: A randomized controlled trial. Parkinson Study Group. *JAMA* **2000**, *284*, 1931–8.

191. Hauser, R. A.; Rascol, O.; Korczyn, A. D.; Jon Stoessl, A.; Watts, R. L.; Poewe, W.; De Deyn, P. P.; Lang, A. E. Ten-year follow-up of Parkinson's disease patients randomized to initial therapy with ropinirole or levodopa. *Mov. Disord.* **2007**, *22*, 2409–17.

192. Constantinescu, R.; Romer, M.; McDermott, M. P.; Kamp, C.; Kieburtz, K. Impact of pramipexole on the onset of levodopa-related dyskinesias. *Mov. Disord.* **2007**, *22*, 1317–9.

193. Katzenschlager, R.; Head, J.; Schrag, A.; Ben-Shlomo, Y.; Evans, A.; Lees, A. J. Fourteen-year final report of the randomized PDRG-UK trial comparing three initial treatments in PD. *Neurology* **2008**, *71*, 474–80.

194. Hely, M. A.; Morris, J. G. L.; Reid, W. G. J.; Trafficante, R. Sydney Multicenter Study of Parkinson's disease: non-L-dopa-responsive problems dominate at 15 years. *Mov. Disord.* **2005**, *20*, 190–9.

195. Rascol, O.; Perez-Lloret, S.; Ferreira, J. J. New treatments for levodopa-induced motor complications. *Mov. Disord. Off. J. Mov. Disord. Soc.* **2015**, *30*, 1451–1460.

196. Stocchi, F.; Arnold, G.; Onofrj, M.; Kwiecinski, H.; Szczudlik, A.; Thomas, A.; Bonuccelli, U.; Van Dijk, A.; Cattaneo, C.; Sala, P.; Fariello, R. G. Improvement of motor function in early Parkinson disease by safinamide. *Neurology* **2004**, *63*, 746–8.

197. Stocchi, F.; Borgohain, R.; Onofrj, M.; Schapira, A. H. V; Bhatt, M.; Lucini, V.; Giuliani, R.; Anand, R. A randomized, double-blind, placebo-controlled trial of safinamide as add-on therapy in early Parkinson's disease patients. *Mov. Disord.* **2012**, *27*, 106–12.

198. Schapira, A. H. V; Stocchi, F.; Borgohain, R.; Onofrj, M.; Bhatt, M.; Lorenzana, P.; Lucini, V.; Giuliani, R.; Anand, R. Long-term efficacy and safety of safinamide as add-on therapy in early Parkinson's disease. *Eur. J. Neurol.* **2013**, *20*, 271–80.

199. Grégoire, L.; Jourdain, V. A.; Townsend, M.; Roach, A.; Di Paolo, T. Safinamide reduces dyskinesias and prolongs L-DOPA antiparkinsonian effect in parkinsonian monkeys. *Parkinsonism Relat. Disord.* **2013**, *19*, 508–14.

200. Borgohain, R.; Szasz, J.; Stanzione, P.; Meshram, C.; Bhatt, M. H.; Chirilineau, D.; Stocchi, F.; Lucini, V.; Giuliani, R.; Forrest, E.; Rice, P.; Anand, R. Two-year, randomized, controlled study of safinamide as add-on to levodopa in mid to late Parkinson's disease. *Mov. Disord.* **2014**, *29*, 1273–80.

201. Poewe, W.; Antonini, A. Novel formulations and modes of delivery of levodopa. *Mov. Disord.* **2015**, *30*, 114–20.

202. van der Brug, M. P.; Singleton, A.; Gasser, T.; Lewis, P. A. Parkinson's disease: From human genetics to clinical trials. *Sci. Transl. Med.* **2015**, *7*, 205ps20–205ps20.

203. Kalia, L. V; Kalia, S. K.; Lang, A. E. Disease-modifying strategies for Parkinson's disease. *Mov. Disord.* **2015**, *30*, 1442–50.

204. Aviles-Olmos, I.; Dickson, J.; Kefalopoulou, Z.; Djamshidian, A.; Ell, P.; Soderlund, T.; Whitton, P.; Wyse, R.; Isaacs, T.; Lees, A.; Limousin, P.; Foltynie, T. Exenatide and the treatment of patients with Parkinson's disease. *J. Clin. Invest.* **2013**, *123*, 2730–6.

205. Schintu, N.; Frau, L.; Ibba, M.; Caboni, P.; Garau, A.; Carboni, E.; Carta, A. R. PPAR-gamma-mediated neuroprotection in a chronic mouse model of Parkinson's disease. *Eur. J. Neurosci.* **2009**, *29*, 954–63.

206. Carta, A. R.; Frau, L.; Pisanu, A.; Wardas, J.; Spiga, S.; Carboni, E. Rosiglitazone decreases peroxisome proliferator receptor-γ levels in microglia and inhibits TNF-α production: new evidences on neuroprotection in a progressive Parkinson's disease model. *Neuroscience* **2011**, *194*, 250–61.

207. Carta, A. R.; Pisanu, A. Modulating microglia activity with PPAR-γ agonists: a promising therapy for Parkinson's disease? *Neurotox. Res.* **2013**, *23*, 112–23.

208. Brauer, R.; Bhaskaran, K.; Chaturvedi, N.; Dexter, D. T.; Smeeth, L.; Douglas, I. Glitazone Treatment and Incidence of Parkinson's Disease among People with Diabetes: A Retrospective Cohort Study. *PLoS Med.* **2015**, *12*, e1001854.

209. Pioglitazone in early Parkinson's disease: a phase 2, multicentre, double-blind, randomised trial. *Lancet. Neurol.* **2015**, *14*, 795–803.

210. Olson, K. E.; Gendelman, H. E. ScienceDirect Immunomodulation as a neuroprotective and therapeutic strategy for Parkinson ' s disease. *Curr. Opin. Pharmacol.* **2016**, *26*, 87–95.

211. Aviles-Olmos, I.; Dickson, J.; Kefalopoulou, Z.; Djamshidian, A.; Kahan, J.; Ell, P.; Whitton, P.; Wyse, R.; Isaacs, T.; Lees, A.; Limousin, P.; Foltynie, T. Motor and cognitive advantages persist 12 months after exenatide exposure in Parkinson's disease. *J. Parkinsons. Dis.* **2014**, *4*, 337–44.

212. Gong, L.; Zhang, Q.-L.; Zhang, N.; Hua, W.-Y.; Huang, Y.-X.; Di, P.-W.; Huang, T.; Xu, X.-S.; Liu, C.-F.; Hu, L.-F.; Luo, W.-F. Neuroprotection by urate on 6-OHDA-lesioned rat model of Parkinson's disease: linking to Akt/GSK3β signaling pathway. *J. Neurochem.* **2012**, *123*, 876–85.

213. Pan, M.; Gao, H.; Long, L.; Xu, Y.; Liu, M.; Zou, J.; Wu, A.; Wei, X.; Chen, X.; Tang, B.; Wang, Q. Serum uric acid in patients with Parkinson's disease and vascular parkinsonism: a cross-sectional study. *Neuroimmunomodulation* **2013**, *20*, 19–28.

214. Schwarzschild, M. A.; Ascherio, A.; Beal, M. F.; Cudkowicz, M. E.; Curhan, G. C.; Hare, J. M.; Hooper, D. C.; Kieburtz, K. D.; Macklin, E. A.; Oakes, D.; Rudolph, A.; Shoulson, I.; Tennis, M. K.; Espay, A. J.; Gartner, M.; Hung, A.; Bwala, G.; Lenehan, R.; Encarnacion, E.; Ainslie, M.; Castillo, R.; Togasaki, D.; Barles, G.; Friedman, J. H.; Niles, L.; Carter, J. H.; Murray, M.; Goetz, C. G.; Jaglin, J.; Ahmed, A.; Russell, D. S.; Cotto, C.; Goudreau, J. L.; Russell, D.; Parashos, S. A.; Ede, P.; Saint-Hilaire, M. H.; Thomas, C.-A.; James, R.; Stacy, M. A.; Johnson, J.; Gauger, L.; Antonelle de Marcaida, J.; Thurlow, S.; Isaacson, S. H.; Carvajal, L.; Rao, J.; Cook, M.; Hope-Porche, C.; McClurg, L.; Grasso, D. L.; Logan, R.; Orme, C.; Ross, T.; Brocht, A. F. D.; Constantinescu, R.; Sharma, S.; Venuto, C.; Weber, J.; Eaton, K. Inosine to increase serum and cerebrospinal fluid urate in Parkinson disease: a randomized clinical trial. *JAMA Neurol.* **2014**, *71*, 141–50.

215. Noyce, A. J.; Bestwick, J. P.; Silveira-Moriyama, L.; Hawkes, C. H.; Giovannoni, G.; Lees, A. J.; Schrag, A. Meta-analysis of early nonmotor features and risk factors for Parkinson disease. *Ann. Neurol.* **2012**, *72*, 893–901.

216. Taymans, J.-M. Can the increasing number of newly developed leucine-rich repeat kinase 2 inhibitors validate or invalidate a potential disease-modifying therapeutic approach for Parkinson's disease? *Expert Opin. Ther. Pat.* **2014**, *24*, 727–30.

217. Herzig, M. C.; Kolly, C.; Persohn, E.; Theil, D.; Schweizer, T.; Hafner, T.; Stemmelen, C.; Troxler, T. J.; Schmid, P.; Danner, S.; Schnell, C. R.; Mueller, M.; Kinzel, B.; Grevot, A.; Bolognani, F.; Stirn, M.; Kuhn, R. R.; Kaupmann, K.; van der Putten, P. H.; Rovelli, G.; Shimshek, D. R. LRRK2 protein levels are determined by kinase function and are crucial for kidney and lung homeostasis in mice. *Hum. Mol. Genet.* **2011**, *20*, 4209–23.

218. Fuji, R. N.; Flagella, M.; Baca, M.; S Baptista, M. A.; Brodbeck, J.; Chan, B. K.; Fiske, B. K.; Honigberg, L.; Jubb, A. M.; Katavolos, P.; Lee, D. W.; Lewin-Koh, S.-C.; Lin, T.; Liu, X.; Liu, S.; Lyssikatos, J. P.; O'Mahony, J.; Reichelt, M.; Roose-Girma, M.; Sheng, Z.; Sherer, T.; Smith, A.; Solon, M.; Sweeney, Z. K.; Tarrant, J.; Urkowitz, A.; Warming, S.; Yaylaoglu, M.; Zhang, S.; Zhu, H.; Estrada, A. A.; Watts, R. J. Effect of selective LRRK2 kinase inhibition on nonhuman primate lung. *Sci. Transl. Med.* **2015**, *7*, 273ra15.

219. Fell, M. J.; Mirescu, C.; Basu, K.; Cheewatrakoolpong, B.; DeMong, D. E.; Ellis, J. M.; Hyde, L. A.; Lin, Y.; Markgraf, C. G.; Mei, H.; Miller, M.; Poulet, F. M.; Scott, J. D.; Smith, M. D.; Yin, Z.; Zhou, X.; Parker, E. M.; Kennedy, M. E.; Morrow, J. A. MLi-2, a Potent, Selective, and Centrally Active Compound for Exploring the Therapeutic Potential and Safety of LRRK2 Kinase Inhibition. *J. Pharmacol. Exp. Ther.* **2015**, *355*, 397–409.

220. Baptista, M. A. S.; Dave, K. D.; Frasier, M. A.; Sherer, T. B.; Greeley, M.; Beck, M. J.; Varsho, J. S.; Parker, G. A.; Moore, C.; Churchill, M. J.; Meshul, C. K.; Fiske, B. K. Loss of leucine-rich repeat kinase 2 (LRRK2) in rats leads to progressive abnormal phenotypes in peripheral organs. *PLoS One* **2013**, *8*, e80705.

221. Lee, H.-J.; Bae, E.-J.; Lee, S.-J. Extracellular α--synuclein-a novel and crucial factor in

Lewy body diseases. *Nat. Rev. Neurol.* **2014**, *10*, 92–8.

222. Valera, E.; Masliah, E. Immunotherapy for neurodegenerative diseases: focus on α-synucleinopathies. *Pharmacol. Ther.* **2013**, *138*, 311–22.

223. Schapira, A. H. V; Olanow, C. W.; Greenamyre, J. T.; Bezard, E. Slowing of neurodegeneration in Parkinson's disease and Huntington's disease: future therapeutic perspectives. *Lancet (London, England)* **2014**, *384*, 545–55.

224. Lindström, V.; Fagerqvist, T.; Nordström, E.; Eriksson, F.; Lord, A.; Tucker, S.; Andersson, J.; Johannesson, M.; Schell, H.; Kahle, P. J.; Möller, C.; Gellerfors, P.; Bergström, J.; Lannfelt, L.; Ingelsson, M. Immunotherapy targeting α-synuclein protofibrils reduced pathology in (Thy-1)-h[A30P] α-synuclein mice. *Neurobiol. Dis.* **2014**, *69*, 134–43.

225. Shahaduzzaman, M.; Nash, K.; Hudson, C.; Sharif, M.; Grimmig, B.; Lin, X.; Bai, G.; Liu, H.; Ugen, K. E.; Cao, C.; Bickford, P. C. Anti-human α-synuclein N-terminal peptide antibody protects against dopaminergic cell death and ameliorates behavioral deficits in an AAV-α-synuclein rat model of Parkinson's disease. *PLoS One* **2015**, *10*, e0116841.

226. Games, D.; Valera, E.; Spencer, B.; Rockenstein, E.; Mante, M.; Adame, A.; Patrick, C.; Ubhi, K.; Nuber, S.; Sacayon, P.; Zago, W.; Seubert, P.; Barbour, R.; Schenk, D.; Masliah, E. Reducing C-terminal-truncated alpha-synuclein by immunotherapy attenuates neurodegeneration and propagation in Parkinson's disease-like models. *J. Neurosci.* **2014**, *34*, 9441–54.

227. Barker, R. A.; Drouin-Ouellet, J.; Parmar, M. Cell-based therapies for Parkinson disease—past insights and future potential. *Nat. Rev. Neurol.* **2015**, *11*, 492–503.

228. Piccini, P.; Brooks, D. J.; Björklund, A.; Gunn, R. N.; Grasby, P. M.; Rimoldi, O.; Brundin, P.; Hagell, P.; Rehncrona, S.; Widner, H.; Lindvall, O. Dopamine release from nigral transplants visualized in vivo in a Parkinson's patient. *Nat. Neurosci.* **1999**, *2*, 1137–40.

229. Piccini, P.; Lindvall, O.; Björklund, A.; Brundin, P.; Hagell, P.; Ceravolo, R.; Oertel, W.; Quinn, N.; Samuel, M.; Rehncrona, S.; Widner, H.; Brooks, D. J. Delayed recovery of movement-related cortical function in Parkinson's disease after striatal dopaminergic grafts. *Ann. Neurol.* **2000**, *48*, 689–95.

230. Widner, H.; Tetrud, J.; Rehncrona, S.; Snow, B.; Brundin, P.; Gustavii, B.; Björklund, A.; Lindvall, O.; Langston, J. W. Bilateral fetal mesencephalic grafting in two patients with parkinsonism induced by 1-methyl-4-phenyl-1,2,3,6-tetrahydropyridine (MPTP). *N. Engl. J. Med.* **1992**, *327*, 1556–63.

231. Freed, C. R.; Greene, P. E.; Breeze, R. E.; Tsai, W.-Y.; DuMouchel, W.; Kao, R.; Dillon, S.; Winfield, H.; Culver, S.; Trojanowski, J. Q.; Eidelberg, D.; Fahn, S. Transplantation of Embryonic Dopamine Neurons for Severe Parkinson's Disease. *N. Engl. J. Med.* **2001**, *344*, 710–719.

232. Kumar, R.; Lozano, A. M.; Kim, Y. J.; Hutchison, W. D.; Sime, E.; Halket, E.; Lang, A. E. Double-blind evaluation of subthalamic nucleus deep brain stimulation in advanced Parkinson's disease. *Neurology* **1998**, *51*, 850–5.

233. Ma, Y.; Feigin, A.; Dhawan, V.; Fukuda, M.; Shi, Q.; Greene, P.; Breeze, R.; Fahn, S.; Freed, C.; Eidelberg, D. Dyskinesia after fetal cell transplantation for parkinsonism: a PET study. *Ann. Neurol.* **2002**, *52*, 628–34.

234. Politis, M.; Oertel, W. H.; Wu, K.; Quinn, N. P.; Pogarell, O.; Brooks, D. J.; Bjorklund, A.; Lindvall, O.; Piccini, P. Graft-induced dyskinesias in Parkinson's disease: High striatal serotonin/dopamine transporter ratio. *Mov. Disord.* **2011**, *26*, 1997–2003.

235. Hagell, P.; Brundin, P. Cell survival and clinical outcome following intrastriatal transplantation in Parkinson disease. *J. Neuropathol. Exp. Neurol.* **2001**, *60*, 741–52.

236. Brederlau, A.; Correia, A. S.; Anisimov, S. V; Elmi, M.; Paul, G.; Roybon, L.; Morizane, A.; Bergquist, F.; Riebe, I.; Nannmark, U.; Carta, M.; Hanse, E.; Takahashi, J.; Sasai, Y.; Funa, K.; Brundin, P.; Eriksson, P. S.; Li, J.-Y. Transplantation of human embryonic stem cell-derived cells to a rat model of Parkinson's disease: effect of in vitro differentiation on graft survival and teratoma formation. *Stem Cells* **2006**, *24*, 1433–40.

237. Park, C.-H.; Minn, Y.-K.; Lee, J.-Y.; Choi, D. H.; Chang, M.-Y.; Shim, J.-W.; Ko, J.-Y.; Koh, H.-C.; Kang, M. J.; Kang, J. S.; Rhie, D.-J.; Lee, Y.-S.; Son, H.; Moon, S. Y.; Kim, K.-S.; Lee, S.-H. In vitro and in vivo analyses of human embryonic stem cell-derived dopamine neurons. *J.*

Neurochem. **2005**, *92*, 1265–76.

238. Zeng, X.; Cai, J.; Chen, J.; Luo, Y.; You, Z.-B.; Fotter, E.; Wang, Y.; Harvey, B.; Miura, T.; Backman, C.; Chen, G.-J.; Rao, M. S.; Freed, W. J. Dopaminergic differentiation of human embryonic stem cells. *Stem Cells* **2004**, *22*, 925–40.

239. Sonntag, K.-C.; Pruszak, J.; Yoshizaki, T.; van Arensbergen, J.; Sanchez-Pernaute, R.; Isacson, O. Enhanced yield of neuroepithelial precursors and midbrain-like dopaminergic neurons from human embryonic stem cells using the bone morphogenic protein antagonist noggin. *Stem Cells* **2007**, *25*, 411–8.

240. Roy, N. S.; Cleren, C.; Singh, S. K.; Yang, L.; Beal, M. F.; Goldman, S. A. Functional engraftment of human ES cell-derived dopaminergic neurons enriched by coculture with telomerase-immortalized midbrain astrocytes. *Nat. Med.* **2006**, *12*, 1259–68.

241. Cooper, O.; Hargus, G.; Deleidi, M.; Blak, A.; Osborn, T.; Marlow, E.; Lee, K.; Levy, A.; Perez-Torres, E.; Yow, A.; Isacson, O. Differentiation of human ES and Parkinson's disease iPS cells into ventral midbrain dopaminergic neurons requires a high activity form of SHH, FGF8a and specific regionalization by retinoic acid. *Mol. Cell. Neurosci.* **2010**, *45*, 258–66.

242. Takahashi, K.; Yamanaka, S. Induction of pluripotent stem cells from mouse embryonic and adult fibroblast cultures by defined factors. *Cell* **2006**, *126*, 663–76.

243. Hargus, G.; Cooper, O.; Deleidi, M.; Levy, A.; Lee, K.; Marlow, E.; Yow, A.; Soldner, F.; Hockemeyer, D.; Hallett, P. J.; Osborn, T.; Jaenisch, R.; Isacson, O. Differentiated Parkinson patient-derived induced pluripotent stem cells grow in the adult rodent brain and reduce motor asymmetry in Parkinsonian rats. *Proc. Natl. Acad. Sci. U. S. A.* **2010**, *107*, 15921–6.

244. Kikuchi, T.; Morizane, A.; Doi, D.; Onoe, H.; Hayashi, T.; Kawasaki, T.; Saiki, H.; Miyamoto, S.; Takahashi, J. Survival of human induced pluripotent stem cell-derived midbrain dopaminergic neurons in the brain of a primate model of Parkinson's disease. *J. Parkinsons. Dis.* **2011**, *1*, 395–412.

245. Kriks, S.; Shim, J.-W.; Piao, J.; Ganat, Y. M.; Wakeman, D. R.; Xie, Z.; Carrillo-Reid, L.; Auyeung, G.; Antonacci, C.; Buch, A.; Yang, L.; Beal, M. F.; Surmeier, D. J.; Kordower, J. H.; Tabar, V.; Studer, L. Dopamine neurons derived from human ES cells efficiently engraft in animal models of Parkinson's disease. *Nature* **2011**, *480*, 547–51.

246. Kirkeby, A.; Grealish, S.; Wolf, D. A.; Nelander, J.; Wood, J.; Lundblad, M.; Lindvall, O.; Parmar, M. Generation of regionally specified neural progenitors and functional neurons from human embryonic stem cells under defined conditions. *Cell Rep.* **2012**, *1*, 703–14.

247. Fasano, C. A.; Chambers, S. M.; Lee, G.; Tomishima, M. J.; Studer, L. Efficient derivation of functional floor plate tissue from human embryonic stem cells. *Cell Stem Cell* **2010**, *6*, 336–47.

248. Grealish, S.; Diguet, E.; Kirkeby, A.; Mattsson, B.; Heuer, A.; Bramoulle, Y.; Van Camp, N.; Perrier, A. L.; Hantraye, P.; Björklund, A.; Parmar, M. Human ESC-derived dopamine neurons show similar preclinical efficacy and potency to fetal neurons when grafted in a rat model of Parkinson's disease. *Cell Stem Cell* **2014**, *15*, 653–65.

249. Morizane, A.; Doi, D.; Kikuchi, T.; Okita, K.; Hotta, A.; Kawasaki, T.; Hayashi, T.; Onoe, H.; Shiina, T.; Yamanaka, S.; Takahashi, J. Direct comparison of autologous and allogeneic transplantation of iPSC-derived neural cells in the brain of a non-human primate. *Stem cell reports* **2013**, *1*, 283–92.

250. Fernández-Santiago, R.; Carballo-Carbajal, I.; Castellano, G.; Torrent, R.; Richaud, Y.; Sánchez-Danés, A.; Vilarrasa-Blasi, R.; Sánchez-Pla, A.; Mosquera, J. L.; Soriano, J.; López-Barneo, J.; Canals, J. M.; Alberch, J.; Raya, Á.; Vila, M.; Consiglio, A.; Martín-Subero, J. I.; Ezquerra, M.; Tolosa, E. Aberrant epigenome in iPSC-derived dopaminergic neurons from Parkinson's disease patients. *EMBO Mol. Med.* **2015**, *7*, 1529–46.

251. Kim, H. S.; Bernitz, J. M.; Lee, D.-F.; Lemischka, I. R. Genomic editing tools to model human diseases with isogenic pluripotent stem cells. *Stem Cells Dev.* **2014**, *23*, 2673–86.

252. Kordower, J. H.; Bjorklund, A. Trophic factor gene therapy for Parkinson's disease. *Mov. Disord.* **2013**, *28*, 96–109.

253. Airaksinen, M. S.; Saarma, M. THE GDNF FAMILY: SIGNALLING, BIOLOGICAL FUNCTIONS AND THERAPEUTIC VALUE. *Nat. Rev. Neurosci.* **2002**, *3*, 383–394.

254. Dianshuai Gao, Y. L. S. S. L. L. and Y. X. *Etiology and Pathophysiology of Parkinson's Disease*; Rana, A. Q., Ed.; InTech, 2011.

255. d'Anglemont de Tassigny, X.; Pascual, A.; López-Barneo, J. GDNF-based therapies, GDNF-producing interneurons, and trophic support of the dopaminergic nigrostriatal pathway. Implications for Parkinson's disease. *Front. Neuroanat.* **2015**, *9*, 10.

256. Pascual, A.; Hidalgo-Figueroa, M.; Gómez-Díaz, R.; López-Barneo, J. GDNF and protection of adult central catecholaminergic neurons. *J. Mol. Endocrinol.* **2011**, *46*, R83–92.

257. Paratcha, G.; Ledda, F.; Ibáñez, C. F. The neural cell adhesion molecule NCAM is an alternative signaling receptor for GDNF family ligands. *Cell* **2003**, *113*, 867–79.

258. Lin, L. F.; Doherty, D. H.; Lile, J. D.; Bektesh, S.; Collins, F. GDNF: a glial cell line-derived neurotrophic factor for midbrain dopaminergic neurons. *Science* **1993**, *260*, 1130–2.

259. Moore, M. W.; Klein, R. D.; Fariñas, I.; Sauer, H.; Armanini, M.; Phillips, H.; Reichardt, L. F.; Ryan, A. M.; Carver-Moore, K.; Rosenthal, A. Renal and neuronal abnormalities in mice lacking GDNF. *Nature* **1996**, *382*, 76–9.

260. Pichel, J. G.; Shen, L.; Sheng, H. Z.; Granholm, A. C.; Drago, J.; Grinberg, A.; Lee, E. J.; Huang, S. P.; Saarma, M.; Hoffer, B. J.; Sariola, H.; Westphal, H. GDNF is required for kidney development and enteric innervation. *Cold Spring Harb. Symp. Quant. Biol.* **1996**, *61*, 445–57.

261. Sánchez, M. P.; Silos-Santiago, I.; Frisén, J.; He, B.; Lira, S. A.; Barbacid, M. Renal agenesis and the absence of enteric neurons in mice lacking GDNF. *Nature* **1996**, *382*, 70–3.

262. Pascual, A.; Hidalgo-Figueroa, M.; Piruat, J. I.; Pintado, C. O.; Gómez-Díaz, R.; López-Barneo, J. Absolute requirement of GDNF for adult catecholaminergic neuron survival. *Nat. Neurosci.* **2008**, *11*, 755–61.

263. Hoffer, B. J.; Hoffman, A.; Bowenkamp, K.; Huettl, P.; Hudson, J.; Martin, D.; Lin, L. F.; Gerhardt, G. A. Glial cell line-derived neurotrophic factor reverses toxin-induced injury to midbrain dopaminergic neurons in vivo. *Neurosci. Lett.* **1994**, *182*, 107–11.

264. Bowenkamp, K. E.; Hoffman, A. F.; Gerhardt, G. A.; Henry, M. A.; Biddle, P. T.; Hoffer, B. J.; Granholm, A. C. Glial cell line-derived neurotrophic factor supports survival of injured midbrain dopaminergic neurons. *J. Comp. Neurol.* **1995**, *355*, 479–89.

265. Tomac, A.; Lindqvist, E.; Lin, L. F.; Ogren, S. O.; Young, D.; Hoffer, B. J.; Olson, L. Protection and repair of the nigrostriatal dopaminergic system by GDNF in vivo. *Nature* **1995**, *373*, 335–9.

266. Winkler, C.; Sauer, H.; Lee, C. S.; Björklund, A. Short-term GDNF treatment provides long-term rescue of lesioned nigral dopaminergic neurons in a rat model of Parkinson's disease. *J. Neurosci.* **1996**, *16*, 7206–15.

267. Gash, D. M.; Zhang, Z.; Ovadia, A.; Cass, W. A.; Yi, A.; Simmerman, L.; Russell, D.; Martin, D.; Lapchak, P. A.; Collins, F.; Hoffer, B. J.; Gerhardt, G. A. Functional recovery in parkinsonian monkeys treated with GDNF. *Nature* **1996**, *380*, 252–5.

268. Nutt, J. G.; Burchiel, K. J.; Comella, C. L.; Jankovic, J.; Lang, A. E.; Laws, E. R.; Lozano, A. M.; Penn, R. D.; Simpson, R. K.; Stacy, M.; Wooten, G. F. Randomized, double-blind trial of glial cell line-derived neurotrophic factor (GDNF) in PD. *Neurology* **2003**, *60*, 69–73.

269. Patel, N. K.; Bunnage, M.; Plaha, P.; Svendsen, C. N.; Heywood, P.; Gill, S. S. Intraputamenal infusion of glial cell line-derived neurotrophic factor in PD: a two-year outcome study. *Ann. Neurol.* **2005**, *57*, 298–302.

270. Slevin, J. T.; Gerhardt, G. A.; Smith, C. D.; Gash, D. M.; Kryscio, R.; Young, B. Improvement of bilateral motor functions in patients with Parkinson disease through the unilateral intraputaminal infusion of glial cell line-derived neurotrophic factor. *J. Neurosurg.* **2005**, *102*, 216–22.

271. Lang, A. E.; Gill, S.; Patel, N. K.; Lozano, A.; Nutt, J. G.; Penn, R.; Brooks, D. J.; Hotton, G.; Moro, E.; Heywood, P.; Brodsky, M. A.; Burchiel, K.; Kelly, P.; Dalvi, A.; Scott, B.; Stacy, M.; Turner, D.; Wooten, V. G. F.; Elias, W. J.; Laws, E. R.; Dhawan, V.; Stoessl, A. J.; Matcham, J.; Coffey, R. J.; Traub, M. Randomized controlled trial of intraputamenal glial cell line-derived neurotrophic factor infusion in Parkinson disease. *Ann. Neurol.* **2006**, *59*, 459–66.

272. Tatarewicz, S. M.; Wei, X.; Gupta, S.; Masterman, D.; Swanson, S. J.; Moxness, M. S. Development of a maturing T-cell-mediated immune response in patients with idiopathic

Parkinson's disease receiving r-metHuGDNF via continuous intraputaminal infusion. *J. Clin. Immunol.* **2007**, *27*, 620–7.

273. Lindholm, D.; Mäkelä, J.; Di Liberto, V.; Mudò, G.; Belluardo, N.; Eriksson, O.; Saarma, M. Current disease modifying approaches to treat Parkinson's disease. *Cell. Mol. Life Sci.* **2015**.

274. Björklund, A.; Kirik, D.; Rosenblad, C.; Georgievska, B.; Lundberg, C.; Mandel, R. J. Towards a neuroprotective gene therapy for Parkinson's disease: use of adenovirus, AAV and lentivirus vectors for gene transfer of GDNF to the nigrostriatal system in the rat Parkinson model. *Brain Res.* **2000**, *886*, 82–98.

275. Kirik, D.; Georgievska, B.; Björklund, A. Localized striatal delivery of GDNF as a treatment for Parkinson disease. *Nat. Neurosci.* **2004**, *7*, 105–10.

276. Salegio, E. A.; Samaranch, L.; Kells, A. P.; Forsayeth, J.; Bankiewicz, K. Guided delivery of adeno-associated viral vectors into the primate brain. *Adv. Drug Deliv. Rev.* **2012**, *64*, 598–604.

277. Bobo, R. H.; Laske, D. W.; Akbasak, A.; Morrison, P. F.; Dedrick, R. L.; Oldfield, E. H. Convection-enhanced delivery of macromolecules in the brain. *Proc. Natl. Acad. Sci. U. S. A.* **1994**, *91*, 2076–80.

278. Marks, W. J.; Bartus, R. T.; Siffert, J.; Davis, C. S.; Lozano, A.; Boulis, N.; Vitek, J.; Stacy, M.; Turner, D.; Verhagen, L.; Bakay, R.; Watts, R.; Guthrie, B.; Jankovic, J.; Simpson, R.; Tagliati, M.; Alterman, R.; Stern, M.; Baltuch, G.; Starr, P. A.; Larson, P. S.; Ostrem, J. L.; Nutt, J.; Kieburtz, K.; Kordower, J. H.; Olanow, C. W. Gene delivery of AAV2-neurturin for Parkinson's disease: a double-blind, randomised, controlled trial. *Lancet. Neurol.* **2010**, *9*, 1164–72.

279. Olanow, C. W.; Bartus, R. T.; Volpicelli-Daley, L. A.; Kordower, J. H. Trophic factors for Parkinson's disease: To live or let die. *Mov. Disord.* **2015**, *30*, 1715–24.

280. Rosenblad, C.; Kirik, D.; Devaux, B.; Moffat, B.; Phillips, H. S.; Björklund, A. Protection and regeneration of nigral dopaminergic neurons by neurturin or GDNF in a partial lesion model of Parkinson's disease after administration into the striatum or the lateral ventricle. *Eur. J. Neurosci.* **1999**, *11*, 1554–66.

281. Oiwa, Y.; Yoshimura, R.; Nakai, K.; Itakura, T. Dopaminergic neuroprotection and regeneration by neurturin assessed by using behavioral, biochemical and histochemical measurements in a model of progressive Parkinson's disease. *Brain Res.* **2002**, *947*, 271–83.

282. Grondin, R.; Zhang, Z.; Ai, Y.; Ding, F.; Walton, A. A.; Surgener, S. P.; Gerhardt, G. A.; Gash, D. M. Intraputamenal infusion of exogenous neurturin protein restores motor and dopaminergic function in the globus pallidus of MPTP-lesioned rhesus monkeys. *Cell Transplant.* **2008**, *17*, 373–81.

283. Gasmi, M.; Brandon, E. P.; Herzog, C. D.; Wilson, A.; Bishop, K. M.; Hofer, E. K.; Cunningham, J. J.; Printz, M. A.; Kordower, J. H.; Bartus, R. T. AAV2-mediated delivery of human neurturin to the rat nigrostriatal system: long-term efficacy and tolerability of CERE-120 for Parkinson's disease. *Neurobiol. Dis.* **2007**, *27*, 67–76.

284. Herzog, C. D.; Dass, B.; Holden, J. E.; Stansell, J.; Gasmi, M.; Tuszynski, M. H.; Bartus, R. T.; Kordower, J. H. Striatal delivery of CERE-120, an AAV2 vector encoding human neurturin, enhances activity of the dopaminergic nigrostriatal system in aged monkeys. *Mov. Disord.* **2007**, *22*, 1124–32.

285. Herzog, C. D.; Dass, B.; Gasmi, M.; Bakay, R.; Stansell, J. E.; Tuszynski, M.; Bankiewicz, K.; Chen, E.-Y.; Chu, Y.; Bishop, K.; Kordower, J. H.; Bartus, R. T. Transgene expression, bioactivity, and safety of CERE-120 (AAV2-neurturin) following delivery to the monkey striatum. *Mol. Ther.* **2008**, *16*, 1737–44.

286. Bartus, R. T.; Baumann, T. L.; Siffert, J.; Herzog, C. D.; Alterman, R.; Boulis, N.; Turner, D. A.; Stacy, M.; Lang, A. E.; Lozano, A. M.; Olanow, C. W. Safety/feasibility of targeting the substantia nigra with AAV2-neurturin in Parkinson patients. *Neurology* **2013**, *80*, 1698–701.

287. Bové, J.; Perier, C. Neurotoxin-based models of Parkinson's disease. *Neuroscience* **2012**, *211*, 51–76.

288. Ungerstedt, U. 6-Hydroxy-dopamine induced degeneration of central monoamine neurons. *Eur. J. Pharmacol.* **1968**, *5*, 107–10.

289. Faull, R. L.; Laverty, R. Changes in dopamine levels in the corpus striatum following lesions in the substantia nigra. *Exp. Neurol.* **1969**, *23*, 332–40.

290. Sauer, H.; Oertel, W. H. Progressive degeneration of nigrostriatal dopamine neurons following intrastriatal terminal lesions with 6-hydroxydopamine: a combined retrograde tracing and immunocytochemical study in the rat. *Neuroscience* **1994**, *59*, 401–15.

291. Przedborski, S.; Levivier, M.; Jiang, H.; Ferreira, M.; Jackson-Lewis, V.; Donaldson, D.; Togasaki, D. M. Dose-dependent lesions of the dopaminergic nigrostriatal pathway induced by intrastriatal injection of 6-hydroxydopamine. *Neuroscience* **1995**, *67*, 631–47.

292. Bezard, E.; Przedborski, S. A tale on animal models of Parkinson's disease. *Mov. Disord.* **2011**, *26*, 993–1002.

293. Giovanni, A.; Sieber, B. A.; Heikkila, R. E.; Sonsalla, P. K. Studies on species sensitivity to the dopaminergic neurotoxin 1-methyl-4-phenyl-1,2,3,6-tetrahydropyridine. Part 1: Systemic administration. *J. Pharmacol. Exp. Ther.* **1994**, *270*, 1000–7.

294. Sonsalla, P. K.; Heikkila, R. E. Neurotoxic effects of 1-methyl-4-phenyl-1,2,3,6-tetrahydropyridine (MPTP) and methamphetamine in several strains of mice. *Prog. Neuropsychopharmacol. Biol. Psychiatry* **1988**, *12*, 345–54.

295. Soto-Otero, R.; Méndez-Alvarez, E.; Hermida-Ameijeiras, A.; Muñoz-Patiño, A. M.; Labandeira-Garcia, J. L. Autoxidation and neurotoxicity of 6-hydroxydopamine in the presence of some antioxidants: potential implication in relation to the pathogenesis of Parkinson's disease. *J. Neurochem.* **2000**, *74*, 1605–12.

296. Hu, X.; Weng, Z.; Chu, C. T.; Zhang, L.; Cao, G.; Gao, Y.; Signore, A.; Zhu, J.; Hastings, T.; Greenamyre, J. T.; Chen, J. Peroxiredoxin-2 protects against 6-hydroxydopamine-induced dopaminergic neurodegeneration via attenuation of the apoptosis signal-regulating kinase (ASK1) signaling cascade. *J. Neurosci.* **2011**, *31*, 247–61.

297. Broom, L.; Marinova-Mutafchieva, L.; Sadeghian, M.; Davis, J. B.; Medhurst, A. D.; Dexter, D. T. Neuroprotection by the selective iNOS inhibitor GW274150 in a model of Parkinson disease. *Free Radic. Biol. Med.* **2011**, *50*, 633–40.

298. Feany, M. B.; Bender, W. W. A Drosophila model of Parkinson's disease. *Nature* **2000**, *404*, 394–8.

299. Liu, Z.; Wang, X.; Yu, Y.; Li, X.; Wang, T.; Jiang, H.; Ren, Q.; Jiao, Y.; Sawa, A.; Moran, T.; Ross, C. A.; Montell, C.; Smith, W. W. A Drosophila model for LRRK2-linked parkinsonism. *Proc. Natl. Acad. Sci. U. S. A.* **2008**, *105*, 2693–8.

300. Venderova, K.; Kabbach, G.; Abdel-Messih, E.; Zhang, Y.; Parks, R. J.; Imai, Y.; Gehrke, S.; Ngsee, J.; Lavoie, M. J.; Slack, R. S.; Rao, Y.; Zhang, Z.; Lu, B.; Haque, M. E.; Park, D. S. Leucine-Rich Repeat Kinase 2 interacts with Parkin, DJ-1 and PINK-1 in a Drosophila melanogaster model of Parkinson's disease. *Hum. Mol. Genet.* **2009**, *18*, 4390–404.

301. Saha, S.; Guillily, M. D.; Ferree, A.; Lanceta, J.; Chan, D.; Ghosh, J.; Hsu, C. H.; Segal, L.; Raghavan, K.; Matsumoto, K.; Hisamoto, N.; Kuwahara, T.; Iwatsubo, T.; Moore, L.; Goldstein, L.; Cookson, M.; Wolozin, B. LRRK2 modulates vulnerability to mitochondrial dysfunction in Caenorhabditis elegans. *J. Neurosci.* **2009**, *29*, 9210–8.

302. Chesselet, M.-F.; Carmichael, S. T. Animal models of neurological disorders. *Neurotherapeutics* **2012**, *9*, 241–4.

303. Rockenstein, E.; Mallory, M.; Hashimoto, M.; Song, D.; Shults, C. W.; Lang, I.; Masliah, E. Differential neuropathological alterations in transgenic mice expressing alpha-synuclein from the platelet-derived growth factor and Thy-1 promoters. *J. Neurosci. Res.* **2002**, *68*, 568–78.

304. Matsuoka, Y.; Vila, M.; Lincoln, S.; McCormack, A.; Picciano, M.; LaFrancois, J.; Yu, X.; Dickson, D.; Langston, W. J.; McGowan, E.; Farrer, M.; Hardy, J.; Duff, K.; Przedborski, S.; Di Monte, D. A. Lack of nigral pathology in transgenic mice expressing human alpha-synuclein driven by the tyrosine hydroxylase promoter. *Neurobiol. Dis.* **2001**, *8*, 535–9.

305. Lee, H.-J.; Patel, S.; Lee, S.-J. Intravesicular localization and exocytosis of alpha-synuclein and its aggregates. *J. Neurosci.* **2005**, *25*, 6016–24.

306. Diógenes, M. J.; Dias, R. B.; Rombo, D. M.; Vicente Miranda, H.; Maiolino, F.; Guerreiro, P.; Näsström, T.; Franquelim, H. G.; Oliveira, L. M. A.; Castanho, M. A. R. B.; Lannfelt, L.; Bergström, J.; Ingelsson, M.; Quintas, A.; Sebastião, A. M.; Lopes, L. V; Outeiro, T. F.

Extracellular alpha-synuclein oligomers modulate synaptic transmission and impair LTP via NMDA-receptor activation. *J. Neurosci.* **2012**, *32*, 11750–62.

307. Angot, E.; Steiner, J. A.; Lema Tomé, C. M.; Ekström, P.; Mattsson, B.; Björklund, A.; Brundin, P. Alpha-synuclein cell-to-cell transfer and seeding in grafted dopaminergic neurons in vivo. *PLoS One* **2012**, *7*, e39465.

308. Mougenot, A.-L.; Nicot, S.; Bencsik, A.; Morignat, E.; Verchère, J.; Lakhdar, L.; Legastelois, S.; Baron, T. Prion-like acceleration of a synucleinopathy in a transgenic mouse model. *Neurobiol. Aging* **2012**, *33*, 2225–2228.

309. Löw, K.; Aebischer, P. Use of viral vectors to create animal models for Parkinson's disease. *Neurobiol. Dis.* **2012**, *48*, 189–201.

310. Lo Bianco, C.; Ridet, J.-L.; Schneider, B. L.; Deglon, N.; Aebischer, P. alpha -Synucleinopathy and selective dopaminergic neuron loss in a rat lentiviral-based model of Parkinson's disease. *Proc. Natl. Acad. Sci. U. S. A.* **2002**, *99*, 10813–8.

311. Decressac, M.; Ulusoy, A.; Mattsson, B.; Georgievska, B.; Romero-Ramos, M.; Kirik, D.; Björklund, A. GDNF fails to exert neuroprotection in a rat α-synuclein model of Parkinson's disease. *Brain* **2011**, *134*, 2302–11.

312. Decressac, M.; Kadkhodaei, B.; Mattsson, B.; Laguna, A.; Perlmann, T.; Björklund, A. α-Synuclein-induced down-regulation of Nurr1 disrupts GDNF signaling in nigral dopamine neurons. *Sci. Transl. Med.* **2012**, *4*, 163ra156.

313. Li, X.; Patel, J. C.; Wang, J.; Avshalumov, M. V; Nicholson, C.; Buxbaum, J. D.; Elder, G. A.; Rice, M. E.; Yue, Z. Enhanced striatal dopamine transmission and motor performance with LRRK2 overexpression in mice is eliminated by familial Parkinson's disease mutation G2019S. *J. Neurosci.* **2010**, *30*, 1788–97.

314. Ramonet, D.; Daher, J. P. L.; Lin, B. M.; Stafa, K.; Kim, J.; Banerjee, R.; Westerlund, M.; Pletnikova, O.; Glauser, L.; Yang, L.; Liu, Y.; Swing, D. A.; Beal, M. F.; Troncoso, J. C.; McCaffery, J. M.; Jenkins, N. A.; Copeland, N. G.; Galter, D.; Thomas, B.; Lee, M. K.; Dawson, T. M.; Dawson, V. L.; Moore, D. J. Dopaminergic neuronal loss, reduced neurite complexity and autophagic abnormalities in transgenic mice expressing G2019S mutant LRRK2. *PLoS One* **2011**, *6*, e18568.

315. Zhou, H.; Huang, C.; Tong, J.; Hong, W. C.; Liu, Y.-J.; Xia, X.-G. Temporal expression of mutant LRRK2 in adult rats impairs dopamine reuptake. *Int. J. Biol. Sci.* **2011**, *7*, 753–61.

316. Dusonchet, J.; Kochubey, O.; Stafa, K.; Young, S. M.; Zufferey, R.; Moore, D. J.; Schneider, B. L.; Aebischer, P. A rat model of progressive nigral neurodegeneration induced by the Parkinson's disease-associated G2019S mutation in LRRK2. *J. Neurosci.* **2011**, *31*, 907–12.

317. Palacino, J. J.; Sagi, D.; Goldberg, M. S.; Krauss, S.; Motz, C.; Wacker, M.; Klose, J.; Shen, J. Mitochondrial dysfunction and oxidative damage in parkin-deficient mice. *J. Biol. Chem.* **2004**, *279*, 18614–22.

318. Gautier, C. A.; Kitada, T.; Shen, J. Loss of PINK1 causes mitochondrial functional defects and increased sensitivity to oxidative stress. *Proc. Natl. Acad. Sci.* **2008**, *105*, 11364–11369.

319. Påhlman, S.; Mamaeva, S.; Meyerson, G.; Mattsson, M. E.; Bjelfman, C.; Ortoft, E.; Hammerling, U. Human neuroblastoma cells in culture: a model for neuronal cell differentiation and function. *Acta Physiol. Scand. Suppl.* **1990**, *592*, 25–37.

320. Presgraves, S. P.; Ahmed, T.; Borwege, S.; Joyce, J. N. Terminally differentiated SH-SY5Y cells provide a model system for studying neuroprotective effects of dopamine agonists. *Neurotox. Res.* **2004**, *5*, 579–98.

321. Tofaris, G. K.; Layfield, R.; Spillantini, M. G. alpha-synuclein metabolism and aggregation is linked to ubiquitin-independent degradation by the proteasome. *FEBS Lett.* **2001**, *509*, 22–6.

322. Danzer, K. M.; Krebs, S. K.; Wolff, M.; Birk, G.; Hengerer, B. Seeding induced by alpha-synuclein oligomers provides evidence for spreading of alpha-synuclein pathology. *J. Neurochem.* **2009**, *111*, 192–203.

323. Watabe, M.; Nakaki, T. Rotenone induces apoptosis via activation of bad in human dopaminergic SH-SY5Y cells. *J. Pharmacol. Exp. Ther.* **2004**, *311*, 948–53.

324. Constantinescu, R.; Constantinescu, A. T.; Reichmann, H.; Janetzky, B. Neuronal differentiation and long-term culture of the human neuroblastoma line SH-SY5Y. *J. Neural*

Transm. Suppl. **2007**, 17–28.

325. Takahashi, K.; Tanabe, K.; Ohnuki, M.; Narita, M.; Ichisaka, T.; Tomoda, K.; Yamanaka, S. Induction of pluripotent stem cells from adult human fibroblasts by defined factors. *Cell* **2007**, *131*, 861–72.

326. Nakagawa, M.; Koyanagi, M.; Tanabe, K.; Takahashi, K.; Ichisaka, T.; Aoi, T.; Okita, K.; Mochiduki, Y.; Takizawa, N.; Yamanaka, S. Generation of induced pluripotent stem cells without Myc from mouse and human fibroblasts. *Nat. Biotechnol.* **2008**, *26*, 101–6.

327. Aasen, T.; Raya, A.; Barrero, M. J.; Garreta, E.; Consiglio, A.; Gonzalez, F.; Vassena, R.; Bilić, J.; Pekarik, V.; Tiscornia, G.; Edel, M.; Boué, S.; Izpisúa Belmonte, J. C. Efficient and rapid generation of induced pluripotent stem cells from human keratinocytes. *Nat. Biotechnol.* **2008**, *26*, 1276–84.

328. Rodríguez-Pizà, I.; Richaud-Patin, Y.; Vassena, R.; González, F.; Barrero, M. J.; Veiga, A.; Raya, A.; Izpisúa Belmonte, J. C. Reprogramming of human fibroblasts to induced pluripotent stem cells under xeno-free conditions. *Stem Cells* **2010**, *28*, 36–44.

329. Okita, K.; Ichisaka, T.; Yamanaka, S. Generation of germline-competent induced pluripotent stem cells. *Nature* **2007**, *448*, 313–7.

330. Raya, A.; Rodríguez-Pizà, I.; Guenechea, G.; Vassena, R.; Navarro, S.; Barrero, M. J.; Consiglio, A.; Castellà, M.; Río, P.; Sleep, E.; González, F.; Tiscornia, G.; Garreta, E.; Aasen, T.; Veiga, A.; Verma, I. M.; Surrallés, J.; Bueren, J.; Izpisúa Belmonte, J. C. Disease-corrected haematopoietic progenitors from Fanconi anaemia induced pluripotent stem cells. *Nature* **2009**, *460*, 53–9.

331. Ebert, A. D.; Yu, J.; Rose, F. F.; Mattis, V. B.; Lorson, C. L.; Thomson, J. A.; Svendsen, C. N. Induced pluripotent stem cells from a spinal muscular atrophy patient. *Nature* **2009**, *457*, 277–80.

332. Marchetto, M. C. N.; Carromeu, C.; Acab, A.; Yu, D.; Yeo, G. W.; Mu, Y.; Chen, G.; Gage, F. H.; Muotri, A. R. A model for neural development and treatment of Rett syndrome using human induced pluripotent stem cells. *Cell* **2010**, *143*, 527–39.

333. Ma, H.; Morey, R.; O'Neil, R. C.; He, Y.; Daughtry, B.; Schultz, M. D.; Hariharan, M.; Nery, J. R.; Castanon, R.; Sabatini, K.; Thiagarajan, R. D.; Tachibana, M.; Kang, E.; Tippner-Hedges, R.; Ahmed, R.; Gutierrez, N. M.; Van Dyken, C.; Polat, A.; Sugawara, A.; Sparman, M.; Gokhale, S.; Amato, P.; P.Wolf, D.; Ecker, J. R.; Laurent, L. C.; Mitalipov, S. Abnormalities in human pluripotent cells due to reprogramming mechanisms. *Nature* **2014**, *511*, 177–183.

334. Ban, H.; Nishishita, N.; Fusaki, N.; Tabata, T.; Saeki, K.; Shikamura, M.; Takada, N.; Inoue, M.; Hasegawa, M.; Kawamata, S.; Nishikawa, S.-I. Efficient generation of transgene-free human induced pluripotent stem cells (iPSCs) by temperature-sensitive Sendai virus vectors. *Proc. Natl. Acad. Sci. U. S. A.* **2011**, *108*, 14234–9.

335. Okita, K.; Yamakawa, T.; Matsumura, Y.; Sato, Y.; Amano, N.; Watanabe, A.; Goshima, N.; Yamanaka, S. An efficient nonviral method to generate integration-free human-induced pluripotent stem cells from cord blood and peripheral blood cells. *Stem Cells* **2013**, *31*, 458–66.

336. Kim, D.; Kim, C.-H.; Moon, J.-I.; Chung, Y.-G.; Chang, M.-Y.; Han, B.-S.; Ko, S.; Yang, E.; Cha, K. Y.; Lanza, R.; Kim, K.-S. Generation of human induced pluripotent stem cells by direct delivery of reprogramming proteins. *Cell Stem Cell* **2009**, *4*, 472–6.

337. Warren, L.; Manos, P. D.; Ahfeldt, T.; Loh, Y.-H.; Li, H.; Lau, F.; Ebina, W.; Mandal, P. K.; Smith, Z. D.; Meissner, A.; Daley, G. Q.; Brack, A. S.; Collins, J. J.; Cowan, C.; Schlaeger, T. M.; Rossi, D. J. Highly efficient reprogramming to pluripotency and directed differentiation of human cells with synthetic modified mRNA. *Cell Stem Cell* **2010**, *7*, 618–30.

338. Carvajal-Vergara, X.; Sevilla, A.; D'Souza, S. L.; Ang, Y.-S.; Schaniel, C.; Lee, D.-F.; Yang, L.; Kaplan, A. D.; Adler, E. D.; Rozov, R.; Ge, Y.; Cohen, N.; Edelmann, L. J.; Chang, B.; Waghray, A.; Su, J.; Pardo, S.; Lichtenbelt, K. D.; Tartaglia, M.; Gelb, B. D.; Lemischka, I. R. Patient-specific induced pluripotent stem-cell-derived models of LEOPARD syndrome. *Nature* **2010**, *465*, 808–12.

339. Ku, S.; Soragni, E.; Campau, E.; Thomas, E. A.; Altun, G.; Laurent, L. C.; Loring, J. F.; Napierala, M.; Gottesfeld, J. M. Friedreich's ataxia induced pluripotent stem cells model intergenerational GAA·TTC triplet repeat instability. *Cell Stem Cell* **2010**, *7*, 631–7.

340. Moretti, A.; Bellin, M.; Welling, A.; Jung, C. B.; Lam, J. T.; Bott-Flügel, L.; Dorn, T.; Goedel,

A.; Höhnke, C.; Hofmann, F.; Seyfarth, M.; Sinnecker, D.; Schömig, A.; Laugwitz, K.-L. Patient-specific induced pluripotent stem-cell models for long-QT syndrome. *N. Engl. J. Med.* **2010**, *363*, 1397–409.

341. Torrent, R.; De Angelis Rigotti, F.; Dell'Era, P.; Memo, M.; Raya, A.; Consiglio, A. Using iPS Cells toward the Understanding of Parkinson's Disease. *J. Clin. Med.* **2015**, *4*, 548–566.

342. Ryan, S. D.; Dolatabadi, N.; Chan, S. F.; Zhang, X.; Akhtar, M. W.; Parker, J.; Soldner, F.; Sunico, C. R.; Nagar, S.; Talantova, M.; Lee, B.; Lopez, K.; Nutter, A.; Shan, B.; Molokanova, E.; Zhang, Y.; Han, X.; Nakamura, T.; Masliah, E.; Yates, J. R.; Nakanishi, N.; Andreyev, A. Y.; Okamoto, S.; Jaenisch, R.; Ambasudhan, R.; Lipton, S. A. Isogenic Human iPSC Parkinson's Model Shows Nitrosative Stress-Induced Dysfunction in MEF2-PGC1α Transcription. *Cell* **2013**, *155*, 1351–1364.

343. Miller, J. D.; Ganat, Y. M.; Kishinevsky, S.; Bowman, R. L.; Liu, B.; Tu, E. Y.; Mandal, P. K.; Vera, E.; Shim, J.; Kriks, S.; Taldone, T.; Fusaki, N.; Tomishima, M. J.; Krainc, D.; Milner, T. A.; Rossi, D. J.; Studer, L. Human iPSC-based modeling of late-onset disease via progerin-induced aging. *Cell Stem Cell* **2013**, *13*, 691–705.

344. Devine, M. J.; Ryten, M.; Vodicka, P.; Thomson, A. J.; Burdon, T.; Houlden, H.; Cavaleri, F.; Nagano, M.; Drummond, N. J.; Taanman, J.-W.; Schapira, A. H.; Gwinn, K.; Hardy, J.; Lewis, P. A.; Kunath, T. Parkinson's disease induced pluripotent stem cells with triplication of the α-synuclein locus. *Nat. Commun.* **2011**, *2*, 440.

345. Byers, B.; Cord, B.; Nguyen, H. N.; Schüle, B.; Fenno, L.; Lee, P. C.; Deisseroth, K.; Langston, J. W.; Pera, R. R.; Palmer, T. D. SNCA Triplication Parkinson's Patient's iPSC-derived DA Neurons Accumulate α-Synuclein and Are Susceptible to Oxidative Stress. *PLoS One* **2011**, *6*, e26159.

346. Chung, C. Y.; Khurana, V.; Auluck, P. K.; Tardiff, D. F.; Mazzulli, J. R.; Soldner, F.; Baru, V.; Lou, Y.; Freyzon, Y.; Cho, S.; Mungenast, A. E.; Muffat, J.; Mitalipova, M.; Pluth, M. D.; Jui, N. T.; Schüle, B.; Lippard, S. J.; Tsai, L.-H.; Krainc, D.; Buchwald, S. L.; Jaenisch, R.; Lindquist, S. Identification and rescue of α-synuclein toxicity in Parkinson patient-derived neurons. *Science* **2013**, *342*, 983–7.

347. Clark, J.; Simon, D. K. Transcribe to survive: transcriptional control of antioxidant defense programs for neuroprotection in Parkinson's disease. *Antioxid. Redox Signal.* **2009**, *11*, 509–28.

348. Chan, P.; Jiang, X.; Forno, L. S.; Di Monte, D. A.; Tanner, C. M.; Langston, J. W. Absence of mutations in the coding region of the alpha-synuclein gene in pathologically proven Parkinson's disease. *Neurology* **1998**, *50*, 1136–7.

349. Schöndorf, D. C.; Aureli, M.; McAllister, F. E.; Hindley, C. J.; Mayer, F.; Schmid, B.; Sardi, S. P.; Valsecchi, M.; Hoffmann, S.; Schwarz, L. K.; Hedrich, U.; Berg, D.; Shihabuddin, L. S.; Hu, J.; Pruszak, J.; Gygi, S. P.; Sonnino, S.; Gasser, T.; Deleidi, M. iPSC-derived neurons from GBA1-associated Parkinson's disease patients show autophagic defects and impaired calcium homeostasis. *Nat. Commun.* **2014**, *5*, 4028.

350. Woodard, C. M.; Campos, B. A.; Kuo, S.-H.; Nirenberg, M. J.; Nestor, M. W.; Zimmer, M.; Mosharov, E. V.; Sulzer, D.; Zhou, H.; Paull, D.; Clark, L.; Schadt, E. E.; Sardi, S. P.; Rubin, L.; Eggan, K.; Brock, M.; Lipnick, S.; Rao, M.; Chang, S.; Li, A.; Noggle, S. A. iPSC-Derived Dopamine Neurons Reveal Differences between Monozygotic Twins Discordant for Parkinson's Disease. *Cell Rep.* **2014**, *9*, 1173–1182.

351. Narendra, D. P.; Jin, S. M.; Tanaka, A.; Suen, D.-F.; Gautier, C. A.; Shen, J.; Cookson, M. R.; Youle, R. J. PINK1 Is Selectively Stabilized on Impaired Mitochondria to Activate Parkin. *PLoS Biol.* **2010**, *8*, e1000298.

352. Seibler, P.; Graziotto, J.; Jeong, H.; Simunovic, F.; Klein, C.; Krainc, D. Mitochondrial Parkin recruitment is impaired in neurons derived from mutant PINK1 induced pluripotent stem cells. *J. Neurosci.* **2011**, *31*, 5970–6.

353. Jiang, H.; Ren, Y.; Yuen, E. Y.; Zhong, P.; Ghaedi, M.; Hu, Z.; Azabdaftari, G.; Nakaso, K.; Yan, Z.; Feng, J. Parkin controls dopamine utilization in human midbrain dopaminergic neurons derived from induced pluripotent stem cells. *Nat. Commun.* **2012**, *3*, 668.

354. Imaizumi, Y.; Okada, Y.; Akamatsu, W.; Koike, M.; Kuzumaki, N.; Hayakawa, H.; Nihira, T.; Kobayashi, T.; Ohyama, M.; Sato, S.; Takanashi, M.; Funayama, M.; Hirayama, A.; Soga, T.; Hishiki, T.; Suematsu, M.; Yagi, T.; Ito, D.; Kosakai, A.; Hayashi, K.; Shouji, M.; Nakanishi, A.;

Suzuki, N.; Mizuno, Y.; Mizushima, N.; Amagai, M.; Uchiyama, Y.; Mochizuki, H.; Hattori, N.; Okano, H. Mitochondrial dysfunction associated with increased oxidative stress and α-synuclein accumulation in PARK2 iPSC-derived neurons and postmortem brain tissue. *Mol. Brain* **2012**, *5*, 35.

355. Ren, Y, Jiang, H, Hu, Z, Fan, K, Wang, J, Janoschka, S, Wang, X, Ge, S, Feng, J. Parkin Mutations Reduce the Complexity of Neuronal Processes in iPSC-derived Human Neurons. *Stem Cells* **2015**, *33*, 68–78.

356. Shaltouki, A.; Sivapatham, R.; Pei, Y.; Gerencser, A. A.; Momčilović, O.; Rao, M. S.; Zeng, X. Mitochondrial Alterations by PARKIN in Dopaminergic Neurons Using PARK2 Patient-Specific and PARK2 Knockout Isogenic iPSC Lines. *Stem Cell Reports* **2015**, *4*, 847–859.

357. Reinhardt, P.; Schmid, B.; Burbulla, L. F.; Schöndorf, D. C.; Wagner, L.; Glatza, M.; Höing, S.; Hargus, G.; Heck, S. A.; Dhingra, A.; Wu, G.; Müller, S.; Brockmann, K.; Kluba, T.; Maisel, M.; Krüger, R.; Berg, D.; Tsytsyura, Y.; Thiel, C. S.; Psathaki, O.-E.; Klingauf, J.; Kuhlmann, T.; Klewin, M.; Müller, H.; Gasser, T.; Schöler, H. R.; Sterneckert, J. Genetic correction of a LRRK2 mutation in human iPSCs links parkinsonian neurodegeneration to ERK-dependent changes in gene expression. *Cell Stem Cell* **2013**, *12*, 354–67.

358. Ohta, E.; Kubo, M.; Obata, F. Prevention of intracellular degradation of I2020T mutant LRRK2 restores its protectivity against apoptosis. *Biochem. Biophys. Res. Commun.* **2010**, *391*, 242–7.

359. Ohta, E.; Nihira, T.; Uchino, A.; Imaizumi, Y.; Okada, Y.; Akamatsu, W.; Takahashi, K.; Hayakawa, H.; Nagai, M.; Ohyama, M.; Ryo, M.; Ogino, M.; Murayama, S.; Takashima, A.; Nishiyama, K.; Mizuno, Y.; Mochizuki, H.; Obata, F.; Okano, H. I2020T mutant LRRK2 iPSC-derived neurons in the Sagamihara family exhibit increased Tau phosphorylation through the AKT/GSK-3 signaling pathway. *Hum. Mol. Genet.* **2015**, *24*, 1–80.

360. Cooper, O.; Seo, H.; Andrabi, S.; Guardia-Laguarta, C.; Graziotto, J.; Sundberg, M.; McLean, J. R.; Carrillo-Reid, L.; Xie, Z.; Osborn, T.; Hargus, G.; Deleidi, M.; Lawson, T.; Bogetofte, H.; Perez-Torres, E.; Clark, L.; Moskowitz, C.; Mazzulli, J.; Chen, L.; Volpicelli-Daley, L.; Romero, N.; Jiang, H.; Uitti, R. J.; Huang, Z.; Opala, G.; Scarffe, L. A.; Dawson, V. L.; Klein, C.; Feng, J.; Ross, O. A.; Trojanowski, J. Q.; Lee, V. M.-Y.; Marder, K.; Surmeier, D. J.; Wszolek, Z. K.; Przedborski, S.; Krainc, D.; Dawson, T. M.; Isacson, O. Pharmacological rescue of mitochondrial deficits in iPSC-derived neural cells from patients with familial Parkinson's disease. *Sci. Transl. Med.* **2012**, *4*, 141ra90.

361. Schwab, A. J.; Ebert, A. D. Neurite Aggregation and Calcium Dysfunction in iPSC-Derived Sensory Neurons with Parkinson's Disease-Related LRRK2 G2019S Mutation. *Stem cell reports* **2015**, *5*, 1039–52.

362. Yahata, N.; Asai, M.; Kitaoka, S.; Takahashi, K.; Asaka, I.; Hioki, H.; Kaneko, T.; Maruyama, K.; Saido, T. C.; Nakahata, T.; Asada, T.; Yamanaka, S.; Iwata, N.; Inoue, H. Anti-Aβ Drug Screening Platform Using Human iPS Cell-Derived Neurons for the Treatment of Alzheimer's Disease. *PLoS One* **2011**, *6*, e25788.

363. Sánchez-Danés, A.; Consiglio, A.; Richaud, Y.; Rodríguez-Pizà, I.; Dehay, B.; Edel, M.; Bové, J.; Memo, M.; Vila, M.; Raya, A.; Izpisua Belmonte, J. C. Efficient generation of A9 midbrain dopaminergic neurons by lentiviral delivery of LMX1A in human embryonic stem cells and induced pluripotent stem cells. *Hum. Gene Ther.* **2012**, *23*, 56–69.

364. Soldner, F.; Hockemeyer, D.; Beard, C.; Gao, Q.; Bell, G. W.; Cook, E. G.; Hargus, G.; Blak, A.; Cooper, O.; Mitalipova, M.; Isacson, O.; Jaenisch, R. Parkinson's disease patient-derived induced pluripotent stem cells free of viral reprogramming factors. *Cell* **2009**, *136*, 964–77.

365. Lin, X.; Parisiadou, L.; Gu, X.-L.; Wang, L.; Shim, H.; Sun, L.; Xie, C.; Long, C.-X.; Yang, W.-J.; Ding, J.; Chen, Z. Z.; Gallant, P. E.; Tao-Cheng, J.-H.; Rudow, G.; Troncoso, J. C.; Liu, Z.; Li, Z.; Cai, H. Leucine-rich repeat kinase 2 regulates the progression of neuropathology induced by Parkinson's-disease-related mutant alpha-synuclein. *Neuron* **2009**, *64*, 807–27.

366. Giralt, A.; Friedman, H. C.; Caneda-Ferrón, B.; Urbán, N.; Moreno, E.; Rubio, N.; Blanco, J.; Peterson, A.; Canals, J. M.; Alberch, J. BDNF regulation under GFAP promoter provides engineered astrocytes as a new approach for long-term protection in Huntington's disease. *Gene Ther.* **2010**, *17*, 1294–308.

367. Alessi, D. R.; Cuenda, A.; Cohen, P.; Dudley, D. T.; Saltiel, A. R. PD 098059 is a specific

inhibitor of the activation of mitogen-activated protein kinase kinase in vitro and in vivo. *J. Biol. Chem.* **1995**, *270*, 27489–94.

368. Dudley, D. T.; Pang, L.; Decker, S. J.; Bridges, A. J.; Saltiel, A. R. A synthetic inhibitor of the mitogen-activated protein kinase cascade. *Proc. Natl. Acad. Sci. U. S. A.* **1995**, *92*, 7686–9.

369. Zeng, X.; Chen, J.; Deng, X.; Liu, Y.; Rao, M. S.; Cadet, J.-L.; Freed, W. J. An in vitro model of human dopaminergic neurons derived from embryonic stem cells: MPP+ toxicity and GDNF neuroprotection. *Neuropsychopharmacology* **2006**, *31*, 2708–15.

370. Xing, B.; Xin, T.; Zhao, L.; Hunter, R. L.; Chen, Y.; Bing, G. Glial cell line-derived neurotrophic factor protects midbrain dopaminergic neurons against lipopolysaccharide neurotoxicity. *J. Neuroimmunol.* **2010**, *225*, 43–51.

371. Villadiego, J.; Méndez-Ferrer, S.; Valdés-Sánchez, T.; Silos-Santiago, I.; Fariñas, I.; López-Barneo, J.; Toledo-Aral, J. J. Selective glial cell line-derived neurotrophic factor production in adult dopaminergic carotid body cells in situ and after intrastriatal transplantation. *J. Neurosci.* **2005**, *25*, 4091–8.

372. Ortega-Sáenz, P.; Pardal, R.; Levitsky, K.; Villadiego, J.; Muñoz-Manchado, A. B.; Durán, R.; Bonilla-Henao, V.; Arias-Mayenco, I.; Sobrino, V.; Ordóñez, A.; Oliver, M.; Toledo-Aral, J. J.; López-Barneo, J. Cellular properties and chemosensory responses of the human carotid body. *J. Physiol.* **2013**, *591*, 6157–73.

373. Carballo-Carbajal, I.; Weber-Endress, S.; Rovelli, G.; Chan, D.; Wolozin, B.; Klein, C. L.; Patenge, N.; Gasser, T.; Kahle, P. J. Leucine-rich repeat kinase 2 induces alpha-synuclein expression via the extracellular signal-regulated kinase pathway. *Cell. Signal.* **2010**, *22*, 821–7.

374. Kulich, S. M.; Chu, C. T. Sustained extracellular signal-regulated kinase activation by 6-hydroxydopamine: implications for Parkinson's disease. *J. Neurochem.* **2001**, *77*, 1058–66.

375. Almeida, R. D.; Manadas, B. J.; Melo, C. V; Gomes, J. R.; Mendes, C. S.; Grãos, M. M.; Carvalho, R. F.; Carvalho, A. P.; Duarte, C. B. Neuroprotection by BDNF against glutamate-induced apoptotic cell death is mediated by ERK and PI3-kinase pathways. *Cell Death Differ.* **2005**, *12*, 1329–43.

376. Luo, Y.; DeFranco, D. B. Opposing roles for ERK1/2 in neuronal oxidative toxicity: distinct mechanisms of ERK1/2 action at early versus late phases of oxidative stress. *J. Biol. Chem.* **2006**, *281*, 16436–42.

377. Kaplan, D. R.; Miller, F. D. Neurotrophin signal transduction in the nervous system. *Curr. Opin. Neurobiol.* **2000**, *10*, 381–91.

378. Cagnol, S.; Chambard, J.-C. ERK and cell death: mechanisms of ERK-induced cell death--apoptosis, autophagy and senescence. *FEBS J.* **2010**, *277*, 2–21.

379. Feng, Y.; He, D.; Yao, Z.; Klionsky, D. J. The machinery of macroautophagy. *Cell Res.* **2014**, *24*, 24–41.

380. Jakobsen, B.; Gramsbergen, J. B.; Møller Dall, A.; Rosenblad, C.; Zimmer, J. Characterization of organotypic ventral mesencephalic cultures from embryonic mice and protection against MPP toxicity by GDNF. *Eur. J. Neurosci.* **2005**, *21*, 2939–48.

381. Chu, C. T.; Plowey, E. D.; Dagda, R. K.; Hickey, R. W.; Cherra, S. J.; Clark, R. S. B. Autophagy in neurite injury and neurodegeneration: in vitro and in vivo models. *Methods Enzymol.* **2009**, *453*, 217–49.

382. Menzies, F. M.; Moreau, K.; Rubinsztein, D. C. Protein misfolding disorders and macroautophagy. *Curr. Opin. Cell Biol.* **2011**, *23*, 190–7.

383. Takei, N.; Nawa, H. mTOR signaling and its roles in normal and abnormal brain development. *Front. Mol. Neurosci.* **2014**, *7*, 28.

384. Hidalgo-Figueroa, M.; Bonilla, S.; Gutiérrez, F.; Pascual, A.; López-Barneo, J. GDNF is predominantly expressed in the PV+ neostriatal interneuronal ensemble in normal mouse and after injury of the nigrostriatal pathway. *J. Neurosci.* **2012**, *32*, 864–72.

385. Chung, S.; Shin, B.-S.; Hwang, M.; Lardaro, T.; Kang, U. J.; Isacson, O.; Kim, K.-S. Neural precursors derived from embryonic stem cells, but not those from fetal ventral mesencephalon, maintain the potential to differentiate into dopaminergic neurons after expansion in vitro. *Stem Cells* **2006**, *24*, 1583–93.

386. Favata, M. F.; Horiuchi, K. Y.; Manos, E. J.; Daulerio, A. J.; Stradley, D. A.; Feeser, W. S.;

Van Dyk, D. E.; Pitts, W. J.; Earl, R. A.; Hobbs, F.; Copeland, R. A.; Magolda, R. L.; Scherle, P. A.; Trzaskos, J. M. Identification of a novel inhibitor of mitogen-activated protein kinase kinase. *J. Biol. Chem.* **1998**, *273*, 18623–32.

387. Du, Y.; Li, X.; Yang, D.; Zhang, X.; Chen, S.; Huang, K.; Le, W. Multiple molecular pathways are involved in the neuroprotection of GDNF against proteasome inhibitor induced dopamine neuron degeneration in vivo. *Exp. Biol. Med. (Maywood).* **2008**, *233*, 881–90.

388. Wong, E.; Cuervo, A. M. Integration of clearance mechanisms: the proteasome and autophagy. *Cold Spring Harb. Perspect. Biol.* **2010**, *2*, a006734.

389. Chao, C. C.; Lee, E. H. Neuroprotective mechanism of glial cell line-derived neurotrophic factor on dopamine neurons: role of antioxidation. *Neuropharmacology* **1999**, *38*, 913–6.

390. Smith, M. P.; Cass, W. A. GDNF reduces oxidative stress in a 6-hydroxydopamine model of Parkinson's disease. *Neurosci. Lett.* **2007**, *412*, 259–63.

391. Chu, Y.; Le, W.; Kompoliti, K.; Jankovic, J.; Mufson, E. J.; Kordower, J. H. Nurr1 in Parkinson's disease and related disorders. *J. Comp. Neurol.* **2006**, *494*, 495–514.

392. Le, W.-D.; Xu, P.; Jankovic, J.; Jiang, H.; Appel, S. H.; Smith, R. G.; Vassilatis, D. K. Mutations in NR4A2 associated with familial Parkinson disease. *Nat. Genet.* **2003**, *33*, 85–9.

393. Sleiman, P. M. A.; Healy, D. G.; Muqit, M. M. K.; Yang, Y. X.; Van Der Brug, M.; Holton, J. L.; Revesz, T.; Quinn, N. P.; Bhatia, K.; Diss, J. K. J.; Lees, A. J.; Cookson, M. R.; Latchman, D. S.; Wood, N. W. Characterisation of a novel NR4A2 mutation in Parkinson's disease brain. *Neurosci. Lett.* **2009**, *457*, 75–9.

394. Siegel, G. J.; Chauhan, N. B. Neurotrophic factors in Alzheimer's and Parkinson's disease brain. *Brain Res. Brain Res. Rev.* **2000**, *33*, 199–227.

395. Mattson, M. P.; Magnus, T. Ageing and neuronal vulnerability. *Nat. Rev. Neurosci.* **2006**, *7*, 278–94.

396. Hunot, S.; Bernard, V.; Faucheux, B.; Boissière, F.; Leguern, E.; Brana, C.; Gautris, P. P.; Guérin, J.; Bloch, B.; Agid, Y.; Hirsch, E. C. Glial cell line-derived neurotrophic factor (GDNF) gene expression in the human brain: a post mortem in situ hybridization study with special reference to Parkinson's disease. *J. Neural Transm.* **1996**, *103*, 1043–52.

397. Mogi, M.; Togari, A.; Kondo, T.; Mizuno, Y.; Kogure, O.; Kuno, S.; Ichinose, H.; Nagatsu, T. Glial cell line-derived neurotrophic factor in the substantia nigra from control and parkinsonian brains. *Neurosci. Lett.* **2001**, *300*, 179–81.

398. Chauhan, N. B.; Siegel, G. J.; Lee, J. M. Depletion of glial cell line-derived neurotrophic factor in substantia nigra neurons of Parkinson's disease brain. *J. Chem. Neuroanat.* **2001**, *21*, 277–88.

399. Bäckman, C. M.; Shan, L.; Zhang, Y. J.; Hoffer, B. J.; Leonard, S.; Troncoso, J. C.; Vonsatel, P.; Tomac, A. C. Gene expression patterns for GDNF and its receptors in the human putamen affected by Parkinson's disease: a real-time PCR study. *Mol. Cell. Endocrinol.* **2006**, *252*, 160–6.

400. Trupp, M.; Belluardo, N.; Funakoshi, H.; Ibáñez, C. F. Complementary and overlapping expression of glial cell line-derived neurotrophic factor (GDNF), c-ret proto-oncogene, and GDNF receptor-alpha indicates multiple mechanisms of trophic actions in the adult rat CNS. *J. Neurosci.* **1997**, *17*, 3554–67.

401. Tomac, A.; Widenfalk, J.; Lin, L. F.; Kohno, T.; Ebendal, T.; Hoffer, B. J.; Olson, L. Retrograde axonal transport of glial cell line-derived neurotrophic factor in the adult nigrostriatal system suggests a trophic role in the adult. *Proc. Natl. Acad. Sci. U. S. A.* **1995**, *92*, 8274–8.

402. Saavedra, A.; Baltazar, G.; Duarte, E. P. Driving GDNF expression: the green and the red traffic lights. *Prog. Neurobiol.* **2008**, *86*, 186–215.

403. Tepper, J. M.; Bolam, J. P. Functional diversity and specificity of neostriatal interneurons. *Curr. Opin. Neurobiol.* **2004**, *14*, 685–92.

404. Björklund, A.; Dunnett, S. B. Dopamine neuron systems in the brain: an update. *Trends Neurosci.* **2007**, *30*, 194–202.

405. Fukuda, T. Network architecture of gap junction-coupled neuronal linkage in the striatum. *J. Neurosci.* **2009**, *29*, 1235–43.

406. Reiner, A.; Shelby, E.; Wang, H.; Demarch, Z.; Deng, Y.; Guley, N. H.; Hogg, V.; Roxburgh, R.; Tippett, L. J.; Waldvogel, H. J.; Faull, R. L. M. Striatal parvalbuminergic neurons are lost in Huntington's disease: implications for dystonia. *Mov. Disord.* **2013**, *28*, 1691–9.

407. Kataoka, Y.; Kalanithi, P. S. A.; Grantz, H.; Schwartz, M. L.; Saper, C.; Leckman, J. F.; Vaccarino, F. M. Decreased number of parvalbumin and cholinergic interneurons in the striatum of individuals with Tourette syndrome. *J. Comp. Neurol.* **2010**, *518*, 277–91.

408. Huertas-Fernández, I.; Gómez-Garre, P.; Madruga-Garrido, M.; Bernal-Bernal, I.; Bonilla-Toribio, M.; Martín-Rodríguez, J. F.; Cáceres-Redondo, M. T.; Vargas-González, L.; Carrillo, F.; Pascual, A.; Tischfield, J. A.; King, R. A.; Heiman, G. A.; Mir, P. GDNF gene is associated with tourette syndrome in a family study. *Mov. Disord.* **2015**, *30*, 1115–20.

409. Yan, Y.; Shin, S.; Jha, B. S.; Liu, Q.; Sheng, J.; Li, F.; Zhan, M.; Davis, J.; Bharti, K.; Zeng, X.; Rao, M.; Malik, N.; Vemuri, M. C. Efficient and rapid derivation of primitive neural stem cells and generation of brain subtype neurons from human pluripotent stem cells. *Stem Cells Transl. Med.* **2013**, *2*, 862–70.

410. Liu, Y.; Liu, H.; Sauvey, C.; Yao, L.; Zarnowska, E. D.; Zhang, S.-C. Directed differentiation of forebrain GABA interneurons from human pluripotent stem cells. *Nat. Protoc.* **2013**, *8*, 1670–1679.

411. Bartus, R. T.; Herzog, C. D.; Chu, Y.; Wilson, A.; Brown, L.; Siffert, J.; Johnson, E. M.; Olanow, C. W.; Mufson, E. J.; Kordower, J. H. Bioactivity of AAV2-neurturin gene therapy (CERE-120): differences between Parkinson's disease and nonhuman primate brains. *Mov. Disord.* **2011**, *26*, 27–36.

412. Luz, M.; Mohr, E.; Fibiger, H. C. GDNF-induced cerebellar toxicity: A brief review. *Neurotoxicology* **2015**, *52*, 46–56.

413. Monville, C.; Torres, E.; Thomas, E.; Scarpini, C. G.; Muhith, J.; Lewis, J.; Finn, J.; Smith, C.; Cai, S.; Efstathiou, S.; Howard, K.; Dunnett, S. B. HSV vector-delivery of GDNF in a rat model of PD: partial efficacy obscured by vector toxicity. *Brain Res.* **2004**, *1024*, 1–15.

414. Ziller, M. J.; Gu, H.; Müller, F.; Donaghey, J.; Tsai, L. T.-Y.; Kohlbacher, O.; De Jager, P. L.; Rosen, E. D.; Bennett, D. A.; Bernstein, B. E.; Gnirke, A.; Meissner, A. Charting a dynamic DNA methylation landscape of the human genome. *Nature* **2013**, *500*, 477–81.

8. ANNEXES

Articles resulted from the participation of the PhD candidate in projects related to the thesis research.

8.1. Using iPS Cells toward the understanding of Parkinson's Disease (Review).

Torrent, R., De Angelis-Rigotti, F., Dell'Era, P., Memo, M., Raya, A., Consiglio, A., *Using iPS cells toward the understanding of Parkinson's disease*, **J. Clin. Med.,** 2015 4: 548-566.

J. Clin. Med. **2015**, *4*, 548-566; doi:10.3390/jcm4040548

OPEN ACCESS
Journal of
Clinical Medicine
ISSN 2077-0383
www.mdpi.com/journal/jcm

Review

Using iPS Cells toward the Understanding of Parkinson's Disease

Roger Torrent [1], Francesca De Angelis Rigotti [1], Patrizia Dell'Era [2], Maurizio Memo [2], Angel Raya [3,4,5,6] and Antonella Consiglio [1,2,*]

1 Institute for Biomedicine of the University of Barcelona (IBUB), Barcelona Science Park, Barcelona 08028, Spain; E-Mails: rtorrent@gmail.com (R.T.); fdeangelisrigotti@ibub.pcb.ub.es (F.D.A.R.)
2 Department of Molecular and Translational Medicine, Fibroblast Reprogramming Unit, University of Brescia, Brescia 25123, Italy; E-Mails: patrizia.dellera@med.unibs.it (P.D.E.); maurizio.memo@med.unibs.it (M.M.)
3 Control of Stem Cell Potency Group, Institute for Bioengineering of Catalonia (IBEC), Barcelona 08028, Spain; E-Mail: araya@ibecbarcelona.eu
4 Institució Catalana de Recerca i Estudis Avançats (ICREA), Barcelona 08010, Spain
5 Center for Networked Biomedical Research on Bioengineering, Biomaterials and Nanomedicine (CIBER-BBN), Madrid 28029, Spain
6 Center of Regenerative Medicine in Barcelona, Dr. Aiguader 88, Barcelona 08003, Spain

* Author to whom correspondence should be addressed; E-Mail: aconsiglio@ibub.pcb.ub.es or consiglio@med.unibs.it; Tel.: +34-93-403-9842; Fax: +34-93-402-155.

Academic Editor: Michael J. Edel

Received: 23 October 2014 / Accepted: 10 February 2015 / Published: 30 March 2015

Abstract: Cellular reprogramming of somatic cells to human pluripotent stem cells (iPSC) represents an efficient tool for *in vitro* modeling of human brain diseases and provides an innovative opportunity in the identification of new therapeutic drugs. Patient-specific iPSC can be differentiated into disease-relevant cell types, including neurons, carrying the genetic background of the donor and enabling *de novo* generation of human models of genetically complex disorders. Parkinson's disease (PD) is the second most common age-related progressive neurodegenerative disease, which is mainly characterized by nigrostriatal dopaminergic (DA) neuron degeneration and synaptic dysfunction. Recently, the generation of disease-specific iPSC from patients suffering from PD has unveiled a recapitulation of disease-related cell phenotypes, such as abnormal α-synuclein accumulation and alterations in autophagy machinery. The use of patient-specific iPSC has a remarkable potential to uncover novel insights of the disease pathogenesis, which in turn will open

new avenues for clinical intervention. This review explores the current Parkinson's disease iPSC-based models highlighting their role in the discovery of new drugs, as well as discussing the most challenging limitations iPSC-models face today.

Keywords: induced pluripotent stem cells; Parkinson's disease; Leucine-rich repeat kinase 2 (LRRK2); dopaminergic neurons

1. Parkinson's Disease

Parkinson's disease (PD) is the second most common neurodegenerative disease in the world after Alzheimer's disease (AD), affecting 2% of the population over the age of 60. The mean duration of the disease from the time of diagnosis to death is approximately 15 years, with a mortality ratio of 2 to 1 in the affected subjects [1].

PD is characterized by debilitating motor deficits, such as tremor, limb rigidity and slowness of movements (bradykinesia) although non-motor features, such as hyposmia, cognitive decline, depression, and disturbed sleep are also present in later stages of the disease [1–3]. Neuropathologically, these motor deficits are caused by the progressive preferential loss of striatal-projecting neurons of the substantia nigra pars compacta; more specifically a subtype of dopaminergic neurons (DAn) patterned for the ventral midbrain (vmDAn). Neuronal loss is typically accompanied by the presence of intra-cytoplasmic ubiquitin-positive inclusions in surviving neurons. These structures are known as Lewy bodies and Lewy neurites and they are mainly composed of the neuronal protein α-synuclein (α-syn). These protein inclusions are not only found throughout the brain but also outside of the CNS. Moreover, microglial activation and an increase in astroglia and lymphocyte infiltration also occur in PD [4].

Approximately 90%–95% of all PD cases are sporadic with no family history. Although disease onset and age are highly correlated, PD occurs when complex mechanisms such as mitochondrial activity, autophagy or degradation via proteasome are dysregulated by environmental influence or PD-specific mutation susceptibility [5].

Studies of rare large families showing classical Mendelian inherited PD have allowed for the identification of 11 genes out of 16 identified disease *loci*. They include dominant mutations in Leucine-rich repeat kinase 2 (*LRRK2*), recessive mutations in Parkin (coded by *PARK2*) and PTEN-induced putative kinase (*PINK1*) [6], as well as both rare dominant mutations and multiplications in the gene encoding α-synuclein (*SNCA*).

Current treatment for PD is limited to targeting only the symptoms of the disease and does not cure or delay disease progression. Therefore, the identification of new and more effective drugs to slow down, stop and even reverse PD is critical. This limited symptomatic treatment is due to the lack of clear understanding of the underlying mechanisms affected during PD. Using patient-specific iPSC-based models to recapitulate the disease from start to finish delivers a more detailed picture of the mechanisms involved in the progression of Parkinson's disease and will aid in the discovery of disease-targeted therapies in the future.

2. Models of Parkinson's Disease

Despite advances in the identification of genes and proteins involved in PD, there are still gaps in our understanding of the underlying mechanisms involved [7,8]. The lack of PD models fully representing the complex mechanisms involved in disease progression, as well as the near impossible task of extracting live neurons from patients has proven the investigation of PD difficult [8]. In general, genetic mouse models do not represent the pathophysiological neurodegeneration and protein aggregation pattern observed in PD patients [9,10], and are thus limited [11,12]. On the other hand, PD animal models of administration of neurotoxins systemically or locally have successfully replicated DAn neurodegeneration, however they fail to recapitulate the degeneration in a slow and progressive manner, nor the formation of Lewy body-like inclusions which occur in PD human pathology [13].

Although the cellular models of PD, mostly based on human neuronal tumor cell lines, have provided helpful insights into alterations in specific subcellular components (such as proteasome, lysosome and mitochondrion), the relevance of these findings for PD pathogenesis is not always immediate. These models do not, however, investigate the defective mechanisms within the predominantly affected cell in PD, the DAn [14]. In addition, all studies involving human tissue have been performed with post-mortem samples, which can only allow for a limited analysis.

The recent discovery of cellular reprogramming to generate induced pluripotent stem cells (iPSC) from patient somatic cells offers a remarkable opportunity to generate disease-specific iPSC [15], and to reproduce at a cellular and molecular level the mechanisms involved in disease progression. The use of iPSC offers not only the possibility of addressing important questions such as the functional relevance of the molecular findings, the contribution of individual genetic variations, patient-specific response to specific interventions, but also helps to recapitulate the prolonged time-course of the disease (Figure 1).

3. Generation of PD-Specific iPSCs

In recent years, neurodegenerative disease research has quickly advanced with the help of stem cell technology reprogramming somatic cells, such as fibroblasts, into induced pluripotent stem cells (iPSC) [15]. Human iPSC share many characteristics with human embryonic stem cells (hESC), including similarities in their morphologies, gene expression profiles, self-renewal ability, and capacity to differentiate into cell types of the three embryonic germ layers *in vitro* and *in vivo* [16]. An important advantage of induced cell reprogramming is represented by the possibility of generating iPSC from patients showing sporadic or familial forms of the disease. These *in vitro* models are composed of cells that carry the patients' genetic variants, some known and others not, that are key to the contribution of disease onset and progression. Moreover, given that iPSC can be further differentiated into neurons, this technology potentially provides, for the first time, an unlimited source of native phenotypes of cells specifically involved in the process related to neuronal death in neurodegeneration *in vitro*.

One issue found in modeling PD with the use of iPSC is to correctly reproduce its late-onset characteristics, since aging is a crucial risk factor. Indeed, at first it was unclear whether disease-specific features of neurodegenerative disorders that usually progressively appear over several years were reproducible *in vitro* over a period of only a few days to a few months. As a consequence, iPSC were initially used to model neurodevelopmental phenotypes and a variety of monogenic early-onset

diseases [17–24]. However, studies using iPSC derived from patients with monogenic and sporadic forms of PD have illustrated these key features of PD pathophysiology, as a late-onset neurodegenerative disorder, after differentiating these iPSC into dopaminergic neurons. Moreover, several inducible factors that cause cell stress, such as mitochondrial toxins [25], growth factor deficiency, or even modulated aging with induced expression of progerin (a protein causing premature aging) [26], have also been used to accelerate and reproduce the phenotypes found during disease progression.

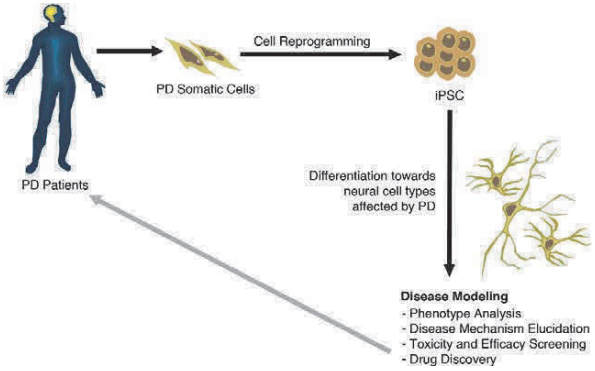

Figure 1. Generation and use of iPSC modelling in PD. Somatic cells from a diseased patient are isolated and then reprogrammed to a pluripotent state (iPSCs). iPSCs can be maintained in culture or induced to differentiate along tissue- and cell-type specific pathways. Differentiated cells can be used to elucidate disease mechanism pathways, as well as for the development of novel therapies.

In this review, the recent work on iPSC-based PD modeling for both sporadic and familial cases will be discussed, as well as how iPSC-based studies are helping in the advancement of novel drug discoveries. These studies give insight for the fundamental understanding of PD pathogenesis, which is critical for the development of new treatments.

4. Modeling Sporadic and Familial PD Using iPSC

Over the last few years, several studies have reported the generation of iPSC from patients suffering from sporadic and genetic forms of PD (Table 1). The first group generated PD-specific iPSC from a sporadic PD patient in 2008 [27]. Over the following year, the Jaenisch's group was able to demonstrate that iPSC derived from PD patients were able to differentiate towards DAn, however, no characteristic signs of progressive neurodegeneration or disease-related phenotypes were observed in those cells [28]. The Jaenisch group generated gene-free iPSC lines from skin fibroblasts of five idiopathic PD patients. Using *in vivo* experiments, they showed that PD-specific iPSC-derived DAn were able to survive and engraft in the rodent striatum for at least 12 weeks. A small number of these cells co-expressed tyrosine hydroxylase (TH) and G-protein-gated inwardly rectifying K+ channel subunit (GIRK2), which are the hallmark characteristics of vmDAn. Remarkably, injection of these iPSC-derived DAn into the brains of 6-OHDA-lesioned rats resulted in motor symptoms improvement [29].

Table 1. Summary of the described PD iPSC modeling publications in this review.

Gene	Publication	Mutation	Number of patients	Isogenic Controls	Cell Type Differentiation	Findings
SNCA	Devine *et al.*, 2011 [30]	Triplication	1	NO	Floor-plate DAn differentiation (21–30 days): 28%–37% $TH^+/TUJ1^+$	mRNA doubled expression of SNCA
	Byers *et al.*, 2011 [31]	Triplication	1	NO	DAn differentiation (50 days): 6%–11% TH^+	Double expression of SNCA, increased susceptibility to OS
	Chung *et al.*, 2013 [32]	A53T	2	YES	Neuronal differentiation (56–84 days): DAn yield not specified.	Increased nitrosative stress, and ER stress, reversed by adding NAB2.
	Ryan *et al.*, 2013 [25]	A53T	1	YES	Kriks's Floor-plate DAn differentiation: ~80% A9 DAn of total neurons.	Diminished spare respiration mitochondrial capacity; increased ROS/RNS and attenuation of MEF2/PGC1α neuroprotective pathway
GBA1	Mazzulli *et al.*, 2011 [33]	N370S/84GG insertion	1	NO	DAn diff. (30 days): 80% $TUJ1^+$, 10% $TH^+/TUJ1^+$	Formation of soluble α-syn oligomers, correlated with a decline of lysosomal proteolysis.
	Schöndorf *et al.*, 2014 [34]	GBA1 (RecNcil/wt) GD (N370S; L444P)	4 GBA1 4 GD	YES	Kriks's Floor-plate DAn differentiation: 15%–20% $TH^+/GIRK2^+/FOXA2^+/VMAT2^+$ There is also further purification of DAn by FACS	Causal relation of GBA1 mutations with increased a-syn and LB inclusions, correlated with autophagic/lysosomal system impairment
PARK2	Jiang *et al.*, 2012 [35]	Exon 3/5 deletion	2	NO	DAn differentiation (70 days): yield not specified	Loss of Parkin function; decreased DA uptake and incorrectly folded DAT protein, with increased OS susceptibility. Transduction of WT PARK2 reversed OS sensitiveness.
	Imaizumi *et al.*, 2012 [36]	Exons 2–4 and 6,7 homozygous deletion	2	NO	DAn differentiation (10 days): yield not specified	Abnormal mitochondrial morphology and impaired mitochondrial homeostasis.
PARK2 *PINK1*	Miller *et al.*, 2013 [26]	PINK1 (Q456X) Parkin (V324a)	1 1	NO	Kriks's Floor-plate DAn differentiation yield not specified	Loss of dendrite lenght and decreased neuronal survival, as seen by decreased *p*-ATK values, when exposing mDA neurons to progerin.

Table 1. *Cont.*

Gene	Publication	Mutation	Number of patients	Isogenic Controls	Cell Type Differentiation	Findings
PINK1	Seibler *et al*., 2013 [37]	C1366T, C509G	3	NO	Floor-plate DAn differentiation: 11%–16% $TH^+/TUJ1^+$	Endogenous mutant PINK1 diminished Parkin recruitment to the mitochondrial membrane under the presence of valynomycin. WT PINK1 rescued Parkin recruitment.
(PINK1)	Cooper *et al*., 2012 [38]	Q456X	2	NO	DAn differentiation (22 days): 35% $TUJ1^+$; 10% TH^+	Increased vulnerability of neural cells to chemical stressors, with common defects to protect against OS.
LRRK2	Nguyen *et al*., 2011 [39]	G2019S, R1441C	2	NO	Floor-plate DAn differentiation (30–35 days): 3.6%–5% TH^+	α-syn accumulation, increased OS genes, and increased susceptibility to hydrogen peroxide.
	Sánchez-Danes *et al*., 2012 [40]	G2019S	7 Sporadic 4 LRRK2 (G2019S)	NO	DAn diff (Lentiviral-mediated forced expression LMX1A in neural precursors) (75 days): 55% $TH^+/TUJ1^+$ (Majority TH^+GIRK2^+)	Reduced neurite lenght and number. Accumulation of α-syn in LRRK2 DAn. Reduction of autophagic flux and accumulation of early autophagosomes.
	Orenstein *et al*., 2013 [41]	G2019S	4 LRRK2 (G2019S)	NO	As described in [40]	Blockage of the CMA degradation pathway due to accumulated α-syn with correlated increased expression of LAMP-2A.
	Reinhardt *et al.*, 2013 [42]	G2019S	2	YES	Floor-plate DAn differentiation (30–35 days): 20% TH/TUJ1/DAPI	Decreased neurite lenght levels. Increased ERK activation levels, and discover of novel genes dysregulated in LRRK2 DAn.

Many laboratories have now successfully recapitulated *in vitro* some of the characteristics of PD, using iPSC as a model compared to the aforementioned studies in which no signs of Parkinson's disease were observed. However, given that PD is a progressive aging disease that affects several cellular mechanisms involving different cell types, each iPSC model highlights only some PD-associated characteristics. Nevertheless, each one of these models has helped to understand some of the fundamental underlying mechanisms as a proof-of-concept. In the last few years, iPSC-model reliability has rapidly improved and has paved the way for the discovery of new complex biomolecular interactions in the pathogenesis of PD. Thus, iPSC modeling has shown to be promising as a tool for drug-screening platforms in the future.

Recently, iPSC-derived DA neurons carrying a triplication of *SNCA*, the coding gene for α-syn protein, have been generated [30,31]. These cells showed enhanced α-syn mRNA and protein levels [30] and increased cell death vulnerability when exposed to oxidative-stress inducers [31]. Using an iPSC model based on the rare missense A53T *SNCA* mutation, Chung *et al*. observed early pathogenic phenotype in patient-derived neurons, compared to isogenic gene-corrected controls. In particular, they observed a connection between nitrosative and ER stress in the context of α-syn toxicity. Interestingly, the levels of CHOP (CCAAT enhancer binding protein homologous protein), a component of ER stress-induced apoptosis, did not change, indicating that in this model cellular pathology was still at an early stage [32]. iPSC-derived DAn, carrying the A53T *SNCA* mutation, also showed α-syn aggregation, altered mitochondrial machinery, thus enhancing basal ROS/RNS production [25]. The increase of RNS production leads to *S*-nitrosylation of the *pro*-survival transcription factor MEF2 and its consequent inhibition, reducing the expression of the mitochondrial master regulator PGC1α and genes that are important for the development and survival of A9 DAn [43]. Interestingly, Ryan *et al*., postulated that the MEF2-PGC1α pathway contributes to the appearance of late-onset phenotypes in PD due to the complex interaction between environmental factors and gene expression. Indeed, when PD-associated pesticides were added below EPA-accepted levels, this was enough to exacerbate oxidative/nitrosative stress, inhibiting MEF2-PGC1α and inducing apoptosis, a late-onset phenotype [25].

Interestingly, α-syn is one of the main pathological readouts for many of the sporadic and familial PD cases that are not related with mutations in *SNCA* [44]. For example, the clinical link between the lysosomal storage disorder Gaucher disease (GD) and PD appears to be based on the fact that mutations in acid *GBA1* gene, which causes GD, contributes to the pathogenesis of synucleinopathies [33,34]. *GBA1* encodes the lysosomal enzyme β-Glucocerebrocidase (GCase), which cleaves the β-glucosyl linkage of GlcCer. Functional loss of GCase activity in iPSC-derived neurons has been associated with compromised lysosomal protein degradation, which in turn induces α-syn accumulation, resulting in neurotoxicity through aggregation-dependent mechanisms [33]. In addition, iPSC-derived neurons carrying the heterozygous mutation in *GBA1* also have shown increased levels of GlcCer, changes in the autophagic/lysosomal system and calcium homeostasis, which may cause a selective threat to DA neurons in PD [34].

Similarly to mutations in *GBA1*, mutations in *PINK1* and *PARK2* are also associated with early onset recessive forms of familial PD [45]. Both proteins, PINK1 and Parkin, are involved in the clearance of mitochondrial damage. Therefore their mutations cause a PD characterized by mitochondrial stress as main feature [46–48]. Under physiological conditions, Parkin, which is localized in the cytoplasm, is translocated to damaged mitochondria in a PINK-dependent manner triggering mitophagy [49]. This has been confirmed in iPSC-derived DA neurons carrying a mutation in *PINK1*. In these cells, Parkin

recruitment to mitochondria was impaired and only over-expression of WT *PINK1* was able to rescue the function [37]. On the other hand, iPSC models for mutation in *PARK2* revealed an increase of oxidative stress. Jiang and colleagues showed that iPSC from patients carrying mutations in *PARK2* enhanced the transcription of monoamine oxidase, the spontaneous release of dopamine and significantly decreased dopamine uptake, increasing susceptibility to reactive oxygen species [35]. Although the incremented oxidative stress has been confirmed in a parallel study, in this study no difference in monoamine oxidase was observed [36]. On the contrary, the oxidative stress was accompanied by a compensation mechanism that involved the activation of the reducing Nrf2A pathway [36].

Mutations in *LRRK2* have been one of the most studied mutations in PD, not only because they are the most common cause of familial PD, but also because clinical symptoms of *LRRK2*-PD are similar to those of idiopathic PD [50]. The most common mutation is the G2019S, which results in hyper-activity of the LRRK2 kinase domain. Although penetrance of this gene has shown to be variable between individuals' age, iPSC model of a G2019S *LRRK2*-PD has recapitulated characteristic features of PD, such as accumulation of α-syn, increase in genes responsible for oxidative stress and enhanced susceptibility to hydrogen peroxide, which is displayed through caspase-3 activation [39]. Furthermore, the expression of key oxidative stress-response genes and α-syn were found to be increased in neurons from *LRRK2*-iPSC, when compared to those differentiated from control iPSC or hESC.

Our group has generated iPSC lines from seven patients with idiopathic PD and four patients carrying G2019S mutation in the *LRRK2* gene [40]. We observed morphological alterations in PD-derived iPSC vmDAn (fewer and shorter neurites) as well as an increase in the number of apoptotic neurons over a long-time culture (2.5 months). Moreover, we found an accumulation of α-syn in *LRRK2*-iPSC derived DAn after a 30 days culture.

Sporadic forms of PD are not as well defined, given that they may be caused by several genetic variants, as well as a strong environmental effect. However, our study revealed that DAn, which were derived from idiopathic PD patients, also showed an increased susceptibility to degeneration *in vitro* after long-term culture [40].

Importantly, the appearance of the neurodegenerative phenotypes in differentiated DAn from either idiopathic or *LRRK2*-associated PD was shown to be the consequence, at least in part, of impaired autophagy. Blockade of autophagy by lysosomal inhibition showed a specific reduction in autophagic flux by LC3-II immunoblotting, suggesting that the clearance of autophagosomes was compromised [40]. Proteins may also enter the autophagic process directly at the lysosome level, via chaperone-mediated autophagy (CMA). Increased co-localization of α-syn with LAMP2A puncta in iPSC-derived *LRRK2* DAn, revealed a compromised degradation of α-syn by CMA [41]. Although both wild-type and mutant LRRK2 inhibit CMA, G2019S LRRK2 protein was more resistant to the CMA-mediated degradation, resulting in α-syn accumulation [41]. Furthermore, the same phenotype was induced by over-expression of wild-type or G2019S *LRRK2* in control iPSC-derived cultures [40] and rescued by LRRK2 inhibition [42]. Indeed, iPSC-derived DAn cultures from isogenic G2019S *LRRK2* lines (mutation being the sole experimental variable) exhibited an increased mutant-specific apoptosis and decreased neurite outgrowth, as well as alterations in the expression of several pERK (phosphorylated ERK) controlled genes, all of which could be rescued by the inhibition of LRRK2 [42]. Moreover, the genetic correction of LRRK2 mutation resulted in the phenotypic rescue of differentiated neurons with improved neurite length to levels comparable to those of controls.

5. Patient-Derived Stem Cells Could Improve Drug Research for PD

An important goal of humanized stem cell-based PD model systems is the screening of potential new drugs that could affect the neurodegenerative process at several levels during its development in specifically affected human cells. Moreover, the availability of such patient-specific stem cell-based model systems could help identifying new pharmacological strategies for the design of personalized therapies. Recently, iPSC-derived forebrain neurons have been used as a platform to screen disease-modifying drugs, highlighting the possibilities of iPSC technology as an *in vitro* cell-based assay system for AD research [51]. A recent study has also taken a significant leap towards personalized medicine for PD patients, by investigating signs of the disease in patient-specific iPSC-derived neurons and testing how the cells respond to drug treatments [38]. The study showed that neurons derived from PD patients carrying mutations in the *PINK1* or *LRRK2* genes display common signs of distress and vulnerability such as abnormalities in mitochondria and increased vulnerability to oxidative stress. However, they found that oxygen consumption rates were lower in cells with mutations in *LRRK2* and higher in cells with the mutations in *PINK1*. Notably, they were able to rescue the phenotype caused by toxins to which the cells were exposed to with various drug treatments, including the antioxidant coenzyme Q10 and rapamycin. Most importantly, the response of iPSC-derived neurons was different depending on the type of familial PD, since drugs that prevented damage to neurons with mutations in *LRRK2,* did not protect neurons with mutations in *PINK1* [38].

In addition, Ryan and colleagues performed a high-throughput screening (HTS) to identify molecules that are capable of protecting DAn from the toxic effect of PD-associated pesticides. They observed that the MEF2-PGC1α pathway contributes to the late-onset PD phenotypes due to the interaction between environmental factors and gene expression [25]. They performed HTS for small molecules capable of targeting the MEF2-PGC1α pathway and they identify isoxazole as new potential therapeutic drug. Isoxazole, not only drove the expression of both MEF2 and PGC1α, but also protected A53T DAn from pesticide-induced apoptosis [25].

Chung and colleagues investigated yeast and iPSC PD models in parallel to discover and reverse phenotypic responses to α-syn. In conjunction to what was previously reported, they showed a connection between α-syn toxicity, accumulation of NO and ER stress [32]. With these results, they took a step further by screening for possible α-syn toxicity suppressors in their iPSC model, to compare with their previous yeast screenings [52–54]. In particular they showed that the ubiquitin ligase Nedd4 and its chemical activator NAB2 [53] are able to rescue the α-syn toxicity in patient-derived neurons [32], opening a door to a new potential drug treatment.

These results encourage the use of iPSC technology as a tool to discover potential therapeutic drugs. However, concluding for what recent studies have unveiled up until now focusing only on genetic forms of PD, it remains to be determined whether this advanced technology can be used also in sporadic patients with uncertain genetic cause of the disease.

6. Limitations of Using iPSC in Disease Modeling: From Overall Neurodegeneration to the Detailed Mechanisms Involved

6.1. Reprogramming and Epigenetic Signatures

Reprogramming increases cell variability due to the introduction of mutations in the genomic DNA [55] and the insertion of exogenous reprogramming genes. Moreover reprogrammed cells maintain a residual DNA methylation signature characteristic of the somatic tissue of origin [56–59] affecting also gene expression [60]. These issues can affect the predisposition of a given line to differentiate into particular cell type independently of the patient's genotype, and will abrogate the possibility of using these lines for cell therapy treatment in the future. To decrease the impact of these technical limitations, more than one clone for each iPSC line is usually analyzed. However, the use of integrating methods, such as lenti- and retro-virus infection for gene transduction, not only increases cell variability, but also maintains residual expression of exogenous reprogramming genes that is only partially lost through cell passaging. The residual expression of reprogramming genes can, not only create problems during cell differentiation, but overall iPSC do not need a constant over expression of reprogramming genes. Indeed, the reprogramming process by which a somatic cell acquires pluripotent potential is not a genetic transformation, but an epigenomic one [61], therefore only a transient expression of reprogramming genes needs to be activated. Alternative methods to the retro- or lenti-viral infection, have been recently adopted. These include the use of non-integrating viral vectors such as Sendai virus [62], episomal vectors [63], protein transduction [64], or transfection of modified mRNA transcripts [65]. These methods of reprogramming are relevant in the context of any future clinical applications of iPSCs in the field of transplantable replacement cell therapies.

As aforementioned, one of the major concerns in iPSC modeling through the reprogramming of somatic cells into iPSCs has been that of resetting the identity of these cells back to an embryonic stage, therefore having to consider the generated iPSC-derived neurons as fetal neurons. Given the slow progression of neurodegenerative diseases, the idea of modeling this type of disease in a dish has been highly doubted. However, despite the typical late-onset of PD, the key cellular and molecular pathological mechanisms may have started before the onset of the disease. Therefore, α-syn accumulation, autophagic clearance and mitochondrial dysfunctions, among other pathological mechanisms afforested, could have been active in the early stages of the disease. The cumulative effect of these abnormalities along with the effect of environmental influence, have been shown to progressively encourage neurodegeneration [25]. In addition the use of cell stressors and inducible aging [26] also have shown the possibility of accelerating the appearance of diseased phenotypes in a dish.

6.2. Reliable Control Lines and Gene-Editing

Comparative studies require an appropriate control that accounts for differences between lines due only to the genotypic background that exists between individuals. This is especially crucial in diseases whose causative mutations do not have a high penetrance. For example, when complex diseases, such as PD, are modeled with patient- and healthy donor-derived iPSC, the patient iPSC tend to show subtle phenotypes that can be masked by genetic background effects [66]. For this reason, it is imperative to remove the excess genetic variation between iPSC clones and controls, to ensure a more reliable comparative analysis. Given that to obtain iPSC from unaffected siblings or parental controls is not often possible, a solution is to

generate isogenic controls directly from the patient iPSCs. In the last years, several research groups have used this approach to correct known mutations [25,26,32,34,42,67], or even utilizing the introduction of the same mutation in control iPSC lines to see the effect of just the mutation itself [42,67]. For this reason, isogenic controls have claimed to be crucial when it comes to assess the impact of any mutation on specific cellular processes. Therefore, editing technologies based on Zinc Fingers Nucleases, TALENs or CRISPR [68], have become indispensable tools in developing comparative studies in iPSC models, allowing for the reduction of iPSC cohorts.

6.3. Cell Differentiation and Sorting

The efficacy of Parkinson's disease iPSC models depends highly on their ability to correctly differentiate neurons into the specific cell type that is affected by the disease (in this case A9 dopaminergic neuronal subtype). Indeed this is critical in order to recapitulate disease features *in vitro* and observe comparative differences between diseased and healthy control lines. Neuronal differentiation of iPSC into DA neurons is not only subjected to high variability of efficiency, depending on the techniques used in a laboratory, but also on the specific ability of each iPSC line. For example, by comparing the studies reported in this review, the percentage of DA neurons compared to the total number of cells varies depending on each cell line, differentiation method and even laboratory group (Table 1). Throughout the field, groups encountered problems in yielding a high percentage of DA neurons within the differentiated population. Therefore, although a number of results are based on the disease phenotype through the identification of TH positive cells by immunocytochemistry, protein immunoblots in which all cell populations are considered skews the data. More specifically, the levels of affected protein in the few TH positive cells may be diluted and missed when mixed with the whole population of differentiate cells when analyzed. Interpretation of these results have been, thus, controversial, especially in the cases in which PD iPSC-derived models have low yield in DA differentiation, which probably cannot go beyond the gross neurodegeneration mechanisms that they have observed. Thus, delving deep inside the biomolecular pathways affected in PD will require a more fine-tuned differentiation protocol that allows the enrichment of the cell type of interest. To achieve this, a novel floor-plate-based strategy described by Kriks and colleagues has become the gold standard in the generation of human A9 vmDA neurons for both transplantation and research purposes [69]. The protocol is based on the concurrent inhibition of two parallel SMAD/TGF-β (transforming growth factor-β) superfamily-signaling pathways, which during CNS development induce no-neuronal fates such as endoderm or mesoderm. This inhibition directs the cell culture to a predetermined neural progenitor fate with an efficiency of at least 80% of $PAX6^+$ neural cells among total cells [70]. Differentiation of these neuronal stem cells into mature vmDAn is then instructed through the molecular guidance of Sonic Hedgehog (SHH), FGF8 and more importantly Wnt signaling pathway induction, which enhances expression of the transcription factors FOXA2 and LMX1A [71,72]. The final step of neuronal maturation is achieved through the use of a cocktail of neurotrophic factors, including BDNF, GDNF, TGFβ3, dbcAMP, and ascorbic acid (Figure 2). Interestingly, the most recent papers reviewed here have started to implement the A9 vmDAn enrichment protocol [25,26,34] with the addition of isogenic-corrected controls [25,34]. Moreover, Schöndorf and colleagues improved the Kriks differentiation protocol thanks to the use of a cell sorting method (Fluorescence-activated cell sorting), which allowed for a 6.1-fold enrichment of the neuronal population. This step of sorting was necessary to

assess reliable biomolecular changes that could not have been assessed with an unsorted heterogenic population [34].

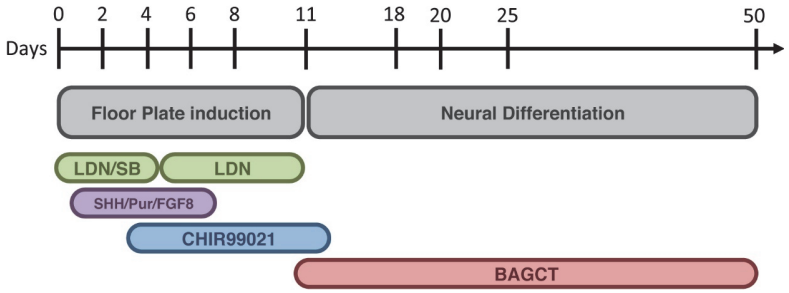

Figure 2. Schematic summary of the novel floor-plate A9 vmDAn differentiation protocol by Kriks [69]. The first stage illustrates floor-plate induction [70], with the appropriate modification in order to reach a more specialized A9 midbrain DA neuronal identity. Exposure to LDN (LDN193189) and SB (SB431542) triggers the Dual-SMAD inhibition. Purmorphamine (Pur), which activates Sonic Hedgehog (SHH) signaling, together with SHH and FGF8 is not sufficient to trigger a selective enrichment of midbrain DA precursors. However, SHH/Pur/FGF8 in combination with exposure to CHIR99021 (a potent GSK3β inhibitor known to strongly activate WNT signaling) allows for a complete enrichment of DA precursors with A9 midbrain identity, by inducing the expression of FOXA2 and LMX1A. Neural differentiation and maturation is achieved through the use of a cocktail of neurotrophic factors BAGCT (BDNF + ascorbic acid + GDNF + dbcAMP + TGFβ3).

On the other hand, to unveil the mechanisms behind pathophysiological processes such as neuroinflammation, the investigation of all cells responsible for the maintenance of CNS homeostasis, such as astrocytes and microglia, is crucial. Nevertheless, the study of a more isolated system may allow investigators to detect early events of a disease that would otherwise be missed.

7. Conclusions and Challenges

PD is a progressive neurodegenerative disease resulting in the gradual loss of vmDA neurons, as well as cytoplasmic inclusions called Lewy Bodies. The exact mechanisms leading to vmDA neuronal death in PD are still unclear, although pathogenic protein aggregation of α-synuclein, mitochondrial dysfunction, oxidative and nitrosative stress, or altered autophagy have been proposed as mechanisms that contribute to this devastating neurodegenerative process. The generation of reliable iPSC-based models for late-onset neurodegenerative disorders, in which the etiology is yet to be uncovered, has proven to be difficult to overcome. However, recent advances in the field have demonstrated the feasibility of developing experimental models of PD based on iPSC from patients of both genetic and idiopathic forms of PD that recapitulate the key features of the disease. The successful generation of these genetic and idiopathic PD models has opened the door bringing to light some of the crucial pathogenic mechanisms responsible for

the initiation and progression of PD, as well as aid in the development of novel drugs that may prevent or rescue neurodegeneration in PD. Recent findings in the field have moved far beyond the proof-of-principle stage, and have started to optimize and standardize these models for the discovery of new aspects of disease biology and new targets for therapeutic intervention. The use of isogenic-corrected controls, more reliable differentiation protocols [25,26,34] and efficient cell-sorting methods [34], have strongly validated the reliability of iPSC models in the context of complex diseases such as PD. Within the field of neuroscience, the opportunity and challenge to combine patient-derived disease-specific stem cells with drug screening technologies with the aim of finding new therapies is now a possibility. In addition, the combination of establishing optimal neuronal differentiation protocols of iPSC using genetic reporters, together with software analysis algorithms, allows for the possibility of automatically tracking each cell over time and to assess any feature of interest, thus providing this system with a powerful tool in drug discovery in the near future.

Moreover, by studying symptomatic and asymptomatic mutation carriers, iPSC technology could also provide a unique opportunity for identifying putative gene-linked PD biomarkers in pre-symptomatic individuals, opening a new novel window for the early diagnosis and individualized treatment in the preclinical phase of the disease.

Acknowledgments

The authors would like to thank all the laboratory members for their helpful discussion and in particular Angelique Di Domenico for editorial comments. Roger Torrent was partially supported by a pre-doctoral fellowship from MINECO. Work in the authors' laboratories is funded by grants from MINECO (RyC-2008-02772, BFU2010-21823), and the ERC-2013-StG grant of the European Research Council (ERC) to Antonella Consiglio, SAF2012-33526, PLE2009-0144, and ACI2010-1117 to Ángel Raya, and a CIBERNED Cooperative Project (to Ángel Raya).

Author Contributions

All the authors contributed to conception and design, data collection and manuscript writing. All the authors approved submission.

Conflicts of Interest

The authors declare no conflict of interest.

References

1. Lees, A.J.; Hardy, J.; Revesz, T. Parkinson's disease. *Lancet* **2009**, *373*, 2055–2066.
2. Obeso, J.A.; Rodriguez-Oroz, M.C.; Goetz, C.G.; Marin, C.; Kordower, J.H.; Rodriguez, M.; Hirsch, E.C.; Farrer, M.; Schapira, A.H.; Halliday, G. Missing pieces in the Parkinson's disease puzzle. *Nat. Med*. **2010**, *16*, 653–661.
3. Schapira, A.H.; Tolosa, E. Molecular and clinical prodrome of Parkinson disease: Implications for treatment. *Nat. Rev. Neurol*. **2010**, *6*, 309–317.

4. Glass, C.K.; Saijo, K.; Winner, B.; Marchetto, M.C.; Gage, F.H. Mechanisms underlying inflammation in neurodegeneration. *Cell* **2010**, *140*, 918–923.
5. Dauer, W.; Przedborski, S. Parkinson's disease: Mechanisms and models. *Neuron*. **2003**, *39*, 889–909.
6. Kim, J.; Byun, J.W.; Choi, I.; Kim, B.; Jeong, H.K.; Jou, I.; Joe, E. PINK1 Deficiency Enhances Inflammatory Cytokine Release from Acutely Prepared Brain Slices. *Exp. Neurobiol*. **2013**, *22*, 38–44.
7. Melrose, H.; Lincoln, S.; Tyndall, G.; Dickson, D.; Farrer, M. Anatomical localization of leucine-rich repeat kinase 2 in mouse brain. *Neuroscience* **2006**, *139*, 791–794.
8. Dawson, T.M.; Ko, H.S.; Dawson, V.L. Genetic animal models of Parkinson's disease. *Neuron* **2010**, *66*, 646–661.
9. Gispert, S.; del Turco, D.; Garrett, L.; Chen, A.; Bernard, D.J.; Hamm-Clement, J.; Korf, H.W.; Deller, T.; Braak, H.; Auburger, G.; *et al*. Transgenic mice expressing mutant A53T human alpha-synuclein show neuronal dysfunction in the absence of aggregate formation. *Mol. Cell Neurosci.* **2003**, *24*, 419–429.
10. Gispert, S.; Ricciardi, F.; Kurz, A.; Azizov, M.; Hoepken, H.H.; Becker, D.; Voos, W.; Leuner, K.; Müller, W.E.; Kudin, A.P.; *et al*. Parkinson phenotype in aged PINK1-deficient mice is accompanied by progressive mitochondrial dysfunction in absence of neurodegeneration. *PLoS ONE* **2009**, *4*, e5777.
11. Chesselet, M.F.; Richter, F. Modelling of Parkinson's disease in mice. *Lancet Neurol.* **2011**, *10*, 1108–1118.
12. Magen, I.; Chesselet, M.F. Genetic mouse models of Parkinson's disease. The state of the art. Prog. *Brain Res.* **2010**, *184*, 53–87
13. Tieu, K. A guide to neurotoxic animal models of Parkinson's disease. *Cold Spring Harb. Perspect. Med.* **2011**, doi:10.1101/cshperspect.a009316.
14. Kume, T.; Kawato, Y.; Osakada, F.; Izumi, Y.; Katsuki, H.; Nakagawa, T.; Kaneko, S.; Niidome, T.; Takada-Takatori, Y.; Akaike, A. Dibutyryl cyclic AMP induces differentiation of human neuroblastoma SH-SY5Y cells into a noradrenergic phenotype. *Neurosci. Lett.* **2008**, *443*, 199–203.
15. Takahashi, K.; Tanabe, K.; Ohnuki, M.; Narita, M.; Ichisaka, T.; Tomoda, K.; Yamanaka, S. Induction of pluripotent stem cells from adult human fibroblasts by defined factors. *Cell* **2007**, *131*, 861–872.
16. Rodríguez-Pizà, I.; Richaud-Patin, Y.; Vassena, R.; González, F.; Barrero, M.J.; Veiga, A.; Raya, A.; Izpisúa Belmonte, J.C. Reprogramming of human fibroblasts to induced pluripotent stem cells under xeno-free conditions. *Stem Cells* **2010**, *28*, 36–44.
17. Ebert, A.D.; Yu, J.; Rose, F.F., Jr.; Mattis, V.B.; Lorson, C.L.; Thomson, J.A.; Svendsen, C.N. Induced pluripotent stem cells from a spinal muscular atrophy patient. *Nature* **2009**, *457*, 277–280.
18. Lee, G.; Papapetrou, E.P.; Kim, H.; Chambers, S.M.; Tomishima, M.J.; Fasano, C.A.; Ganat, Y.M.; Menon, J.; Shimizu, F.; Viale, A.; *et al*. Modelling pathogenesis and treatment of familial dysautonomia using patient-specific iPSCs. *Nature* **2009**, *461*, 402–406.

19. Raya, A.; Rodriguez-Piza, I.; Guenechea, G.; Vassena, R.; Navarro, S.; Barrero, M.J.; Consiglio, A.; Castella, M.; Rio, P.; Sleep, E.; *et al*. Disease-corrected haematopoietic progenitors from Fanconi anaemia induced pluripotent stem cells. *Nature* **2009**, *460*, 53–55.
20. Carvajal-Vergara, X.; Sevilla, A.; D'Souza, S.L.; Ang, Y.S.; Schaniel, C.; Lee, D.F.; Yang, L.; Kaplan, A.D.; Adler, E.D.; Rozov, R.; *et al*. Patient-specific induced pluripotent stem-cell-derived models of LEOPARD syndrome. *Nature* **2010**, *465*, 808–812.
21. Ku, S.; Soragni, E.; Campau, E.; Thomas, E.A.; Altun, G.; Laurent, L.C.; Loring, J.F.; Napierala, M.; Gottesfeld, J.M. Friedreich's ataxia induced pluripotent stem cells model intergenerational GAATTC triplet repeat instability. *Cell Stem Cell* **2010**, *7*, 631–637.
22. Moretti, A.; Bellin, M.; Welling, A.; Jung, C.B.; Lam, J.T.; Bott-Flugel, L.; Dorn, T.; Goedel, A.; Hohnke, C.; Hofmann, F.; *et al*. Patient-specific induced pluripotent stem-cell models for long-QT syndrome. *N. Engl. J. Med.* **2010**, *363*, 1397–1409.
23. Rashid, S.T.; Corbineau, S.; Hannan, N.; Marciniak, S.J.; Miranda, E.; Alexander, G.; Huang-Doran, I.; Griffin, J.; Ahrlund-Richter, L.; Skepper, J.; *et al*. Modeling inherited metabolic disorders of the liver using human induced pluripotent stem cells. *J. Clin. Invest.* **2010**, *120*, 3127–3136.
24. Zhang, J.; Lian, Q.; Zhu, G.; Zhou, F.; Sui, L.; Tan, C.; Mutalif, R.A.; Navasankari, R.; Zhang, Y.; Tse, H.F.; *et al*. A human iPSC model of Hutchinson Gilford Progeria reveals vascular smooth muscle and mesenchymal stem cell defects. *Cell Stem Cell* **2011**, *8*, 31–45.
25. Ryan, S.D.; Dolatabadi, N.; Chan, S.F.; Zhang, X.; Akhtar, M.W.; Parker, J.; Soldner, F.; Sunico, C.R.; Nagar, S.; Talantova, M.; *et al*. Isogenic human iPSC Parkinson's model shows nitrosative stress-induced dysfunction in mef2-pgc1alpha transcription. *Cell* **2013**, *155*, 1351–1364.
26. Miller, J.D.; Ganat, Y.M.; Kishinevsky, S.; Bowman, R.L.; Liu, B.; Tu, E.Y.; Mandal, P.K.; Vera, E.; Shim, J.W.; Kriks, S.; *et al*. Human iPSC-based modeling of late-onset disease via progerin-induced aging. *Cell Stem Cell* **2013**, *13*, 691–705.
27. Park, I.H.; Arora, N.; Huo, H.; Maherali, N.; Ahfeldt, T.; Shimamura, A.; Lensch, M.W.; Cowan, C.; Hochedlinger, K.; Daley, G.Q. Disease-specific induced pluripotent stem cells. *Cell* **2008**, *134*, 877–886.
28. Soldner, F.; Hockemeyer, D.; Beard, C.; Gao, Q.; Bell, G.W.; Cook, E.G.; Hargus, G.; Blak, A.; Cooper, O.; Mitalipova, M.; *et al*. Parkinson's disease patient-derived induced pluripotent stem cells free of viral reprogramming factors. *Cell* **2009**, *136*, 964–977.
29. Hargus, G.; Cooper, O.; Deleidi, M.; Levy, A.; Lee, K.; Marlow, E.; Yow, A.; Soldner, F.; Hockemeyer, D.; Hallett, P.J.; *et al*. Differentiated Parkinson patient-derived induced pluripotent stem cells grow in the adult rodent brain and reduce motor asymmetry in Parkinsonian rats. *Proc. Natl. Acad. Sci. USA* **2010**, *107*, 15921–15926.
30. Devine, M.J.; Ryten, M.; Vodicka, P.; Thomson, A.J.; Burdon, T.; Houlden, H.; Cavaleri, F.; Nagano, M.; Drummond, N.J.; Taanman, J.W.; *et al*. Parkinson's disease induced pluripotent stem cells with triplication of the alpha-synuclein locus. *Nat. Commun.* **2011**, *2*, doi:10.1038/ncomms1453.
31. Byers, B.; Cord, B.; Nguyen, H.N.; Schüle, B.; Fenno, L.; Lee, P.C.; Deisseroth, K.; Langston, J.W.; Pera, R.R.; Palmer, T.D. SNCA triplication Parkinson's patient's iPSC-derived DA neurons accumulate α-synuclein and are susceptible to oxidative stress. *PLoS ONE* **2011**, *6*, e26159.

32. Chung, C.Y.; Khurana, V.; Auluck, P.K.; Tardiff, D.F.; Mazzulli, J.R.; Soldner, F.; Baru, V.; Lou, Y.; Freyzon, Y.; Cho, S.; *et al*. Identification and rescue of α-synuclein toxicity in Parkinson patient-derived neurons. *Science* **2013**, *342*, 983–987.
33. Mazzulli, J.R.; Xu, Y.H.; Sun, Y.; Knight, A.L.; McLean, P.J.; Caldwell, G.A.; Sidransky, E.; Grabowski, G.A.; Krainc, D. Gaucher disease glucocerebrosidase and α-synuclein form a bidirectional pathogenic loop in synucleinopathies. *Cell* **2011**, *146*, 37–52.
34. Schöndorf, D.C.; Aureli, M.; McAllister, F.E.; Hindley, C.J.; Mayer, F.; Schmid, B.; Sardi, S.P.; Valsecchi, M.; Hoffmann, S.; Schwarz, L.K.; *et al*. iPSC-derived neurons from GBA1-associated Parkinson's disease patients show autophagic defects and impaired calcium homeostasis. *Nat. Commun*. **2014**, *5*, doi:10.1038/ncomms5028.
35. Jiang, H.; Ren, Y.; Yuen, E.Y.; Zhong, P.; Ghaedi, M.; Hu, Z.; Azabdaftari, G.; Nakaso, K.; Yan, Z.; Feng, J. Parkin controls dopamine utilization in human midbrain dopaminergic neurons derived from induced pluripotent stem cells. *Nat. Commun.* **2012**, *3*, doi:10.1038/ncomms1669.
36. Imaizumi, Y.; Okada, Y.; Akamatsu, W.; Koike, M.; Kuzumaki, N.; Hayakawa, H.; Nihira, T.; Kobayashi, T.; Ohyama, M.; Sato, S.; *et al*. Mitochondrial dysfunction associated with increased oxidative stress and α-synuclein accumulation in PARK2 iPSC-derived neurons and postmortem brain tissue. *Mol. Brain.* **2012**, *5*, doi:10.1186/1756-6606-5-35.
37. Seibler, P.; Graziotto, J.; Jeong, H.; Simunovic, F.; Klein, C.; Krainc, D. Mitochondrial Parkin recruitment is impaired in neurons derived from mutant PINK1 induced pluripotent stem cells. *J. Neurosci.* **2011**, *31*, 5970–5976.
38. Cooper, O.; Seo, H.; Andrabi, S.; Guardia-Laguarta, C.; Graziotto, J.; Sundberg, M.; McLean, J.R.; Carrillo-Reid, L.; Xie, Z.; Osborn, T.; *et al*. Pharmacological rescue of mitochondrial deficits in iPSC-derived neural cells from patients with familial Parkinson's disease. *Sci. Transl. Med.* **2012**, *4*, doi:10.1126/scitranslmed.3003985.
39. Nguyen, H.N.; Byers, B.; Cord, B.; Shcheglovitov, A.; Byrne, J.; Gujar, P.; Kee, K.; Schule, B.; Dolmetsch, R.E.; Langston, W.; *et al*. LRRK2 Mutant iPSC-Derived DA Neurons Demonstrate Increased Susceptibility to Oxidative Stress. *Cell Stem Cell* **2011**, *8*, 267–280.
40. Sanchez-Danes, A.; Richaud-Patin, Y.; Carballo-Carbajal, I.; Jimenez-Delgado, S.; Caig, C.; Mora, S.; Di Guglielmo, C.; Ezquerra, M.; Patel, B.; Giralt, A.; *et al*. Disease-specific phenotypes in dopamine neurons from human iPS-based models of genetic and sporadic Parkinson's disease. *EMBO Mol. Med.* **2012**, *4*, 380–395.
41. Orenstein, S.J.; Kuo, S.-H.; Tasset, I.; Arias, E.; Koga, H.; Fernandez Carasa, I.; Cortes, E.; Honig, L.S.; Dauer, W.; Consiglio, A.; *et al*. Interplay of LRRK2 with chaperone-mediated autophagy. *Nat. Neurosci.* **2013**, *16*, 394–406.
42. Reinhardt, P.; Schmid, B.; Burbulla, L.F.; Schöndorf, D.C.; Wagner, L.; Glatza, M.; Höing, S.; Hargus, G.; Heck, S.A.; Dhingra, A.; *et al*. Genetic correction of a LRRK2 mutation in human iPSCs links parkinsonian neurodegeneration to ERK-dependent changes in gene expression. *Cell Stem Cell* **2013**, *12*, 354–367.

43. Clark, J.; Simon, D.K. Transcribe to survive: Transcriptional control of antioxidant defense programs for neuroprotection in Parkinson's disease. *Antiox. Redox Signal.* **2009**, *11*, 509–528.
44. Chan, P.; Jiang, X.; Forno, L.S.; Di Monte, D.A.; Tanner, C.M.; Langston, J.W. Absence of mutations in the coding region of the alpha-synuclein gene in pathologically proven Parkinson's disease. *Neurology* **1998**, *50*, 1136–1137.
45. Klein, C.; Djarmati, A.; Hedrich, K.; Schäfer, N.; Scaglione, C.; Marchese, R.; Kock, N.; Schüle, B.; Hiller, A.; Lohnau, T.; *et al*. PINK1, Parkin, and DJ-1 mutations in Italian patients with early-onset parkinsonism. *Eur. J. Hum. Genet.* **2005**, *13*, 1086–1093.
46. Singleton, A.B.; Farrer, M.J.; Bonifati, V. The genetics of Parkinson's disease: Progress and therapeutic implications. *Mov. Disord.* **2013**, *28*, 14–23.
47. Tan, J.M.M.; Dawson, T.M. Parkin blushed by PINK1. *Neuron* **2006**, *50*, 527–529.
48. Okatsu, K.; Oka, T.; Iguchi, M.; Imamura, K.; Kosako, H.; Tani, N.; Kimura, M.; Go, E.; Koyano, F.; Funayama, M.; *et al.* PINK1 autophosphorylation upon membrane potential dissipation is essential for Parkin recruitment to damaged mitochondria. *Nat. Commun*. **2012**, *3*, doi:10.1038/ncomms2016.
49. Narendra, D.P.; Jin, S.M.; Tanaka, A.; Suen, D.F.; Gautier, C.A.; Shen, J.; Cookson, M.R.; Youle, R.J. PINK1 is selectively stabilized on impaired mitochondria to activate Parkin. *PLoS Biol.* **2010**, *8*, e1000298.
50. Haugarvoll, K.; Rademakers, R.; Kachergus, J.M.; Nuytemans, K.; Ross, O.A.; Gibson, J.M.; Tan, E.K.; Gaig, C.; Tolosa, E.; Goldwurm, S.; *et al*. LRRK2 R1441C parkinsonism is clinically similar to sporadic Parkinson disease. *Neurology* **2008**, *70*, 1456–1460.
51. Yahata, N.; Asai, M.; Kitaoka, S.; Takahashi, K.; Asaka, I.; Hioki, H.; Kaneko, T.; Maruyama, K.; Saido, T.C.; Nakahata, T.; *et al*. Anti-Aβ drug screening platform using human iPS cell-derived neurons for the treatment of Alzheimer's disease. *PLoS ONE* **2011**, *6*, e25788.
52. Gitler, A.D.; Chesi, A.; Geddie, M.L.; Strathearn, K.E.; Hamamichi, S.; Hill, K.J.; Caldwell, K.A.; Caldwell, G.A.; Cooper, A.A.; Rochet, J.S.; *et al*. α-Synuclein is part of a diverse and highly conserved interaction network that includes PARK9 and manganese toxicity. *Nat. Genet.* **2009**, *41*, 308–315.
53. Tardiff, D.F.; Jui, N.T.; Khurana, V.; Tambe, M.A.; Thompson, M.L.; Chung, C.Y.; Kamadurai, H.B.; Kim, H.T.; Lancaster, A.K.; Caldwell, K.A.; *et al*. Yeast Reveal a "Druggable" Rsp5/Nedd4 Network that Ameliorates α-synuclein Toxicity in Neurons. *Science* **2013**, *343*, 979–983.
54. Cooper, A.A.; Gitler, A.D.; Cashikar, A.; Haynes, C.M.; Hill, K.J.; Bhullar, B.; Liu, K.; Xu, K.; Strathearn, K.E.; Liu, F.; *et al*. α-synuclein blocks ER-Golgi traffic and Rab1 rescues neuron loss in Parkinson's models. *Science* **2006**, *313*, 324–328.
55. Gore, A.; Li, Z.; Fung, H.L.; Young, J.E.; Agarwal, S.; Antosiewicz-Bourget, J.; Canto, I.; Giorgetti, A.; Israel, M.A.; Kiskinis, E.; *et al*. Somatic coding mutations in human induced pluripotent stem cells. *Nature* **2011**, *471*, 63–67.
56. Kim, K.; Doi, A.; Wen, B.; Ng, K.; Zhao, R.; Cahan, P.; Kim, J.; Aryee, M.J.; Ji, H.; Ehrlich, L.I.; *et al*. Epigenetic memory in induced pluripotent stem cells. *Nature* **2010**, *467*, 285–290.

57. Marchetto, M.C.; Yeo, G.W.; Kainohana, O.; Marsala, M.; Gage, F.H.; Muotri, A.R. Transcriptional signature and memory retention of human-induced pluripotent stem cells. *PLoS ONE* **2009**, *4*, e7076.
58. Hussein, S.M.; Batada, N.N.; Vuoristo, S.; Ching, R.W.; Autio, R.; Närvä, E.; Ng, S.; Sourour, M.; Hämäläinen, R.; Olsson, C.; *et al*. Copy number variation and selection during reprogramming to pluripotency. *Nature* **2011**, *471*, 58–62.
59. Lister, R.; Pelizzola, M.; Kida, Y.S.; Hawkins, R.D.; Nery, J.R.; Hon, G.; Antosiewicz-Bourget, J.; O'Malley, R.; Castanon, R.; Klugman, S.; *et al*. Hotspots of aberrant epigenomic reprogramming in human induced pluripotent stem cells. *Nature* **2011**, *471*, 68–73.
60. Laurent, L.C.; Ulitsky, I.; Slavin, I.; Tran, H.; Schork, A.; Morey, R.; Lynch, C.; Harness, J.V.; Lee, S.; Barrero, M.J.; *et al*. Dynamic changes in the copy number of pluripotency and cell proliferation genes in human escs and ipscs during reprogramming and time in culture. *Cell Stem Cell* **2011**, *8*, 106–118.
61. Ma, H.; Morey, R.; O'Neil, R.C.; He, Y.; Daughtry, B.; Schultz, M.D.; Hariharan, M.; Nery, J.R.; Castanon, R.; Sabatini, K.; *et al*. Abnormalities in human pluripotent cells due to reprogramming mechanisms. *Nature* **2014**, *511*, 177–183.
62. Ban, H.; Nishishita, N.; Fusaki, N.; Tabata, T.; Saeki, K.; Shikamura, M.; Takada, N.; Inoue, M.; Hasegawa, M.; Kawamata, S.; *et al*. Efficient generation of transgene-free human induced plutipotent stem cells (iPSCs) by temperature-sensitive Sendai virus vectors. *Proc. Natl. Acad. Sci. USA* **2011**, *108*, 13234–14239.
63. Okita, K.; Matsumura, Y.; Sato, Y.; Okada, A.; Morizane, A.; Okamoto, S.; Hong, H.; Nakagawa, M.; Tanabe, K.; Tezuka, K.; *et al*. A more efficient method to generate integration-free human iPS cells. *Nat. Methods* **2011**, *8*, 409–412.
64. Kim, D.; Kim, C.H.; Moon, J.I.; Chung, Y.G.; Chang, M.Y.; Han, B.S.; Ko, S.; Yang, E.; Cha, K.Y.; Lanza, R.; *et al*. Generation of human induced pluripotent stem cells by direct delivery of reprogramming proteins. *Cell Stem Cell* **2009**, *4*, 472–476.
65. Warren, L.; Manos, P.D.; Ahfeldt, T.; Loh, Y.H.; Li, H.; Lau, F.; Ebina, W.; MAndal, P.K.; Smith, Z.D.; Meissner, A.; *et al*. Highly efficient reprogramming to pluripotency and directed differentiation of human cells with synthetic modified mRNA. *Cell Stem Cell* **2010**, *7*, 618–630.
66. International Parkinson Disease Genomics Consortium; Nalls, M.A.; Plagnol, V.; Hernandez, D.G.; Sharma, M.; Sheerin, U.M.; Saad, M.; Simón-Sánchez, J.; Schulte, C.; Lesage, S.; *et al*. Imputation of sequence variants for identification of genetic risks for Parkinson's disease: A meta-analysis of genome-wide association studies. *Lancet* **2011**, *377*, 641–649.
67. Liu, G.H.; Qu, J.; Suzuki, K.; Nivet, E.; Li, M.; Montserrat, N.; Yi, F.; Xu, X.; Ruiz, S.; Zhang, W.; *et al*. Progressive degeneration of human neural stem cells caused by pathogenic LRRK2. *Nature* **2012**, *491*, 603–607.
68. Kim, H.S.; Bernitz, J.; Lee, D.F.; Lemischka, I.R. Genomic editing tools to model human diseases with isogenic pluripotent stem cells. *Stem Cells Dev.* **2014**, *23*, 2673–2686.
69. Kriks, S.; Shim, J.W.; Piao, J.; Ganat, Y.M.; Wakeman, D.R.; Xie, Z.; Carrillo-Reid, L.; Auyeung, G.; Antonacci, C.; Buch, A.; *et al*. Dopamine neurons derived from human ES cells efficiently engraft in animal models of Parkinson's disease. *Nature* **2011**, *480*, 547–551.

70. Chambers, S.M.; Fasano, C.A.; Papapetrou, E.P.; Tomishima, M.; Sadelain, M.; Studer, L. Highly efficient neural conversion of human ES and iPS cells by dual inhibition of SMAD signaling. *Nat. Biotechnol.* **2001**, *27*, 275–280.
71. Muroyama, Y.; Fujihara, M.; Ikeya, M.; Kondoh, H.; Takada, S. Wnt signaling plays an essential role in neuronal specification of the dorsal spinal cord. *Genes Dev.* **2002**, *16*, 548–553.
72. Joksimovic, M.; Yun, B.A.; Kittappa, R.; Anderegg, A.M.; Chang, W.W.; Taketo, M.M.; McKay, R.D.; Awatrami, R.B. Wnt antagonism of Shh facilitates midbrain floor plate neurogenesis. *Nat. Neurosci.* **2009**, *12*, 125–131.

8.2. Aberrant epigenome in iPSC-derived dopaminergic neurons from Parkinson's disease patients (Research article).

Fernández-Santiago, R., Carballo-Carbajal, I., Castellano, G., **Torrent, R.,** Richaud, Y., Sánchez-Danès, A., Vilarrassa-Blasi, R., Sánchez-Pla, A., Mosquera, J.L., Soriano, J., López-Barneo, J., Canals J.M., Alberch, J., Raya, A., Vila, M., Consiglio, A., Martín-Subero, J.I., Ezquerra, M., Tolosa, E., *Aberrant epigenom in iPSC-derived dopaminergic neurons from Parkinson's disease patients,* ***EMBO Mol Med,*** 2015 7: 1529-46.

Our group has collaborated with Eduardo Tolosa group in a study regarding the epigenetic background analysis of DA neurons derived from iPSC from PD patients (both LRRK2-PD and ID-PD), in comparison with healthy CTL lines, aiming to identify pathological mechanisms that could cause neuronal death in PD brain patients [250].
The results of this study demonstrated extensive DNA methylation changes in iPSC-derived DA neurons of PD patients. Specifically, in comparison with CTLs, DA neurons derived from PD were epigenetically disregulated, as shown by 75% of all differentially methylated CpG sites (DMCpGs) remaining unchanged during differentiation of iPSC DA neurons derived from PD patients, whereas only 40% of DMCpGs were found unchanged in the CTL lines. These data suggests an incomplete epigenomic remodelling in PD. Moreover, non of these epigenetic differences were found between keratinocytes nor iPSC between PD and CTL lines, suggesting that this molecular defect remains latent in keratinocytes from PD patients, and only become exposed when their fate is DA neurons.
Subsequently, the transcriptome of DA neurons derived from iPSC was analyzed and found that some of the genes associated with DMCpGs were involved in neural functions and also in regulating transcriptional activity. Among different genes affected, a decreased expression of FOXA1, NR3C1, and HNF4 was found. Interestingly, theses genes are involved in the development and maintenance of DA neuronal fate in adults mammals [414]. This study describes an imbalance in the regulation of transcipcional activity of these genes, which could justify the diseased phenotype described by Sánchez-Danès [102].

Specifically, I have participated in:

1. Providing fresh pellets of iPSC-derived DA neuronal differentiation, performed as previously described [363], from the following individuals: 4 CTL (SP15 #2, SP11 #1, SP09 #4, SP17 #2); 4 LRRK2-PD (SP13 #4, SP12 #3, SP06 #2, SP05 #1); and 6 ID-PD (SP02 #1, SP16 #2, SP10#1, SP04 #2, SP08 #1, SP01 #1).
2. Characterization of iPSC-derived DA neuronal differentiations (see Figure 1).
3. Identification of protein expression deregulation in PD iPSC-derived DA neurons. Here we performed immunoblots of DAn differentiations for the transcription factors PAX6, and OTX2. As well, we performed immunostaining in order to assess collocalitzation of TH neurons for OTX2, PAX6 and the transmembrane protein DCC (see Supplementary Figure EV3).

Published online: October 29, 2015

Research Article

SOURCE DATA | TRANSPARENT PROCESS | OPEN ACCESS

EMBO Molecular Medicine

Aberrant epigenome in iPSC-derived dopaminergic neurons from Parkinson's disease patients

Rubén Fernández-Santiago[1,2,3,*], Iria Carballo-Carbajal[2,4,†], Giancarlo Castellano[5,†], Roger Torrent[6], Yvonne Richaud[7,8], Adriana Sánchez-Danés[6], Roser Vilarrasa-Blasi[5], Alex Sánchez-Pla[9,10], José Luis Mosquera[9], Jordi Soriano[11], José López-Barneo[2,12], Josep M Canals[2,3,13], Jordi Alberch[2,3,13], Ángel Raya[7,8,14], Miquel Vila[2,4,14], Antonella Consiglio[6,15,‡], José I Martín-Subero[5,‡], Mario Ezquerra[1,2,3,‡,**] & Eduardo Tolosa[1,2,3,16,‡]

Abstract

The epigenomic landscape of Parkinson's disease (PD) remains unknown. We performed a genomewide DNA methylation and a transcriptome studies in induced pluripotent stem cell (iPSC)-derived dopaminergic neurons (DAn) generated by cell reprogramming of somatic skin cells from patients with monogenic LRRK2-associated PD (L2PD) or sporadic PD (sPD), and healthy subjects. We observed extensive DNA methylation changes in PD DAn, and of RNA expression, which were common in L2PD and sPD. No significant methylation differences were present in parental skin cells, undifferentiated iPSCs nor iPSC-derived neural cultures not-enriched-in-DAn. These findings suggest the presence of molecular defects in PD somatic cells which manifest only upon differentiation into the DAn cells targeted in PD. The methylation profile from PD DAn, but not from controls, resembled that of neural cultures not-enriched-in-DAn indicating a failure to fully acquire the epigenetic identity own to healthy DAn in PD. The PD-associated hypermethylation was prominent in gene regulatory regions such as enhancers and was related to the RNA and/or protein downregulation of a network of transcription factors relevant to PD (FOXA1, NR3C1, HNF4A, and FOSL2). Using a patient-specific iPSC-based DAn model, our study provides the first evidence that epigenetic deregulation is associated with monogenic and sporadic PD.

Keywords DNA methylation; dopaminergic neuron; induced pluripotent stem cell; Parkinson's disease; transcription factor
Subject Categories Chromatin, Epigenetics, Genomics & Functional Genomics; Neuroscience; Stem Cells
DOI 10.15252/emmm.201505439 | Received 15 May 2015 | Revised 24 September 2015 | Accepted 28 September 2015 | Published online 29 October 2015
EMBO Mol Med (2015) 7: 1529–1546

Introduction

Parkinson's disease (PD) is a neurodegenerative disorder associated with the progressive loss of dopaminergic neurons (DAn) in the

1 Laboratory of Neurodegenerative Disorders, Department of Neurology, Hospital Clínic of Barcelona, Institut d'Investigacions Biomèdiques August Pi i Sunyer (IDIBAPS), University of Barcelona (UB), Barcelona, Spain
2 Centro de Investigación Biomédica en Red de Enfermedades Neurodegenerativas (CIBERNED), Madrid, Spain
3 Cell Therapy Program, Faculty of Medicine, University of Barcelona (UB), Barcelona, Spain
4 Neurodegenerative Diseases Research Laboratory, Hospital Vall d'Hebron, Vall d'Hebron Research Institute (VHIR), Universitat Autònoma de Barcelona (UAB), Barcelona, Spain
5 Department of Pathological Anatomy, Pharmacology and Microbiology, University of Barcelona (UB), Institut d'investigacions Biomèdiques August Pi i Sunyer (IDIBAPS), Barcelona, Spain
6 Institute for Biomedicine (IBUB), University of Barcelona (UB), Barcelona, Spain
7 Control of Stem Cell Potency Group, Institute for Bioengineering of Catalonia (IBEC), Barcelona, Spain
8 Centre for Networked Biomedical Research on Bioengineering, Biomaterials and Nanomedicine (CIBER-BBN), Zaragoza, Spain
9 Department of Statistics, University of Barcelona (UB), Barcelona, Spain
10 Department of Statistics, Vall d'Hebron Research Institute (VHIR), Barcelona, Spain
11 Departament d'Estructura i Constituents de la Matèria (ECM), Facultat de Física, University of Barcelona (UB), Barcelona, Spain
12 Institute of Biomedicine of Seville (IBiS), Hospital Universitario Virgen del Rocío, Consejo Superior de Investigaciones Científicas (CSIC), University of Seville, Seville, Spain
13 Department of Cell Biology, Immunology and Neuroscience, Faculty of Medicine, Institut d'Investigacions Biomèdiques August Pi i Sunyer (IDIBAPS), University of Barcelona (UB), Barcelona, Spain
14 Institució Catalana de Recerca i Estudis Avançats (ICREA), Barcelona, Spain
15 Department of Molecular and Translational Medicine, University of Brescia and National Institute of Neuroscience, Brescia, Italy
16 Movement Disorders Unit, Department of Neurology, Hospital Clínic of Barcelona, Institut d'Investigacions Biomèdiques August Pi i Sunyer (IDIBAPS), University of Barcelona (UB), Barcelona, Spain
*Corresponding author. Tel: +34 932 275 400 ext. 4814; Fax: +34 935 275 783; E-mail: ruben.fernandez.santiago@gmail.com
**Corresponding author. Tel: +34 932 275 400 ext. 4814; Fax: +34 935 275 783; E-mail: ezquerra@clinic.ub.es
†These authors contributed equally to this work
‡Co-senior authors

substantia nigra pars compacta (SNpc) (Lang & Lozano, 1998a,b). Yet PD is recognized as a systemic disease affecting other tissues apart from the nervous system (Hoepken *et al*, 2008; Beach *et al*, 2010; Shannon *et al*, 2012). Although most cases are sporadic, around 5–10% encompass monogenic forms caused by pathogenic mutations in PD-associated genes (Farrer, 2006). Among these, missense mutations in the leucine-rich repeat kinase 2 (*LRRK2*) gene are the most frequent cause of familial PD (Paisan-Ruiz *et al*, 2004; Zimprich *et al*, 2004) and also of the common sporadic form. The *LRRK2* G2019S mutation alone explains up to 6% familial and 3% sporadic PD cases in Europeans (Di Fonzo *et al*, 2005; Gilks *et al*, 2005) and up to 20% of total cases among Ashkenazy Jews (Ozelius *et al*, 2006) or 40% in North African Berbers (Lesage *et al*, 2006). In addition, *LRRK2*-associated PD (L2PD) is clinical and neuropathologically similar to sporadic PD (sPD) lacking *LRRK2* mutations (Healy *et al*, 2008), thus representing a valuable system to investigate the most common form of disease. Moreover, the reduced penetrance of G2019S in L2PD suggests the involvement, akin to sPD, of yet unknown disease-modifying factors (Healy *et al*, 2008).

Genetic and epigenetic alterations contribute to the physiopathology of diseases (Bergman & Cedar, 2013). In PD, beyond largely studied genetic defects, the epigenomic landscape of disease remains unknown (Urdinguio *et al*, 2009; van Heesbeen *et al*, 2013). Epigenetic modifications are inheritable changes of gene expression without alterations in the DNA sequence which can virtually capture the influence of environmental factors (Feil & Fraga, 2011). Thus, epigenetic alterations can reflect the relationship among factors which have been postulated to play a role in complex neurodegenerative disorders such as the individual genetic background, the environment, and the aging process. To date, epigenetic studies in central nervous system disorders have been hampered by the inaccessibility to disease targeted cells from patients, and especially of DAn from the SNpc in PD. The few published reports in PD were performed in blood cells using single gene candidate approaches (Kontopoulos *et al*, 2006; Pieper *et al*, 2008; de Boni *et al*, 2011; Jin *et al*, 2014) or human postmortem cortex and cerebellum representing end-points of disease (Desplats *et al*, 2011; IPDGC, 2011; Masliah *et al*, 2013). Results from these studies have been sometimes conflicting and did not yield robust associations. In addition, previous studies on iPSC-derived DAn did not explore in the role of the epigenome in PD (Byers *et al*, 2011; Nguyen *et al*, 2011; Seibler *et al*, 2011; Cooper *et al*, 2012; Jiang *et al*, 2012; Sanchez-Danes *et al*, 2012b; Rakovic *et al*, 2013; Reinhardt *et al*, 2013; Ryan *et al*, 2013; Schondorf *et al*, 2014).

In the present study, we investigated the epigenome of PD by performing a genomewide DNA methylation study of CpG dinucleotides and a transcriptome study using an *in vitro* PD model of patient-specific disease-relevant cells (DAn). This cell system consisted in induced pluripotent stem cell (iPSC)-derived DAn generated upon cell reprogramming of parental skin cells from L2PD patients carrying the G2019S mutation ($n = 4$), sPD patients without *LRRK2* mutations ($n = 6$), and gender- and age-matched healthy subjects ($n = 4$) (Sanchez-Danes *et al*, 2012a,b). Studied cell lines were similar in PD and controls as regards their properties and their maturation state and included 30-day morphologically and functionally mature ventromedial (vm)-DAn which were mostly of the A9 subtype (Sanchez-Danes *et al*, 2012b). The goal of our study was to explore for the first time the epigenomic landscape of PD using iPSC-derived DAn, and to compare the methylome of the common sPD form with the uniquely resembling L2PD monogenic form.

Results

Studied cell lines from PD patients and healthy controls were generated and characterized in parallel blind to researcher in a previous study (Sanchez-Danes *et al*, 2012b) using a 30-days differentiation protocol (Sanchez-Danes *et al*, 2012a) (Table 1, Fig 1 and Materials and Methods). Resulting iPSC-derived DAn had similar morphological and functional properties as well as similar full DAn maturation state in PD and controls (Fig 1) (Sanchez-Danes *et al*, 2012b). Yet consistently with the late onset of disease, the DAn cells from PD patients developed specific neurodegenerative phenotypes upon long-term culture (75-days) including impaired axonal outgrowth, deficient autophagic vacuole clearance, and accumulation of α-synuclein (SNCA) (Sanchez-Danes *et al*, 2012b; Orenstein *et al*, 2013).

Epigenetic changes are associated with monogenic and sporadic PD

We performed a comprehensive genomewide DNA methylation analysis of 30-days iPSC-derived DAn using the Illumina 450k methylation platform (Bibikova *et al*, 2011). Unsupervised hierarchical clustering of CpGs methylation values showed different DNA methylation profiles between both forms of PD (L2PD and sPD) and controls indicating robust differences between PD and controls (Figs 2A and EV1A). We further detected 1,261 differentially methylated CpG sites (DMCpGs) in L2PD and 2,512 in sPD with respect to controls under an absolute mean methylation difference above 0.25 (Bibikova *et al*, 2011) and an adjusted P below 0.05 (Figs 2B and EV1B, and Table EV1). Most DMCpGs in L2PD were common to sPD (78%) and no significant methylation differences were found when comparing L2PD and sPD using the same criteria mentioned above, indicating that L2PD and sPD share similar methylation profiles. Accordingly, both groups were merged for further analysis. In all PD subjects, we identified 2,087 DMCpGs as compared to controls including hypermethylation in 1,046 regions and hypomethylation in 1,041. DMCpGs mostly affected gene bodies and promoters but were also enriched at intergenic regions. Hypermethylated DMCpGs were more often located outside CpG islands, shores, or shelves (73% vs. 31% in background, $P < 0.4 \times 10^{-14}$) (Fig 2C). Notably, genes associated with DMCpGs were largely involved in neural functions and transcription factor (TF) activity (Table EV2). These data indicate that DAn from PD patients show epigenetic abnormalities. They also indicate that monogenic L2PD and the sporadic form of PD share similar DNA methylation changes.

Epigenetic changes manifest only in DAn from PD patients

We further investigated whether those DNA methylation changes observed in DAn were already present in fibroblasts or in undifferentiated iPSCs from the same subjects by analyzing a subset of representative individuals (two L2PD, two sPD, and three controls). Isogenic fibroblasts and iPSCs from these subjects showed no methylation differences between PD and controls neither for the

Table 1. Summary of clinical features and iPSC-derived DAn cell line details from PD patients and gender- and age-matched healthy controls.

Cell line code	Code previous study[Ref.]	Subject type	*LRRK2* mutation	Family history of PD	Gender	Age at donation	Age at onset	Initial symptoms[a]	L-DOPA response	Code of selected IPSCs clones	Cell ratio $TUJ1^+/DAPI^+$ (neurons)[b]	Cell ratio $TH^+/TUJ1^+$ (DA neurons)[c]
C-01	SP-15	Control	No	No	Female	47	–	–	–	15-2	34.7	45.0
C-02	SP-11	Control	No	No	Female	48	–	–	–	11-1	40.0	59.9
C-03	SP-09	Control	No	No	Male	66	–	–	–	9-4	52.2	55.5
C-04	SP-17	Control	No	No	Male	52	–	–	–	17-2	54.0	65.8
PD-01	SP-13	L2PD	G2019S	Yes	Female	68	57	T	Good	13-4	47.0	65.2
PD-02	SP-02	sPD	No	No	Male	55	48	T	N/A	2-1	20.6	42.2
PD-03	SP-05	L2PD	G2019S	Yes	Male	66	52	B	Good	5-1	39.9	49.6
PD-04	SP-16	sPD	No	No	Female	51	48	B	N/A	16-2	32.1	55.2
PD-05	SP-06	L2PD	G2019S	Yes	Male	44	33	T	Good	6-2	40.9	61.9
PD-06	SP-10	sPD	No	No	Male	58	50	D	Good	10-2	35.0	41.1
PD-07	SP-12	L2PD	G2019S	Yes	Female	63	49	T	Good	12-3	42.7	60.0
PD-08	SP-04	sPD	No	No	Male	46	40	B	Good	4-2	52.1	47.3
PD-09	SP-01	sPD	No	No	Female	63	58	T and B	N/A	1-1	32.2	44.9
PD-10	SP-08	sPD	No	No	Female	66	60	T	Good	8-1	41.6	67.1

N/A, not assessed; C, control.
[a]Initial symptoms; T, tremor; B, bradykinesia; D, foot dystonia.
[b]Ratio of neurons/total cells, estimated by immunofluorescence as the ratio of TUJ1 (neuron-specific class III b-tubulin)-positive cells/DAPI-positive cells.
[c]Ratio of iPSC-derived DAn/total neurons, estimated by immunofluorescence as the ratio of TH (tyrosine hydroxylase)-positive cells/TUJ1-positive cells.
[b] and [c] were calculated blind to researcher upon three independent differentiations as previously described (Sanchez-Danes *et al*, 2012b).

2,087 DMCpGs detected in iPSC-derived DAn (Fig 2D) nor for any other given CpG (Fig EV1C) under an absolute mean methylation difference above 0.25 (Bibikova *et al*, 2011) and an adjusted *P* below 0.05. Yet fibroblasts, undifferentiated iPSCs and iPSC-derived DAn showed distinct DNA methylomes as expected for each specific cell type (Doi *et al*, 2009; Hochedlinger & Plath, 2009) (Fig EV1D). Interestingly, a total of 75% of all the 2,087 DMCpGs did not change in the differentiation from iPSCs to DAn in PD patients, whereas only 40% DMCpGs remained unchanged in controls, suggesting an incomplete epigenomic remodeling in PD in spite of the successful reprogramming and differentiation into mature DAn (Sanchez-Danes *et al*, 2012b) (Table EV3 and Fig EV2). These findings suggest that latent molecular defects in skin cells from PD patients become uncovered upon differentiation into DAn. This is compliant with the idea of PD as a systemic disease affecting other tissues apart from the nervous system (Hoepken *et al*, 2008; Beach *et al*, 2010; Shannon *et al*, 2012) including molecular defects which were previously reported in fibroblasts from L2PD or sPD patients (Papkovskaia *et al*, 2012; Ambrosi *et al*, 2014; Yakhine-Diop *et al*, 2014). In addition, to address the extent of the methylation changes attributed to DAn alone in the context of cell heterogeneity inherent to iPSC-derived DAn systems, we differentiated iPSCs from the same subjects into neural cultures not-enriched-in-DAn by omitting the lentiviral-mediated forced expression of the ventral midbrain determinant LMX1A and the supplementation with DAn patterning factors. This protocol results in a > 4-fold depletion in the number of DAn (See Materials and Methods and (Sanchez-Danes *et al*, 2012a)). In neural cultures not-enriched-in-DAn, we did not find methylation differences between PD and controls under an absolute mean methylation difference above 0.25 (Bibikova *et al*, 2011) and an adjusted *P* below 0.05 (Fig EV1C). Moreover, the methylation profile from PD DAn was closer to that from neural cultures not-enriched-in-DAn as compared to control DAn (Fig 2D). For any given comparison and using the same restrictive cutoffs mentioned above, we found that the overall methylation variability referred to all samples was attributable, in decreasing order, to (i) the different cell types as expected, (ii) the condition health/disease only in iPSC-derived DAn, and (iii) inter-individual differences in a relative lesser extent. Altogether, these results indicate that the identified PD epigenetic changes are specific for DAn cells and consist in the failure of PD DAn to fully acquire the mature epigenetic identity own to healthy DAn.

Gene and protein expression changes occur along with methylation changes

We next studied the transcriptome of iPSC-derived DAn by using gene expression microarrays. Compliant to the methylome analysis, no differentially expressed gene (DEG) was found between L2PD and sPD, being most of DEGS in L2PD (93%) shared in sPD. As compared to controls, we identified 437 DEGs in the PD group as a whole under an adjusted *P* below 0.05 (Fig 3A and B, and Table EV4). These findings are in line with two previous studies reporting expression changes associated with PD in DAn, at least with L2PD (sPD not studied) (Nguyen *et al*, 2011; Reinhardt *et al*, 2013). Upregulated DEGs ($n = 254$) were largely involved in neural functions and transcription factor regulatory activity, whereas down-regulated DEGs ($n = 183$) affected basic homeostasis (Table EV5). One upregulated DEG was *SNCA* (> 2.5-fold), a gene involved in familial PD and sPD whose encoded protein, α-synuclein, aggregates in Lewy body inclusions which represent a hallmark of PD (Lang & Lozano, 1998a,b). Another upregulated DEG was *SYT11* (> 5-fold) which has been top-linked associated to PD across genomewide association studies (Nalls *et al*, 2014). We subsequently selected seven genes involved in neural functions from the top-30 list of upregulated DEGs (*OTX2*, *PAX6*, *ZIC1*, *SYT11*, *DCT*, *DCC*, and *NEFL*)

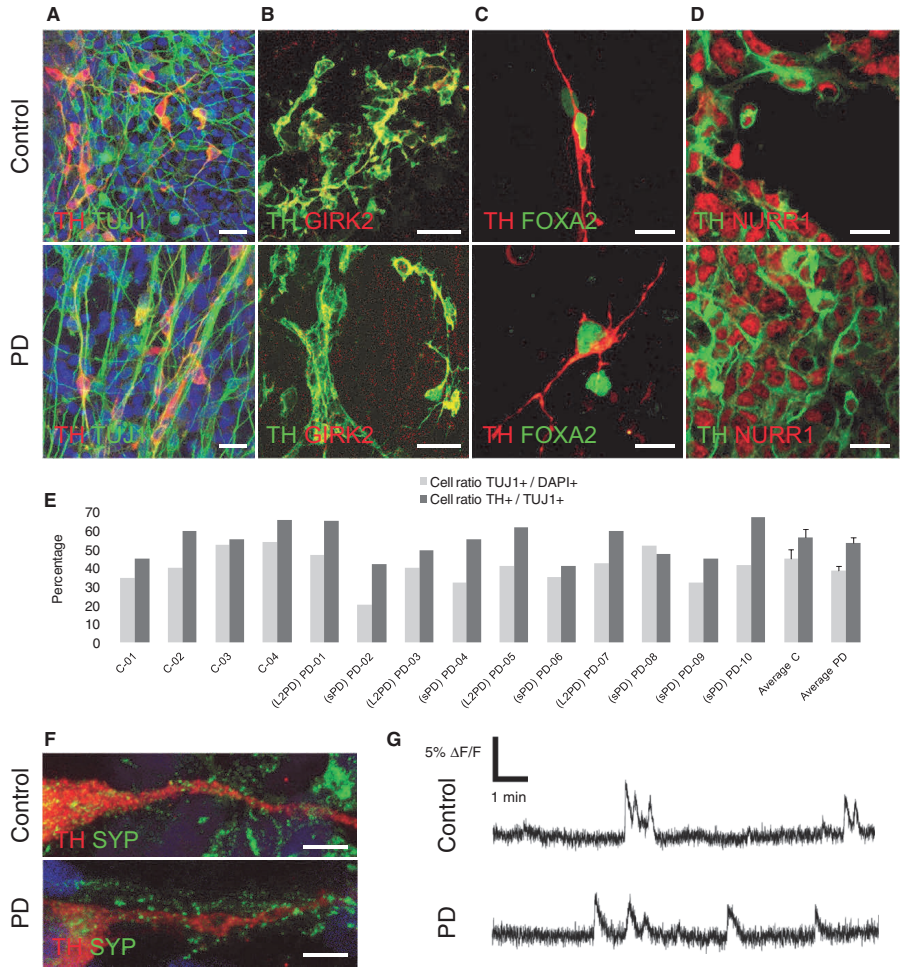

Figure 1. Generation and characterization of iPSC-derived DAn.

A–G After iPSC-based reprogramming of fibroblasts, we generated DAn from PD patients (n = 10) and gender- and age-matched healthy controls (n = 4) using a 30-day differentiation protocol. Blind to researcher, resulting iPSC-derived DAn showed similar properties and maturation state in PD and controls. Specifically, studied iPSC-derived DAn encompassed 30-day ventromedial (vm)-DAn-enriched cultures of morphologically mature DAn showing typical bipolar morphology, lacking PD neural phenotypes, mostly of the A9 subtype, and showing properties of tyrosine hydroxylase $(TH)^+$ mature neurons. Representative immunocytochemical analyses of vmDAn from PD patients and controls showed that (A) TUJ1-positive cells expressing neural tubulin III (TUJ1) co-expressed TH (Scale bar, 25 μm); (B) co-expressed the A9 subtype marker of inward rectifier K^+ channel GIRK2 (Scale bar, 25 μm); (C) co-expressed the A9 subtype marker of transcription factor Forkhead Box A2 (FOXA2) (Scale bar, 12.5 μm); and (F) co-expressed the synaptic vesicle protein synaptophysin (SYP) which was located along neurites (Scale bar, 5 μm). (D) The 1-week neural progenitor cells (NPCs) from which iPSC-derived DAn were generated strongly expressed DAn progenitor markers such as the nuclear-related receptor 1 NURR1 (Scale bar, 12.5 μm). (E) We observed similar and comparable cell counts of total neurons in PD and controls as quantified by TUJ-1/DAPI and of DAn as quantified by TH/TUJ1. Selected DAn cells were generated upon 2-6 iPSC lines per subject (See methods). Error bars indicate SEM. C, control; TUJ1, neuron-specific class III b-tubulin. (G) Calcium imaging assay revealed strong spontaneous neuronal activity. %ΔF/F indicates the relative change in fluorescence of the monitored neurons. Collectively, these results indicate that the iPSC-derived DAn used our study were sufficiently mature for the studied parameters to be functional and to spontaneously form active neural networks in a similar and comparable manner for PD and controls.

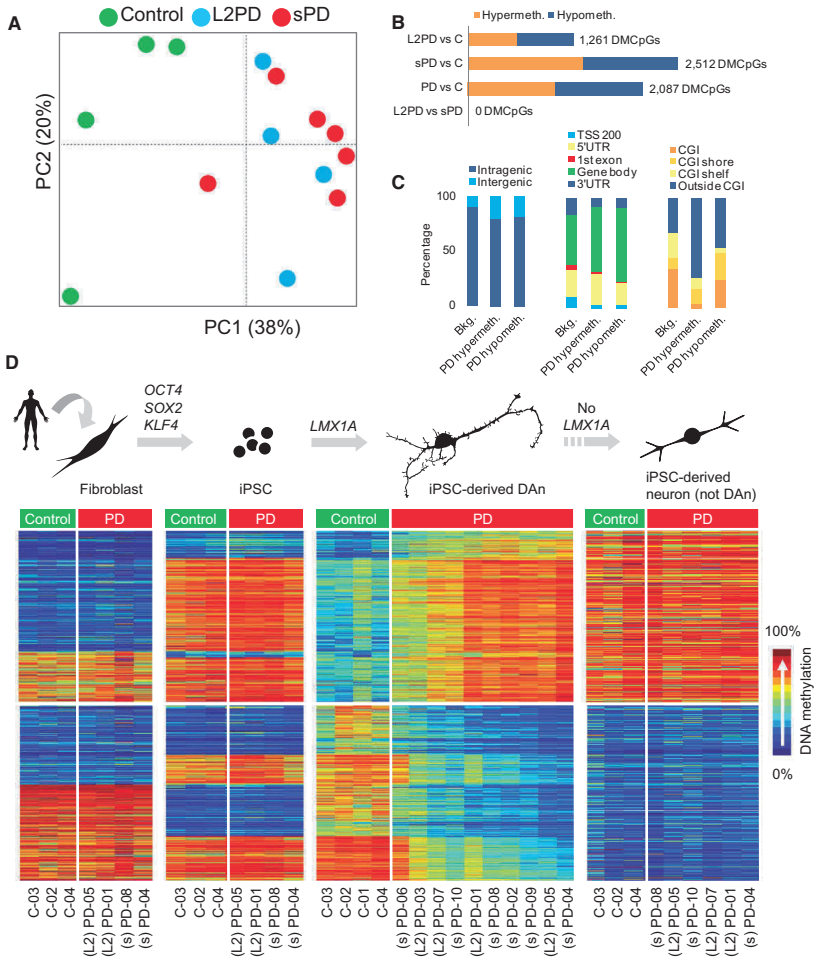

Figure 2. DNA methylation analysis of iPSC-derived DAn from monogenic LRRK2-associated PD (L2PD) and sporadic PD (sPD) patients across the cell types involved in the cell reprogramming and differentiation processes.

A Principal component analysis (PCA) of methylation data from 28,363 CpG sites with variable methylation values (SD > 0.1) in iPSC-derived DAn cell lines (n = 14). This analysis shows different DNA methylation profiles between PD patients and controls, and no differences between L2PD and sPD. PC, principal component.

B Bar diagram showing the number of differentially methylated CpGs (DMCpGs) among iPSC-derived DAn lines (n = 14) as detected in multiple comparisons. This analysis indicates that L2PD and sPD share similar DNA methylation changes with respect to controls. Hypermeth, hypermethylation; hypometh, hypomethylation.

C Relative distribution of DMCpGs in PD iPSC-derived DAn lines (n = 10) across inter- and intragenic regions (left), across different gene-related regions (middle), and within CpG islands (CGI), CGI shores, CGI shelves, or outside CGI (right). Bkg, background (methylation platform).

D DNA methylation analysis across the cell types involved in the cell reprogramming and differentiation processes and also iPSC-derived neural cultures not-enriched-in-DAn. Scheme of the cell reprogramming and differentiation protocols (upper part of the panel). Heatmaps and density color code of the 2,087 DMCpGs identified in iPSC-derived DAn from PD patients with respect to controls (n = 14), as well as their methylation status in parental fibroblasts (n = 9), undifferentiated iPSCs (n = 9), and iPSC-derived neurons (not-DAn) (n = 9) (lower part of the panel) (Wilcoxon rank test for independent samples with delta-beta above |0.25| and FDR-adjusted $P < 0.05$).

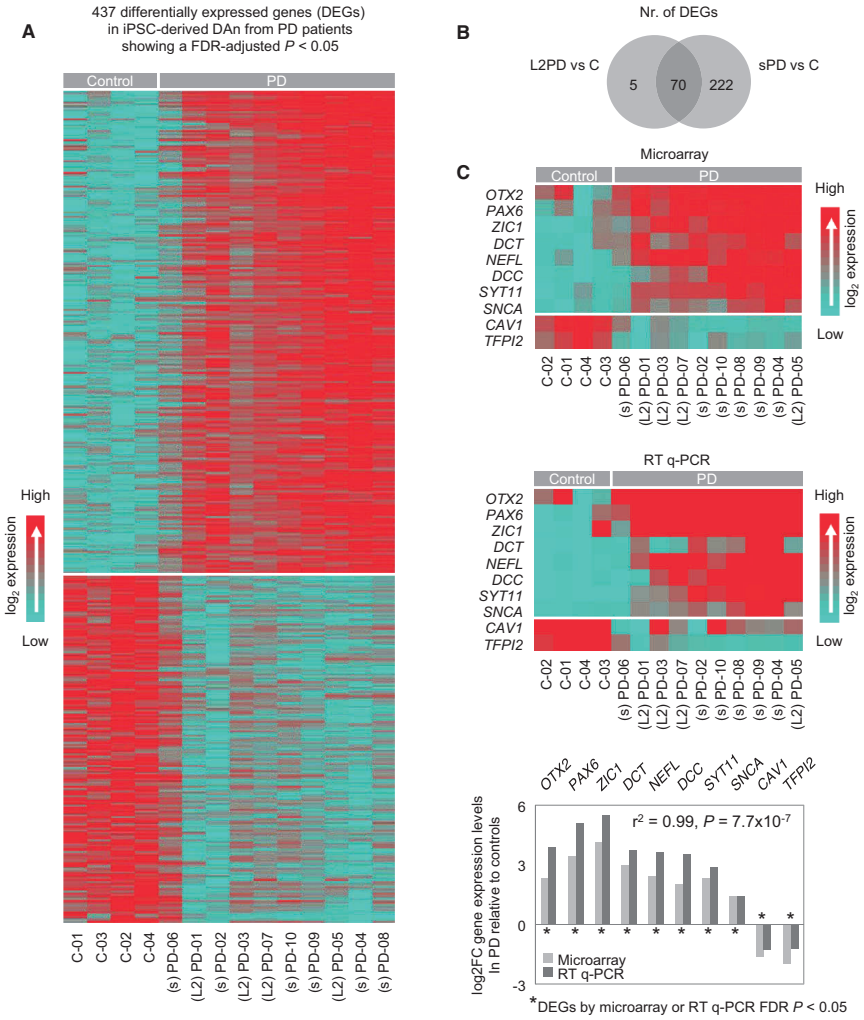

Figure 3. Genomewide gene expression analysis of iPSC-derived DAn from PD patients and controls.

A Heatmap showing the 437 differentially expressed genes (DEGs) detected in PD patients with either L2PD (L2) or sPD (s) as compared to controls (C) (n = 14), and density color code for gene expression levels. This analysis indicates that L2PD and sPD share similar gene expression changes with respect to controls. A total of 254 DEGs were upregulated in PD whereas 183 showed significant downregulation (Linear model with empirical bayes moderation of the variance similar to ANOVA with FDR-adjusted $P < 0.05$).

B Venn diagram representing the number of DEGs in iPSC-derived DAn from PD patients with respect to healthy subjects (n = 14) showing that most DMCpGs in L2PD were common to sPD.

C Technical validation of 10 top DEGs in PD iPSC-derived DAn as compared to controls (n = 14) identified by genomewide gene expression study (upper heat-map) and validated by real-time qPCR (lower heat-map). Relative gene expression and statistical significances were calculated using the ΔΔCt method and *GAPDH*, *ACTB*, and *PPIA* as endogenous controls. Pearson correlation analysis between microarray and real-time qPCR data showed a high degree of correlation (r^2 = 0.99, $P = 7.7 \times 10^{-7}$) (bottom graph). L2, *LRRK2*-associated PD; s, sporadic PD.

and *SNCA* to validate the array data by real-time qPCR (Fig 3C) and to study their protein expression levels by immunoblot. We detected a > 2-fold protein upregulation of all genes except *NEFL* (Fig EV3A). Moreover, protein expression of some DEGs co-localized at the single-cell level with the DAn marker tyrosine hydroxylase (Fig EV3C). These findings point toward the presence of gene and also protein expression changes in DAn from PD patients which occur simultaneously along with DNA methylation changes.

PD DNA mehtylation changes are associated with gene expression

We then analyzed the relationship between gene expression and DNA methylation levels in iPSC-derived DAn from PD patients. We found a significant correlation in 17% of the 2,087 DMCpGs (n = 353) involving 239 different genes (Fig 4A and B). The percentage of correlation between methylation and expression was similar to that reported in other studies (Kulis *et al*, 2012). Of the 353 unique correlating DMCpGs, a total of 73% showed an inverse association of DNA methylation and expression, whereas the remaining 27% DMCpGs were positively associated (Table EV6). DMCpGs showing inverse association were situated in introns and 5′ untranslated regions, whereas those with positive association were enriched in introns (Fig 4C). Globally, DMCpGs showing association with gene expression were more frequently located in introns (49%) than in 5′ regions (24%). These findings suggest that, as reported in cell differentiation and cancer (Jones, 2012; Kulis *et al*, 2012, 2013), PD gene-body DNA methylation changes play a role in regulating gene expression, both inversely and positively.

Differential DNA methylation in PD is enriched in enhancer elements

We further studied the potential molecular mechanisms underlying the association between DNA methylation and gene expression. We analyzed our data in the context of recently available functional chromatin states (Ernst *et al*, 2011). Hypermethylated DMCpGs were highly enriched in enhancer elements (35% vs. 12% in the background, $P = 0.3 \times 10^{-14}$), while hypomethylated DMCpGs were enriched in Polycomb-repressed regions (31% vs. 12% in the background, $P = 0.2 \times 10^{-14}$) (Fig 4D). When considering only the DMCpGs correlating with gene expression, DMCpGs with inverse correlation were located in promoters and enhancers, whereas DMCpGs with positive correlation were associated with repressed regions (Fig 4E). These results suggest that PD-associated DNA methylation changes target functionally active sequences.

PD enhancer hypermethylation is associated with the downregulation of a TFs network

We next inquired whether the DMCpGs identified in PD patients were enriched for transcription factor (TF)-binding sites (TFBSs). To this end, we overlapped our data with TFBS clusters generated by ChIP-seq in the Encyclopedia of DNA Elements project (Dunham *et al*, 2012; Gerstein *et al*, 2012; Lee *et al*, 2012). We found enrichment for binding sites of 23 TFs in PD-hypermethylated DMCpGs and of only two TFs in PD-hypomethylated DMCpGs (Fig 5A and Table EV7). Since the PD-associated hypermethylation affected most prominently to enhancer elements (35%) (Fig 4D), we focused on this chromatin state and observed that 65% of all PD hypermethylated enhancers became demethylated from iPSCs to DAn in controls, whereas only 8% significantly lost methylation in PD patients which overall retained higher methylation levels (Table EV3 and Fig 2D). Furthermore, among the 23 TFs showing TFBS enrichment, we found reduced gene expression of four TFs, namely *FOXA1*, *NR3C1*, *HNF4A*, and *FOSL2*, whose downregulation was also significantly associated with increased methylation levels at enhancer DMCpGs in PD (Fig 5B–D). Moreover, variable expression of these TFs together with the expression of other TFs was coordinated in PD DAn (Fig 6), suggesting that the expression level of a TF network, rather than that of individual TFs, was associated with the hypermethylation of enhancers in PD. In addition, *HNF4A* and *FOSL2* showed a significant downregulation of protein levels as detected by immunoblot, whereas *NR3C1* showed a downregulation trend which did not reach significance (Figs 7A and EV3B, and Source data for Fig 7). These data complement recent work linking TF binding to enhancers and tissue-specific hypomethylation (Stadler *et al*, 2011; Hon *et al*, 2013; Xie *et al*, 2013; Ziller *et al*, 2013), and also downregulation of TF networks to enhancer hypermethylation (Agirre *et al*, 2015). Our findings suggest that the incomplete epigenetic remodeling observed for the 2,087 DMCpGs identified in iPSC-derived DAn from PD patients might be mediated by the aberrant downregulation of a network of key TFs whose deficiency could prevent their target sites to become demethylated during the differentiation from iPSCs to DAn.

Discussion

We report the first genomewide DNA methylation study of iPSC-derived DAn in PD. We found that DAn from PD patients are epigenetically altered with respect to healthy controls and that DAn from monogenic L2PD and sPD share similar DNA methylation abnormalities. These methylation changes cannot be explained by technical biases since all iPSC-derived DAn lines were equally generated and characterized in parallel, blind to the researcher, and differentiated DAn had similar morphological and functional properties (Sanchez-Danes *et al*, 2012b). We also found that the PD-associated methylation changes were not present in parental skin cells or undifferentiated iPSCs and become uncovered only upon differentiation into the DAn cells targeted in PD. In addition, the methylation profile of DAn from PD patients, with either monogenic or sporadic PD, resembled that of neural cultures not-enriched-in-DAn indicating a failure to fully acquire the epigenetic identity own to healthy DAn in PD. We also detected that gene and protein expression changes occur simultaneously along with methylation alterations in PD and that these alterations are similar in monogenic L2PD and sPD. Finally, we found that the DNA methylation changes present in PD DAn are partially associated with gene expression, target gene regulatory sequences such as enhancers, and correlate with the RNA and protein downregulation of a network of TFs.

The lack of DNA methylation differences between DAn from patients with L2PD and sPD provides the proof-of-concept of common or at least converging epigenomic changes in these disease forms (Zhu *et al*, 2011). However, one limitation of our work is that we studied only one monogenic form of PD (L2PD) and therefore

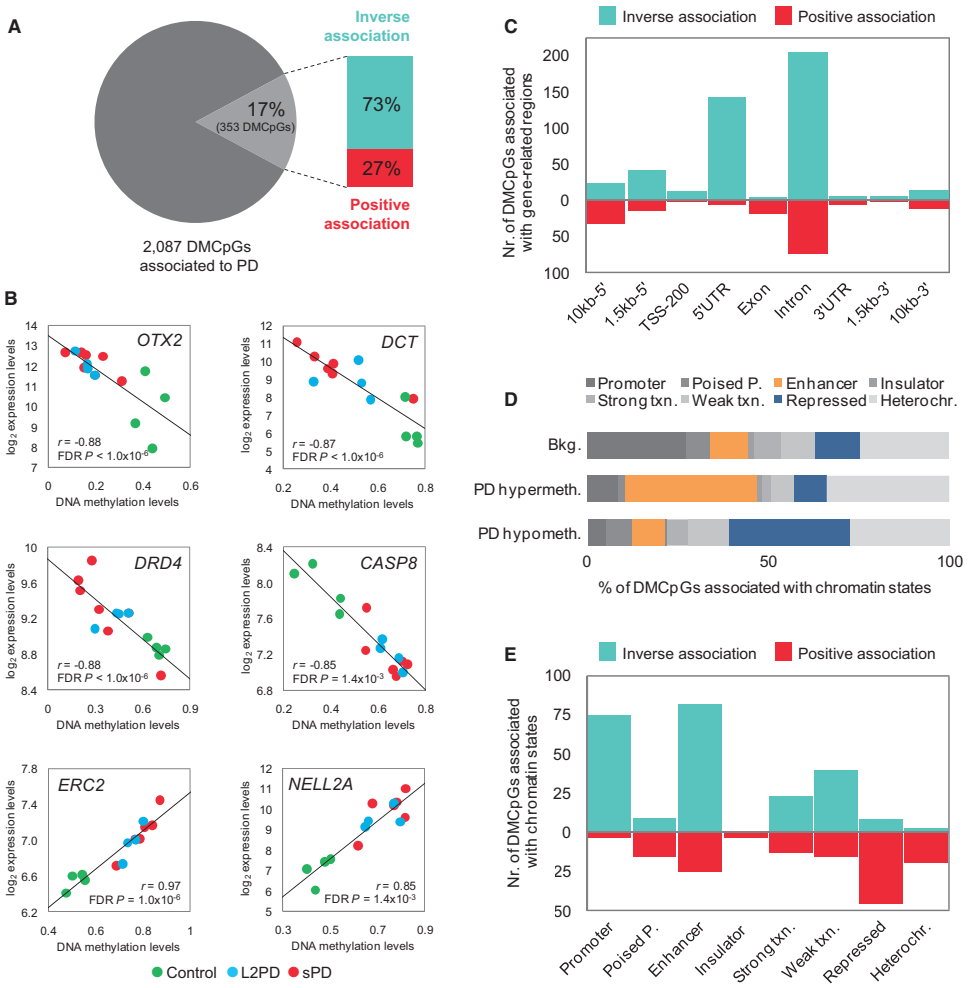

Figure 4. Correlation between DNA methylation values of differentially methylated CpGs (DMCpGs) and expression levels of the associated genes in PD iPSC-derived DAn.

A Graphical representation of the percentage of DMCpGs associated with gene expression.

B Examples of genes showing significant correlation including a brief functional description: *OTX2*, transcription factor for midbrain DAn development which blocks *LMX1A*; *DCT*, dopachrome tautomerase, induced by *OTX2*, is a detoxifying enzyme of DA metabolites involved in the synthesis of neuromelanin; *DRD4*, DA receptor type 4; *CASP8*, apoptosis extrinsic pathway member inducing *CASP3*; *ERC2*, cytoskeleton organizer at nerve terminals for neurotransmission; *NELL2*, neural epidermal growth factor-like 2 involved in neural differentiation.

C Counts of DMCpGs associated with gene expression across gene-related regions.

D Relative distribution of DMCpGs across chromatin states. Poised P, poised promoter; Txn, transcription; Heterochr, heterochromatin.

E Counts of DMCpGs associated with gene expression across chromatin states.

Data information: In (A) and (B), $n = 14$ cell lines, Spearman correlation analysis with FDR-adjusted $P < 0.05$.

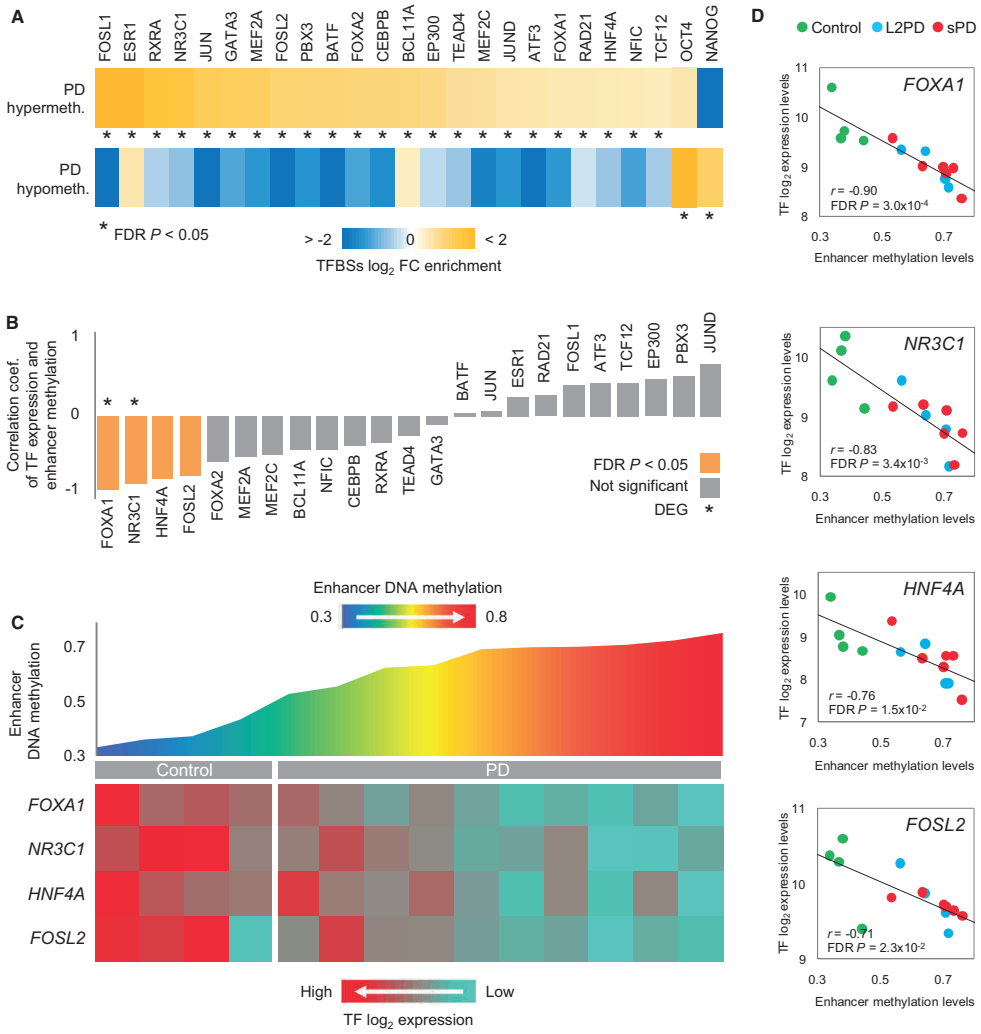

Figure 5. Association between gene expression levels of transcription factors (TFs) and DNA methylation levels at PD-hypermethylated enhancers from PD iPSC-derived DAn.

A Relative enrichment of TF-binding sites (TFBSs) overlapping with the 2,087 DMCpGs detected in PD iPSC-derived DAn (n = 10). This analysis shows an enrichment of binding sites for 23 TFs in regions hypermethylated in PD.

B Bar plot showing the results of the Spearman correlation analysis between levels of TF gene expression and of average DNA methylation at the 376 enhancer sites hypermethylated in PD iPSC-derived DAn (n = 10). Coef, coefficient.

C Graphical representation of average methylation at PD-associated enhancers and gene expression of the key TFs *FOXA1*, *NR3C1*, *HNF4A*, and *FOSL2* in iPSC-derived DAn (n = 14).

D Scatter plots of key TF gene expression and DNA methylation levels at enhancers in iPSC-derived DAn (n = 14).

Data information: Fisher's exact test with a FDR-adjusted $P < 0.05$ in (A), and Spearman correlation analysis with FDR $P < 0.05$ in (B) and (D).

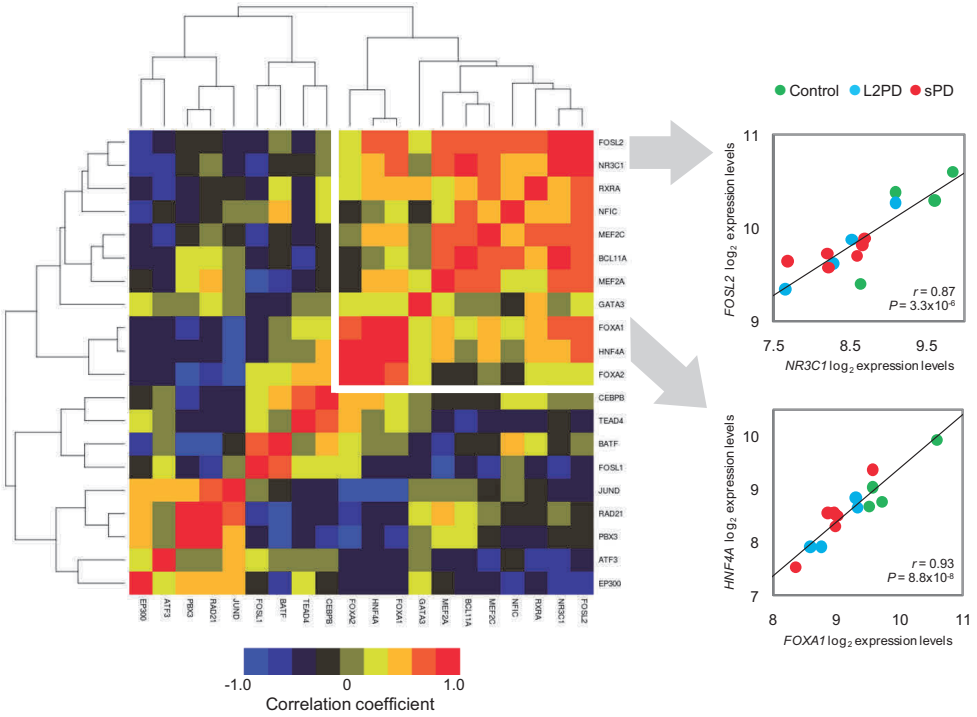

Figure 6. Correlation matrix of gene expression levels among TFs showing TF-binding sites (TFBS) enrichment at PD-hypermethylated enhancers.
Pearson correlation coefficients and correlation *P*-values were calculated evaluating TF gene expression levels in iPSC-derived DAn from PD patients and controls (n = 14) under a 2-tailed Student's *t*-test. Among TFs showing coordinated expression, maximal correlation was observed for *FOXA1*, *FOXA2*, *NR3C1*, *HNF4A*, and *FOSL2*.

the epigenetic involvement in other PD familial forms remains to be explored. Our findings are compliant with the observation that L2PD is clinical and neuropathologically similar to sPD lacking *LRRK2* mutations (Healy *et al*, 2008). Yet the interpretation of our results requires further considerations. First, the epigenome is expected to reflect the influence from the environment and thus one possibility is that unknown environmental factors could trigger epigenomic changes in PD patients. This environmental contribution would be expectable for sPD (Feil & Fraga, 2011), but the age-dependent reduced penetrance of the *LRRK2* G2019S mutation together with its identification not only in monogenic but also in sPD cases (Healy *et al*, 2008) could also support an environmental involvement in L2PD (Farrer, 2006; Urdinguio *et al*, 2009). Second, an alternative possibility is that the genetic background from PD patients could drive DNA methylation changes not only in monogenic L2PD as expectable but also in sPD. In this regard, it has been described that sPD could be caused by an accumulation of common polygenic alleles with relatively low effect sizes (Escott-Price *et al*, 2015). Thus, a possible integrative interpretation of our findings is that cumulative genetic risk factors such as single nucleotide polymorphisms (SNPs) or copy number variants (CNVs) in sPD, or *LRRK2* mutations in L2PD, alone or in combination with still unknown environmental factors could be underlying the common epigenetic changes detected in both disease forms. These environmental and/or genetic factors arising from different but converging pathways could ultimately cause common end-point alterations in L2PD and sPD.

The PD epigenetic changes were present only in iPSC-derived DAn but not in undifferentiated iPSC, in fibroblasts, nor in iPSC-derived neural cultures not-enriched-in-DAn. These results indicate that the PD-associated DNA methylation changes are specific of DAn but not of other types since neural cultures not-enriched-in-DAn did not reveal methylation differences. They also suggest that molecular defects, of an environmental and/or genetic origin as discussed above, should be carried from the PD patient, latent in fibroblasts, and manifested only upon differentiation into DAn. Here it should be mentioned that although in PD when and where the degenerative process starts is unclear, and the related underlying

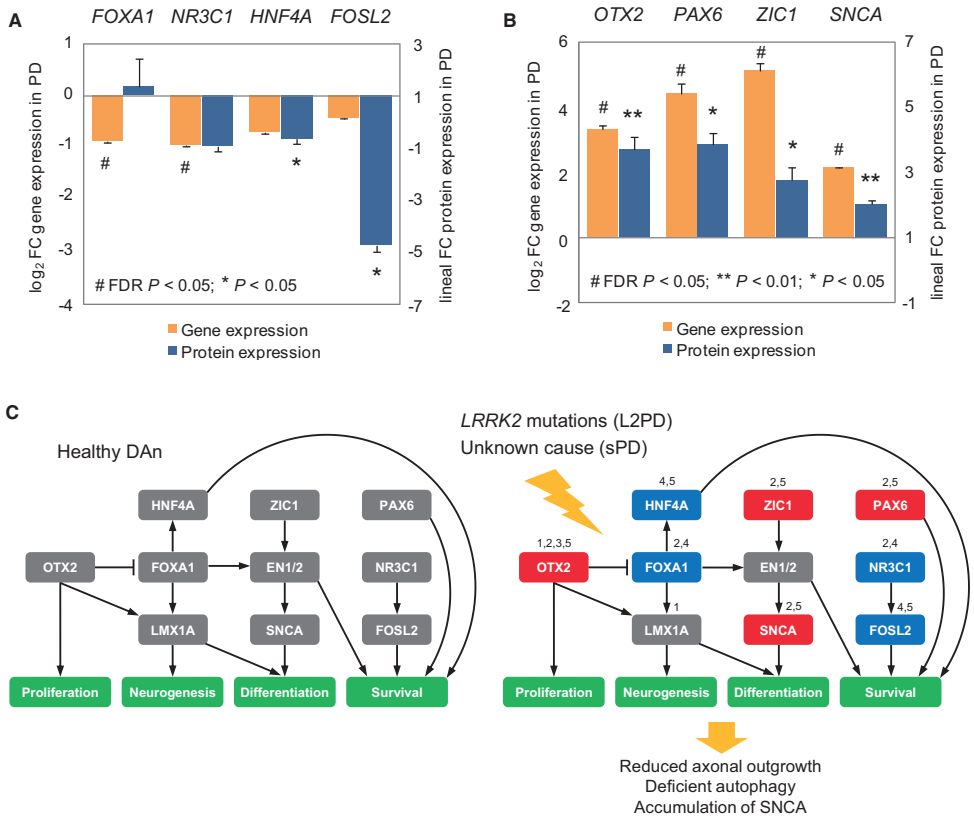

Figure 7. Gene and protein expression of PD downregulated key TFs and proposed theoretic model.

A, B Graphical representation of gene and protein expression of the key TFs *FOXA1*, *NR3C1*, *HNF4A*, and *FOSL2* (A) (see also Fig EV3B and Source data for Fig 7), or of the PD upregulated genes (B) (see also Fig EV3A and Source data for Fig 7) identified in iPSC-derived DAn from PD patients, normalized to the expression of controls, and expressed, respectively, as $\log_2$ or lineal fold change (FC) values. (For gene expression, linear model with empirical bayes moderation of the variance similar to ANOVA with FDR-adjusted $P < 0.05$; for protein expression, two-tailed Student's *t*-test (**$P < 0.01$, *$P < 0.05$). Samples were studied at least in three independent experiments. Data are represented as group mean ± SEM).

C Proposed model in which deficits of the key TFs *FOXA1*, *NR3C1*, *HNF4A*, and *FOSL2* relevant to PD lead to DNA methylation changes. Key 1 denotes differentially methylated gene, key 2 denotes DEG, key 3 denotes significant correlation of DNA methylation with proximal gene expression, key 4 denotes significant correlation of key TF gene expression with distal DNA methylation at enhancers, and key 5 denotes differentially expressed protein. Blue-shaded boxes indicate gene expression downregulation, whereas red-shaded boxes indicate upregulation. Illustration of our model was built by selecting most prominent alterations detected by unbiased genomewide approaches in our study.

Source data are available online for this figure.

biological changes remain unknown, several works have reported molecular defects in fibroblasts from L2PD and also from other PD monogenic forms (Hoepken *et al*, 2008; Rakovic *et al*, 2013; Ambrosi *et al*, 2014; Yakhine-Diop *et al*, 2014). In this context, our findings are compatible with the emerging notion of PD as a systemic disease affecting other tissues apart from the nervous system (Beach *et al*, 2010; Shannon *et al*, 2012).

The methylation profile from PD DAn resembled that of neural cultures not-enriched-in-DAn indicating a failure in PD to fully acquire the epigenetic identity own to healthy DAn. The methylation changes identified in PD occurred in spite of the apparently normal dopaminergic phenotypes observed in our early 30-days DAn cultures which consisted in functionally and morphologically mature DAn which were similar in PD and controls

(Sanchez-Danes *et al*, 2012b). This is in agreement with previous studies describing normal dopaminergic phenotypes in PD iPSC-derived DAn (Byers *et al*, 2011; Nguyen *et al*, 2011; Cooper *et al*, 2012; Rakovic *et al*, 2013; Reinhardt *et al*, 2013) with the exception of one Parkin study reporting altered dopamine release and uptake (Jiang *et al*, 2012). However, we found that the epigenetic changes detected in our early 30-days DAn cultures antedated late (75-days), spontaneous (not-drug induced), PD-associated phenotypes which were previously described in our model and included impaired axonal outgrowth, deficient autophagic vacuole clearance, and accumulation of α-synuclein (Sanchez-Danes *et al*, 2012b; Orenstein *et al*, 2013). Consistent with our methylation findings, these PD phenotypes were also common in DAn from L2PD and sPD patients (Sanchez-Danes *et al*, 2012b). Yet although the early DNA methylation changes reported here antedated these long-term PD phenotypes potential causality needs to be explored in future works.

As reported in cell differentiation and cancer (Jones, 2012; Kulis *et al*, 2012, 2013), we found that the identified epigenetic changes correlate partially with expression, indicating that PD gene-body DNA methylation changes play a role in the regulation of gene expression. We also found that the PD DNA hypermethylation changes are prominent at enhancer regulatory regions. In line with other studies (Agirre *et al*, 2015), we also found that in PD, the hypermethylation of enhancers appears to be related to the downregulation of a network of key TFs, rather than of individual TFs. These data complement recent work linking TF binding to enhancers and tissue-specific hypomethylation (Stadler *et al*, 2011; Hon *et al*, 2013; Xie *et al*, 2013; Ziller *et al*, 2013) and suggest a theoretic model in which the incomplete epigenetic remodeling in PD DAn might be related to the downregulation of a network of key TFs whose deficiency could prevent their binding sites to become demethylated during the differentiation from iPSCs to DAn. Key TFs from this network have been previously associated with the specification of the substantia nigra (*FOXA1*, *NR3C1*, and *HNF4*) and of fetal brain (*FOSL2*) (Ziller *et al*, 2013). Of these, *FOXA1* is involved in maintaining the dopaminergic phenotype in adult mesodienchepalic DAn (Stott *et al*, 2013; Domanskyi *et al*, 2014), whereas the glucocorticoid receptor *NR3C1* regulates DAn neurodegeneration in PD (Ros-Bernal *et al*, 2011). Downregulation of *HNF4A* has been reported in blood from PD patients as a PD biomarker correlating with motor symptoms severity (Potashkin *et al*, 2012; Santiago & Potashkin, 2015), whereas *FOSL2* has been linked to dyskinesia, a major side effect in the DA substitutive treatment with L-DOPA (Cao *et al*, 2010). Since these TFs seem to be relevant to the development and maintenance of midbrain DAn in PD (Lahti *et al*, 2011, 2012), their deficiency might be related to impairments in the maintenance of a differentiated DAn epigenetic cellular identity in PD (Holmberg & Perlmann, 2012). In this theoretic model, the upregulation of gene and protein expression of other TFs (*OTX2*, *PAX6*, or *ZIC1*) and genes (*SNCA*, *DCC*, or *DCT*) (Figs 7B and EV3A, and Source data for Fig 7) might transiently circumvent deficits of the network of key TFs, at least in early culture stages.

One hypothesis proposes the neurodevelopmental origin of neurodegenerative diseases in the sense that molecular mechanisms occurring during development are abnormally recapitulated in neurodegenerative disease processes (Goedert *et al*, 1993; Schafer & Stevens, 2010). For example, a recent study showed that neural degeneration in Alzheimer's disease involves the abnormal re-activation of cellular self-destruction mechanisms which take place during neural development (Nikolaev *et al*, 2009). Since we found that the epigenetic pattern from PD iPSC-derived DAn showed certain similarities to neural cultures not-enriched-in-DAn, our data could be interpreted in light of this theory pointing towards the presence of possible developmental epigenetic defects associated with PD. In addition, developmental deficits of TFs which are key in the differentiation of DAn have been recently linked to PD (Laguna *et al*, 2015).

We showed that iPSC-derived DAn from PD patients exhibit epigenomic and transcriptomic alterations, and therefore, our findings may have implications for future cell replacement therapies. The use of pluripotent stem cells has proved as a valuable *in vitro* system to investigate disease, as well as a promising tool for brain transplantation and dopaminergic restoration in PD. Yet the generation of DAn for cell replacement is still matter of research (Lindvall & Bjorklund, 2011). Recently, the autologous transplantation of iPSC-derived neurons into the striatum of healthy monkeys has been suggested to be advantageous as compared to allogenic grafts, at least in terms of reduced immunogenicity (Morizane *et al*, 2013). Our study suggests that future cell therapeutic strategies should pay attention to the correct epigenomic status of the reprogrammed dopaminergic cells, especially when using patient own cells. In summary, using a patient-specific iPSC-based DAn system, our study provides the first evidence that epigenetic deregulation is associated with both monogenic and sporadic PD.

Materials and Methods

PD patients and generation of iPSC-derived DAn

We used mature iPSC-derived DAn lines of 30-days of differentiation generated and characterized in parallel blind to researcher previously (Sanchez-Danes *et al*, 2012b) using a published protocol (Sanchez-Danes *et al*, 2012a). Expanded subject information, cell characterization, and technical details are extensively described in these precedent studies where they should be consulted. Of these, a summary presented in Table 1, Fig 1, and here as it follows. Arm surface skin biopsies of 3 mm of diameter were obtained from *LRRK2* PD patients carrying the G2019S mutation (L2PD, $n = 4$); sporadic PD patients lacking family history of PD and mutations in known PD genes (sPD, $n = 6$); and gender- and age-matched healthy individuals without neurological disease history (controls, $n = 4$). Primary cultures of keratinocytes or fibroblasts were reprogrammed using retroviral delivery of *OCT4*, *KLF4*, and *SOX2* to generate 2–6 iPSC lines per individual ($n = 50$ lines). Of these, we selected the two more homogenous lines per subject which were thoroughly characterized and shown to be fully reprogrammed to pluripotency. For the directed differentiation of iPSC to ventral midbrain dopaminergic neurons (vmDAn), we used a 30-days protocol based on the lentiviral-mediated forced expression of the vmDAn determinant *LMX1A* together with DAn patterning factors and co-culture with mouse PA6 feeding cells to provide trophic factor support. DAn

pellets were obtained by mechanic separation of the PA6 layer with a finely drawn Pasteur pipette. Differentiated cells were 30-days vmDAn-enriched cultures of morphologically fully mature DAn lacking PD neural phenotypes (Sanchez-Danes *et al*, 2012b), mostly of the A9 subtype which showed properties of TH^+ mature neurons: (i) electrophysiological analysis showed action potentials, (ii) the majority of DAn presented the typical bipolar morphology, (iii) co-expressed the A9 subtype marker GIRK2, and (iv) co-expressed the DA transporter (DAT). Collectively, studied iPSC-derived DAn were sufficiently mature, in a similar and comparable manner for both PD and control cultures, to be functional and to spontaneously form active neural networks.

Calcium fluorescence imaging of iPSC-derived DAn

We used the cell-permeant fluorescence dye Fluo-4-AM (Life Technologies) in combination with an imaging device to monitor spontaneous activity in PD and control cells. This fluorescence probe becomes active upon binding with calcium, therefore signaling the occurrence of action potentials in the neurons. Cultures of either PD or control cells were cultured in 30-mm-diameter petri dishes for 30-days and their activity monitored as follows. Prior to imaging, the culture dish was first washed with 4 ml PBS at room temperature to remove the original culture medium. The culture was next incubated for 30 min in a solution that contained 1 ml of recording medium (RM, consisting of 128 mM NaCl, 1 mM $CaCl_2$, 1 mM $MgCl_2$, 45 mM sucrose, 10 mM glucose, and 0.01 M Hepes; treated to pH 7.4) and 4 μg/ml of Fluo-4. The culture was then washed with fresh RM to remove residual free Fluo-4, and finally, a volume of 4 ml of RM was left in the dish for actual recordings. The culture dish was mounted on a Zeiss inverted microscope equipped with a CMOS camera (Hamamatsu Orca Flash 2.8) and an arc lamp for fluorescence. Gray-scale images of neuronal activity were acquired at intervals of 50 ms, and in a field of view that contained on the order of 100 cells. Cultures were visualized for 30 min at room temperature. The acquired data was next analyzed to extract the fluorescence traces for each neuron. In order to compare the fluorescence traces among neurons and cultures, the raw fluorescence signal $F(t)$ of a given neuron was normalized as $F^*(t) = \%\Delta F/F = 100 * (F(t) - F0)/F0$, where $F0$ is the fluorescence signal of the neuron at rest. Spontaneous neuronal activations were revealed in the fluorescence signal as a sharp increase of typically a 10% respect to the resting state.

Generation of iPSC-derived neural cultures not-enriched-in-DAn

iPSC-derived neural cultures not-enriched-in-DAn were generated as technical controls from a subset of PD patients ($n = 6$) and healthy subjects ($n = 3$) using the previously described protocol (Sanchez-Danes *et al*, 2012a) but omitting the lentiviral expression of the vmDAn determinant *LMX1A* and DAn patterning factors. The lentiviral delivery of LMX1A results in a > 4-fold enrichment of the total final number of DAn to ~30% as compared to only ~7% without LMX1A (Sanchez-Danes *et al*, 2012a). Embryoid body (EB) formation was induced for forced aggregation and maintained in suspension in the presence of MEF condition medium for 3 days. EBs were then maintained for 10 days in ultralow attachment plates in N2B27 medium in the presence of FGF2. After that, EBs were transferred to matrigel-coated plastic chamber slides and cultured in the differentiation medium in the absence of FGF2 for 30-days. The medium for each condition was changed every other day.

DNA, RNA, and protein isolation

DNA, RNA, and proteins were isolated from one million cells using the Allprep DNA-RNA-Protein kit (QIAGEN). Concentration and quality of DNA and RNA were, respectively, determined in a Nanodrop 1000 Spectrophotometer and in an Agilent 2100 Bioanalyzer. Total protein concentration was assessed with the BCA assay (Thermo Scientific).

DNA methylation analysis

The EZ DNA Methylation Kit (Zymo Research) was used for bisulfite conversion of 1,000 ng genomic DNA. Bisulfite-converted DNA was hybridized onto the Infinium Human Methylation 450K BeadChip Kit (Illumina) which covers 99% of the RefSeq genes and 96% of CpG islands at a single-base resolution (refer to Product Datasheet: http://www.illumina.com/products/methylation_450_beadchip_kits.ilmn). We have previously demonstrated a correlation coefficient of findings above 95% between the Illumina 450k platform and whole-genome bisulfite sequencing (Kulis *et al*, 2012). The Infinium methylation assay was carried out following criteria requested for this platform (Bibikova *et al*, 2011). All the array experiments were performed simultaneously at the same day, and PD and control samples were randomized at each BeadChip, ruling out any potential batch effect. Array data were analyzed by minfi package available through Bioconductor (Kasper Daniel Hansen and Martin Aryee. Minfi: Analyze Illumina's 450k methylation arrays. R package version 3.0.1). To exclude technical biases, we used an optimized pipeline with several filters developed at the Unidad de Hematopatología at IDIBAPS (Kulis *et al*, 2012). From the initial dataset of 485,512 sites (excluding probes detecting SNPs), we removed those with poor detection P-values ($P > 0.01$, $n = 670$) and those with sex-specific DNA methylation ($n = 6{,}614$). The remaining 478,228 sites were used for downstream analyses. Single CpG quantitative methylation values (beta values) in each sample were calculated as the ratio of the methylated signal intensity to the sum of methylated and unmethylated signals. Resulting quantitative methylation values ranged from 0, fully unmethylated, to 1, fully methylated CpGs. DNA from pure mouse PA6 cell cultures was included as a control sample that did not hybridize at readable levels in the human Illumina 450k methylation array, therefore not influencing methylation findings.

Genomic annotation of CpGs

The 450k Human Methylation Array data was annotated using the current hg19 version of the UCSC Genome Browser as reference sequence. We assigned the CpGs into discrete categories according to their location with respect to gene-related regions: 10-kb 5′ region (10,000 to 1,501 bp upstream of the transcriptional start site (TSS)), 1.5-kb 5′ region (1,500 to 201 bp upstream of the TSS), TSS 200 (200 to 1 bp upstream of the TSS), 5′ UTR, gene first exon, gene

body (from the first intron to the last exon), 3′ UTR, 1.5-kb 3′ region (1 to 1,500 bp downstream of the 3′UTR), 10-kb 3′ region (1,501 to 10,000 bp downstream of the 3′UTR), and intergenic regions. Owing to the presence of alternative transcription start sites and regions containing more than one gene, some CpGs were assigned multiple gene annotations. For the DMCpGs location relative to a CpG island (CGI), we used the categories: within CGI, in CGI shore (up to 2 kb from the CGI edge), in CGI shelf (from 2 to 4 kb from the CGI edge), and outside CGI.

Statistics: identification of differentially methylated CpGs

For each CpG, we computed the difference between the DNA methylation level in the two groups under comparison. Subsequently, CpGs were considered differentially methylated (DMCpGs) when showing a delta-beta methylation difference above |0.25| and a false discovery rate (FDR)-adjusted *P* Wilcoxon rank test for independent samples below 0.05. A delta-beta above |0.20| is detectable with a 99% confidence in our methylation platform (Bibikova *et al*, 2011). Consistently, the same cutoff of delta-beta above |0.25| and FDR-adjusted $P < 0.05$ was used in our study to identify statistically significant methylation differences (DMCpGs) between cases and controls in iPSC-derived DAn, fibroblasts, undifferentiated iPSC, and iPSC-derived neural cultures not-enriched-in-DAn for any given comparison.

Statistics: Gene expression analysis and identification of differentially expressed genes

We hybridized 100 ng of RNA onto the Genechip Human Exon 1.0 ST Array (Affymetrix) which covers > 96% of the human transcriptome. Using a robust multi-array analysis (RMA) algorithm (Irizarry *et al*, 2003), pre-processing of microarray data resulted in single gene $\log_2$-transformed values from 36,079 transcripts (22,014 Entrez RefSeq. genes). We filtered out (i) genes with group mean signals < 50 percentile of all signals, and (ii) genes with standard deviation (SD) < 50 percentile of all SDs. The remaining 4,686 Entrez RefSeq genes were used for downstream analysis. RNA from pure mouse PA6 cell cultures was included as a control sample that did not hybridize at readable levels in the Affymetrix human array, therefore not influencing expression findings. We used the Bioconductor Limma package to detect differentially expressed genes (DEGs) under a linear model with empirical bayes moderation of the variance similar to ANOVA developed to adjust for small sample size in microarray studies (Smyth, 2004). A FDR-adjusted $P < 0.05$ was used to identify DEGs.

Real-time quantitative RT–PCR

We analyzed by real-time qPCR the expression levels of ten DEGs identified by the genomewide gene expression microarray: *OTX2, PAX6, ZIC1, DCT, NEFL, DCC, SYT11, SNCA, CAV1,* and *TFPI2* (Fig 3). cDNA was synthesized using the High Capacity cDNA Reverse Transcription kit (Applied Biosystems). We used 1 ng of cDNA for each real-time qPCR. Gene amplification was done using pre-designed Taqman Gene Expression assays in a StepOnePlus Real-time PCR System (Applied Biosystems). The $\log_2$ fold change (FC) values and statistical significances of DEGs were calculated using the ΔΔCt method in the DataAssist v3.0 software (Applied Biosystems). We normalized the expression of DEGs to the housekeeping genes glyceraldehydes-3-phosphate dehydrogenase (*GAPDH*), beta-actin (*ACTB*), and cyclophylin A (*PPIA*). Pearson correlation between microarray and real-time qPCR data was computed using the SPSS 16.0 software. Commercially available assay numbers are as it follows: *OTX2* (hs00222238_m1), *PAX6* (hs00240871_m1), *ZIC1* (hs00602749_m1), *DCT* (hs01098278_m1), *NEFL* (hs00196245_m1), *DCC* (hs00180437_m1), *SYT11* (hs00383056_m1), *SNCA* (hs01103383_m1), *CAV1* (hs00971716_m1), *TFPI2* (hs00197918_m1), *GAPDH* (hs02758991_g1), *ACTB* (hs01060665_g1), and *PPIA* (hs04194521_s1).

Biological enrichment analysis

To determine whether genes associated with DMCpGs (1,178 genes/2,087 CpGs) or DEGs ($n = 437$) in PD were enriched in particular gene ontology (GO) terms, we used the Functional Annotation Tool (FAT) of the Database for Annotation, Visualization and Integrated Discovery (DAVID) (Huang da *et al*, 2009). Multiple hypothesis test correction was performed using the Benjamini & Hochberg algorithm (Benjamini, 1995).

Correlation of DNA methylation and expression data

Based on common gene annotations, DNA methylation data from 2,087 PD-associated DMCpGs and gene expression data from all 36,079 transcripts were overlapped. We detected 2,430 annotating pairs. Subsequently, Spearman correlation analysis was done under a FDR-adjusted $P < 0.05$.

Transcriptional and epigenomic characterization of differentially methylated sites

We analyzed our data in the context of functional chromatin states using the NHEK keratinocyte as background cell line (Ernst *et al*, 2011) which is similar to the cells used to generate iPSCs in our study. We considered regions with states 1 and 2 (designated as "active promoter" and "weak promoter") as "promoter regions"; state 3 as "poised promoters"; states 4, 5, 6, and 7 (designated as "strong enhancer" and "weak/poised enhancer") as "enhancer regions"; state 8 as "insulator"; states 9 and 10 (designated as "transcriptional transition" and "transcriptional elongation") as "strong transcription regions"; state 11 as "weak transcription"; state 12 as "Polycomb repressed"; and states 13, 14, and 15 (designated as "heterochromatin (nuclear lamina)" and "repetitive heterochromatin") as "heterochromatin regions".

Transcription factor analysis

We overlapped the methylation data from 2,087 PD DMCpGs with transcription factor (TF)-binding site (TFBS) clusters generated by ChIP-seq in the ENCODE project (Dunham *et al*, 2012; Gerstein *et al*, 2012; Lee *et al*, 2012) and available at the UCSC Genome Browser (http://genome.ucsc.edu/cgi-bin/hgTrackUi?db=hg19&g=wgEncodeHaibTfbs). For each TF, we calculated the $\log_2$ ratio of the proportion of TFBSs in the lists of hyper- and hypomethylated DMCpGs as compared to that in the whole methylation array (Table EV7). A Fisher exact test with a FDR-adjusted $P < 0.05$

resulted in 25 significant TFs. Of these, 23 TFs showed enrichment of binding sites at PD-hypermethylated DMCpGs. Spearman correlation analysis was done under a FDR $P < 0.05$ to study the association between average methylation levels at hypermethylated DMCpGs from enhancer sites, annotated in the NHEK background, and the gene expression of related TFs.

Immunoblotting

We used the following primary antibodies: rabbit anti-FOXA1 (Abcam, 1:500, #ab23738), rabbit anti-NR3C1 (Santa Cruz, 1:2,000, #sc1002), goat anti-HNF4A (Santa Cruz, 1:1,000, #sc6556), rabbit anti-FOSL2 (Santa Cruz, 1:500, #sc604), rabbit anti-OTX2 (Millipore, 1:1,000, #ab9566), rabbit anti-PAX6 (Covance, 1:500, #prb278p), rabbit anti-ZIC1 (Abcam, 1:1,000, #ab72694), mouse anti-SYT11 (Santa Cruz, 1:500, #sc365991), rabbit anti-DCT (Santa Cruz, 1:250, #sc25544), mouse anti-DCC (BD Pharmigen, 1:2,000, #554223), mouse anti-SNCA (BD Transduction Laboratories, 1:500, #610787), mouse anti-NEFL (Sigma, 1:500, #5139), mouse anti-β-actin (Sigma, 1:5,000, #A5441), and mouse anti-α-tubulin (Sigma, 1:10,000, #T5168). Nitrocellulose membranes were incubated overnight at 4°C with primary antibodies diluted in 2% BSA/PBS. Appropriate secondary antibody (anti-mouse and anti-rabbit from Amersham Biosciences, or anti-goat from Santa Cruz), coupled to horseradish peroxidase and diluted in 1% milk powder/PBS (1:5,000 dilution), were incubated 1 h at room temperature, followed by repeated washing with PBS. Immunoreactive bands were visualized using the Super-Signal Femto Chemiluminescent Substrate (Pierce) in the ImageQuant RT ECL imaging system (GE Healthcare). Protein band intensity was quantified by densitometry using the ImageJ Software. A total of 10 PD samples and four controls were studied for OTX2, PAX6, ZIC1, SYT11, DCT, DCC, SNCA, and NEFL. In the case of FOXA1, NR3C1, HNF4A, and FOSL2, six PD cases and three controls were analyzed as to illustrate extremes of a gene expression continuum that gradually increases from PD to controls. In both cases, a two-tailed Student's *t*-test was used to compare the PD and control groups. All samples were assayed in at least three independent experiments. Data in Figs 7A and B, and EV3A and B are represented as group mean ± SEM.

Immunofluorescence

iPSC-derived DAn were grown on plastic cover slide chambers, fixed with 4% paraformaldehyde, and then permeabilized with 0.5% Triton X-100 in TBS. Cells were then blocked in 0.5% Triton X-100 with 3% donkey serum for 2 h before 4°C overnight incubation with the appropriate primary antibodies. We used the following antibodies: mouse anti-TH (Chemicon, 1:1,000, #mab5280), rabbit anti-TH (Sigma, 1:1,000, #t8700), mouse anti-TUJ1 (Covance, 1:500, #mms435p), rabbit anti-GIRK2 (Sigma, 1:40, #P8122), goat anti-FOXA2 (R&D Systems, 1:100, #AF2400), rabbit anti-NURR1 (Santa Cruz, 1:200, #sc-991), mouse anti-SYP (Millipore, 1:500, #MAB332), rabbit anti-OTX2 (Millipore, 1:1,000, #ab9566), rabbit anti-PAX6 (Covance, 1:100, #prb278p), and mouse anti-DCC (BD Pharmigen, 1:250, #554223). Secondary antibodies used were all from the Alexa Fluor Series (Invitrogen, all 1:500). Images were taken using a Leica SP5 confocal microscope. For quantification of stained cells, randomly 300 cells per differentiated aggregate were counted (average 5–6 differentiated aggregates per experiment). Data points represent the average of at least three independent experiments. To visualize nuclei, slides were stained with 0.5 μg/ml DAPI (4′,6-diamidino-2-phenylindole) and then mounted with PVA/DABCO.

The paper explained

Problem
As a complex multifactorial neurodegenerative disorder, pathogenic mechanisms of Parkinson's disease (PD) remain poorly understood. This is in part due to the inaccessibility to the dopaminergic neurons (DAn) targeted by disease which are only available postmortem.

Results
Upon cell reprogramming of somatic skin cells (fibroblasts) into induced pluripotent stem cells (iPSC), we generated DAn from patients with sporadic PD (sPD) (90-95% of cases) and patients with a less frequent familial form caused by mutations in the gene *LRRK2* (L2PD). Using genomewide approaches, we found large epigenomic (DNA methylation) and gene expression changes in DAn from PD patients as compared to healthy subjects. Interestingly, these changes were largely similar in sPD and familial L2PD. In addition, the PD epigenetic changes were specific for DAn since fibroblasts, iPSCs, or other neural types (not-DAn) derived from the same PD patients did not show epigenetic abnormalities. Moreover, the PD epigenetic changes affected prominently to regulatory regions (hypermethylation of enhancers) and were related to the gene or protein downregulation of a network of transcription factors which is relevant to PD.

Impact
Using a patient-specific iPSC-derived DAn model, our findings indicate that: (i) epigenetic deregulation occurs in PD, (ii) PD-associated changes are similar in the sporadic and the L2PD familial form suggesting common etiologic processes and potential applicability of common therapeutic treatments, and (iii) future iPSC-based cell therapy strategies should pay attention to the correct epigenomic status of the reprogrammed DAn if using patient own cells.

Study approval

This study has been conducted conforming the principles of the Declaration of Helsinki and the Belmont Report. The Commission on Guarantees for Donation and Use of Human Tissues and Cells of the Instituto de Salud Carlos III (ISCIII) and the local ethics committee at the Hospital Clínic de Barcelona approved the study. All subjects gave written informed consent prior to their participation in the study.

Accession number

Genomewide DNA methylation and gene expression datasets generated in this study have been deposited in the Gene Expression Omnibus (GEO) under accession GSE16453. Summaries of analyses on these crude data may be found at Tables EV1, EV3, EV4, and EV6.

Expanded View for this article is available online.

Acknowledgements
We are indebted to the patients with PD who have participated in this study and to their relatives. We are grateful to Prof. Carlos López-Otín and to Dr. Ariadna Laguna Tuset for critical reading of this manuscript. We thank Manel

Fernández and Cristina Muñoz for excellent technical assistance. We also acknowledge Carla Sureda and Ana Molgosa for helpful assistance with the neuronal differentiation of iPSCs. We are grateful to the Spanish National Genotyping Centre (CeGen, http://www.cegen.org) and to the Advanced Fluorescence Microscopy Unit of the Institut de Biologia Molecular de Barcelona (IBMB). Part of this work was developed at the Centre de Recerca Biomèdica Cellex and the Centre Esther Koplowitz, Barcelona, Spain. The study was funded by the Instituto de Salud Carlos III (ISCIII) through the Cooperative Projects program of the Centro de Investigación Biomédica en Red de Enfermedades Neurodegenerativas (CIBERNED) (to E.T., M.V., A.R., J.A. y J.L.-B.). Additional support was provided by the Spanish Ministry of Economy and Competitiveness (MINECO) grant FIS2010-21924-C02-02 and the Generalitat de Catalunya grant 2009SGR14 (to J.S.), the Fundación Botín (to J.L.-B.), the SAF program of the Spanish Ministry of Innovation and Science (to J.L.-B., J.M.C. and J.A), the Spanish Cell Therapy Network (Red de Terapia Celular) of the ISICIII (to J.M.C.), the SAF2012-33526 grant and the Cell Therapy Network (TerCel nodes RD12/0019/0019,/0003, and/0033) of the ISCIII (to A.R.), the PIE14/00061 grant of the ISICIII/FEDER (to A.R., R.F.-S. and M.E.), the FIS project PI10/849 of the ISCIII (to M.V.), the BFU2013-49157-P grant, as well as the ERC-2012-StG grant of the European Research Council (ERC) (to A.C.), and the Mendelian Forms of Parkinson's Disease grant (MEFOPA) of the EC (to E.T.). R.F.-S. was supported by a Marie Skłodowska-Curie contract of the EC and IDIBAPS, and by a Juan de la Cierva contract of the Spanish Ministry of Economy and Competitiveness (MINECO), I.C.-C. by a CIBERNED contract, J.I.M.-S. by a Ramón y Cajal contract of the MINECO, and M.E. by a Miguel Servet contract of the ISCIII.

Author contributions

RF-S and ME conceived the study. IC-C and GC contributed equally to this work. RF-S, AC, JIM-S, ME, and ET jointly supervised research. RF-S, IC-C, AR, MV, AC, JIM-S, and ME conceived and designed the experiments. RF-S, IC-C, RT, YR, AS-D, RV-B, JS, and ME performed the experiments. RF-S, IC-C, GC, AS-P, JLM, JIM-S, and ME performed statistical analyses. RF-S, IC-C, GC, JS, JL-B, JMC, JA, AR, MV, AC, JIM-S, ME, and ET analyzed the data. GC, AR, MV, AC, JIM-S, and ET contributed reagents, materials, or analysis tools. RF-S, IC-C, GC, AS-D, JL-B, JMC, JA, AR, MV, AC, JIM-S, ME, and ET wrote the paper.

Conflict of interest

The authors declare that they have no conflict of interest.

References

Agirre X, Castellano G, Pascual M, Heath S, Kulis M, Segura V, Bergmann A, Esteve A, Merkel A, Raineri E *et al* (2015) Whole-epigenome analysis in multiple myeloma reveals DNA hypermethylation of B cell-specific enhancers. *Genome Res* 25: 478 – 487

Ambrosi G, Ghezzi C, Sepe S, Milanese C, Payan-Gomez C, Bombardieri CR, Armentero MT, Zangaglia R, Pacchetti C, Mastroberardino PG *et al* (2014) Bioenergetic and proteolytic defects in fibroblasts from patients with sporadic Parkinson's disease. *Biochim Biophys Acta* 1842: 1385 – 1394

Beach TG, Adler CH, Sue LI, Vedders L, Lue L, White Iii CL, Akiyama H, Caviness JN, Shill HA, Sabbagh MN *et al* (2010) Multi-organ distribution of phosphorylated alpha-synuclein histopathology in subjects with Lewy body disorders. *Acta Neuropathol* 119: 689 – 702

Benjamini Y (1995) Controlling the false discovery rate: a practical and powerful approach to multiple testing. *J R Stat Series B* 57: 289 – 300

Bergman Y, Cedar H (2013) DNA methylation dynamics in health and disease. *Nat Struct Mol Biol* 20: 274 – 281

Bibikova M, Barnes B, Tsan C, Ho V, Klotzle B, Le JM, Delano D, Zhang L, Schroth GP, Gunderson KL *et al* (2011) High density DNA methylation array with single CpG site resolution. *Genomics* 98: 288 – 295

de Boni L, Tierling S, Roeber S, Walter J, Giese A, Kretzschmar HA (2011) Next-generation sequencing reveals regional differences of the alpha-synuclein methylation state independent of Lewy body disease. *Neuromolecular Med* 13: 310 – 320

Byers B, Cord B, Nguyen HN, Schule B, Fenno L, Lee PC, Deisseroth K, Langston JW, Pera RR, Palmer TD (2011) SNCA triplication Parkinson's patient's iPSC-derived DA neurons accumulate alpha-synuclein and are susceptible to oxidative stress. *PLoS ONE* 6: e26159

Cao X, Yasuda T, Uthayathas S, Watts RL, Mouradian MM, Mochizuki H, Papa SM (2010) Striatal overexpression of DeltaFosB reproduces chronic levodopa-induced involuntary movements. *J Neurosci* 30: 7335 – 7343

Cooper O, Seo H, Andrabi S, Guardia-Laguarta C, Graziotto J, Sundberg M, McLean JR, Carrillo-Reid L, Xie Z, Osborn T *et al* (2012) Pharmacological rescue of mitochondrial deficits in iPSC-derived neural cells from patients with familial Parkinson's disease. *Sci Transl Med* 4: 141ra190

Desplats P, Spencer B, Coffee E, Patel P, Michael S, Patrick C, Adame A, Rockenstein E, Masliah E (2011) Alpha-synuclein sequesters Dnmt1 from the nucleus: a novel mechanism for epigenetic alterations in Lewy body diseases. *J Biol Chem* 286: 9031 – 9037

Di Fonzo A, Rohe CF, Ferreira J, Chien HF, Vacca L, Stocchi F, Guedes L, Fabrizio E, Manfredi M, Vanacore N *et al* (2005) A frequent LRRK2 gene mutation associated with autosomal dominant Parkinson's disease. *Lancet* 365: 412 – 415

Doi A, Park IH, Wen B, Murakami P, Aryee MJ, Irizarry R, Herb B, Ladd-Acosta C, Rho J, Loewer S *et al* (2009) Differential methylation of tissue- and cancer-specific CpG island shores distinguishes human induced pluripotent stem cells, embryonic stem cells and fibroblasts. *Nat Genet* 41: 1350 – 1353

Domanskyi A, Alter H, Vogt MA, Gass P, Vinnikov IA (2014) Transcription factors Foxa1 and Foxa2 are required for adult dopamine neurons maintenance. *Front Cell Neurosci* 8: 275

Dunham I, Kundaje A, Aldred SF, Collins PJ, Davis CA, Doyle F, Epstein CB, Frietze S, Harrow J, Kaul R *et al* (2012) An integrated encyclopedia of DNA elements in the human genome. *Nature* 489: 57 – 74

Ernst J, Kheradpour P, Mikkelsen TS, Shoresh N, Ward LD, Epstein CB, Zhang X, Wang L, Issner R, Coyne M *et al* (2011) Mapping and analysis of chromatin state dynamics in nine human cell types. *Nature* 473: 43 – 49

Escott-Price V, Nalls MA, Morris HR, Lubbe S, Brice A, Gasser T, Heutink P, Wood NW, Hardy J, Singleton AB *et al* (2015) Polygenic risk of Parkinson disease is correlated with disease age at onset. *Ann Neurol* 77: 582 – 591

Farrer MJ (2006) Genetics of Parkinson disease: paradigm shifts and future prospects. *Nat Rev Genet* 7: 306 – 318

Feil R, Fraga MF (2011) Epigenetics and the environment: emerging patterns and implications. *Nat Rev Genet* 13: 97 – 109

Gerstein MB, Kundaje A, Hariharan M, Landt SG, Yan KK, Cheng C, Mu XJ, Khurana E, Rozowsky J, Alexander R *et al* (2012) Architecture of the human regulatory network derived from ENCODE data. *Nature* 489: 91 – 100

Gilks WP, Abou-Sleiman PM, Gandhi S, Jain S, Singleton A, Lees AJ, Shaw K, Bhatia KP, Bonifati V, Quinn NP *et al* (2005) A common LRRK2 mutation in idiopathic Parkinson's disease. *Lancet* 365: 415 – 416

Goedert M, Jakes R, Crowther RA, Six J, Lubke U, Vandermeeren M, Cras P, Trojanowski JQ, Lee VM (1993) The abnormal phosphorylation of tau

protein at Ser-202 in Alzheimer disease recapitulates phosphorylation during development. *Proc Natl Acad Sci USA* 90: 5066 – 5070

Healy DG, Falchi M, O'Sullivan SS, Bonifati V, Durr A, Bressman S, Brice A, Aasly J, Zabetian CP, Goldwurm S *et al* (2008) Phenotype, genotype, and worldwide genetic penetrance of LRRK2-associated Parkinson's disease: a case-control study. *Lancet Neurol* 7: 583 – 590

van Heesbeen HJ, Mesman S, Veenvliet JV, Smidt MP (2013) Epigenetic mechanisms in the development and maintenance of dopaminergic neurons. *Development* 140: 1159 – 1169

Hochedlinger K, Plath K (2009) Epigenetic reprogramming and induced pluripotency. *Development* 136: 509 – 523

Hoepken HH, Gispert S, Azizov M, Klinkenberg M, Ricciardi F, Kurz A, Morales-Gordo B, Bonin M, Riess O, Gasser T *et al* (2008) Parkinson patient fibroblasts show increased alpha-synuclein expression. *Exp Neurol* 212: 307 – 313

Holmberg J, Perlmann T (2012) Maintaining differentiated cellular identity. *Nat Rev Genet* 13: 429 – 439

Hon GC, Rajagopal N, Shen Y, McCleary DF, Yue F, Dang MD, Ren B (2013) Epigenetic memory at embryonic enhancers identified in DNA methylation maps from adult mouse tissues. *Nat Genet* 45: 1198 – 1206

Huang da, Sherman BT, Lempicki RA (2009) Systematic and integrative analysis of large gene lists using DAVID bioinformatics resources. *Nat Protoc* 4: 44 – 57

IPDGC (2011) A two-stage meta-analysis identifies several new loci for Parkinson's disease. *PLoS Genet* 7: e1002142

Irizarry RA, Hobbs B, Collin F, Beazer-Barclay YD, Antonellis KJ, Scherf U, Speed TP (2003) Exploration, normalization, and summaries of high density oligonucleotide array probe level data. *Biostatistics* 4: 249 – 264

Jiang H, Ren Y, Yuen EY, Zhong P, Ghaedi M, Hu Z, Azabdaftari G, Nakaso K, Yan Z, Feng J (2012) Parkin controls dopamine utilization in human midbrain dopaminergic neurons derived from induced pluripotent stem cells. *Nat Commun* 3: 668

Jin H, Kanthasamy A, Harischandra DS, Kondru N, Ghosh A, Panicker N, Anantharam V, Rana A, Kanthasamy AG (2014) Histone hyperacetylation upregulates pkcdelta in dopaminergic neurons to induce cell death: relevance to epigenetic mechanisms of neurodegeneration in Parkinson's disease. *J Biol Chem* 289: 34743 – 34767

Jones PA (2012) Functions of DNA methylation: islands, start sites, gene bodies and beyond. *Nat Rev Genet* 13: 484 – 492

Kontopoulos E, Parvin JD, Feany MB (2006) Alpha-synuclein acts in the nucleus to inhibit histone acetylation and promote neurotoxicity. *Hum Mol Genet* 15: 3012 – 3023

Kulis M, Heath S, Bibikova M, Queiros AC, Navarro A, Clot G, Martinez-Trillos A, Castellano G, Brun-Heath I, Pinyol M *et al* (2012) Epigenomic analysis detects widespread gene-body DNA hypomethylation in chronic lymphocytic leukemia. *Nat Genet* 44: 1236 – 1242

Kulis M, Queiros AC, Beekman R, Martin-Subero JI (2013) Intragenic DNA methylation in transcriptional regulation, normal differentiation and cancer. *Biochim Biophys Acta* 1829: 1161 – 1174

Laguna A, Schintu N, Nobre A, Alvarsson A, Volakakis N, Jacobsen JK, Gomez-Galan M, Sopova E, Joodmardi E, Yoshitake T *et al* (2015) Dopaminergic control of autophagic-lysosomal function implicates Lmx1b in Parkinson's disease. *Nat Neurosci* 18: 826 – 835

Lahti L, Saarimaki-Vire J, Rita H, Partanen J (2011) FGF signaling gradient maintains symmetrical proliferative divisions of midbrain neuronal progenitors. *Dev Biol* 349: 270 – 282

Lahti L, Peltopuro P, Piepponen TP, Partanen J (2012) Cell-autonomous FGF signaling regulates anteroposterior patterning and neuronal differentiation in the mesodiencephalic dopaminergic progenitor domain. *Development* 139: 894 – 905

Lang AE, Lozano AM (1998a) Parkinson's disease. First of two parts. *N Engl J Med* 339: 1044 – 1053

Lang AE, Lozano AM (1998b) Parkinson's disease. Second of two parts. *N Engl J Med* 339: 1130 – 1143

Lee ST, Xiao Y, Muench MO, Xiao J, Fomin ME, Wiencke JK, Zheng S, Dou X, de Smith A, Chokkalingam A *et al* (2012) A global DNA methylation and gene expression analysis of early human B-cell development reveals a demethylation signature and transcription factor network. *Nucleic Acids Res* 40: 11339 – 11351

Lesage S, Durr A, Tazir M, Lohmann E, Leutenegger AL, Janin S, Pollak P, Brice A (2006) LRRK2 G2019S as a cause of Parkinson's disease in North African Arabs. *N Engl J Med* 354: 422 – 423

Lindvall O, Bjorklund A (2011) Cell therapeutics in Parkinson's disease. *Neurotherapeutics* 8: 539 – 548

Masliah E, Dumaop W, Galasko D, Desplats P (2013) Distinctive patterns of DNA methylation associated with Parkinson disease: identification of concordant epigenetic changes in brain and peripheral blood leukocytes. *Epigenetics* 8: 1030 – 1038

Morizane A, Doi D, Kikuchi T, Okita K, Hotta A, Kawasaki T, Hayashi T, Onoe H, Shiina T, Yamanaka S *et al* (2013) Direct comparison of autologous and allogenic transplantation of iPSC derived neural cells in the brain of a nonhuman primate. *Stem Cell Rep* 1: 283 – 292

Nalls MA, Pankratz N, Lill CM, Do CB, Hernandez DG, Saad M, DeStefano AL, Kara E, Bras J, Sharma M *et al* (2014) Large-scale meta-analysis of genome-wide association data identifies six new risk loci for Parkinson's disease. *Nat Genet* 46: 989 – 993

Nguyen HN, Byers B, Cord B, Shcheglovitov A, Byrne J, Gujar P, Kee K, Schule B, Dolmetsch RE, Langston W *et al* (2011) LRRK2 mutant iPSC-derived DA neurons demonstrate increased susceptibility to oxidative stress. *Cell Stem Cell* 8: 267 – 280

Nikolaev A, McLaughlin T, O'Leary DD, Tessier-Lavigne M (2009) APP binds DR6 to trigger axon pruning and neuron death via distinct caspases. *Nature* 457: 981 – 989

Orenstein SJ, Kuo SH, Tasset I, Arias E, Koga H, Fernandez-Carasa I, Cortes E, Honig LS, Dauer W, Consiglio A *et al* (2013) Interplay of LRRK2 with chaperone-mediated autophagy. *Nat Neurosci* 16: 394 – 406

Ozelius LJ, Senthil G, Saunders-Pullman R, Ohmann E, Deligtisch A, Tagliati M, Hunt AL, Klein C, Henick B, Hailpern SM *et al* (2006) LRRK2 G2019S as a cause of Parkinson's disease in Ashkenazi Jews. *N Engl J Med* 354: 424 – 425

Paisan-Ruiz C, Jain S, Evans EW, Gilks WP, Simon J, van der Brug M, Lopez de Munain A, Aparicio S, Gil AM, Khan N *et al* (2004) Cloning of the gene containing mutations that cause PARK8-linked Parkinson's disease. *Neuron* 44: 595 – 600

Papkovskaia TD, Chau KY, Inesta-Vaquera F, Papkovsky DB, Healy DG, Nishio K, Staddon J, Duchen MR, Hardy J, Schapira AH *et al* (2012) G2019S leucine-rich repeat kinase 2 causes uncoupling protein-mediated mitochondrial depolarization. *Hum Mol Genet* 21: 4201 – 4213

Pieper HC, Evert BO, Kaut O, Riederer PF, Waha A, Wullner U (2008) Different methylation of the TNF-alpha promoter in cortex and substantia nigra: implications for selective neuronal vulnerability. *Neurobiol Dis* 32: 521 – 527

Potashkin JA, Santiago JA, Ravina BM, Watts A, Leontovich AA (2012) Biosignatures for Parkinson's disease and atypical parkinsonian disorders patients. *PLoS ONE* 7: e43595

Rakovic A, Shurkewitsch K, Seibler P, Grunewald A, Zanon A, Hagenah J, Krainc D, Klein C (2013) Phosphatase and tensin homolog (PTEN)-induced

putative kinase 1 (PINK1)-dependent ubiquitination of endogenous Parkin attenuates mitophagy: study in human primary fibroblasts and induced pluripotent stem cell-derived neurons. *J Biol Chem* 288: 2223 – 2237

Reinhardt P, Schmid B, Burbulla LF, Schondorf DC, Wagner L, Glatza M, Hoing S, Hargus G, Heck SA, Dhingra A *et al* (2013) Genetic correction of a LRRK2 mutation in human iPSCs links parkinsonian neurodegeneration to ERK-dependent changes in gene expression. *Cell Stem Cell* 12: 354 – 367

Ros-Bernal F, Hunot S, Herrero MT, Parnadeau S, Corvol JC, Lu L, Alvarez-Fischer D, Carrillo-de Sauvage MA, Saurini F, Coussieu C *et al* (2011) Microglial glucocorticoid receptors play a pivotal role in regulating dopaminergic neurodegeneration in parkinsonism. *Proc Natl Acad Sci USA* 108: 6632 – 6637

Ryan SD, Dolatabadi N, Chan SF, Zhang X, Akhtar MW, Parker J, Soldner F, Sunico CR, Nagar S, Talantova M *et al* (2013) Isogenic human iPSC Parkinson's model shows nitrosative stress-induced dysfunction in MEF2-PGC1alpha transcription. *Cell* 155: 1351 – 1364

Sanchez-Danes A, Consiglio A, Richaud Y, Rodriguez-Piza I, Dehay B, Edel M, Bove J, Memo M, Vila M, Raya A *et al* (2012a) Efficient generation of A9 midbrain dopaminergic neurons by lentiviral delivery of LMX1A in human embryonic stem cells and induced pluripotent stem cells. *Hum Gene Ther* 23: 56 – 69

Sanchez-Danes A, Richaud-Patin Y, Carballo-Carbajal I, Jimenez-Delgado S, Caig C, Mora S, Di Guglielmo C, Ezquerra M, Patel B, Giralt A *et al* (2012b) Disease-specific phenotypes in dopamine neurons from human iPS-based models of genetic and sporadic Parkinson's disease. *EMBO Mol Med* 4: 380 – 395

Santiago JA, Potashkin JA (2015) Network-based metaanalysis identifies HNF4A and PTBP1 as longitudinally dynamic biomarkers for Parkinson's disease. *Proc Natl Acad Sci USA* 112: 2257 – 2262

Schafer DP, Stevens B (2010) Synapse elimination during development and disease: immune molecules take centre stage. *Biochem Soc Trans* 38: 476 – 481

Schondorf DC, Aureli M, McAllister FE, Hindley CJ, Mayer F, Schmid B, Sardi SP, Valsecchi M, Hoffmann S, Schwarz LK *et al* (2014) iPSC-derived neurons from GBA1-associated Parkinson's disease patients show autophagic defects and impaired calcium homeostasis. *Nat Commun* 5: 4028

Seibler P, Graziotto J, Jeong H, Simunovic F, Klein C, Krainc D (2011) Mitochondrial Parkin recruitment is impaired in neurons derived from mutant PINK1 induced pluripotent stem cells. *J Neurosci* 31: 5970 – 5976

Shannon KM, Keshavarzian A, Mutlu E, Dodiya HB, Daian D, Jaglin JA, Kordower JH (2012) Alpha-synuclein in colonic submucosa in early untreated Parkinson's disease. *Mov Disord* 27: 709 – 715

Smyth GK (2004) Linear models and empirical bayes methods for assessing differential expression in microarray experiments. *Stat Appl Genet Mol Biol* 3: Article3

Stadler MB, Murr R, Burger L, Ivanek R, Lienert F, Scholer A, van Nimwegen E, Wirbelauer C, Oakeley EJ, Gaidatzis D *et al* (2011) DNA-binding factors shape the mouse methylome at distal regulatory regions. *Nature* 480: 490 – 495

Stott SR, Metzakopian E, Lin W, Kaestner KH, Hen R, Ang SL (2013) Foxa1 and foxa2 are required for the maintenance of dopaminergic properties in ventral midbrain neurons at late embryonic stages. *J Neurosci* 33: 8022 – 8034

Urdinguio RG, Sanchez-Mut JV, Esteller M (2009) Epigenetic mechanisms in neurological diseases: genes, syndromes, and therapies. *Lancet Neurol* 8: 1056 – 1072

Xie M, Hong C, Zhang B, Lowdon RF, Xing X, Li D, Zhou X, Lee HJ, Maire CL, Ligon KL *et al* (2013) DNA hypomethylation within specific transposable element families associates with tissue-specific enhancer landscape. *Nat Genet* 45: 836 – 841

Yakhine-Diop SM, Bravo-San Pedro JM, Gomez-Sanchez R, Pizarro-Estrella E, Rodriguez-Arribas M, Climent V, Aiastui A, Lopez de Munain A, Fuentes JM, Gonzalez-Polo RA (2014) G2019S LRRK2 mutant fibroblasts from Parkinson's disease patients show increased sensitivity to neurotoxin 1-methyl-4-phenylpyridinium dependent of autophagy. *Toxicology* 324: 1 – 9

Zhu H, Lensch MW, Cahan P, Daley GQ (2011) Investigating monogenic and complex diseases with pluripotent stem cells. *Nat Rev Genet* 12: 266 – 275

Ziller MJ, Gu H, Muller F, Donaghey J, Tsai LT, Kohlbacher O, De Jager PL, Rosen ED, Bennett DA, Bernstein BE *et al* (2013) Charting a dynamic DNA methylation landscape of the human genome. *Nature* 500: 477 – 481

Zimprich A, Biskup S, Leitner P, Lichtner P, Farrer M, Lincoln S, Kachergus J, Hulihan M, Uitti RJ, Calne DB *et al* (2004) Mutations in LRRK2 cause autosomal-dominant Parkinsonism with pleomorphic pathology. *Neuron* 44: 601 – 607

8.3. Activity and High-Order effective connectivity alteration in Sanfilippo C Patient-specific neuronal networks (Research Paper).

Canals, I., Soriano, J., Orlandi J.G., Torrent, R., Richaud-Patin, Y., Jiménez-Delgado S., Merlin, S., Follenzi, A., Consiglio, A., Vilageliu, L., Grinberg, D., Raya, A., *Activity and High-Order Effective Connectivity Alterations in Sanfilippo C Patient-Specific Neuronal Networks,* 2015, Stem Cell Reports, 5: 546-57.

Here, our group has collaborated with Daniel Grinberg and Luïsa Vilageliu, in the generation of iPSC lines from two patients with Sanfilippo type C syndrome (SFC), a lysosomal storage disorder with inheritable progressive neurodegeneration, as well as two healthy donors (WT). Mature neurons obtained from patient-specific iPSC lines recapitulated the main known phenotypes of the disease, not present in genetically corrected patient-specific iPSC-derived cultures. Moreover, neuronal networks organized in vitro from mature patient-derived neurons showed early defects in neuronal activity, network-wide degradation, and altered effective connectivity. Our findings establish the importance of iPSC-based technology to identify early functional phenotypes, which can in turn shed light on the pathological mechanisms occurring in Sanfilippo syndrome. This technology also has the potential to provide valuable readouts to screen compounds, which can prevent the onset of neurodegeneration.

Specifically, I have participated to:

1. The generation of teratomas in SCID mice, in order to test the *in vivo* capacity of these iPSC to spontaneously differentiate into cell derivatives of the three embryo germ layers (See Figure 1G).
2. Characterization of *in vitro* neural differentiation of Control (WT) and SFC-specific iPSC lines. Specifically, we performed immunofluorescence staining for MAP2 (a mature neuronal marker) and GFAP (Astrocyte marker), in order to assess the capacity of each line to differentiate into mature neurons. In addition we also characterize this neurons with SYNAPSIN, a marker for synapses, in order to assess that the differentiated neurons are functionally active (See Figure 2).
3. Characterization of *in vitro* neural differentiation of WT and SFC-specific iPSC at 9 weeks of culture: lysosome alterations in SFC-iPSC-derived neurons. We immunostained the neural cultures with MAP2 and LAMP2. Immunoanalysis of LAMP2 staining per neuronal area in MAP2 neurons, show significant differences between controls and patients (Figures 4D and 4E).

Stem Cell Reports
Article

OPEN ACCESS

Activity and High-Order Effective Connectivity Alterations in Sanfilippo C Patient-Specific Neuronal Networks

Isaac Canals,[1,2,3] Jordi Soriano,[4] Javier G. Orlandi,[4] Roger Torrent,[3] Yvonne Richaud-Patin,[5,6] Senda Jiménez-Delgado,[5,6] Simone Merlin,[7] Antonia Follenzi,[7] Antonella Consiglio,[3,8] Lluïsa Vilageliu,[1,2,3] Daniel Grinberg,[1,2,3,*] and Angel Raya[5,6,9,*]

[1]Departament de Genètica, Facultat de Biologia, Universitat de Barcelona, 08028 Barcelona, Spain
[2]Centro de Investigación Biomédica en Red de Enfermedades Raras, 28029 Madrid, Spain
[3]Institut de Biomedicina de la Universitat de Barcelona, 08028 Barcelona, Spain
[4]Departament d'Estructura i Constituents de la Matèria, Universitat de Barcelona, 08028 Barcelona, Spain
[5]Centre de Medicina Regenerativa de Barcelona and Control of Stem Cell Potency Group, Institut de Bioenginyeria de Catalunya, 08028 Barcelona, Spain
[6]Centro de Investigación Biomédica en Red en Bioingeniería, Biomaterials y Nanomedicina, 28029 Madrid, Spain
[7]Health Sciences Department, Universita' del Piemonte Orientale, 28100 Novara, Italy
[8]Department of Molecular and Translational Medicine, University of Brescia, 25123 Brescia, Italy
[9]Institució Catalana de Recerca i Estudis Avançats, 08010 Barcelona, Spain
*Correspondence: dgrinberg@ub.edu (D.G.), araya@cmrb.eu (A.R.)
http://dx.doi.org/10.1016/j.stemcr.2015.08.016

SUMMARY

Induced pluripotent stem cell (iPSC) technology has been successfully used to recapitulate phenotypic traits of several human diseases in vitro. Patient-specific iPSC-based disease models are also expected to reveal early functional phenotypes, although this remains to be proved. Here, we generated iPSC lines from two patients with Sanfilippo type C syndrome, a lysosomal storage disorder with inheritable progressive neurodegeneration. Mature neurons obtained from patient-specific iPSC lines recapitulated the main known phenotypes of the disease, not present in genetically corrected patient-specific iPSC-derived cultures. Moreover, neuronal networks organized in vitro from mature patient-derived neurons showed early defects in neuronal activity, network-wide degradation, and altered effective connectivity. Our findings establish the importance of iPSC-based technology to identify early functional phenotypes, which can in turn shed light on the pathological mechanisms occurring in Sanfilippo syndrome. This technology also has the potential to provide valuable readouts to screen compounds, which can prevent the onset of neurodegeneration.

INTRODUCTION

Sanfilippo syndrome, also known as mucopolysaccharidosis type III (MPS III), is a lysosomal storage disorder (LSD) with an autosomal recessive inheritance pattern. Four different subtypes have been described (type A, OMIM 252900; type B, OMIM 252920; type C, OMIM 252930; and type D, OMIM 252940), which share clinical characteristics, including severe early onset CNS degeneration that typically results in death within the second or third decade of life (Valstar et al., 2008). Each subtype is caused by mutations in a different gene encoding for enzymes involved in the degradation pathway of the glycosaminoglycan (GAG) heparan sulfate (Neufeld and Muenzer, 2001). The lack of activity of any of these enzymes leads to the accumulation of partially degraded heparan sulfate chains within the lysosomes. Subtype C (MPS IIIC) is caused by mutations in the *HGSNAT* gene, encoding acetyl-CoA α-glucosaminide N-acetyltransferase (EC 2.3.1.78), a lysosomal membrane enzyme. The prevalence of MPS IIIC ranges between 0.07 and 0.42 per 100,000 births, depending on the population (Poupetová et al., 2010). The *HGSNAT* gene was identified by two independent groups in 2006 (Fan et al., 2006; Hřebíček et al., 2006), and 64 different mutations have been identified since then (Human Gene Mutation Database Professional 2014.3). A mouse model has been very recently developed (Martins et al., 2015), but a cellular model for Sanfilippo type C has yet to be developed.

The ability to reprogram somatic cells back to a pluripotent state (Takahashi and Yamanaka, 2006; Takahashi et al., 2007) has created new opportunities for generating in vitro models of disease-relevant cells differentiated from patient-specific induced pluripotent stem cell (iPSC) lines (recently reviewed by Cherry and Daley, 2013; Inoue et al., 2014; Trounson et al., 2012). This approach has been shown to be particularly useful in the case of congenital or early-onset monogenic diseases. In particular, iPSC-based models of various LSD have been established, including Gaucher disease (Mazzulli et al., 2011; Panicker et al., 2012; Park et al., 2008; Schöndorf et al., 2014; Tiscornia et al., 2013), Hurler syndrome (Tolar et al., 2011), Pompe disease (Higuchi et al., 2014; Huang et al., 2011), Sanfilippo B syndrome (Lemonnier et al., 2011), and Niemann-Pick type C1 (Maetzel et al., 2014; Trilck et al., 2013). In all these cases, disease-relevant cell types derived from patient-specific iPSCs not only displayed morphologic, biochemical, and/or functional hallmarks of the disease but also have

the capacity of being used as a drug-screening platform to find therapies that are capable of reverting LSD-related phenotypes.

In this study, we set out to test whether patient-specific iPSC-derived cells could be used to investigate the existence of early functional alterations prior to the appearance of disease-related phenotypes identified in patients. For this purpose, we generated iPSCs from fibroblasts of Sanfilippo C syndrome patients (SFC-iPSCs) and differentiated them into neurons, which recapitulate the pathological phenotypes observed in vivo, such as low acetyl-CoA α-glucosaminide N-acetyltransferase activity, accumulation of GAGs, and an increase in lysosome size and number. Moreover, we found that neural networks organized in vitro from control iPSC-derived neurons grew in complexity over time, as quantified in terms of neuronal activity, network activity, and effective connectivity, a measure of neuronal network function as defined by information theory and analyzed through generalized transfer entropy (GTE) methods. In contrast, networks of SFC-iPSC-derived neurons showed early defects in neuronal activity and alterations in effective connectivity and network organization over time.

The identification of early functional phenotypes in SFC-iPSC-derived neurons attests to the validity of iPSC-based technology to model pre-symptomatic stages of human diseases, thus widening the spectrum of potential applications of somatic cell reprogramming for biomedical research.

RESULTS

Generation and Characterization of Patient-Specific iPSCs

Fibroblasts from two unrelated Spanish patients with Sanfilippo type C syndrome (SFC6 and SFC7) and two healthy individuals (WT1 and WT2) were collected. Patient SFC6 was a compound heterozygote carrying a splicing mutation (c.633+1G > A) and a missense mutation (c.1334T > C; p.L445P), both of which were found only in this patient (Canals et al., 2011). This patient was also carrying the Robertsonian translocation der(13;14)(q10;q10), which is the most common chromosome rearrangement in humans and is usually phenotypically silent (Engels et al., 2008). Patient SFC7 was a homozygote for the most prevalent mutation in Spanish patients, accounting for 50% of the mutated alleles (Canals et al., 2011), affecting another splicing site (c.372-2A > G), which results in residual enzyme activity (Matos et al., 2014) and a typically less severe clinical progression. The effects of these mutations on the splicing process and the transferase protein have been previously described (Canals et al., 2011).

Fibroblasts were reprogrammed at early passages (5–7) through the retroviral delivery of *SOX2*, *KLF4*, and *OCT4* (3F) or *SOX2*, *KLF4*, *OCT4*, and c-*MYC* (4F) to generate up to 15 independent iPSC lines for each individual. We selected clones displaying embryonic stem cell-like morphology and positive alkaline phosphatase staining. Four clones representing each individual were chosen to be thoroughly characterized and shown to be fully reprogrammed, as judged by the silencing of the reprogramming transgenes, activation of endogenous pluripotency-associated factors, expression of pluripotency-associated transcription factors and surface markers, demethylation of *OCT4* and *NANOG* promoters, pluripotent differentiation ability in vitro and/or in vivo, and karyotype stability after more than 15 passages (Figures 1A–1G and S1A–S1F; Table S1).

Patient-Specific Neurons Recapitulate Known Sanfilippo C Phenotypes

Wild-type (WT)- and SFC-iPSCs were then differentiated to pure masses of neural precursors using a previously described protocol (Cho et al., 2008) that involves the formation of embryoid bodies and the culture of neural precursor cells to form spherical neural masses (SNMs), which can be expanded and subsequently differentiated to mature neurons after culturing them for several weeks in neuronal induction medium (Figure 2A; see Supplemental Experimental Procedures for further details). SNMs derived from WT- and SFC-iPSC lines homogeneously expressed neural progenitor markers such as PAX6, NESTIN, and SOX2, as well as proliferation markers such as Ki67 (Figure S2). Furthermore, when iPSC-derived SNMs were cultured in neuronal induction media supplemented with N2 and B27, differentiation into mature and synaptically active neurons was evident within 3 to 5 weeks (Figures 2B and 2C). After about 3 weeks in neuronal medium, the cultures formed dense neuronal networks and stained for dendritic marker MAP2 and synaptic marker SYNAPSIN. Under these conditions, SNMs mainly generated MAP2-positive mature neurons (63% ± 3% of differentiated cells, mean ± SEM; n = 37), but also GFAP-positive cells (10% ± 1% of differentiated cells, mean ± SEM; n = 37), confirming their neurogenic capacity (Figure 2B). MAP2-positive neurons showed expression of SYNAPSIN, indicating their capability to form synapses (Figure 2C).

Mutation analysis confirmed that SFC-iPSCs bore the mutations present in the patients' fibroblasts, resulting in the expected splicing defects (data not shown). SFC-iPSCs showed no detectable acetyl-CoA α-glucosaminide N-acetyltransferase activity, consistent with the low enzyme activity levels found in patients' fibroblasts (1.78% and 3.02% of that of WT fibroblasts for SFC6 and SFC7, respectively; Figure 3A). Similarly, SNMs and neural cultures

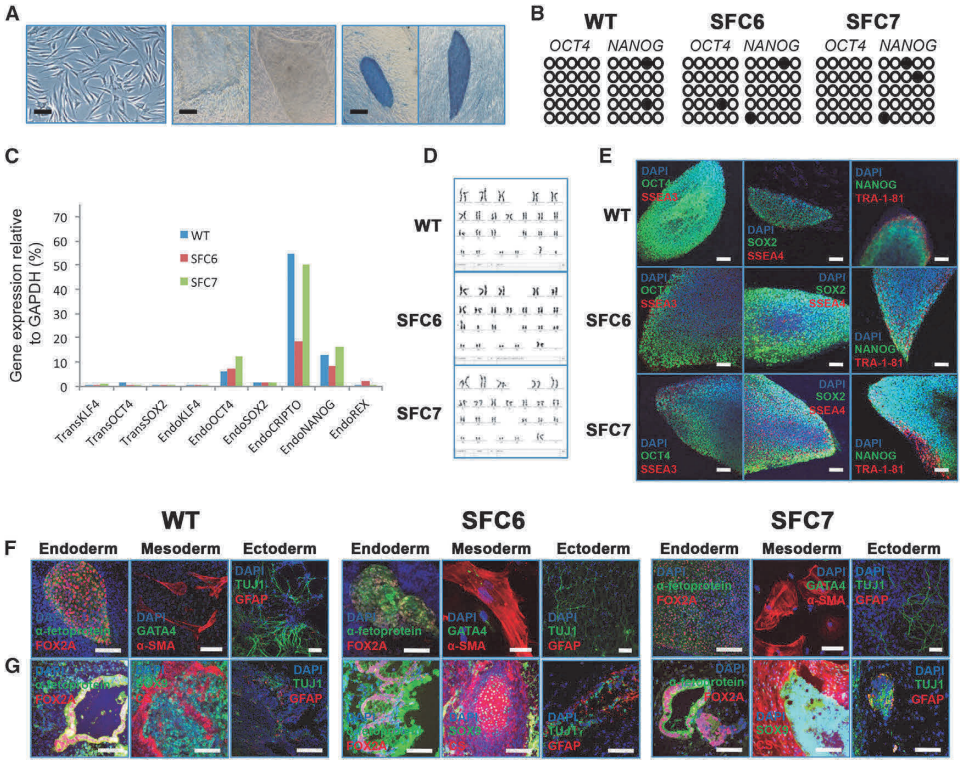

Figure 1. Generation and Characterization of Control and SFC-iPSC Lines Using 3 Reprogramming Factors

A total of 17 independent iPSC lines were obtained after reprogramming control (WT1 and WT2) and SFC (SFC6 and SFC7) fibroblasts with retroviruses expressing *OCT4*, *SOX2*, and *KLF4*. Two lines per fibroblast sample were selected for complete characterization: WT1-iPS#3.1, WT1-iPS#3.6, WT2-iPS#3.1, WT2-iPS#3.2, SFC6-iPS#3.1, SFC6-iPS#3.2, SFC7-iPS#3.1, and SFC7-iPS#3.2. Shown are representative images of the characterization of WT (WT1-iPS#3.6), SFC6 (SFC6-iPS#3.1), and SFC7 (SFC7-iPS#3.1) iPSC lines.

(A) Left: SFC fibroblasts before being transduced with retroviruses carrying reprogramming factors. The scale bar represents 50 μm. Center: Typical human embryonic stem cell (hESC)-like colonies obtained after SFC fibroblast reprogramming. The scale bar represents 400 μm. Right: Positive alkaline phosphatase staining of the hESC-like SFC-iPSC colonies. The scale bar represents 400 μm.

(B) Bisulfite genomic sequencing of the *OCT4* and *NANOG* promoters showing demethylation pattern in WT-, SFC6-, and SFC7-iPSCs.

(C) RT-qPCR analyses of the expression levels of the indicated retroviral-derived reprogramming factors (TRANS-) and endogenous (ENDO-) genes in WT-, SFC6- and SFC7-iPSC.

(D) Karyotype of WT-, SFC6-, and SFC7-iPSCs, which are identical to that of parent fibroblasts (including the known balanced Robertsonian translocation der[13;14][q10;q10] of SFC6).(E) Representative colonies of WT-, SFC6-, and SFC7-iPSCs stained positive for the pluripotency markers OCT4, SOX2, and NANOG (green) and SSEA3, SSEA4, and TRA-1-81 (red). The scale bar represents 100 μm.

(F) Immunofluorescence analyses with specific markers on WT-, SFC6-, and SFC7-iPSCs differentiated in vitro to generate cell derivatives of all three primary germ layers. Endoderm, α-fetoprotein (green), FOX2A (red); mesoderm, GATA4 (green), α-SMA (red); and ectoderm, TUJ1 fetoprotein (green), GFAP (red). The scale bar represents 100 μm.

(G) Immunofluorescence analyses with specific markers on sections from the same teratoma induced after injecting WT-, SFC6-, or SFC7-iPSCs, showing cell derivatives of the three embryo germ layers. Endoderm, α-fetoprotein (green), FOX2A (red); mesoderm, SOX9 (green), CS (red); and ectoderm, TUJ1 fetoprotein (green), GFAP (red). The scale bar represents 100 μm.

See also Figure S1 and Table S1.

derived from SFC-iPSCs showed low enzyme activity levels, representing less than 1% of those found in control cells (Figures 3C and 3D). Total GAG content in patients' fibroblasts approximately doubled that of control cells (Figure 3E). In contrast, SFC-iPSC-derived neural cultures accumulated GAG over time, reaching statistically significant

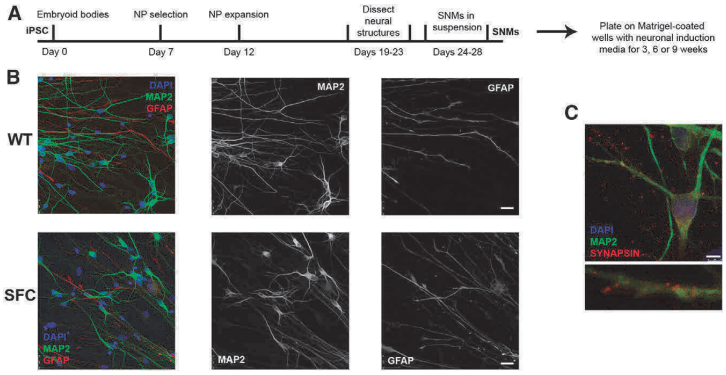

Figure 2. Neural Differentiation of Control and SFC-Specific iPSC Lines

(A) Scheme illustrating the differentiation protocol from iPSC to mature neurons through the establishment of SNMs enriched in neural progenitors (NPs).

(B) Left images show immunofluorescence analyses on representative neural differentiation cultures from SNMs derived from WT2-iPSC#3.1 (WT) and SFC7-iPSC#4.8 (SFC) iPSC lines, stained for typical markers of mature neurons (MAP2 in green) and astrocytes (GFAP in red). Central and right images display the green and red channels in white, for clarity. Similar results were obtained from neural differentiation cultures of SNMs derived from WT1-iPSC#3.1, WT1-iPSC#3.6, WT1-iPSC#4.10, WT1-iPSC#4.12, WT2-iPSC#3.2, WT2-iPSC#4.2, WT2-iPSC#4.5, SFC6-iPSC#3.1, SFC6-iPSC#3.2, SFC6-iPSC#4.6, SFC6-iPSC#4.7, SFC7-iPSC#3.1, SFC7-iPSC#3.2, and SFC7-iPSC#4.9 iPSC lines. The scale bar represents 50 μm.

(C) Representative image of the immunofluorescence analysis of a neuron differentiated from SNMs derived from the SFC7-iPSC#4.8 iPSC line, stained with MAP2 (green), a mature neuronal marker, and SYNAPSIN (red), a marker for synapses (upper image). Magnification of a neuron prolongation with specific staining for SYNAPSIN (lower image). Similar stainings were obtained from neural differentiation cultures of SNMs derived from WT1-iPSC#3.1, WT1-iPSC#3.6, WT1-iPSC#4.10, WT1-iPSC#4.12, WT2-iPSC#3.1, WT2-iPSC#3.2, WT2-iPSC#4.2, WT2-iPSC#4.5, SFC6-iPSC#3.1, SFC6-iPSC#3.2, SFC6-iPSC#4.6, SFC6-iPSC#4.7, SFC7-iPSC#3.1, SFC7-iPSC#3.2, and SFC7-iPSC#4.9 iPSC lines. The scale bar represents 5 μm.

See also Figure S2.

differences compared with controls only after 9 weeks of culture (Figure 3F).

Gene-corrected controls were generated by lentiviral (LV) complementation of SNMs with WT cDNA for the *HGSNAT* gene under a cytomegalovirus (CMV) promoter (LV.CMV.HGSNAT.ires.GFP; Figure S3A). The vector also expressed *GFP* downstream of an internal ribosome entry site element. Neural cells differentiated from gene-corrected SNMs showed high activity of the enzyme, between 50- and 150-fold higher than those differentiated from WT-SNMs transduced with a control LV.CMV.GFP vector (Figures S3B–S3E), demonstrating long-term sustained transgene expression. Gene complementation of SFC-derived neural cultures prevented the statistically significant accumulation of GAG observed in *GFP*-transduced SCF cells after 9 weeks of differentiation, when compared with control cells (Figure 3F).

Analysis by transmission electron microscopy (TEM) revealed marked differences in lysosomes between controls and patients, which increased along time. Whereas lysosomes for control cultures showed typical morphology and size, we found only large vacuoles with an empty-like appearance in patients' samples (Figure 4A), similar to those described in a mouse model of Sanfilippo B (Vitry et al., 2010). These vacuoles were derived from lysosomes, as judged by positive immuno-gold staining for LAMP1 (Figure 4B). The differences in lysosome size increased with culture time and reached 80% for both patients compared with controls at 9 weeks (Figure 4C). In addition, immunostaining for LAMP2 in isolated neurons of these cultures analyzed 9 weeks after differentiation showed significant differences between controls and patients (Figures 4D and 4E), consistent with the 80% detected by the TEM analysis, and illustrating that these differences can be detected specifically in iPSC-derived neurons. After transduction with the *HGSNAT* cDNA, some cells presented lysosomes with a morphology between the affected type and those of WT, suggesting a partial correction (Figure 4A).

Network-Broad Activity Alterations in Sanfilippo C Neuronal Cultures

Next, we allowed control- and SFC-iPSC-derived neurons to form networks and used a calcium fluorescence imaging assay to monitor functional neuronal activity after 3, 6, and 9 weeks. Typical recordings of spontaneous activity at week 9 for the different conditions are shown in Movies S1, S2, and S3. WT-iPSC-derived neurons showed repeated firing episodes of large amplitude ("bursts") that were not present in SFC6-iPSC neurons. SFC7-iPSC neurons showed a slightly richer activity than SFC6-iPSC neurons, but the amplitude of the bursts was still low compared with WT-iPSC neurons (Figure 5A). Gene complementation with *HGSNAT* significantly changed the activity of the patient-specific iPSC-derived neurons, and both SCF6- and SCF7-iPSC-derived neurons exhibited activity patterns similar to those of WT.

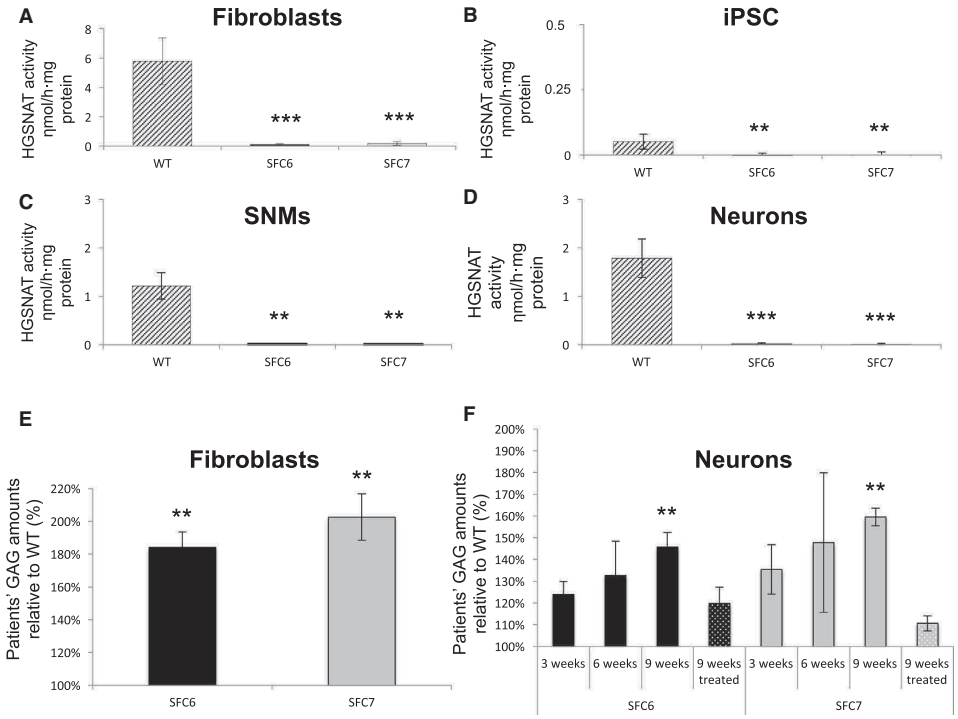

Figure 3. HGSNAT Activity and GAG Storage in Control and SCF-Specific Cell Types

(A–D) Analyses of the HGSNAT enzyme activity expressed in nmol × h^{-1} × mg^{-1} protein for the WT-, SFC6-, and SFC7-fibroblasts (A), iPSCs (B), SNMs (C), and neurons (D). The data show mean ± SD of three independent experiments performed in triplicate (WT1, SFC6, and SFC7 fibroblasts and iPSCs, SNMs, and neurons derived from the WT1-iPSC#3.6, SFC6-iPSC#3.1, and SFC7-iPSC#3.1 iPSC lines), and three independent experiments performed in duplicate (WT2 fibroblasts and iPSC, SNMs, and neurons derived from the WT1-iPSC#3.1, WT1-iPSC#4.10, WT2-iPSC#3.1, WT2-iPSC#3.2, WT2-iPSC#4.2, WT2-iPSC#4.5, SFC6-iPSC#3.2, SFC6-iPSC#4.6, SFC6-iPSC#4.7, SFC7-iPSC#3.2, SFC7-iPSC#4.8, and SFC7-iPSC#4.9 iPSC lines). **p < 0.01 (WT versus patients), ***p < 0.001 (WT versus patients).

(E) Analyses of the GAG levels expressed as percentage of WT levels, in WT1-, SFC6-, and SFC7-fibroblasts (E) and neurons differentiated for 3, 6, and 9 weeks from SNMs derived from the SFC6-iPSC#3.1 and SFC7-iPSC#3.1 iPSC lines or after 9 weeks from gene-complemented (treated) SNMs derived from the SFC6-iPSC#3.1 and SFC7-iPSC#3.1 iPSC lines, relative to neurons differentiated at the same time points from SNMs derived from the WT1-iPSC#3.6 iPSC line (F). The data show mean ± SD of three independent experiments performed in duplicate. **p < 0.01 (WT versus patients).

See also Figure S3.

The overall network performance was first quantified by means of two standard descriptors: (1) neuronal activity, which was defined as the average number of bursting episodes per neuron during the 30 min recording time, and (2) fraction of active neurons, which was defined as the ratio between those cells that showed at least one bursting episode and the total population monitored (see detailed definition and measurement in Experimental Procedures). We first considered the scenario of cultures that were not transduced to test the reliability of our analysis. The network activity for WT cultures was close to 1, indicating that most of the neurons in the network were active (Figure 5B). Activity was maintained within experimental error at weeks 6 and 9. This stability of WT measurements allowed us to associate possible changes in activity due solely to the disorder. Indeed, neuronal activity in the patients' neurons showed a gradual decrease, although the loss of activity was more evident in networks of SFC6-iPSC-derived neurons (Figure 5B).

We next considered the cultures that were transduced by LV.CMV.GFP and LV.CMV.HGSNAT.ires.GFP and carried out identical measurements (Figure 5C). For clarity, we compared the relative change in activity of the cultures from patients with respect to their WT counterparts (namely, WT solely transduced with *GFP* or WT transduced with both *GFP* and *HGSNAT*). We verified that WT

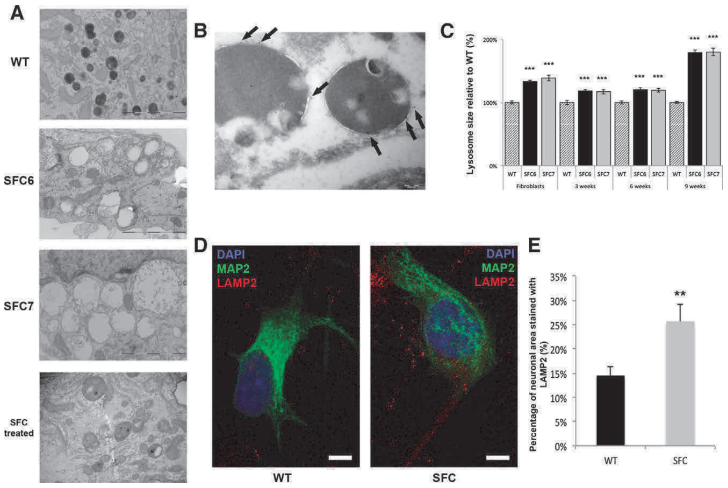

Figure 4. Lysosome Alterations in SFC-iPSC-Derived Neurons

(A) TEM micrograph representative of WT-, SFC6-, SFC7-, and gene-complemented SFC6-iPSC-derived neurons after 9 weeks of differentiation, showing lysosomal-derived accumulation vesicles (dark in the WT, empty-like in both patients, and gray in the gene-complemented sample). Neural cultures for these experiments were derived from SNMs established from the WT1-iPSC#3.6, SFC6-iPSC#3.1, and SFC7-iPSC#3.1 iPSC lines. The scale bar represents 2 μm.

(B) Immuno-gold analysis with anti-LAMP1 antibodies of SFC6-iPSC#3.1-derived neurons after 9 weeks of differentiation demonstrating the lysosomal origin of accumulation vesicles (gold particles indicated by black arrows). The scale bar represents 0.2 μm.

(C) Comparative analysis of lysosome size in WT, SFC6, and SFC7 samples, measured in TEM micrographs of fibroblasts and iPSC-derived neurons at the indicated times of differentiation. Neurons were the most abundant cell type in these preparations and were readily identified thanks to their round-shaped nuclei with weakly compacted chromatin and prominent nucleolus, scarce electrodense cytoplasm with numerous organelles, and synaptic contacts. The values shown indicate the size of SFC6 and SFC7 lysosomes in each cell type relative to the size of WT lysosomes in equivalent samples. The data show means ± SE of at least 200 lysosomes for each sample, obtained in 3 independent experiments. ***$p < 0.001$ (patients versus WT).

(D and E) Representative images of the immunoanalysis of LAMP2 staining per neuronal area in neurons (MAP2-positive cells) differentiated from WT (line WT2-iPSC#3.1, left image) and SFC (line SFC7-iPSC#4.8, right image) iPSC lines (D) and comparative analysis between control and patients at 9 weeks of differentiation (E). The values indicate the percentage of MAP2 stained area also stained for LAMP2. The data show mean ± SE of at least 15 neurons for each sample, obtained in 3 independent experiments. **$p < 0.01$ (patients versus controls).

See also Figure S4.

GFP-transduced neurons showed the same trend as the untransduced ones within statistical error. SFC6 and SFC7 neuronal networks gradually decayed in activity, and at week 9, activity loss reached about 70% and 45%, respectively, compared with controls. The reproducibility of this trend (evidenced by the small error bars and their similar trends in Figures 5B and 5C) indicates that the transduction protocol itself did not influence the behavior of the neurons and the development of the network. On the other hand, *HGSNAT*-transduced cultures showed a significant increase in activity over time, reaching activity levels similar to controls at 9 weeks (Figure 5C).

The analysis of the fraction of active neurons in the network allowed further characterization of the differences between the *HGSNAT*-treated and untreated cultures. As shown in Figure 5D, *GFP*-only SFC6 and SFC7 exhibited at week 9 about 70% and 50% less active neurons, respectively, compared with WT controls. However, after transduction with *HGSNAT*, both SFC6 and SFC7 maintained a fraction of active neurons comparable with the WTs. We also include in Figure 5E the values of network activity at week 9 (corresponding to the time point of Figure 5C). GFP-transduced SFC6 and SFC7 cultures showed a significant loss of network activity, while the corresponding *HGSNAT*-transduced counterparts reached activity levels indistinguishable from the control condition.

Effective Connectivity Degradation in Patient-Specific Neuronal Networks

Effective network connectivity was determined by identifying causal influences among neurons through GTE, an information theory method that allows drawing a functional map of neuronal interactions in the network (Orlandi et al., 2014; Stetter et al., 2012). A total of 30 cultures were analyzed, extending from week 3 to 9, and including all the conditions (WT, SFC, and gene-corrected SFC). Figure 6 provides the connectivity maps of three representative neuronal cultures at weeks 3 and 9, comparing the WT and SFC7 case with and without *HGSNAT* transduction. The WT and SFC7-*HGSNAT*-transduced cultures displayed comparable network structures, where most of the neurons established a similar pattern of connections with other neurons including a uniform increase in connectivity. In contrast, in the *GFP*-only SFC7 cultures, strong

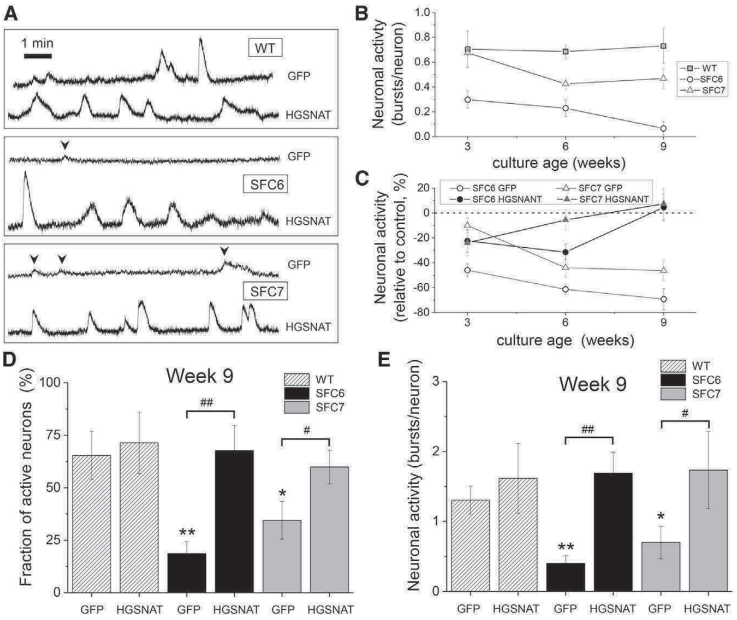

Figure 5. Altered Neuronal Activity in SFC-Derived Neuronal Networks

(A) Representative traces of spontaneous neuronal activity at week 9 of differentiation analyzed by calcium fluorescence imaging. Top traces correspond to control (*GFP*-transduced) neuronal networks; bottom traces correspond to gene complemented (*HGSNAT*-transduced) networks. Sharp increases in the fluorescence signal denote bursting episodes. Firings events of low amplitude (arrowheads) correspond to single spikes.

(B) Neuronal activity (total number of firings per neuron monitored along 30 min recording) of three independent untransduced cultures, at 3, 6, and 9 weeks after differentiation for each cell line and at each time point.

(C) Relative change in activity of control (*GFP*-transduced) or gene complemented (*HGSNAT*-transduced) SFC6 and SFC7 neuronal networks with respect to their equivalent WT networks. Three independent cultures were analyzed for each cell line at each time point.

(D) Fraction of active neurons at week 9 in control (*GFP*-transduced) or gene complemented (*HGSNAT*-transduced) WT, SFC6, and SFC7 neuronal networks. Three independent cultures were analyzed for each cell line at each time point.

(E) Neuronal activity of control (*GFP*-transduced) or gene complemented (*HGSNAT*-transduced) WT, SFC6, or SFC7 neuronal networks at week 9 of differentiation. In (B) through (E), error bars are root-mean-square error. Three independent cultures were analyzed for each line at each time point. *$p < 0.05$ (patients versus WT), **$p < 0.01$ (patients versus WT), #$p < 0.05$ (*GFP*- versus *HGSNAT*-transduced), ##$p < 0.01$ (*GFP*- versus *HGSNAT*-transduced).

connections were formed only within a subset of neurons, leaving most of the remaining neurons weakly connected or disconnected, particularly at week 9. In general, from the total of 30 cultures analyzed for network effective connectivity, this extreme feature was almost exclusive to SFC6 and SFC7 cultures at week 9, with 4 of 6 cultures showing such a trait. All 9 WT cultures at any week showed uniform connectivity characteristics, and of the 15 *HGSNAT*-transduced cultures analyzed, only 1 SFC6-transduced culture at week 9 exhibited this extreme trait.

As a complementary measure of network connectivity, we also analyzed the cultures for the existence of assortativity (Newman, 2002). A network is said to be assortative when nodes with many connections preferentially connect to one another. In turn, nodes with few connections also tend to connect to one another. Conversely, a network is said to be disassortative if nodes with many connections tend to connect with nodes with few connections. In our experiments, of a total of 30 analyzed cultures, 24 were assortative and 6 disassortative. Interestingly, 4 of the disassortative networks corresponded to the SFC6 and SFC7 cultures at week 9 (see, e.g., Figure 6, bottom central panel).

Each of the above analyses (i.e., the presence of unconnected neurons and disassortativity traits) is not significant when observed independently. However, their concurrent presence is highly indicative of network-wide changes in SFC6 and SFC7 untreated cultures compared with WT and *HGSNAT*-transduced ones. Indeed, a combined Fisher's permutation test yields an achieved significance level (ASL) of 0.02 between the SFC and WT cultures and an ASL of 0.03 between the SFC and SFC-*HGSNAT* transduced cultures, whereas the ASL between SFC-*HGSNAT* and WT is 0.46, showing no statistically significant differences. The reasonable significance of the former group supports the idea that the disorder causes important network topology changes, ultimately driving the affected networks toward a state of high fragility.

DISCUSSION

In this work, we have generated a neuronal model of Sanfilippo type C by reprogramming fibroblasts from two patients using the iPSC technology. The generation of a

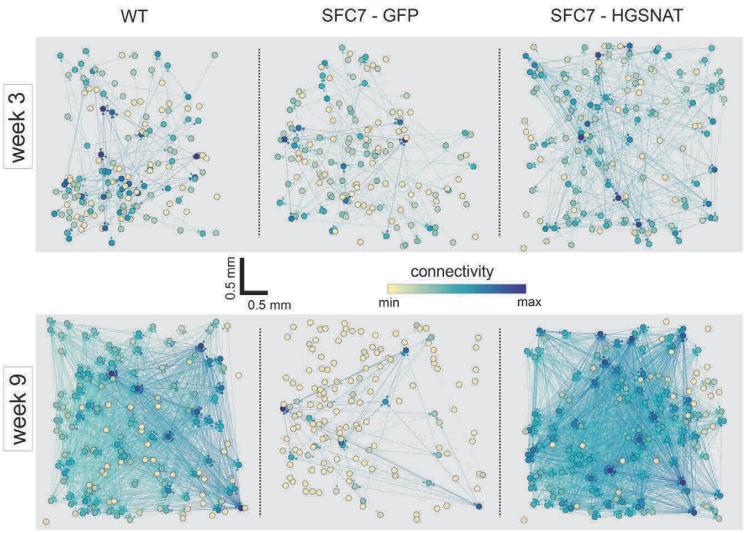

Figure 6. Alterations in Effective Connectivity in SFC-Derived Neuronal Networks

Structure of representative WT and control (*GFP*-transduced) or gene complemented (*HGSNAT*-transduced) SFC7-iPSC-derived neuronal networks at 3 (top) and 9 (bottom) weeks of differentiation, as reconstructed through GTE methods. In all the depicted networks, circles show the actual position of the neurons in the culture and are color-coded according to their relative connectivity. For easier visualization, the number of neurons in each network is limited to 150, which are randomly chosen from the original set, and only those connections with p values < 0.002 are represented.

neuronal model is relevant because the main features of the disease cannot be studied in fibroblasts. The fact that we used samples from two patients validates the results and allows the detection of slight inter-individual differences, although the study of additional Sanfilippo type C patient-specific iPSCs would be necessary to generalize our conclusions.

iPSC technology has been widely used to model different types of diseases, including those affecting the CNS (Durnaoglu et al., 2011; Okano and Yamanaka, 2014). Some other LSDs have been modeled using iPSC technology, which were later differentiated to the human cellular type of interest for each case. For Pompe's disease, cardiomyocytes exhibit the highest accumulation of glycogen, impaired autophagy, vacuolation, mitochondrial aberrances, and shorter survival times, features that were reverted after the overexpression of the normal gene (Huang et al., 2011). In the case of Hurler disease, hematopoietic and non-hematopoietic cells showed GAG accumulation and could be rescued by introducing the normal copy of the gene (Tolar et al., 2011). For Sanfilippo B syndrome, patient-derived neurons presented storage vesicles and Golgi disorganization (Lemonnier et al., 2011). In the case of Gaucher disease, iPSC-derived macrophages showed impaired lysosomal function and red blood cell clearance, recapitulating the hallmarks of the disease in this cell type, which could be reverted after administration of the recombinant enzyme (Panicker et al., 2012). Moreover, Gaucher disease-specific macrophages and neurons displayed low enzyme activity that could be partially rescued using small compounds with chaperone activity (Tiscornia et al., 2013); and dopaminergic neurons accumulated glucosylceramide and α-synuclein and showed autophagy and lysosomal defects and dysregulation of calcium homeostasis, all of which could be reverted after gene correction (Schöndorf et al., 2014). Finally, for Niemann-Pick type C1, iPSC-derived neurons exhibited spontaneous action potentials, confirming their maturation and accumulated cholesterol (Trilck et al., 2013). In another work regarding this disease, hepatic and neuronal cells presented lower cell viability, cholesterol storage, and impaired autophagy, features that could be reverted after gene correction (Maetzel et al., 2014). In many of these studies, the phenotypes observed could not be analyzed in fibroblasts, highlighting the importance of developing iPSC-derived models. Gene complementation provides an important experimental control that allows the assurance that the phenotypes detected are due to the genetic defect in the patient, rather than reprogramming artifacts.

In the present study, enzyme activity was dispensable for reprogramming and iPSC maintenance. This is in contrast with Fanconi anemia (Raya et al., 2009; Navarro et al., 2014), and also with Sanfilippo type B (Lemonnier et al., 2011) and Pompe disease (Higuchi et al., 2014), in all of which gene complementation was needed to achieve reprogramming. We hypothesize that the dispensability of enzyme activity for iPSC generation and maintenance might be related to overall low lysosomal activity in these cells. Thus, all the iPSCs generated in the present study (from either controls or SFC patients) showed relatively small numbers of lysosomes in comparison with fibroblasts, as judged by immunostaining with LAMP2

(Figure S4). Moreover, enzyme activity was very low in control iPSCs compared with fibroblasts (Figures 3A and 3B), as were the activities of other lysosomal enzymes (β-hexosaminidase and β-glucocerebrosidase; data not shown), in agreement with previous results (Tiscornia et al., 2013). Taken together, all these data suggest that iPSCs present a small number of lysosomes in comparison with other cell types.

To reduce the variability associated with neural differentiation of iPSCs (Falk et al., 2012), we established iPSC-derived SNMs consisting of neural progenitor cells that can be expanded and subsequently differentiated to neurons and glia (Cho et al., 2008). Mature human neurons that exhibit the principal features of the disease have been successfully generated after culturing iPSC-derived neural precursors cells for 3 to 9 weeks in neuronal differentiation medium. iPSC differentiation, including mature and functional neurons as the main cellular type, was proved through the expression of mature neuronal markers as well as synaptic proteins. Importantly, neuronal cultures derived from SFC patients showed lack of enzyme activity and an accumulation of GAGs and alteration of lysosomes. Apart from the lack of enzyme activity, which is always lacking in SFC cultures, other alterations appeared to be progressive. GAGs accumulated over time, but in our experiments, these differences did not reach statistical significance versus controls until 9 weeks (around 50% respect to control), which could indicate a lower rate of synthesis and storage in this cell type compared to fibroblasts. Lysosomal alterations displayed through TEM/LAMP1 and immunostaining with LAMP2 were first noticed at 3 to 6 weeks and became dramatic at 9 weeks (almost doubled in size). This timeline of appearance of alterations is in concordance with the progressive nature of the disease and highlights current difficulties in predicting the extent of neurological decline, because the lack of enzyme activity is not predictive, and the analysis of GAG storage and lysosome size and number requires invasive techniques.

The fact that our SFC-iPSC-derived neural cultures developed alterations that recapitulated those seen in patients prompted us to investigate whether we could detect early functional alterations predating known pathological signs of the disease. For this purpose, we used calcium imaging to analyze neuronal function in patients' cells. An important decrease in spontaneous activity of SFC neurons compared with WT controls was already detected at 3 weeks of differentiation, particularly for the most severe case (SFC6). The different behavior in SFC6 and SFC7 could be due to the particular features of their mutations. In this regard, we have recently showed that the c.372-2G > A mutation, borne by SFC7, gives rise to a protein lacking 4 amino acids that has some residual activity (Matos et al., 2014). These data suggest that the decline of neuronal activity correlates with the severity of the neurological phenotype observed in patients.

Moreover, we combined a direct quantification of neuronal activity with advanced functional connectivity analyses framed in the context of transfer entropy (TE) (Stetter et al., 2012). The latter provided evidences for broad changes in network structure, unraveling extensive disconnection of neurons, the emergence of a subset of highly connected cells, and the evolution of the network toward a disassortative structure. Although the presence of unconnected neurons is a clear indicator of a dysfunctional network, the existence of assortative or disassortative traits is not. Indeed, several naturally occurring networks may fall into one kind or another (Honey et al., 2007; Pan et al., 2010). Theoretical studies (Schmeltzer et al., 2014) and experiments in vitro (Teller et al., 2014) have shown that assortative networks are resilient to attack since the highly connected nodes shape a core that preserves the functionality of network. In contrast, disassortative networks are highly vulnerable, since the targeted loss of the few highly connected nodes may cause network-wide failure (Newman, 2002). These ideas, translated to our study, suggest that the affected, disassortative cultures could completely collapse upon such targeted damage, making them highly vulnerable networks.

Our results and analyses suggest that the disorder notably disrupts the topology of the network. In the context of the patients, these alterations could significantly affect the normal operation of the brain. Such an aspect is important in the framework of studies that highlight the relation between altered network topology upon disease and the degradation of brain's operability and cognitive tasks (Bassett and Bullmore, 2009; van den Heuvel and Sporns, 2013).

The spontaneous activity of SFC-derived neurons was recovered after transduction, in the SNM stage, with lentiviruses carrying the WT *HGSNAT* cDNA, and subsequent differentiation. The lack of recovery at 3 weeks and the partial recovery at 6 weeks contrast with the total recovery at 9 weeks of differentiation. We believe these differences are due to the fact that LV transduction was around 60% efficient, which could initially slow down the development of the network compared with the WT case. At later stages, we hypothesize that the large fraction of healthy neurons suffices to foster broad circuit connectivity and, ultimately, high neuronal activity. We note that the high expression levels of the transduced cells do not seem to alter their individual activity. Indeed, the WT-derived cultures overexpressing the *HGSNAT* cDNA did not show any significant alteration in these properties. However, our results indicate that the transduced cells do play a role in maintaining or restoring broad network activity and connectivity. Thus, we conclude that neuronal network activity and

development could be reestablished with a therapeutic approach that rescues only a fraction (though sufficiently high) of the total neurons. However, GAG storage or lysosome appearance by TEM showed only partial reversion after 9 weeks of differentiation. Whether longer times are needed for complete reversion of these features, or whether this is not at all possible, will require further investigation. The availability of the human cellular model described here provides an excellent tool to investigate this and other issues.

In summary, the cellular model introduced here reproduces the major features of the Sanfilippo type C syndrome, especially specific neuronal traits. We have demonstrated that most of the phenotypic features of this neuronal model can be reversed after gene complementation, using lentiviruses overexpressing the cDNA of the *HGSNAT* gene. Moreover, our neuronal model could be used as a tool to test different possible therapeutic strategies. This is particularly relevant because no cellular model was available for Sanfilippo type C syndrome, and a mouse model has only very recently been developed (Martins et al., 2015). Our findings prove the usefulness of iPSC-derived neuronal models to detect early functional phenotypes that can shed light onto the molecular and cellular processes that lead to the brain dysfunction in these patients, as well as providing valuable readouts for screening of potential therapeutic compounds that prevent, rather than revert, the onset of neurodegeneration. Moreover, the neuronal activity and effective connectivity analyses could be applicable to other neurodegenerative diseases in which iPSC-based models are available, such as Parkinson's or Alzheimer's disease, autism, and others. Further studies are needed to establish whether this technique would be able to detect differences in the neuronal activity or the network structure before the onset of disease. Such an approach could foster the development of in vivo analyses for early diagnosis of patients affected by neurological diseases, as well as their monitoring during potential treatments.

EXPERIMENTAL PROCEDURES

A complete description of experimental procedures can be found in Supplemental Experimental Procedures.

Network Reconstruction

Network reconstruction was carried out by identifying causal influences between neurons through TE (Schreiber, 2000; Stetter et al., 2012; Vicente et al., 2011). TE is an information-theoretic measure that identifies the flow of information between two time traces. The measure is model free (i.e., it does not require previous knowledge of the dynamics of the system) and is able to detect linear and non-linear interactions between any pair of traces. In a more formal description of TE, one considers two signals X and Y (any two neuronal fluorescence traces in our case), with the goal to assess the influence of X on Y (X → Y). TE measures the amount of uncertainty reduced in predicting the future of Y by taking into account both the pasts of Y and X, rather than the past of Y alone. Mathematically, this operation can be written as

$$TE_{X\to Y} = \sum P(Y_t, Y_t^k, X_t^k) log\left(\frac{P(Y_t \mid Y_t^k, X_t^k)}{P(Y_t \mid Y_t^k)}\right)$$

where Y_t denotes the value of Y at time t and Y_t^k the past k-th values of Y. $P(\cdot)$ is the probability of observing that particular sequence, whereas $P(\cdot|\cdot)$ is the conditional probability. The sum is performed over all possible values of Y_t, Y_t^k, X_t^k.

There are different variations of the TE measure depending on the data under analysis, for example, fMRI (Honey et al., 2007), magnetoencephalography (Wibral et al., 2011), spike trains (Ito et al., 2011), or fluorescence data, as in our case. Here we use a version named GTE (Orlandi et al., 2014; Stetter et al., 2012) that was specifically developed for neuronal fluorescence signals (see Stetter et al., 2012, for details).

The analysis of the recorded spontaneous activity traces within the context of GTE was as follows. We initially computed the first derivative of the fluorescence trace and the resulting values binned with n = 2 intervals for TE computation. TE was then applied to all pairs of neurons in the network. TE assigns a score for every neuronal pair, but only those pairs with scores above a given significance level were considered putative connections. Significance was established by comparing the raw TE scores and the bootstrapped versions (to account for bias) and those obtained by shuffling the data from only the presynaptic neuron. Bootstrapped versions were obtained by generating surrogates of the fluorescence data for every neuronal pair while preserving temporal correlations between the pairs. For the representative networks, a paired *Z* test was performed with the bias-corrected and shuffled scores, and only those values above the 97.5th percentile ($p < 0.002$) were considered putative connections. For the connectivity and assortativity analysis, only the connections with the top 10% bias-corrected score were considered.

Statistical Analysis

Differences between conditions respect to controls were evaluated using a Mann-Whitney non-parametric U test, and statistical significance was set at $p < 0.05$, except for the network reconstruction experiment (see above).

SUPPLEMENTAL INFORMATION

Supplemental Information includes Supplemental Experimental Procedures, four figures, three tables, and three movies and can be found with this article online at http://dx.doi.org/10.1016/j.stemcr.2015.08.016.

ACKNOWLEDGMENTS

The authors would like to thank M. Cozar of the Genetics Department (UB) and the Institut de Bioquímica Clínica, Barcelona, for helpful insights and A. di Domenico for critical reading of the manuscript. We are also grateful for the permanent support,

including financial aid, from Jonah's Just Begun – Foundation to Cure Sanfilippo, Association Sanfilippo Sud, Fundación Stop Sanfilippo, and Asociación MPS España. This study was partially funded by grants from MINECO (SAF2011-25431, SAF2012-33526, BFU2010-21823), the Catalan Government (2014SGR932, 2009SGR971, and 2009SGR14), ISCIII (Red de Terapia Celular – TerCel RD12/0019/0019, FIS2010-21924-C02-02), and the ERC-2013-StG grant of the European Research Council to A.C. I.C. was partially supported by a grant from the University of Barcelona (APIF).

Received: January 29, 2015
Revised: August 26, 2015
Accepted: August 26, 2015
Published: September 24, 2015

REFERENCES

Bassett, D.S., and Bullmore, E.T. (2009). Human brain networks in health and disease. Curr. Opin. Neurol. *22*, 340–347.

Canals, I., Elalaoui, S.C., Pineda, M., Delgadillo, V., Szlago, M., Jaouad, I.C., Sefiani, A., Chabás, A., Coll, M.J., Grinberg, D., and Vilageliu, L. (2011). Molecular analysis of Sanfilippo syndrome type C in Spain: seven novel HGSNAT mutations and characterization of the mutant alleles. Clin. Genet. *80*, 367–374.

Cherry, A.B.C., and Daley, G.Q. (2013). Reprogrammed cells for disease modeling and regenerative medicine. Annu. Rev. Med. *64*, 277–290.

Cho, M.-S., Hwang, D.-Y., and Kim, D.-W. (2008). Efficient derivation of functional dopaminergic neurons from human embryonic stem cells on a large scale. Nat. Protoc. *3*, 1888–1894.

Durnaoglu, S., Genc, S., and Genc, K. (2011). Patient-specific pluripotent stem cells in neurological diseases. Stem Cells Int. *2011*, 212487.

Engels, H., Eggermann, T., Caliebe, A., Jelska, A., Schubert, R., Schüler, H.M., Panasiuk, B., Zaremba, J., Latos-Bieleńska, A., Jakubowski, L., et al. (2008). Genetic counseling in Robertsonian translocations der(13;14): frequencies of reproductive outcomes and infertility in 101 pedigrees. Am. J. Med. Genet. A. *146A*, 2611–2616.

Falk, A., Koch, P., Kesavan, J., Takashima, Y., Ladewig, J., Alexander, M., Wiskow, O., Tailor, J., Trotter, M., Pollard, S., et al. (2012). Capture of neuroepithelial-like stem cells from pluripotent stem cells provides a versatile system for in vitro production of human neurons. PLoS ONE *7*, e29597.

Fan, X., Zhang, H., Zhang, S., Bagshaw, R.D., Tropak, M.B., Callahan, J.W., and Mahuran, D.J. (2006). Identification of the gene encoding the enzyme deficient in mucopolysaccharidosis IIIC (Sanfilippo disease type C). Am. J. Hum. Genet. *79*, 738–744.

Higuchi, T., Kawagoe, S., Otsu, M., Shimada, Y., Kobayashi, H., Hirayama, R., Eto, K., Ida, H., Ohashi, T., Nakauchi, H., and Eto, Y. (2014). The generation of induced pluripotent stem cells (iPSCs) from patients with infantile and late-onset types of Pompe disease and the effects of treatment with acid-α-glucosidase in Pompe's iPSCs. Mol. Genet. Metab. *112*, 44–48.

Honey, C.J., Kötter, R., Breakspear, M., and Sporns, O. (2007). Network structure of cerebral cortex shapes functional connectivity on multiple time scales. Proc. Natl. Acad. Sci. U S A *104*, 10240–10245.

Hřebíček, M., Mrázová, L., Seyrantepe, V., Durand, S., Roslin, N.M., Nosková, L., Hartmannová, H., Ivánek, R., Cízkova, A., Poupetová, H., et al. (2006). Mutations in TMEM76* cause mucopolysaccharidosis IIIC (Sanfilippo C syndrome). Am. J. Hum. Genet. *79*, 807–819.

Huang, H.-P., Chen, P.-H., Hwu, W.-L., Chuang, C.-Y., Chien, Y.-H., Stone, L., Chien, C.-L., Li, L.-T., Chiang, S.-C., Chen, H.-F., et al. (2011). Human Pompe disease-induced pluripotent stem cells for pathogenesis modeling, drug testing and disease marker identification. Hum. Mol. Genet. *20*, 4851–4864.

Inoue, H., Nagata, N., Kurokawa, H., and Yamanaka, S. (2014). iPS cells: a game changer for future medicine. EMBO J. *33*, 409–417.

Ito, S., Hansen, M.E., Heiland, R., Lumsdaine, A., Litke, A.M., and Beggs, J.M. (2011). Extending transfer entropy improves identification of effective connectivity in a spiking cortical network model. PLoS ONE *6*, e27431.

Lemonnier, T., Blanchard, S., Toli, D., Roy, E., Bigou, S., Froissart, R., Rouvet, I., Vitry, S., Heard, J.M., and Bohl, D. (2011). Modeling neuronal defects associated with a lysosomal disorder using patient-derived induced pluripotent stem cells. Hum. Mol. Genet. *20*, 3653–3666.

Maetzel, D., Sarkar, S., Wang, H., Abi-Mosleh, L., Xu, P., Cheng, A.W., Gao, Q., Mitalipova, M., and Jaenisch, R. (2014). Genetic and chemical correction of cholesterol accumulation and impaired autophagy in hepatic and neural cells derived from Niemann-Pick Type C patient-specific iPS cells. Stem Cell Reports *2*, 866–880.

Martins, C., Hůlková, H., Dridi, L., Dormoy-Raclet, V., Grigoryeva, L., Choi, Y., Langford-Smith, A., Wilkinson, F.L., Ohmi, K., DiCristo, G., et al. (2015). Neuroinflammation, mitochondrial defects and neurodegeneration in mucopolysaccharidosis III type C mouse model. Brain *138*, 336–355.

Matos, L., Canals, I., Dridi, L., Choi, Y., Prata, M.J., Jordan, P., Desviat, L.R., Pérez, B., Pshezhetsky, A.V., Grinberg, D., et al. (2014). Therapeutic strategies based on modified U1 snRNAs and chaperones for Sanfilippo C splicing mutations. Orphanet J. Rare Dis. *9*, 180.

Mazzulli, J.R., Xu, Y.-H., Sun, Y., Knight, A.L., McLean, P.J., Caldwell, G.A., Sidransky, E., Grabowski, G.A., and Krainc, D. (2011). Gaucher disease glucocerebrosidase and α-synuclein form a bidirectional pathogenic loop in synucleinopathies. Cell *146*, 37–52.

Navarro, S., Moleiro, V., Molina-Estevez, F.J., Lozano, M.L., Chinchon, R., Almarza, E., Quintana-Bustamante, O., Mostoslavsky, G., Maetzig, T., Galla, M., et al. (2014). Generation of iPSCs from genetically corrected Brca2 hypomorphic cells: implications in cell reprogramming and stem cell therapy. Stem Cells *32*, 436–446.

Neufeld, E.F., and Muenzer, J. (2001). The mucopolysaccharidoses. In The Metabolic and Molecular Bases of Inherited Disease, C.R. Scriver, A.L. Beaudet, W.S. Sly, and D. Valle, eds. (New York: McGraw-Hill), pp. 3421–3452.

Newman, M.E. (2002). Assortative mixing in networks. Phys. Rev. Lett. *89*, 208701.

Okano, H., and Yamanaka, S. (2014). iPS cell technologies: significance and applications to CNS regeneration and disease. Mol. Brain *7*, 22.

Orlandi, J.G., Stetter, O., Soriano, J., Geisel, T., and Battaglia, D. (2014). Transfer entropy reconstruction and labeling of neuronal connections from simulated calcium imaging. PLoS ONE *9*, e98842.

Pan, R.K., Chatterjee, N., and Sinha, S. (2010). Mesoscopic organization reveals the constraints governing Caenorhabditis elegans nervous system. PLoS ONE *5*, e9240.

Panicker, L.M., Miller, D., Park, T.S., Patel, B., Azevedo, J.L., Awad, O., Masood, M.A., Veenstra, T.D., Goldin, E., Stubblefield, B.K., et al. (2012). Induced pluripotent stem cell model recapitulates pathologic hallmarks of Gaucher disease. Proc. Natl. Acad. Sci. U S A *109*, 18054–18059.

Park, I.H., Arora, N., Huo, H., Maherali, N., Ahfeldt, T., Shimamura, A., Lensch, M.W., Cowan, C., Hochedlinger, K., and Daley, G.Q. (2008). Disease-specific induced pluripotent stem cells. Cell *134*, 877–886.

Poupetová, H., Ledvinová, J., Berná, L., Dvoráková, L., Kozich, V., and Elleder, M. (2010). The birth prevalence of lysosomal storage disorders in the Czech Republic: comparison with data in different populations. J. Inherit. Metab. Dis. *33*, 387–396.

Raya, A., Rodríguez-Pizà, I., Guenechea, G., Vassena, R., Navarro, S., Barrero, M.J., Consiglio, A., Castellà, M., Río, P., Sleep, E., et al. (2009). Disease-corrected haematopoietic progenitors from Fanconi anaemia induced pluripotent stem cells. Nature *460*, 53–59.

Schmeltzer, C., Soriano, J., Sokolov, I.M., and Rüdiger, S. (2014). Percolation of spatially constrained Erdős-Rényi networks with degree correlations. Phys. Rev. E Stat. Nonlin. Soft Matter Phys. *89*, 012116.

Schöndorf, D.C., Aureli, M., McAllister, F.E., Hindley, C.J., Mayer, F., Schmid, B., Sardi, S.P., Valsecchi, M., Hoffmann, S., Schwarz, L.K., et al. (2014). iPSC-derived neurons from GBA1-associated Parkinson's disease patients show autophagic defects and impaired calcium homeostasis. Nat. Commun. *5*, 4028.

Schreiber, T. (2000). Measuring information transfer. Phys. Rev. Lett. *85*, 461–464.

Stetter, O., Battaglia, D., Soriano, J., and Geisel, T. (2012). Model-free reconstruction of excitatory neuronal connectivity from calcium imaging signals. PLoS Comput. Biol. *8*, e1002653.

Takahashi, K., and Yamanaka, S. (2006). Induction of pluripotent stem cells from mouse embryonic and adult fibroblast cultures by defined factors. Cell *126*, 663–676.

Takahashi, K., Tanabe, K., Ohnuki, M., Narita, M., Ichisaka, T., Tomoda, K., and Yamanaka, S. (2007). Induction of pluripotent stem cells from adult human fibroblasts by defined factors. Cell *131*, 861–872.

Teller, S., Granell, C., De Domenico, M., Soriano, J., Gómez, S., and Arenas, A. (2014). Emergence of assortative mixing between clusters of cultured neurons. PLoS Comput. Biol. *10*, e1003796.

Tiscornia, G., Vivas, E.L., Matalonga, L., Berniakovich, I., Barragán Monasterio, M., Eguizábal, C., Gort, L., González, F., Ortiz Mellet, C., García Fernández, J.M., et al. (2013). Neuronopathic Gaucher's disease: induced pluripotent stem cells for disease modelling and testing chaperone activity of small compounds. Hum. Mol. Genet. *22*, 633–645.

Tolar, J., Park, I.H., Xia, L., Lees, C.J., Peacock, B., Webber, B., McElmurry, R.T., Eide, C.R., Orchard, P.J., Kyba, M., et al. (2011). Hematopoietic differentiation of induced pluripotent stem cells from patients with mucopolysaccharidosis type I (Hurler syndrome). Blood *117*, 839–847.

Trilck, M., Hübner, R., Seibler, P., Klein, C., Rolfs, A., and Frech, M.J. (2013). Niemann-Pick type C1 patient-specific induced pluripotent stem cells display disease specific hallmarks. Orphanet J. Rare Dis. *8*, 144.

Trounson, A., Shepard, K.A., and DeWitt, N.D. (2012). Human disease modeling with induced pluripotent stem cells. Curr. Opin. Genet. Dev. *22*, 509–516.

Valstar, M.J., Ruijter, G.J.G., van Diggelen, O.P., Poorthuis, B.J., and Wijburg, F.A. (2008). Sanfilippo syndrome: a mini-review. J. Inherit. Metab. Dis. *31*, 240–252.

van den Heuvel, M.P., and Sporns, O. (2013). Network hubs in the human brain. Trends Cogn. Sci. *17*, 683–696.

Vicente, R., Wibral, M., Lindner, M., and Pipa, G. (2011). Transfer entropy—a model-free measure of effective connectivity for the neurosciences. J. Comput. Neurosci. *30*, 45–67.

Vitry, S., Bruyère, J., Hocquemiller, M., Bigou, S., Ausseil, J., Colle, M.-A., Prévost, M.-C., and Heard, J.M. (2010). Storage vesicles in neurons are related to Golgi complex alterations in mucopolysaccharidosis IIIB. Am. J. Pathol. *177*, 2984–2999.

Wibral, M., Rahm, B., Rieder, M., Lindner, M., Vicente, R., and Kaiser, J. (2011). Transfer entropy in magnetoencephalographic data: quantifying information flow in cortical and cerebellar networks. Prog. Biophys. Mol. Biol. *105*, 80–97.